Crossflow Ultrafiltration of Raw Municipal Wastewater

investigations using PVDF tubular membranes

Crossflow Ultrafiltration of Raw Municipal Wastewater

investigations using PVDF tubular membranes

PROEFSCHRIFT

ter verkrijging van de graad van doctor
aan de Technische Universiteit Delft,
op gezag van de Rector Magnificus prof. dr. ir. J.T. Fokkema,
voorzitter van het College voor Promoties,
in het openbaar te verdedigen op donderdag 19 Juni 2008 om 12:30 uur

Aldo Maria RAVAZZINI
Dottore in Ingegneria per l' Ambiente e il Territorio
(Politecnico di Milano, Italië)
geboren te Milano.

Dit proefschrift is goedgekeurd door de promotor:
Prof. dr. ir. J.H.J.M. Van der Graaf

Samenstelling promotiecommissie:

Rector Magnificus,	voorzitter
Prof. dr. ir. J.H.J.M. Van der Graaf,	Technische Universiteit Delft, promotor
Prof. dr. ing. F. Malpei,	Politecnico di Milano
Prof. dr. G. Amy,	UNESCO-IHE/Technische Universiteit Delft
Prof. dr. ing. H. Ødegaard,	Norges Teknisk-Naturvitenskapelige Universiteit
Prof. dr. ing. T. Melin,	RWTH Universität Aachen
Prof. dr. ir. W.H. Rulkens,	Wageningen Universiteit
Dr. ir. A.F. van Nieuwenhuijzen,	Technische Universiteit Delft

ISBN 978-90-8957-004-8

Printed by GILDEPRINT Drukkereijn b.v., Enschede, NL.

Preface

Only dead fishes go with the flow
(S.Benni)

I encountered the sentence that opens this text a couple of years ago, in a half humorous -half serious book that I was reading by chance. As I read those few words, I loved them. They contain so much of me: the water that I love, the fishes that I love (I am crazy about fishing), and my stubbornness (or *independence*, to give it a more positive connotation).

More notably here, they nicely describe my attitude at the time I finished the University and I chose to become a researcher in The Netherlands.

After several years the experience in The Netherlands is over. As *Promovendus* at the TU-Delft, I was able to conduct research with considerable autonomy. This fulfilled my expectations, but I admit that if I had been open to listen to some wise suggestions, it would have taken certainly less time and less mistakes.

I enjoyed the same freedom and I committed avoidable mistakes also during the writing of this dissertation. Probably, if at least this time I had followed some of the wise suggestions I received, the final outcome would have been "thinner" and equally significant. On the opposite, the product in your hands is again a direct product of the naïve sentence quoted at the opening.

Indeed, this dissertation attempts to communicate not only the major findings and results, but also the details of the experiments and the reasoning I followed. On one side, I wanted that nothing significant should be wasted. On the other, that all the interested people were able to understand, or criticise, and improve the work.

The consequence is that the dissertation is very long, but it allows (hopefully) distinct levels of reading. I present my conclusions: it would really make me happy if anyone could find a single idea to continue with or to oppose, and would develop it further.

This book is dedicated to my grandmother *Nonna Elide* and to my little niece *Beatrice*, as main events of their lives marked the period that this dissertation was firstly thought and then written. Nonna Elide showed me that in life only a few things matter and even fewer are important. At the time that she left us, Beatrice stepped in and taught another piece of the same lesson: life never stops, on the contrary, it always blooms again.

I did not quite learn the lesson of my grandmother, and I often run after minor details. I will try to keep the teaching in mind and when this experience will be over, all my energies will go to the people I love and I kept waiting. Another season starts, something good will result.

Contents

Notation

List of symbols

α_{cake}	specific cake resistance (Hermia)	$[m^{-1} \cdot kg^{-1}]$
α_c	average specific cake resistance	$[m \cdot kg^{-1}]$
α_{pb}	average pore blocking parameter	$[m^2 \cdot kg^{-1}]$
α_{pc}	average pore constriction parameter	$[m^3 \cdot kg^{-1}]$
A	membrane area	$[m^2]$
A_m	permeable membrane area	$[m^2]$
C_b	bulk solution concentration	$[kg \cdot m^{-3}]$
δ	thickness of fouling layer	$[m]$
δ_m	membrane thickness	$[m^{-1}]$
d	tube diameter	$[m]$
d_{max}	maximum coagulant dosage (Chapter 8)	$[mg/L]$
ΔJ	flux gap	$[LMH] = [L \cdot m^{-2}h^{-1}]$
ΔP	pressure difference	$[bar]$
ΔR	resistance gap	$[m^{-1}]$
ΔR_{30}	resistance increase during 30 min	$[m^{-1}]$
ΔR_{vol}	resistance increase at fixed permeate volume	$[m^{-1}]$
Δt	time interval	$[s]$
ϵ	porosity of cake layer	$[-]$
η	dynamic viscosity	$[Pa \cdot s^{-1}]$
Θ	conversion	$[-]$
f	friction factor	$[-]$
G	mean velocity gradient	$[s^{-1}]$
J	permeate flux	$[LMH] = [L \cdot m^{-2}h^{-1}]$
J_0	starting flux during fitting ($t = 0$)	$[LMH]$

J_{start}	starting measured flux value	$[LMH]$
J^*	back-transport flux	$[LMH] = [L \cdot m^{-2} h^{-1}]$
k	fouling coefficient for blocking laws	[various]
k_c	fouling rate cake filtration	$[m^{-4}]$
k_i	fouling rate constant for fitting	[various]
k_{pb}	fouling rate pore blocking	$[m^{-1}]$
k_{pc}	fouling rate pore constriction	$[m^{-3}]$
K	permeability	$[L \cdot m^{-2} h^{-1} bar^{-1}]$
ν	kinematic viscosity	$[m^2 \cdot s^{-1}]$
M	mass	$[kg]$
m_c	cake mass	$[kg]$
n	power coefficient for blocking laws	$[-]$
π	constant (3.1415 ...)	$[-]$
P	pressure	$[bar]$
P	power (Chapter 4)	$[W]$
ρ	density	$[kg \cdot m^{-3}]$
R	resistance to filtration	$[m^{-1}]$
R_{bf}	residual resistance after backflush	$[m^{-1}]$
R_{mem}	membrane resistance	$[m^{-1}]$
Re	Reynolds Number	$[-]$
r_p	particle radius	$[m]$
r_p	equivalent pore radius (Chapter 6)	$[m]$
τ	shear stress at membrane wall	$[Pa]$
T	temperature	$[°C]$
u_{cr}	crossflow velocity	$[m \cdot s^{-1}]$
$Volume_{bf}$	backflush volume	$[m^3]$
ξ	pump efficiency	$[-]$

List of abbreviations

$Al_2(SO_4)_3$	Aluminium Sulphate
bioN	Biological Nitrogen
BOD	Biological Oxygen Demand
BSA	Bovine Serum Albumin
CP	Concentration Polarisation
COD	Chemical Oxygen Demand
DOC	Dissolved Organic Carbon

DOM	Dissolved Organic Matter
CWF	Clean Water Flux
DBP	Disinfection By-Product
EfOM	Effluent Organic Matter
EPS	Extracellular Polymeric Substances
$FeCl_3$	Ferrum Chloride
K	Potassium
MBR	Membrane BioReactor
MF	Microfiltration
MFI	Modified Fouling Index
MWCO	Molecular Weight Cut-Off
NEN	Nederlands Normalisatie Instituut
NF	Nanofiltration
NOM	Natural Organic Matter
P	Phosphorous
PA	Polyamide
$PACl$	Poly-Aluminium Chloride
PAN	Polyacrylonitrile
p.e.	population equivalent
PE	Polyethilene
PESU	Poly(ethersulphone)
PLC	Programmable Logic Controller
PP	Polypropylene
PSD	Particle Size Distribution
PVDF	Polyvinylidenfluoride (membrane material)
SEM	Scanning Electron Microscope
SOC	Synthetic Organic Compounds
SMP	Soluble Microbial Products
TMP	Trans-membrane Pressure
TOC	Total Organic Carbon
TSS	Total Suspended Solids
UF	Ultrafiltation
RO	Reverse Osmosis
SPV	Specific Produced Volume
WWTP	Wastewater Treatment Plant
WFD	Water Framework Directive

Chapter 1

Introduction

Where the role of this research within wastewater treatment is (hopefully) explained.

1.1 Generalities on wastewater treatment in Europe

The current standard of wastewater treatment in European countries is represented by a combination of mechanical, chemical and biological processes that takes place in a centralised wastewater treatment plant (WWTP). Next to this, there exist several options for the decentralised (local) treatment, which are commonly applied at isolated housing. However, in the EU countries, the large majority of the produced wastewater is delivered to a centralised sewer network (EUROSTAT, 2003).

The traditional WWTP is designed as a series of treatment steps, as represented in Figure 1.1.

During the treatment train, undesired matter is progressively removed. Primary treatment aims at rough material and large particles. Secondary treatment generally targets organic and inorganic dissolved substances, including nutrients: most of the Nitrogen and significant quantities of Phosphorous are removed here. Finally, a tertiary step can be added, which can be for disinfection or for further removal of nutrients or suspended solids.

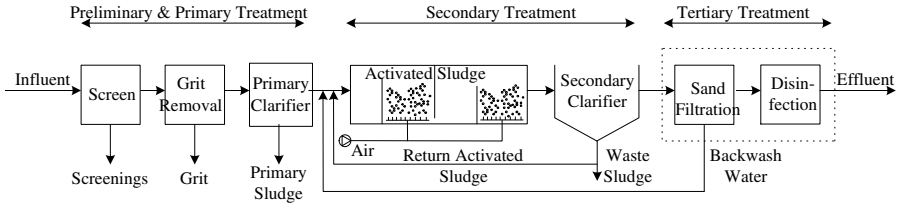

Figure 1.1: *Typical flow scheme of conventional activated sludge process (optional steps in the dotted box). Adapted from Metcalf & Eddy, 2003.*

The primary treatments are usually physical-chemical (mechanical with chemical aids), secondary treatments are biological, and tertiary treatments can be either physical-chemical (i.e. coagulation, rapid filtration, disinfection) or biological (bioN removal). The biological treatment provides the reduction of the most of the bulk parameters COD (Chemical Oxygen Demand) and BOD (Biological Oxygen Demand) and partially of the main nutrients. Therefore it can be considered as the "heart" of the process. The pollutants are either consumed or incorporated into the biological matter which is subsequently removed in the form of sludge.
Decentralised systems usually reproduce this scheme in a simplified form, i.e. simple mechanical pre-treatments precede a less-efficient biological process.

In all cases, the treatment of wastewater is conceived as the way to get rid of polluting and hazardous material before the final discharge of the effluent, which usually takes place in a receiving water body.

The water quality at discharge is dictated by law through the aid of a few key-parameters. Table 1.1 reports the actual European legislation for WWTP discharge (Urban Waste Water Treatment Directive, 91/271/EEC); other specific laws usually exist at National level.

However, it should be noted that nowadays the point of view toward wastewater treatment is changing. At worldwide level, it is common perception that because of human activities and climate changes, in many inhabited areas the quality and quantity of water sources are depleting. Water is emerging as a unique valuable product to be managed properly at any level of the water-cycle, including wastewater treatment. And in facts, we are witnessing the develop-

Table 1.1: *Discharge limits in the EU directive 91/271/EEC*

Parameter		maximum concentration at discharge			
TSS	$(mg \cdot L^{-1})$	60	(2–10,000 *p.e.*);	35	($> 10,000$ *p.e.*)
BOD_5 (20°C)	$(mgO_2 \cdot L^{-1})$	25			
COD_5	$(mgO_2 \cdot L^{-1})$	125			
N [a]	$(mg \cdot L^{-1})$	15	(10–100,000 *p.e.*);	10	($> 100,000$ *p.e.*)
P [a]	$(mg \cdot L^{-1})$	2	(10–100,000 *p.e.*);	1	($> 100,000$ *p.e.*)

[a] = only for "sensitive areas", i.e. subject to eutrophication, as identified in the Annex II.A(a) of the directive itself

ment of increasingly tight water-use regulations, more severe discharge policy and increasing number of wastewater reuse projects (Bixio *et al.*, 2005).

In Europe, this trend has been embraced by the Water Framework Directive (WFD, 2000/60/EC). The WFD aims at a good chemical and ecological status of the surface water, through the adoption of adequate measures. The main instrument will be the harmonization of the existing European directives and legislation which should be completed by 2015. The European Commission identified 33 priority substances for which Community legislation is likely to be implemented (nutrients, biological parameters, pesticides, heavy metals, hormone disrupters and medicinal substances, Communication 581/2002/EEC). These priority substances are considered to be hazardous enough that their levels need to be systematically reduced in all European countries (some of them even to zero-discharge value). In addition to those 33 priority substances, new discharge limits will also be established for "relevant area-specific" substances, thus at river basin level (STOWA, 2007; Broseliske and Verkerk, 2004; Salgot and Huertas, 2003).

The WFD also spells out that an integrated approach to water resources management should favour municipal wastewater reclamation and reuse on a larger scale, for both augmenting water supply and decreasing the impact of human activities on the environment (Bixio *et al.*, 2008; Bixio and Wintgens, 2006).

1.2 Membranes in wastewater treatment

Because of their intrinsic characteristics, membranes are playing a significant role in the recent developments of wastewater treatment (Fane, 2005). Membranes provide both rejection of harmful pathogens and clarification, which makes them suitable for the upgrade of standard WWTP effluent and for the production of reusable water (STOWA, 2005; Te Poele, 2006; Roorda, 2002; Rautenbach and Vossenkaul, 2001). Consequently, the installed capacity of membranes for this purpose is rapidly increasing (Wintgens *et al.*, 2005).

There exist several kinds of membrane processes, operating according to different principles. In wastewater treatment the most commonly applied are pressure-driven processes.

Pressure-driven membrane processes can be classified on the basis of the pore size. Obviously, smaller components are retained by increasingly small pore sizes (see Table 1.2).

Table 1.2: *Classification of membrane processes with pore size and removable components*

Process	Pores (nm)	Removable components
microfiltration (MF)	100-1000	suspended and micro particles, various pathogens
ultrafiltration (UF)	10-100	colloids, (partially) macromolecules, viruses
nanofiltration (NF)	1-10	macromolecules, multivalent ions, (partially) divalent ions
reverse osmosis (RO)	0.1-1	divalent ions, (not completely) monovalent ions

Although the four membrane processes of Table 1.2 can be combined in a variety of schemes, the typical applications in the treatment of municipal wastewater are the following ones:

- MF and UF of secondary/tertiary effluent from a conventional WWTP, as additional polishing step;
- MF/UF followed by RO for the production of high purity water from

WWTP effluent (so-called double membrane system);

- membrane bioreactors (MBR).

In all the cases, a biological treatment precedes the membrane-based step, providing the bulk reduction of the organic load (COD, BOD) and the main nutrients (N and P).

The most relevant limitation to the application of membrane process is membrane *fouling*. Fouling is the decay of the process performances due to the accumulation of materials at the membrane surface and within its pore. The visible consequences are either a reduction in the produced throughput, or a higher energy expenditure to maintain it. Therefore, fouling affects the stability and the economic of membrane processes directly.

Fouling depends upon the characteristics of the feed water and the membrane, but also on the operating conditions. Although stable operations with membrane systems are well proved, fouling is still poorly understood and the design of membrane process often requires expensive and tedious pilot testing (Evenblij, 2006; Judd, 2006; Te Poele, 2006; Laabs, 2004). For this reason, when the feed water is a complex and variable mixture like wastewater, the development of new membrane applications presents high risks.

This dissertation exactly reports on the investigations for the development of a novel membrane process using raw wastewater.

1.3 Direct Ultrafiltration: an interesting option

1.3.1 Direct membrane filtration: definition

Although this is not common practice in municipal wastewater treatment, membrane filtration can exist as stand-alone process as well. For instance, this is the case during several industrial applications, where membranes are applied to specific waste streams to recover either the solvent or the suspended material (Baker, 2004; Judd and Jefferson, 2003; Mulder, 1996).

When this concept is applied specifically to untreated wastewater, it seems appropriate to refer to it as *Direct Membrane Filtration*, as in van Nieuwen-

huijzen, 2000a. This name emphasizes the absence of biological treatment, and avoids confusion with other common expressions. For instance, "Membrane Filtration", usually refers to the filtration of WWTP effluent, and "Direct Filtration" to the rapid filtration of effluent without coagulation (Metcalf & Eddy, 2003). However, since membrane filtration provides the separation of constituents rather than "removal", this process has also been referred to as Direct Membrane Separation (DMS) (Ahn et al., 2001).

Figure 1.2 represents the basic concept of direct membrane filtration. The feed to the membrane is untreated wastewater, which is split into two main streams, one "rejected" (the *retentate*) and one "purified" (the *permeate*).

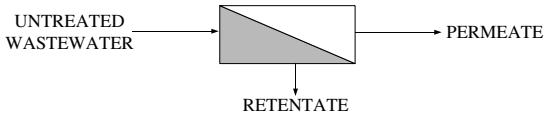

Figure 1.2: *Schematic representation of Direct Membrane Filtration*

The evident challenge is that due to the low quality of the feed water the membrane is considerably exposed to fouling.

The main positive aspect is that in principle it is possible to select the proper membrane size to achieve the desired separation of components. If the wastewater carries valuable components, thanks to the membrane they can be concentrated in the retentate or isolated in the "purified" permeate. If the most valuable product is the water, i.e. the solvent itself, the quality of the permeate will certainly increase with decreasing membrane pore size.

With respect to the traditional concept of wastewater treatment and discharge, direct membrane filtration is definitively a pro-active way to look at wastewater as a potential resource.

1.3.2 Direct ultrafiltration of raw sewage

This dissertation concerns a specific type of direct membrane filtration: direct ultrafiltration of raw sewage. This process is completely new and under development, as at the moment of writing only limited researches have been completed

or initiated on this subject (Hao *et al.*, 2005; Rulkens *et al.*, 2005; Sethi and Jubi, 2002; van Nieuwenhuijzen *et al.*, 2000b; Ahn *et al.*, 1998).

Figure 1.3 shows a concept diagram of direct ultrafiltration of raw sewage. The raw wastewater is regarded as a mixture of valuable compounds (water and nutrients) and undesired elements (summarized as Total Suspended Solids TSS and pathogens). The UF membrane realizes the separation of the desired-undesired compounds by constituting a barrier to particulate, colloids and bacteria.
The produced permeate is water free of particles, microorganisms and bacteria, and is rich in soluble COD and nutrients. The concentrate contains the removed particulate, microorganisms and bacteria.

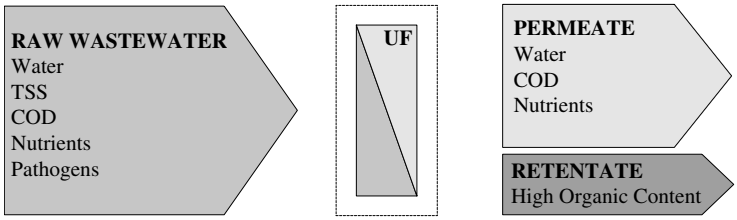

Figure 1.3: *Separation of constituents during Direct Ultrafiltration of municipal wastewater*

Figure 1.4 shows a schematic flow diagram of the process. The feed water undergoes simple mechanical pre-treatments and is collected in a buffer tank, after which it is fed to the membrane. The pre-treatments are meant to remove large particles and debris, in order to avoid clogging problems in the membrane system. The buffer tank equalizes the flow and receives the retentate stream, which allows maintaining a low solids concentration at the membrane inlet meanwhile enabling sedimentation and purging of the solid content.

One of the most evident characteristics of the system is its simplicity, especially noteworthy when Figure 1.4 is compared to Figure 1.1. There exist other appealing features, that make it interesting to explore the feasibility, the performances and the boundaries of direct ultrafiltration of the processs.
In the following, the expected positive and negative features are discussed.

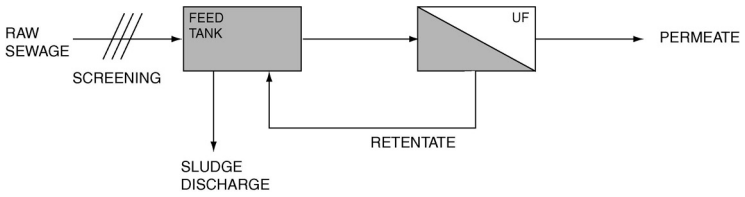

Figure 1.4: *Schematic representation of Direct Ultrafiltration*

Advantages and potential

Purely physical (-chemical) process : Direct membrane filtration is a purely physical process; chemicals are required for cleaning purposes. The typical limitations of the biological processes can be overcome (long start-up period, toxicity to the biomass, difficulties in handling discontinuous flow and temperature variations). Because of their modularity, membrane plants can be scaled-up and resized rapidly, adapting to changes in water flow. Operation could be discontinuous to meet seasonal variations, as for tourist areas.

Excellent particles removal : The UF membrane is a total barrier to particles, which can be expected to be completely removed. This is obtained without any chemical addition, thus avoiding chemical contamination of the rejected sludge.

Excellent pathogens removal : The efficiency of UF in the removal of pathogens of all kinds is already a well-established fact (Wintgens *et al.* 2005; EPA, 2001; Madaeni, 1998; Madaeni *et al.* 1995). The removal mechanism is size exclusion, therefore the complete removal of larger pathogens is guarateed (protozoa, helmints and bacteria). Small viruses and deformable bacteria could actually permeate the membrane; nevertheless, the level of sanitation achieved in one single step has been demonstrated excellent also for application with (partially) untreated wastewater (Hao *et al.*, 2005; Sethi and Juby, 2002).

Clear filtrate : The turbidity of UF filtrate can be expected to be always below 1 NTU. This is a relevant accomplishment in respect to reuse regulations, which always require very low turbidity, usually $< 2NTU$ (Salgot and Huertas, 2003).

Nutrients separation : The Phosphorous (P), Nitrogen (N) and Potassium

(K) present in soluble form in the feed water, will permeate the UF membrane and will be found in the filtrate. This is the expected pattern for ammonia, dissolved orthophosphates and dissolved K. The N:P:K ratio in direct UF permeate is very interesting with respect to the requirements of crops such as soybeans, corn and wheat (Evenblij *et al.*, 2002). Therefore, they may be regarded as valuable nutrients for irrigation purposes, lessening the needs for additional fertilizers and lessening the discharge of nutrients in surface waters. On a longer term scale, isolating P and N in the particle-free permeate may favour the development of technologies for the recovery of nutrients from wastewater.

Sludge quality : The concentrate contains the removed particulate, microorganisms and bacteria. When thickened, it is comparable to primary sludge with high organic content. Therefore, it could be treated with anaerobic digestion, eventually, generating energy for plant use. Given the absence of additional chemicals in the sludge, sludge reuse can be considered, depending on the feed water composition.

Availability of feed source: In the industrialized countries the most of domestic and industrial wastewater is collected in a sewer network and conveyed to a WWTP. Consequently, municipal wastewater is the most available wastewater-source both in terms of quantity and easiness of access. A process capable of reclaiming municipal wastewater would be readily applicable avoiding the necessity of separated collection systems or other dedicated infrastructures. Additionally, the water production can be realized anywhere along the existing sewer mains, and not only at the existing WWTP. This allows generating reusable water in the vicinity of the reuse location, which is often recognized as an obstacle to the feasibility of reuse projects, because of the cost of water transport (STOWA, 2001).

Negative features

High fouling attitude : Raw sewage is a complex mixture of all the possible components that may generate fouling. Additionally, its composition varies strongly from day to day. Achieving stable operation may prove challenging.

Odour and Stability of the permeate : Depending on the modality of transport in the sewer, the wastewater fed to the UF is most of the time anaerobic, and so is the permeate. Therefore, noxious odours may arise when the permeate is stored. The storage of the permeate may be problematic also because

the presence of nutrients and dissolved organics favours bacterial regrowth and algal blooming. Eventually, water could be produced on demand, or stabilized with some additional treatment (e.g. wetlands systems or ponds)

Emerging pollutants : Heavy metals and hazardous substances are known (or suspected) to have adverse effects on aquatic environment and human health. Unfortunately, they cannot be consistently removed by UF (Snyder, 2005), which may demand for an accurate management of both the (waste)-water sources and the reuse application.

1.3.3 Potential applications

Direct UF of municipal wastewater can be regarded either as a end-of-pipe treatment or simply as a side process to generate reusable water.

The first option relies on the fact that it is possible to successfully treat the waste stream purged by the system. For instance, one possibility is that the waste stream is concentrated to suspended solids values similar to those of conventional sludge and is treated as such.

The second option is simpler, because it focuses on the filtration process only. Referring to the concept of "sewer mining" (Butler and Cormick, 1995), it is possible to imagine a process that *extracts* water from the sewage and returns the waste stream to the sewer, instead of locally treating it. Water could be extracted on demand, allowing economical savings and simplifying technical issues.

In the following, a selection of potential applications is proposed.

Direct reuse in agriculture : Irrigation is the most water-consuming activity and requires low water quality (Bixio and Wintgens, 2006; Salgot and Huertas, 2003; Lazarova and Bahri, 2005). The presence of nutrients and dissolved organic load is valuable to increase crops productivity and realize saving on fertilizers (Evenblij *et al.*, 2002). Accurate management of the agricultural practices can help to protect water bodies from nutrients run-off, and eventually from the high ammonium concentration. Figure 1.5 illustrates how this concept is applicable for both isolated housing and existing sewer networks.

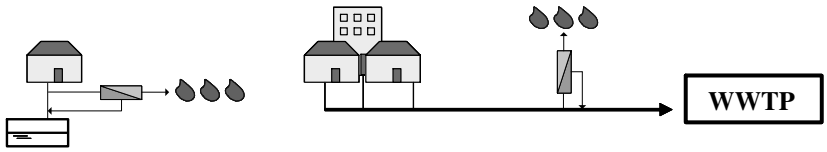

Figure 1.5: *Examples of direct UF for irrigation purposes for isolated housing and existing sewer systems*

Advanced pre-treatment: In tourist areas WWTPs often results in temporary overloading during peak season. Also, little area may be available for upgrading them. Direct UF can provide a small-footprint solution to significantly reduce both the organic load to the WWTP and the water flow, and it can be activated when necessary.

In details, in an integrated water management system direct UF can be used:

- as preliminary treatment in the WWTP, for advanced particle removal (in this case the sludge is extracted and the permeate with reduced organic content is further treated; Figure 1.6, right);

- to extract water everywhere along the sewer mains, for instance for irrigation purposes during the summer period (the water flow is reduced and the organic load left to the WWTP is easily settleable, see Figure 1.6, left).

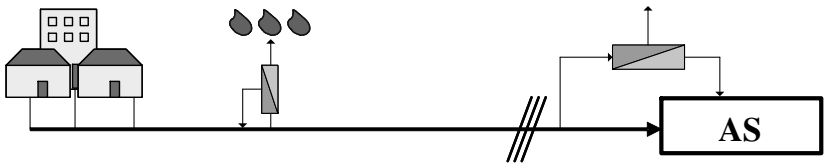

Figure 1.6: *Example applications of direct UF for overloaded WWTP*

Further membrane filtration: Direct UF permeate may represent a source for NF or RO, similarly to the practice in double membrane systems for water reclamation (see Paragraph 1.2). Direct UF would be the starting point for

the production of high purity water by means of physical chemical treatments, which could be interesting for industrial water reuse.

Since the dissolved organic content of the UF permeate is high, additional treatment steps could be necessary before further membrane filtration. Some hypothetical options are shown in Figure 1.7.

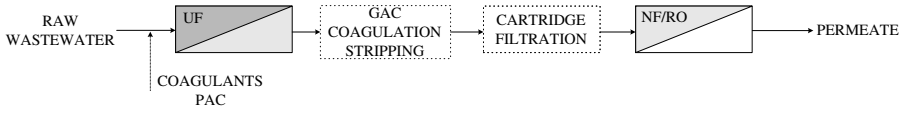

Figure 1.7: *Membrane-based complete wastewater treatment for water reclamation*

Developing this concept a little further, by including options for waste stream treatment and nutrient recovery, it is possible to conceive a new approach to wastewater treatment, fully built on membrane filtration. The separation characteristics of membranes are exploited to recover most of the valuable products contained in the sewage, which moves in the direction of the recent trend of sustainability of the water cycle. Figure 1.8 represents a flow diagram of this concept, as presented by Rulkens *et al.* (2005).

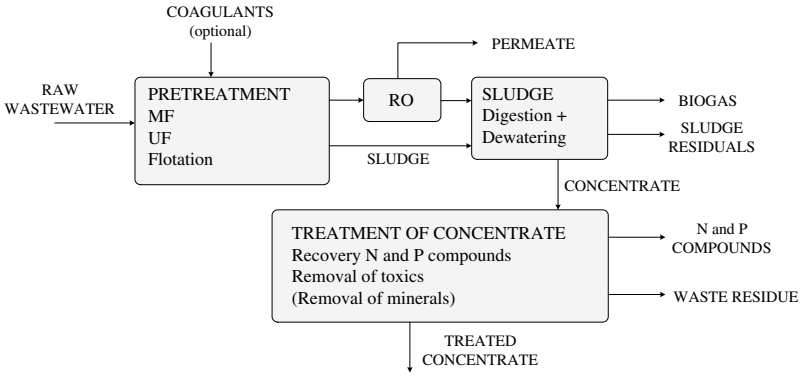

Figure 1.8: *Complete wastewater treatment based on membrane filtration (from Rulkens et al., 2005)*

1.4 Objectives and structure of the thesis

1.4.1 Background and objectives of the thesis

This thesis deals with the experimental activities conducted at the Delft University of Technology for the development of the novel process *Direct Ultrafiltration of Raw Sewage*.

Preliminary tests of crossflow direct ultrafiltration were conducted in 1999 by A. Nieuwenhuizen and H. Evenblij, in the frame of investigations about physical-chemical pre-treatments for advanced particle removal (Evenblij, 1999; van Nieuwenhuijzen, 2000a; van Nieuwenhuijzen, 2002). In the following, they also explored the potential for agricultural reuse (Evenblij, 2001) The promising results led to the research that is presented here.

The general objective of the work is to gain knowledge over the filtration characteristics of crossflow ultrafiltration of untreated sewage, in order to assess the feasibility of the process.

The principal means of investigation are filtration experiments, supported by chemical-physical analyses of the treated water and mathematical modelling. At first, raw sewage is tested at various operating conditions aiming at identifying the optimal ones. Afterward, it is investigated if performances can be improved by simple pre-treatments (sedimentation and coagulation), that could be added without altering the potential of the concept.

1.4.2 Structure of the thesis

The thesis is composed of 10 Chapters; their content is briefly presented in the following.

Chapter 1 is the Introduction that you are reading.

Chapter 2 introduces the general concepts that underlay this research. This includes notions of particles stability in wastewater, fundamentals of membrane filtration and an insight on the fouling process. The information is supported by literature references.

Chapter 3 presents a literature review specifically about ultrafiltration of

(partially) untreated wastewater.

Chapter 4 moves into the specific of this research, by describing the material and methods used during the experimental activities.

Chapter 5, 7 and 8 presents the results of the experiments with raw sewage (Chapter 5) and partially refined sewage (Chapter 7 and 8). The interpretation of results is supported by the interpolation of filtration data with the *blocking laws*, introduced in Chapter 6.

Chapter 9 includes a calculation exercise, based on the findings of the previous chapters. An hypothetical design is compared with existing membrane technologies in order to estimate the cost of water production with direct ultrafiltration.

Finally, Chapter 10 draws the conclusions of this work and traces directions for further research.

Chapter 2

Fundamentals

The basics to understand low-pressure membrane filtration and membrane fouling are introduced. The overview starts describing the characteristics of particles in wastewater and continues explaining how coagulant addition can modify these characteristics. The design and the operational aspects of membrane systems relevant to this dissertation are reported briefly. Finally, membrane fouling is discussed in detail.

2.1 Particles in municipal wastewater

Municipal wastewater is a complex mixture of "particles" in water. The "particles" originates from the source water, the human discharges (domestic or industrial) and the "aquatic life" growing in the wastewater itself (e.g., bacteria).

A typical classification includes inorganic matter (clay, oxides, silica, etc.), organic matter (especially macromolecules such as humic substances, proteins and polysaccharides) and living and dead micro-organisms.

Excluding large objects and rough materials such as hair and debris, the size of "particles" in wastewater varies from a few nanometer (macromolecules) to a few millimeters (sand grains). Whilst large particles behaviour depends mainly on the usual macro-physic forces (e.g. gravity, shear, etc.), smaller particles are subject to a wide range of electrostatic interactions. In particular, the class of colloids is very reactive with respect to aggregation and repulsion phenomena,

which has relevant consequences during membrane filtration.

The issues of particle size and stability are considered in the following.

2.1.1 Suspended solids, colloids, dissolved substances

Water is an excellent solvent for many substances; consequently, these substances can be found in wastewater in a *dissolved* form. Relatively insoluble substances are found in *particulate* form, which includes *suspended solids* and *colloids*.

With respect to particle size, the three mentioned classes of particles can be ordered as follows: suspended solids > colloids > dissolved substances. However, there is not such a thing as a sharp boundary in size that separates them. The shapes of particles is of the utmost variety, which makes it difficult to define an exact particle "size". Additionally, in wastewater treatment there is very little standardization about the classes of particle size.

Suspended Solids In wastewater practice the determination of total suspended solids (TSS) is done by filtration over a porous media. The material of the filter as well as the nominal pore size varies with the different protocols: the pore size ranges from little above 1 μm to a few μm (Metcalf & Eddy, 2003; Standard Methods, 1998; NEN).

Dissolved Solids Total dissolved solids (TDS) are usually measured by evaporation after filtration. The most applied definition, included also in the well known IAWQ activated sludge model, refers to the remaining fraction after filtration over a 0.45 μm membrane. Standard Methods (1998) includes in the "dissolved" class much larger particles, i.e. the dry solids in the filtrate through a medium with nominal pore size of 2 μm. On the opposite, some researches suggest that a upper threshold of 0.1 μm would be more adequate to identify dissolved material (Gregory, 2006; STOWA 1999, 2000).

Colloids The class of colloids is placed between Suspended and Dissolved Solids. Metcalf & Eddy (2003) indicate the colloidal range between 0.01 and 1 μm, whereas Levine *et al.* (1991) and Gregory (2006) refer to particles with at least one dimension in the range 0.001–1 μm. Van Nieuwenhuijzen (2002)

distinguishes between supracolloids (1.2–5 μm), colloids (0.45–1.2 μm) and semi-dissolved (0.1–0.45 μm).

Figure 2.1 compares the size of typical particles in water. It is clear that according to the various definitions, monocell organisms as bacteria can be classified in turn as suspended solids or colloids, or that single particles of clay and viruses can be classified either as colloidal or dissolved.

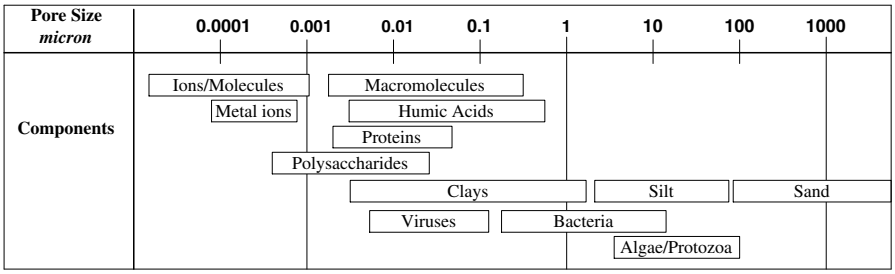

Figure 2.1: *Size of typical particles in water (after Gregory, 2006; Te Poele, 2005; Laabs 2004; Metcalf & Eddy, 2003; van Nieuwenhuijzen, 2002)*

There is of course not sharp change in properties with the particle size; however, it is important to note that for particles with "characteristics" size below 1 μm *diffusion* becomes important and *surface interactions* turn more relevant than "volume" forces such as gravity, fluid drag and hydrodynamics in general (Gregory, 2006; Ripperger, 2002). This is a typical feature of colloids and therefore, in the following, colloids refer to the general acception of submicron particles.

Concerning the inferior size limit of the colloidal class, it is probably correct to extend it to the size of the aggregates of macromolecules, proteins and polysaccharides, which exhibit typical colloidal properties (Jaruttushirak *et al.*, 2002; Lee *et al.* 2004, 2006).

2.1.2 Stability of colloids in wastewater

Particles in stable colloidal suspensions like wastewater are generally negatively charged (Knoppert and van der Heide, 1990). The cause is a surface negative

charge mainly originated by (Gregory, 2006; Bratby, 2006):

- induced reactions at the surface (e.g. dissolution of ions for crystalline solids, surface ionization of carboxyl and amine groups);

- isomorphous substitution (e.g. substitution of cations in the grid of clay materials);

- adsorbtion of ions or polymers (e.g. for hydrophobic/hydrophilic interactions).

In the following, some relevant aspects of colloidal stability are explained in detail.

Stability of hydrophilic and hydrophobic colloids

Hydrophilic colloids are water-soluble macromolecules such as humic acids, proteins, polysaccharides, etc... (Gregory, 2006). The hydrophilic character originates from the presence of amino (-NH_2), hydroxyl (-OH) and carboxyl groups (COOH). These functional groups tend to establish hydrogen bonds with the surrounding water molecules, creating a "layer" of surrounding *bound water* (see Figure 2.2, left). The achieved configuration is stable in a thermodynamic sense, and hydrophilic colloids will remain in solution indefinitively if a change in temperature, pH or salt concentration does not occur.

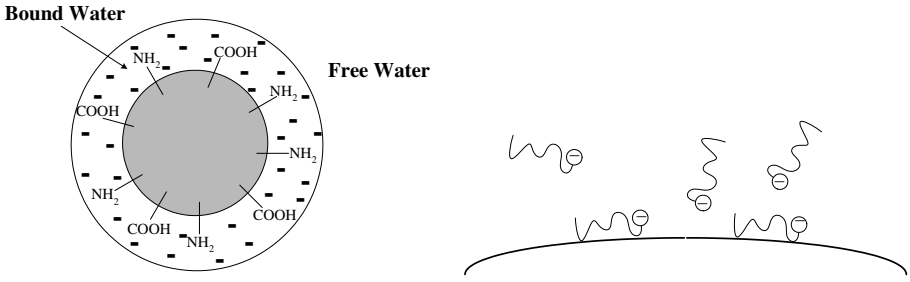

Figure 2.2: *Bound water surroundings hydrophylic colloids (left, after Henze, 1992) and adsorption of surfactants on hydrophobic colloids surface (right, after Gregory, 2006)*

Hydrophobic colloids are substances insoluble in water, but dispersed as very small particles. They do not present polar or ionic groups, nor hydrogen-bonding sites. Typical examples are inorganic materials such as clay and oxides (Gregory, 2006). Differently from hydrophylic colloids, they are thermodinamically instable, which means that they would reach a more stable energy state by aggregating to each other. However, this does not happen because of kinetic reasons, and because dissolved organic substances often adsorb on the surface of hydrophobic colloids, providing a surface charge. A typical example is the adsorption of anionic surfactants, where the hydrophobic tails provide adhesion with the colloidal surface and the hydrophilic head can be ionized (see Figure 2.2, right).

Electrical double layer, diffuse layer and zeta potential

Independently of the origin of the surface charge, a charged surface immersed in a solution of ions affects the ions distribution. Typically, ions of the opposite charge (*counter-ions*) will be attracted in order to maintain electrical neutrality, forming the so-called *electrical double layer*. Figure 2.3 represents the case of a flat infinite surface (left, Stern-Gouy-Chapman model) and a spherical particle (right).

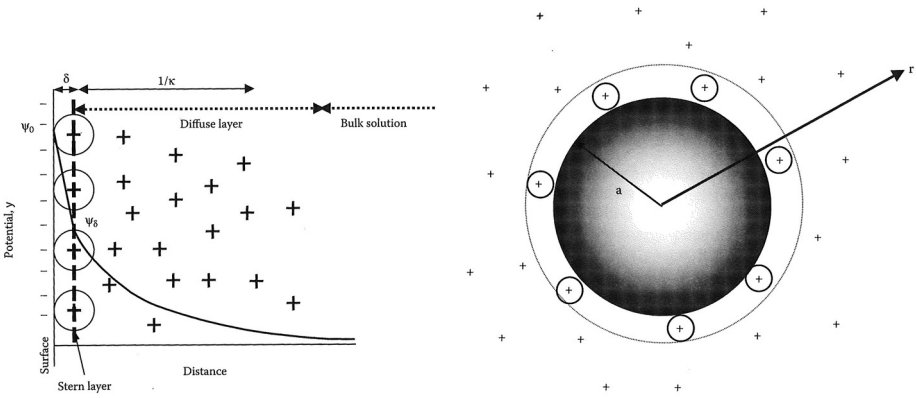

Figure 2.3: *Electrical double layer for a flat infinite surface (left) and for a spherical particle (right); from Gregory (2006)*

It can be noted (Figure 2.3, left) that the non-negligible size of the counter ions allows for a finite minimum distance from the charged surface, which is known as the *Stern layer*. The Stern layer contains only a certain fraction of the total counterions charge, whereas the rest is distributed in the *diffuse layer*.

Another fundamental concept is that there exists a plane of shear which separates the fixed and the mobile charge. The exact position of such plane cannot be determined with accuracy, however, for practical purposes it can be assumed in the proximity of the Stern plane.

The electric potential at the plane of shear is known as *zeta potential* ξ. The zeta potential has great influence on the electrical interactions of charged particles and its value can be measured rather easily by electrophoretic mobility.

DLVO theory

A quantitative discussion of the stability of colloids is possible based on the *DLVO theory* (Deragyn - Landau - Verwey - Overbeek). This theory considers only Van der Waals and electrical double-layer interactions, nevertheless it is sufficient to the purpose of understanding colloidal behaviour.

The *DLVO* theory shows that van der Waals attractive forces predominate at small distances, whereas double layer repulsion at intermediate distances. The system can be described by a potential energy diagram as the one presented in figure 2.4.

The most relevant finding is that there exist two minimums of potential energy separated by a energy barrier. Because this barrier is much higher than the thermal energy of the particles, it will be hardly surmounted by the approaching particles, which will not come into contact. Therefore, the suspension results colloidally stable.

The destabilization of the colloidal suspension can be achieved by reducing the zeta potential, thus reducing the thickness of the diffuse layer, hence decreasing the energy barrier. Simple modifications of the chemistry of the solution are sufficient to this purpose, such as the increase of ionic strength (i.e. increasing salt concentration), pH modifications, or the dosing of specific counterions to be adsorbed at the particle surface. This is usually the aim of coagulant addition.

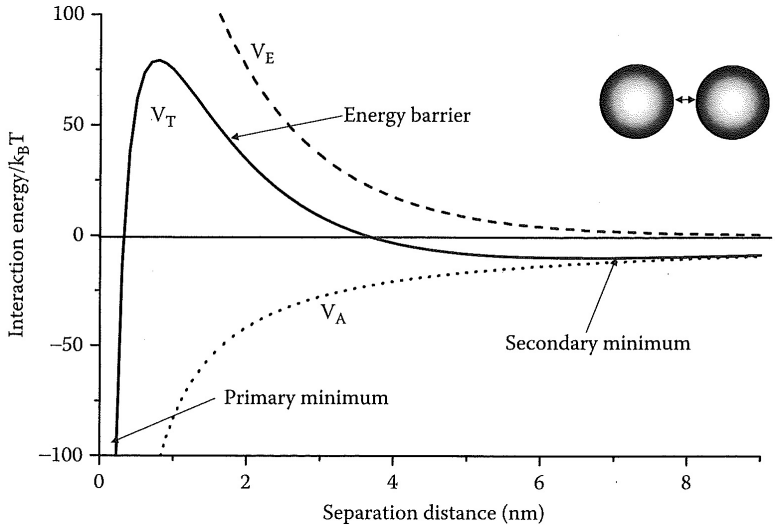

Figure 2.4: *DLVO potential energy diagram (from Gregory, 2006)*

Non-DLVO interactions

Other interactions exist that are not included in the DLVO theory, such as hydration effects, hydrophobic attraction, steric repulsion and polymer bridging. Some of these will be introduced and described in the following. For details and further reading see Gregory (2006), Bratby (2006), and for extension to the DLVO theory van Oss (1993) and Brant and Chirdless (2002).

2.1.3 Organic matter

As previously mentioned, a certain fraction of particles in wastewater is composed by organic matter. Organic matter includes colloidal particles and is a primary issue with respect to membrane filtration.

Organic matter originates from all the sources that compose the wastewater: the original drinking water, the human activities (metabolism, cooking, use of synthetic compounds, etc.), the surface run-off and the bacterial activity during wastewater transport. A vast number of organics is relevant to wastewater treatment, which are often grouped in a few large categories: Natural

Organic Matter (NOM), Effluent Organic Matter (EfOM), soluble microbial products (SMP) and extracellular polymeric substances (EPS). In the following, this nomenclature is explained and the principal chemical components are named.

NOM is a collective name for the organic substances occurring in natural waters, mostly originating from biodegradation of plants and animal remains. Therefore, NOM is a typical issue during the membrane filtration of surface water for drinking water production.

According to Hong and Elimelech (1997) and Gregory (2006), a major fraction of dissolved organic matter in the aquatic environment is contributed by humic substances, i.e. macromolecules of low to moderate weight, negatively charged at the pH range of natural water. During the characterization of organic matter in surface water from different rivers, Lee *et al.* (2004) identified humic substances but also organic acids, proteins and polysaccharides, most likely of bacterial and algal origin.

SMP and EPS concerns the presence of bacteria in natural waters and wastewaters.

SMP are defined as *cellular components that are released during cell lysis, diffuse through the cell membranes, are lost during synthesis or can be excreted* (Laspidou and Rittmann, 2002). They can essentially be produced for substrate metabolism or from cell decay.

EPS are biological polymers produced by bacteria and located outside or at the cell surface. Among other functions, they are fundamental for the bacterial adhesion to surfaces and for the aggregation in flocs and biofilms (Laspidou and Rittmann, 2002; Fleming and Wingender, 2001a,b).

Because of the analytical methods for their determination, SMP and EPS cannot be distinguished in engineering practice (Te Poele, 2006). Furthermore in recent times a unified theory for SMP and EPS has been proposed (Laspidou and Rittmann, 2002). In both cases the main components are proteins and polysaccharides, and to a minor extent, nucleic acids and lipids (Fleming and Wingender, 2001a).

The term EfOM is the correspondent to NOM for biologically treated wastewater, and is commonly used during secondary and tertiary filtration of effluent. EfOM includes refractory NOM conveyed from the drinking water source, synthetic organic compounds (SOC), disinfection by-products (DBP) and SMP originating from the biological treatment (Shon *et al.*, 2005). An extensive char-

acterization of EfOM of secondary effluent was conducted by Jarusutthirak *et al.* (2002), after isolation of various fractions. Using advanced isolation techniques, the presence of proteins, polysaccharides, humic and fulvic acids was ascertained. In particular, polysaccharides and proteins were found abundant in the colloidal fraction.

All the "classes"of organic components indicated above are suspected to contribute to decrease membrane performances, i.e. to cause *fouling*, by accumulating on the membrane surface or into the pores.

Fouling from humic substances is reported by Lahoussine-Turcaud *et al.* (1990), Yuan *et al.* (2002), Hong and Elimelech (1997), Thorsen T. (1999). Concernign NOM in general, Lee *et al.* (2004, 2006) found that the residuals left on the membrane after filtration of surface water were mostly proteins and polysaccharides both in macromolecular or colloidal form.

SMP and EPS are expected to attach to the membranes and to consolidate deposits of material on the membrane surface. Influence on fouling has been reported both for SMP (Laabs *et al.* (2003) and EPS by (Nagaoka, 1996; Kim *et al.*, 2005) although a clear relationship is not fully acknowledged yet (Rosenberg *et al.*, 2005; Evenblij, 2006; Te Poele, 2006).

Fouling from EfOM is an obvious consequence of fouling by NOM, EPS and SMP, since they are actually the same components. Example studies can be Te Poele (2005), Laabs *et al.* (2003), De Carolis, (2001). The findings by Jarusutthirak *et al.* (2002) confirms that EfOM contributes to fouling both as single macromolecules and as colloidal aggregates.

2.2 Coagulation-Flocculation

2.2.1 Introduction

Coagulation and flocculation concern the destabilization of particles in suspension and the successive formation of larger aggregates. In wastewater treatment, this practice is commonly applied in order to favour the removal of colloids in processes such as sedimentation, flotation and filtration (including membrane filtration).

The process is two-steps:

- colloids are de-stabilized, which can be theoretically done by increasing ionic strength or neutralizing the particle charge;

- the collision of destabilized colloids leads to the formation of larger particles. The rate of successful aggregations is influenced by the number of collisions and by the collision efficiency, which depends on a proper destabilization.

2.2.2 Definitions

Conventionally in water and wastewater treatment the word *coagulation* refers to the destabilization process, and the word *flocculation* to the formation of aggregates.

However, in colloidal science, *coagulation* is the process of destabilizing colloids by charge neutralization, which leads to the formation of small and dense aggregates (*coagula*), whereas *flocculation* is the process of aggregating colloids by polymer bridging, which produces larger and more open aggregates: *flocs* (Gregor, 2006).

Although during this dissertation the first definition will be normally applied, traces of the second are found in the commercial distinction of destabilizing agents: hydrolyzing metals are usually referred to as coagulants and polymers as flocculants.

2.2.3 The coagulation-flocculation process

In practice, the coagulation-flocculation process consists of two successive phases: rapid mixing and slow stirring.

Corresponding to the definitions of the previous paragraph, from an operational point of view *coagulation* is the process of dosing an additive to the wastewater and promoting the interaction between the colloidal particles and the additive, whereas *flocculation* is the promotion of the formation of aggregates by some form of fluid motion.

Coagulation is therefore obtained by a short, intensive mixing, whereas flocculation by a longer and less intensive slow-stirring (orthokinetic flocculation).

2.2.4 Metallic hydrolyzing coagulants

Metallic coagulants such as aluminium and ferric salts are the most widely used destabilizing agents.

In water, these salts dissociate and the trivalent metal ions Fe^{3+} and Al^{3+} are hydrated, i.e. surrounded by water molecules oriented with the (negatively charged) oxygen "end" towards the cations. Given the high charge of the cations, hydration may lead to water lysis, i.e. *hydrolysis*: a hydrogen ion is released into the solution and a reduced positive charge is left to the metal group (see Figure 2.5).

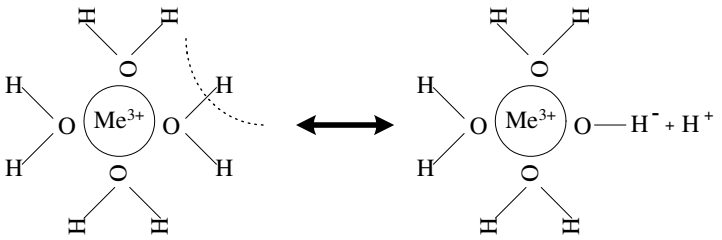

Figure 2.5: *Schematic of hydrolysis with metal salts (4 water molecules shown, 2 omitted)*

Two remarks are particularly relevant:

- given the release of H^+, hydrolysis is dependent on the value of pH (high pH promotes dissociation);

- there exists a sequence of hydrolysis equilibria, depending on the pH, that generates several hydrolysis products (*Me* represents the metal cation and the hydrating water molecules are omitted):

  $Me^{3+} \rightarrow Me(OH)^{2+} \rightarrow Me(OH)_2^+ \rightarrow Me(OH)_3 \rightarrow Me(OH)_4^-$

The action of metal hydrolyzing coagulants can develop in two different ways:

- hydrolysis product can adsorb and neutralize (negative) particle charge, leading to colloid destabilization and coagulation;

- the metal hydroxides $Me(OH)_n$ have limited solubility in water and tend to precipitate, giving the so-called *sweep coagulation*. The solubility diagrams for Fe(III) and Al(III) are shown in Figure 2.6.

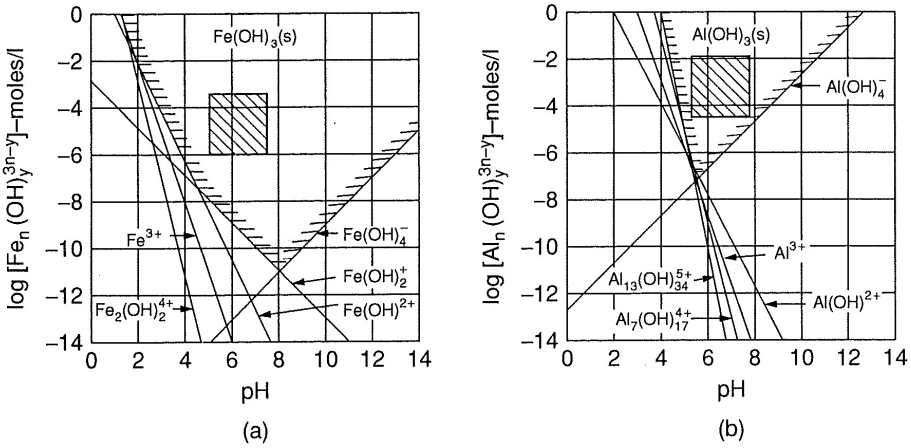

Figure 2.6: *Solubility diagrams for Fe(III) (left), and Al(III) (right); from Bratby (2006)*

Sweep coagulation occurs at higher coagulant dosage than charge neutralization. Nevertheless, it is more commonly applied. The reason is that sweep coagulation leads to faster aggregation and give stronger and larger flocs. Additionally, it does not strictly depend on the nature of the particles to be removed (clays, bacteria, organics, oxides, etc.).

This can be partially explained with the higher number of collisions during sweep coagulation, and because of the less narrow optimal dosage range. Charge neutralization may indeed rapidly turn into charge reversal and re-stabilization when coagulant dosages are excessive.

The major limitation to the application of large coagulant dosages with sweep coagulation is instead the formation of large quantities of chemical sludge (precipitates).

Some common ions, such as sulfates, may improve the floc formation, whereas low temperatures decrease the coagulation performances (less for prehydroliyzed coagulants such as $PACl$)(Gregory, 2006). Hydroxide flocs produced by sweep

coagulation are weaker than the flocs produced by polymeric flocculants. Since breakage can be irreversible, at high shear conditions the latest are preferred.

2.2.5 Organic polymers

A polymer is a long-chain molecule consisting of one or more repetitive unit (*monomer*). The overall structure can be linear or branched, although linear polymers are the most applied. Other characteristics features are the charge (anionic, cationic and nonionic = uncharged), the molecular weight and the charge density. Charged polymers are also called *polyelectrolites*.

A polymer in solution presents a typical *random coil* configuration. However, if ionizable groups are present, they can become charged and eventually repel each other and originate a more open structure. In this case also the ionic strength of the solution contributes to determine the exact final configuration of the molecule.

Polymers adsorb on particle surface through the usual interactions: electrostatic interaction, hydrophobic interaction, hydrogen bonding, ion binding (i.e. like-charge groups are kept together by the mediation of some ion of opposed charge). The adsorption is never complete, in the sense that whereas some segments of the polymer chain are adsorbed (*trains*), others project into the solution as loops (*intermediate*) or *tails* (see Figure 2.7).

It is exactly this feature that enables *polymer bridging*.

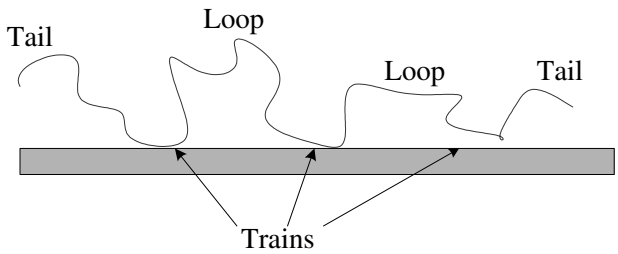

Figure 2.7: *Adsorption of polymers (from Gregory, 2006)*

When two particles collide and at least one of them has an adsorbed poly-

mer, the extending segments may attach to the other surface thus realizing aggregation by "bridging" (see Figure 2.8).

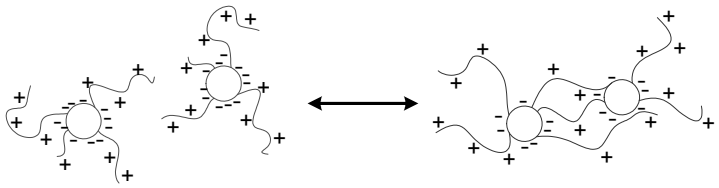

Figure 2.8: *Schematic of polymer bridging*

In order to realize a successful aggregation it is essential that sufficient particle surface is left free, so that during a collision the segments of polymer extending over the surface may attach (Bratby, 2006). Furthermore, the polymer should not cover the entire particle surface, otherwise it could provoke re-stabilization by charge reversal. Consequently, on one side there exists an optimal dosage for the most effective coagulation, and on the other side overdosing may occur (Kim *et al.*, 2001a).

Polymers may induce particle destabilization also by charge neutralization. In this case, at the light of the previous definitions, they might be referred to as *coagulant* rather than *flocculant*.

Charge neutralization is more likely to occur with low-molecular weight polyelectrolite, such as polyDADMAC. The application range is very narrow, because re-stabilization by change reversal easily occurs, and this may reflect onto operational difficulties especially when the feed water quality is not constant (Gregory, 2006).

High molecular weight polyelectolytes produce a high number of bridging bonds, sometimes inducing also a local heterogeneity of charge (*electrostatic patch arrangement*, Bratby 2006). This leads to the formation of definitively stronger flocs, which, combined to the wider effective dosage range, makes bridging the preferred coagulation-flocculation mechanisms in practice.

It must be noted that although bridging flocculation gives stronger and larger flocs than those formed by metal salts, their rupture can be equally irreversible, i.e. when flocs break they do not readily reform (Gregory, 2006; Kim *et al.*, 2001a).

Polymers are often used as *coagulant aids*, i.e. in combination with hydrolyzing metal coagulants to strengthen the flocs (Bratby, 2004; Gregory, 2006; van Nieuwenhuijzen 2002).

2.3 Membrane filtration

2.3.1 Pressure driven membrane processes

There exists several definitions of the word *membrane*, also because there is large variety of membrane types and applications. From a very general point of view a membrane is an interphase that separates two phases and is responsible for the transport of components from one to the other. In water and wastewater treatment, a membrane can be more simply defined as a perm-selective barrier that realizes the separation of components of a given solution.

In many cases the separation is achieved by complete rejection (impermeability), but in some others it results from the different velocities with which different substance can pass through the membrane.

The transport through the membrane is originated by a *driving force*. There exists a number of driving forces, for instance electrical potential, concentration gradient and pressure. Almost always in wastewater treatment pressure is the input provided to achieve the separation. The pressure across the two sides of the membrane is referred to as Trans-Membrane Pressure (TMP, see Figure 2.9).

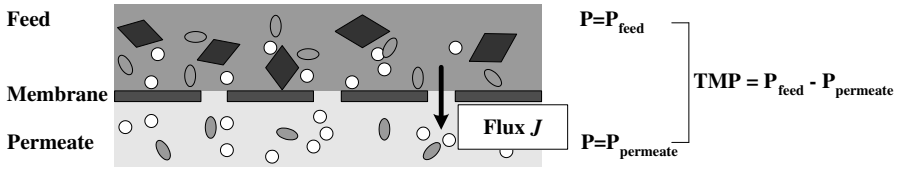

Figure 2.9: *Schematic representation of membrane separation*

Pressure driven membrane processes are classified according to the membrane pore size, which is the primary parameter to determine the ability of the membrane to retain a certain substance: constituents bigger than the pore size cannot pass. From larger to smaller pore size, four membrane processes are distinguished: microfiltration (MF), ultrafiltration (UF), nanofiltration (NF) and

reverse osmosis (RO).

MF and UF membranes are made of finely porous media, whereas RO membranes are known as "dense" and do not present a real porous structure.

When the pore size decreases, increasing pressure is required to operate the membrane process. Therefore, MF and UF are low-pressure processes whereas NF and RO are high-pressure. Table 2.1 summarizes these concepts.

Table 2.1: *Classification of membrane processes with pore size (adapted from Mulder, 1996 and Koros et al., 1996)*

Process	Pore Size (nm)	TMP (*bar*)
Microfiltration	100–1000	0.1–2
Ultrafiltration	10–100	0.1–2
Nanofiltration	1–10	4–20
Reverse Osmosis	0.1-1	10–30

2.3.2 Process parameters

Permeate flux and resistance

The application of the transmembrane pressure produces the *permeate* flow through the membrane. The flow through a unit area per unit time is called *flux*, expressed in $m^3/(m^2 \cdot s)$, m/s or more commonly $L/(m^2 \cdot h)$. For convenience, in this dissertation the flux unit $L/(m^2 \cdot h)$ is written as LMH.

Assuming that the permeate flow through the tortuous membrane pores is laminar, the filtration of pure solvent is described by an adaptation of the Darcy's Law (Lojikine *et al.*, 1992) :

$$J = \frac{TMP}{\eta_p \cdot R} \tag{2.1}$$

where:

J = permeation flux (LMH)
η_p = dynamic viscosity of the permeate ($Pa \cdot s$)

R = resistance to filtration (m^{-1})

The permeate flux is therefore inversely proportional to the dynamic viscosity and the resistance.

The viscosity is a function of temperature. In water and wastewater treatment it is usual to assume permeate viscosity equal to that of pure water, which can be calculated according to Huisman (1996):

$$\eta_p = \frac{479 \cdot 10^{-3}}{(T + 42.5)^{1.5}} \tag{2.2}$$

where:

η_p = dynamic viscosity of the permeate ($Pa \cdot s$)
T = temperature (°C)

When the object of filtration is not pure water, a contribution to the resistance to filtration may arise from the solutes and other transported substances, which cause *fouling* (described in detail in the following Paragraph 2.4). Therefore, during membrane filtration, the total resistance is often expressed as the sum of the membrane resistance R_{mem} and the additional resistance from fouling R_f :

$$R = R_{mem} + R_f \tag{2.3}$$

Permeability

The proportionality between flux and the applied pressure is known as *permeability* K ($L \cdot m^{-2} h^{-1} bar^{-1}$):

$$K = \frac{J}{TMP} \tag{2.4}$$

Permeability accounts for viscosity and resistance, therefore its value is not constant and in particular it decreases during filtration, because of the occurrence of fouling. Nevertheless, the permeability with respect to pure water at a reference temperature is often used as a characterizing property of a membrane.

Rejection and selectivity

As mentioned previously, the reason for membrane filtration is the separation of components. With low-pressure membranes the separation process is dominated to a large extent by particle size and pore size issues. For more dense membranes, other factors prevail, first of all diffusion phenomena.

When size is no longer the determining factor, the molecular weight cut off (MWCO) is used to characterize the membrane. The MWCO is the molecular weight of a solute giving 90% rejection factor with a given membrane.

The rejection factor R is defined as follows (Koros *et al.*, 1996):

$$R = 1 - \frac{c_{i,p}}{c_{i,feed}} \tag{2.5}$$

where:

$c_{i,p}$ = concentration of component i in the permeate (mg/L)
$c_{i,feed}$ = concentration of component i in the feed (mg/L)

Although there is not a straightforward relation between pore size and molecular weight cut off, Figure 2.10 provides an overview of the removal capabilities of the various membrane processes with respect to a number of components, based on particle size and with reference to the MWCO.

2.3.3 Materials and configurations

Membrane materials

The membranes applied in water and wastewater treatment are manufactured from different materials, such as organics, ceramic and metals. The most commonly applied are polymeric materials produced by inversion phase, although ceramic membranes are decreasing in cost and becoming more attractive (Mulder, 1996; Baker, 2004). Table 2.2 reports some of the materials in use.

As a general rule, ceramic membranes have superior mechanical strength and resistance to chemical cleaning, oxidising agents and high temperatures. Polymeric materials have a moderate resistance to pH variations, with the exception of cellulose acetate. Only PTFE and PVDF are highly stable with respect to organic solvents.

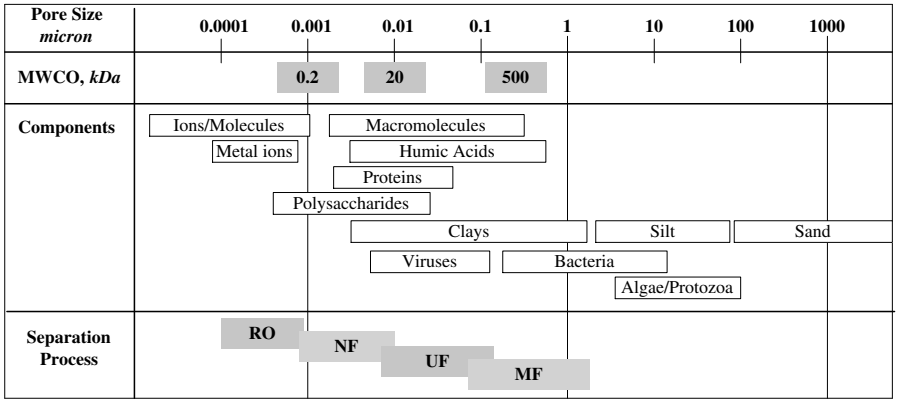

Figure 2.10: *Classification of membrane processes according to pore size, MWCO and particle size (sources: Laabs, 2004; Stephenson et al., 2000; Metcalf & Eddy, 2003; van Nieuwenhuijzen, 2002)*

Table 2.2: *Commonly applied membrane materials (adapted from Judd and Jefferson, 2000; Mulder, 1996)*

Material		Type	applications
Cellulose Acetate	CA	organic	UF, NF, RO
Polyamide	PA	organic	NF, RO
Polyacriylonitrile	PAN	organic	UF, RO
Polysulphone	PSU	organic	UF, RO
Poly(ethersulphone)	PESU	organic	UF, RO
Poly(vinylidene fluoride)	PVDF	organic	MF,UF
Polyethilene	PE	organic	MF,UF
Polytertafluoroethane	PTFE	organic	
Titanium Oxide	TiO_2	ceramic	UF, NF
Zircon Oxide	ZrO_2	ceramic	UF, NF
Aluminimoxide	y-Al_2O_3	metallic	

Since most of the contaminants in water and wastewater have hydrophobic character and would adsorb on hydrophobic surfaces, hydrophilic materials are preferred. When necessary, the hydrophilic character is obtained by surface modification, via chemical oxidation, chemical reactions, plasma treatment or grafting (Judd and Jefferson, 2000; Kilduff *et al.*, 2002).

The membrane structure can be isotropic or anisotropic. Whereas isotropic membranes have a uniform composition and structure, anisotropic membranes (also called asymmetric), consist of different layers. Usually, a thin selective top layer is casted over a more porous layer that provides mechanical strength (Baker, 2004).

Membrane configuration

Membrane *configuration* refers to the membrane geometry and the way it is mounted and oriented with respect to the feed water flow. The configuration is fundamental to determine the process performance and the applicability to a water with certain characteristics.

An ideal configuration would provide: high membrane areas per volume ratio, high turbulence, low energy expenditure, easy cleaning and maintenance. However, some of these features are conflicting. Consequently there exists a number of configurations, in terms of membranes and membrane modules, tailored on the various applications.

All the membranes are manufactured in two geometry, as flat sheet or cylinder. These two geometries are the basis for five principal configurations:

- pleated filter cartridge
- plate-and-frame
- spiral wound
- tubular
- hollow fibre/ capillary

Table 2.3 reports the field of application of the various configurations to the different membrane processes, together with the area/volume ratio and the achievable degree of turbulence.

Table 2.3: *Application of the various membrane configurations to membrane processes (adapted from Baker, 2004 and Judd and Jefferson, 2000)*

Configuration	Area/Vol (m^2/m^3)	Turbulence promotion	Applications
Pleated cartridge	500–1,500	very poor	MF
Plate-and-frame	100–300	fair	MF, UF, RO
Spiral wound	800–1,200	poor	UF, NF, RO
Tubular	150–300	very good	MF, UF, NF
Capillary (inside-out)	1,500–5,000	good	MF,UF
Hollow fibres (outide-in)	10,000–20,000	very poor	MF,UF,RO

2.3.4 Process fundamentals

Crossflow and dead-end filtration

Using membranes, there exist two basics modes of operation: dead-end and crossflow, illustrated in Figure 2.11.

During dead-end operations the flow is perpendicular to the membrane and the entire filtration volume is passed through the membrane. In contrast, during crossflow filtration the feed flow is tangential to the membrane surface and is split into two streams: the permeate and the *retentate* (or *concentrate*).

During dead-end operations all the transported materials accumulate on the membrane surface, whereas during crossflow filtration most of them are carried away in the retentate. Crossflow configuration is more suitable for treating water with high solids content and higher permeation fluxes can be achieved.

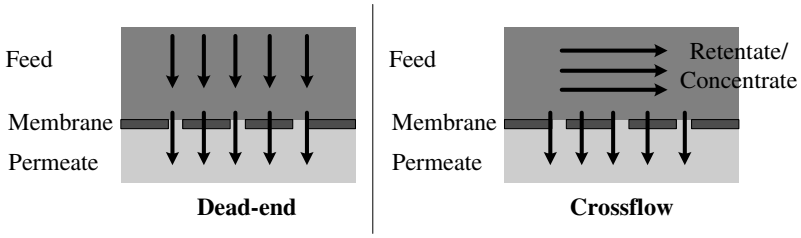

Figure 2.11: *Schematic drawing of dead-end and crossflow operation*

However, these advantages are counterbalanced by a larger energy expenditure for the recirculation of the retentate flow.

Recently, an intermediate mode of operation has been introduced: semi dead-end. In this case the membrane is mostly used in dead-end mode but sometimes the filtration is interrupted and the accumulated solids are flushed away.

Backflush and forward flush

During filtration the permeate flows across the membrane in a certain direction. For cleaning purposes, the direction of the flow can be inverted, which produces the removal of (a fraction of) the accumulated solids. This operation, represented in Figure 2.12, is called *backflush* (or *backwash*). Usually the backflush is performed using permeate; the resulting mixture of permeate and solids is discharged as retentate.

Another common hydraulic cleaning method is the *forward flush*, i.e. a cross-flow at high flow rates (see Figure 2.12). The addition of air can improve the efficiency of the forward flush, because of the scouring effects of air bubbles.

Conversion

The ratio of the produced permeate volume and the total feed volume is called the *conversion* (or *recovery*). In a continuous system the conversion Θ, usually expressed as percentage, can also be expressed in terms of flow (Judd and Jefferson, 2000):

$$\Theta = \frac{Q_p}{Q_{feed}} \tag{2.6}$$

where:

Q_p = permeate flow $(m^3 \cdot s^{-1})$
Q_{feed} = feed flow $(m^3 \cdot s^{-1})$

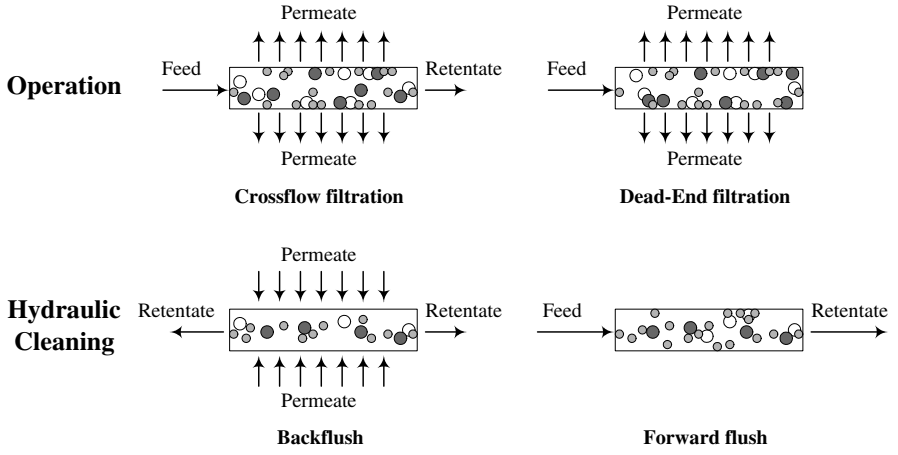

Figure 2.12: *Schematic drawing of backflush and forward flush for tubular inside-out membranes*

A dead-end system can formally achieve 100% conversion, although this is never the case. In practice, a fraction of the produced permeate is always used for cleaning purposes.

Waters with remarkable solids content are usually treated in crossflow systems with low recovery per passage. During nanofiltration and reverse osmosis, conversion is typically below 20% (Judd and Jefferson, 2000). To deal with this fact membrane systems are operated in a number of ways.

Batch operations

Membrane systems are operated in batch or continuous mode. Batch system modes include simple batch and modified batch (topped-off batch and feed-and-bleed), which are semi-continuous modes of operation. Continuous systems can comprise a single membrane system or multiple staged elements.

For the purpose of this dissertation, the description of batch systems is sufficient.

The simple batch mode is typically used for small applications. The feed water circulates through the membrane modules and the concentrate flows back

into the feed tank. After several passages through the membrane, the feed is concentrated to the desired value and discharged, as all the retained solids accumulated in the tank (see Figure 2.13).

Batch mode requires the least membrane area and the largest process tank.

The topped-off batch mode has the variant that as permeate is removed, an equal volume of fresh feed is added to the process tank. Only when certain conditions are reached (e.g. a threshold solid concentration or resistance value), the system switches to batch mode, the feed water is concentrated to the final value and the system is eventually cleaned.

Modified batch can be the preferred mode of operation for industrial applications where maximum solid concentration is the objective .

In feed-and-bleed batch operation, after the passage through the membrane system, the process fluid is divided into two streams: one (small) that returns to the process tank, and the other that is recirculated through the membrane system (see Figure 2.13). The main advantages with respect to the topped-off mode is a lower energy cost, plus the turnover of the process tank that occurs at a much slower rate.

Figure 2.13: *Schematic diagrams of simple batch (left) and feed-and-bleed (right) operations*

It must be noted that also during batch operation the membrane system can be composed by a number of elements in series or in parallel. Often, element in series are placed to fully exploit the energy used for circulating the feed flow (Baker, 2004; Judd and Jefferson, 2000).

2.4 Membrane Fouling

2.4.1 Definitions

In membrane filtration *fouling* is a crucial concept. The Union of Pure and Applied Chemistry (UPAC) defines it as *the loss of performance of a membrane due to deposition of suspended or dissolved substances on its external surfaces, at its pore openings, or within its pores* (Koros *et al.*, 1996).

From this definition it emerges that fouling is a complex phenomenon that includes several mechanisms. The starting point is that it concerns the negative impact of the interactions between the feed water and the membrane on the filtration process. One first issue is whether these interactions take place in the proximity of the membrane surface (at the solute-membrane interface), or on the membrane surface, or inside its pores. A second issue is whether the effects are temporary or permanent, i.e. some cleaning procedure can remove (part of) the fouling.

In literature, two approaches can be found. Some authors (van der Berg and Smolders, 1990; Lojkine, 1992; Ahn *et al.*, 1998; Bacchin *et al.*, 2002) use the term fouling to indicate strictly the "tenacious" interactions that take place on the membrane and that would not be reversed by a release of the driving force. Other authors prefer to consider within "fouling" each mechanisms induced by the filtration process that leads to a decrease of performance. The major distinction becomes operational and is between *reversible* and *irreversible* fouling, where the reversible fouling can be removed by a modification of the operating conditions (interruption of filtration, forward flush, backflush) and the irreversible fouling requires a chemical cleaning.

2.4.2 Fouling mechanisms

In practice, for all membrane separation processes, it is possible to classify four principal fouling mechanisms, which are summarized in Figure 2.14:

- Concentration polarisation: the increased concentration of rejected solutes in the vicinity of the membrane surface favours a number of phenomena (raise of osmotic pressure, scaling, gel formation) that increase the required transmembrane pressure for operation;

- Pore blocking: particles enter the membrane pores and obstruct them, so that the number of pore channels available for permeation is reduced;

- Pore narrowing (or constriction): particles, colloids and molecules that enter the membrane pores depose/adsorb at the walls and reduce the cross section available for permeation:

- Gel (or cake) layer formation: particles and other materials that do not enter the membrane pores accumulate at the surface originating a more or less dense and more or less permeable layer. When the constituents of the gel layer interact with each other and with the membrane surface, this type of fouling can prove difficult to remove as well.

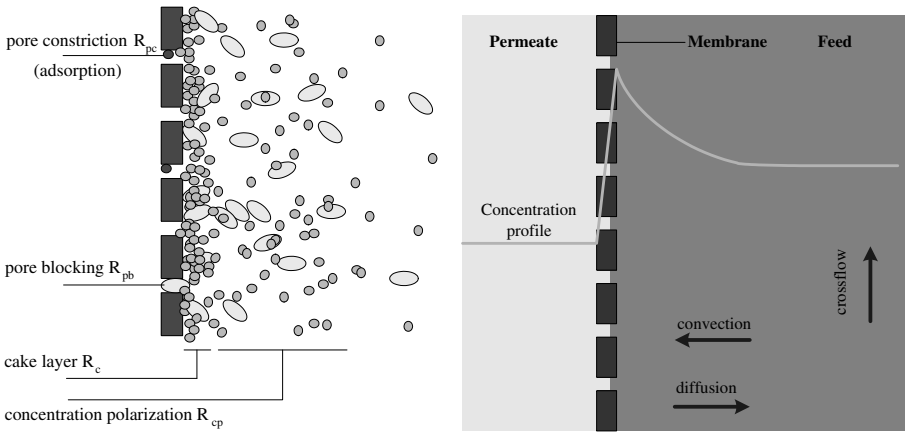

Figure 2.14: *Summary of fouling mechanisms (left) and detail of concentration polarisation (right)*

The only mechanism that does not take place on the membrane itself is concentration polarisation. In facts, some authors include concentration polarisation among the fouling mechanisms and other prefers to regard it as separate.

The concept of concentration polarisation is derived by the RO applications, where the increasing osmotic pressure of the solutes (mainly molecules and ions), can induce a backwards transport of solvent from the permeate side to the feed side of the membrane. This is not the case during MF and UF, because ions and macromolcules permeate the membrane and the accumulation of higher MWCO rather results in gel/cake layer formation. Consequently, the required increasing expenditure of pressure can be interpreted as to overcome the cake

layer resistance rather than to overcome concentration polarisation.

In literature, one common approach is to neglect the contribution of concentration polarisation for particulate crossflow micro- and ultrafiltration (Vyas *et al.*, 2001; Blatt *et al.*, 1970; Porter, 1972). On the contrary, other researches extend the notion of concentration polarisation to large particles (colloids), finally concluding the equivalence of the osmotic pressure model with the gel layer model (Chen *et al.*, 1997; Song and Elimelech, 1995).

In this dissertation the first notion is used and concentration polarisation is neglected. The main effect of the accumulation of colloids is cake formation. Therefore, the considered fouling mechanisms are pore blocking, pore narrowing and cake layer formation.

2.4.3 Factors affecting fouling

Fouling appears to result from the combination of three major variables:

- feed water characteristics: particle size distribution, chemical properties of the solutes and chemical properties of the solution (e.g. pH, ionic strength, etc...)
- membrane characteristics: pore size, roughness, porosity, structure and chemical properties
- operating conditions: permeation drag, pressure, hydrodynamics.

During ultrafiltration of wastewater particulate fouling involves suspended solids and colloids but also microorganisms and bacterial cells. Macromolecules may participate to fouling individually or aggregating in colloids. Single molecules and ions may not represent individually a problem but may be involved in cake formation and similar.

Particle size is crucial to determine particle transport and whether particles can penetrate the pores and permeate or foul the membrane internally.

Particle charge is fundamental to determine the interactions among particles and with the membrane, which affect the actual particle size at the boundary layer, the compactness and the adhesion forces in the filter cake, and the penetration and deposition into the membrane pores.

Particle compressibility may affect cake characteristics.

The role of the operating condition is less straightforward, although evident. In an extensive review of particulate fouling during crossflow microfiltration, Lojkine (1992) noted that observed flux can often be empirically related to the crossflow velocity, and that the particle size distribution in the filter cake is different from the particle size distribution of the feed water, which would be a consequence of the hydrodynamics. It is also common knowledge that increasing permeate flux and transmembrane pressure produces higher fouling (see for instance Hong and Elimelech, 1997; Choi *et al.* 2005 about flux, and Velasco *et al.*, 2003; Visvanathan and Ben Aim, 1989 about pressure).

Recently, Ripperger and Altmann (2002) showed (SEM) pictures of cake layers whose structure could be modified by varying the operating parameters. Vyas *et al.* (2001) suggested the possibility of desired size separation without changing the membrane pore size by modifying the operational parameters crossflow velocity and TMP.

In the following, the overall effects of particle characteristics and operating conditions during crossflow ultrafiltration is described in detail.

2.4.4 Transport and adhesion of foulants

Transport to and from the membrane

The most important driving mechanism to bring particles to the membrane surface is convection, which is a direct consequence of the permeate flux. The transport in the opposite direction, i.e. the so-called back-transport, is traditionally ascribed to Brownian diffusion, in case of small particles and macromolecules, or to hydrodynamic phenomena for larger particles. A number of mechanisms have been considered; Table 2.4 summarizes the so-called back-transport (or *mass transfer*) models and mechanisms.

Most of these mechanisms concern the effect of the crossflow velocity related to the particle size and shape. A common conclusion is that larger particles are more easily back-transported than small ones (Bacchin, 2002; Ripperger, 2002; Kim *et al.* 2001a; Lahussine-Thurcaud *et al.*, 1990; Chellam and Wiesner, 1998).

However, also the concentration of the solution and the particle charge can affect particle motion (Bowen and Jenner, 1984; Huisman *et al.*, 1999).

The combination of the existing forces determines the degree of dispersion of the solution with respect to the convective transport. In other words, it

Table 2.4: *Back-transport models*

Model	Back-transport	References
Concentration polarisation (CP)	brownian diffusion	Porter (1972)
Deposition Theory	lift force	
	diffusion + lift force	Madsen (1977)
Friction force	crossflow drag force	Ebner (1981)
Improved lift force	lateral migration	Green and Belfort (1980)
	(tubular-pinch effect)	Altena and Belfort(1984)
Convective	convection parallel to membrane (shear stress)	Vassilief *et al.*(1985)
Improved CP	shear stress and diffusion	Zydney and Colton (1986)
		Song and Elimelech (1995)
	shear induced diffusion	Davis and Leighton (1987)
		Romero and Davids (1988)

determines whether a certain particle reaches the membrane surface or not.

On the basis of characteristic values of the particle size, charge and relative distance among particles, Lahoussine-Turcaud *et al.* (1990) and Fred Fu and Dempsey (1998) presented examples of calculations of the applied forces in the case of dissolved and colloidal matter. One example from Fred Fu (1998) for "typical" ultrafiltration conditions is shown in Figure 2.15.

Deposition and characteristics of the deposit

When a particle or an aggregate reaches the proximity of the membrane surface, i.e. the boundary layer, the hydrodynamic effects are absent and the interactions with the membrane surface determines whether it deposes, adheres to, or permeates. Relevant aspects are again the particle surface charge (Huisman *et al.*, 2000; Yiantsios and Karabelas, 1998) and the physical-chemical characteristics of the membrane, among which its charge (Brant and Childress, 2002), hydrophobicity (Brant and Childress, 2002; Laabs *et al.*, 2003; Huisman *et al.*, 2000) and its roughness.

However, according to (Bowen *et al.* 1995b), Jacob *et al.* (1998) and Huisman *et al.* (2000), the membrane-particle interactions dominate only for the

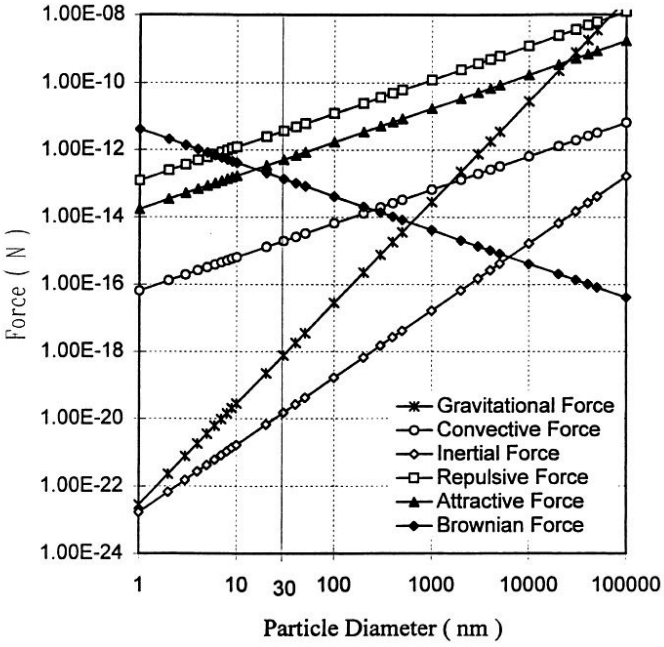

Figure 2.15: *Comparison of various forces with particle diameters, (particle sizes from 1 nm to 100 μm and particle separation distance about 10 nm; from Fred Fu, 1998)*

time that a few layers of particle depose onto the membrane surface, whereas the particle-particle interactions prevail in the following.

If the transport is interpreted as a convection-diffusion problem, the accumulation of material is described by an increasing concentration profile, which may lead to the formation of a gel layer when the stability of the suspension is overcome (Michaels, 1968). In the other cases the accumulation is described as a step concentration profile, i.e. a filter cake. A few authors have developed models to combine these two approaches (Chen *et al.*, 1997; Bacchin *et al.* 2002).

In this dissertation the notion of filter cake is used.

With respect to the resistance to filtration, the main aspects of the filter

cake are thickness and structure, often identified with its porosity.

As it is derived from all the transport theory (see Table 2.4), cake thickness is affected by the amount of particles and by the tangential shear forces due to the crossflow velocity and turbulence.

The arrangement of the deposit is affected by particle size distribution and surface interactions. Although more literature has been concerned with the effect of particle size (see review in Loijkine *et al.*, 1992; Fred Fu and Dempsey, 1998) other authors suggest that the effect of surface interactions on cake voidage is predominant (Mc Donough *et al.*, 1998) or not negligible (Bowen and Jenner, 1995b; Bacchin *et al.* 2002).

For non-interactive particles, the resistance of a cake layer of particles is estimated using the Carman-Kozeny equation (Altena and Belfort, 1983), and it is found that the resistance increases with decreasing particle radius and cake porosity:

$$R_{pl} = \frac{180(1-\epsilon)^2\delta_l}{(2r_p)^2\epsilon^3} \tag{2.7}$$

where:
R_{pl} = resistance of the particle layer (m^{-1})
ϵ = porosity of the layer $(-)$
δ_l= thickness of the layer (m)
r_p = particle radius (m)

The finding that larger particle cause lower fouling, was confirmed by many, among which Vyas *et al.* (2000). However, it must be noted that the particles involved into fouling may differ substantially from the approximation of rigid sphere, and that the relationship between cake voidage and permeability can be not straightforward. For instance, there can exist dead-end voids and some hydrophilic molecules (e.g. proteins and polysaccharides) can bind water molecules (*hydration*, see Paragraph 2.1.2).

For interactive particles, a higher surface repulsion means lower packing density and therefore increased porosity. This explains why any modification to the chemistry of the solution, such as increasing ionic strength, modifying the pH or dosing counter ions, affects both the penetration of particles through the

membrane and the voidage of the cake layer, by changing the surface charge (Velasco *et al.*, 2003; Huisman *et al.*, 2000).

For colloids, all the possible interactions have been recalled in literature: van der Waals, electrical double layer, hydration effects, hydrophobicity, steric interaction of adsorbed layer and polymer bridging.

Dynamics of the filter cake

Finally, during filtration the deposition of materials evolves with time and the characteristics of the filter cake may change.

The pressure applied on a multilayer deposit of compressible particles results in an increase of resistance which is usually expressed by a power law (Belter *et al.*, 1988):

$$\alpha_{cake} = \alpha_0 \cdot \Delta P^s \tag{2.8}$$

where:
α_{cake} = specific cake resistance $(m \cdot kg^{-1})$
α_0 = reference constant per unit value of P
ΔP = pressure difference (Pa)
s = *compressibility coefficient* $(-)$

The value of s varies within $= 0$ for rigid incompressible cake and near 1 for highly compressible cake.

The value of α_0 is conceptually related to the size and shape of the particles within the deposit, however in practice it is a reference value measured or estimated at specific conditions, e.g. at $TMP = 0.5$ *bar* (Roorda, 2004) or at the beginning of filtration (Ho and Zidney, 2000).

The effect of compressibility is usually related to the decreased filter bed voidage, as for instance during filtration of yeast cells in Zydney *et al.*, (1989) and Vyas *et al.* (2001). However, Meireles *et al.* (2002) showed that an important effect is the deformation of the particles of the bottom layer, which can directly reduce the number of membrane pores open to filtration.

Another mechanism was emphasized by Harmant and Aimar (1998), who showed that in a multilayer deposit the bottom layers are subjected to the drag forces applied to the above layers. When the cake grows these forces may

overcome the forces of repulsion between the bottom layer ad the membrane, and a loose layer is turned into irreversible fouling ("filtration induced coagulation").

Also other recent modelling work suggested that the effect of pressure redistribution inside the filter cake has been underestimated by conventional theory and engineering practice (Vorobiev, 2006).

2.4.5 Operating modes

A membrane process can be operated in three different modes: at constant TMP, at constant flux and with some combination of the first two.

The operating mode may have strong consequences on the formation of fouling.

During operation at constant TMP, the value of the driving force TMP is imposed. After some time, because of the occurrence of fouling the overall resistance R starts increasing (see Equation 2.3) and the produced permeate flux decreasing (see Equation 2.1).

Whereas the driving force TMP remains constant, the reduced flux transports a smaller amount of materials to the membrane. Consequently, the growing rate of the deposit slows down and the material already deposited is subject to a constant force. Because of these mechanisms, it is likely that at some point a pseudo-steady state is reached (see Figure 2.16). Therefore, operation at constant TMP can be said to be "self-limiting".

In contrast, during operation at constant flux, the permeate flux value is imposed and the TMP is produced consequently (Equation 2.1).

At a microscopic level, operating at constant flux allows to minimize the actual TMP during filtration, thus reducing at the minimum value the forces acting on the deposited material at the actual flux. However, when resistance increases, TMP also increases and the deposited particles are subject to increasingly high pressure. This typically results in a sudden acceleration of the fouling rate (see Figure 2.17). Operating at constant flux can be said a "self-accelerating" process.

Obviously the operational mode can also be dynamic, i.e. the TMP and flux value are manipulated (decreased) to maintain the resistance (or TMP) values within certain thresholds.

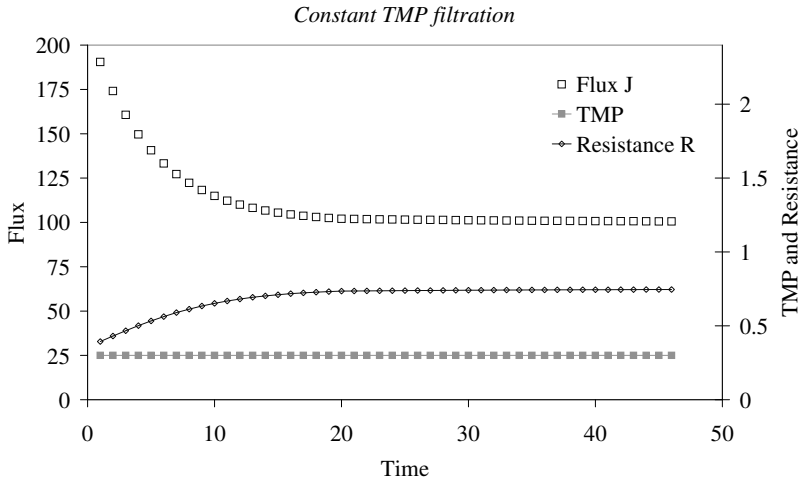

Figure 2.16: *Reconstructed typical diagrams of operation at constant TMP*

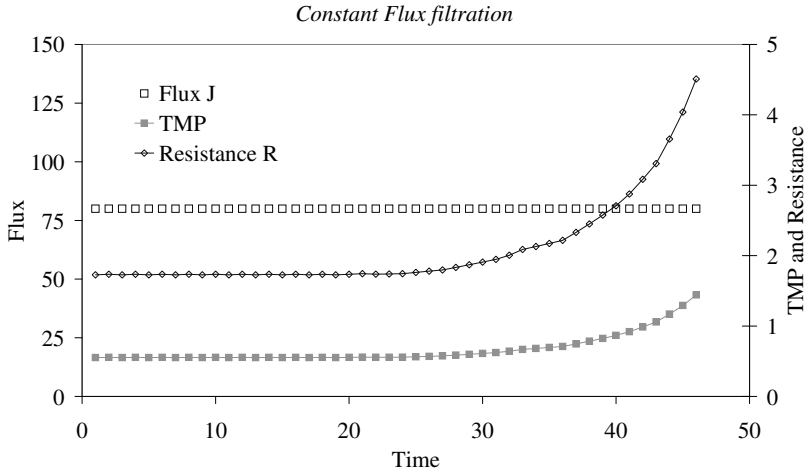

Figure 2.17: *Reconstructed typical diagrams of operation at constant flux*

Whether the constant flux or the constant TMP mode is more beneficial for fouling control is probably a pointless discussion.

Often, finer particles in the cake are observed in constant flux mode (Tarabara *et al.*, 2002; Vyas *et al.* 2002), Lojkine *et al.* 1992; Foley *et al.*, 2005). Consequently, Tarabara *et al.* (2002) suggest that constant pressure operation is preferential as particle size decreases. Differently, Vyas *et al.* (2002) suggest to minimize fouling and optimize process performances by operating in a mixed mode, at constant TMP initially and at constant flux in the following.

Operating at constant flux usually results in a higher permeate volume production *vs.* TMP increase. From this, Hao *et al.* (2006), Ho and Zidney (2002) and Defrance and Jaffrin, (1999) suggest constant flux operating mode.

2.4.6 Critical flux

The description of the operation at constant flux would not be complete without mentioning the concept of "critical flux" for crossflow microfiltration (Field *et al.*, 1995).

Its original formulation spells that: *The critical flux hypothesis for MF is that on start-up there exists a flux below which a decline of flux with time does not occur; above it fouling is observed. This flux is the critical flux and its value depends on the hydrodynamics and probably other variables.*

The concept is that for any membrane process there exists a flux value that, because of the hydrodynamics and other variables, will not allow deposition of materials. However, in opposition to this, it is also possible to conceive a feed suspension for which the interactions of the particles with the membrane are so strong that deposition would occur at zero flux, which means that the critical flux would not exist.

The following remarks can be made:

- The original definition determines that the filtration starts from a clean membrane;
- When fouling is interpreted in terms of foulant transport and deposition, the role of hydrodynamics on the critical flux is obvious. The higher the shear stress at the wall, the higher the critical flux;
- When the membrane-pores are partially occluded or the foulants deposition has an irregular pattern, the "local" flux value for certain pores

can be higher than the observed average flux value, thus overcoming the critical flux (*local critical flux concept*; Cho and Fane, 2002)

In practice all filtration-separation processes lead to some fouling extent. Chen *et al.* (1997) noted that also at the values below the apparent critical flux, when the flux is increased and decreased a little hysteresis is produced in the TMP *vs.* flux plot. Therefore, other "weaker" definitions of critical flux exist. For instance, referring to the fact that different fouling is observed when a certain flux value is produced suddenly by a pump, or is obtained by delicate progressive TMP increase, Defrance and Jaffrin (1999) described the critical flux as *the limit below which, when the flux is set by a pump, a stable filtration can be sustained for a long period with constant* TMP.

The concept of critical flux is at the base of the way several membrane systems are operated. Since constant flux mode certainly favours the design and operation of a membrane system (the filtrate flow is constant and well known), many plants aim at operating at constant flux in the sub-critical region, thus reducing the needs for membrane cleaning and replacement.

However, it is possible to operate in the sub-critical region also at constant TMP, which can be ascertained by measuring that the delivered permeate flux is constant (Defrance and Jaffrin, 1999). Song and Elimelech (1995) demonstrated that in laminar flow there exists a minimum pressure value (*critical pressure*) to hold a particle at the membrane surface; therefore they showed that fouling is a balance problem induced by operating pressures higher than the critical pressure.

2.4.7 Filterability and Reversibility

During the filtration process, regardless of the underlaying fouling mechanisms, the most evident phenomenon is the increase of resistance. Therefore, fouling is usually described by means of two characteristics: *filterability* and *reversibility*.

Filterability is the increase of filtration resistance over time (or filtrated volume); the expression "good filterability" indicates that the resistance increase is small.

The term is often used as to indicate a property of the feed water, however it must be noted that filterability depends on the membrane materials and the operating conditions.

Reversibility is the extent to which an observed increase of resistance can be removed with an hydraulic cleaning. Therefore, the definition is strictly operational.

While measuring filterability, good practice should be to apply a strong hydraulic cleaning and make sure that all the removable fouling is removed. However, in most cases the term reversibility is used with respect to the specific hydraulic cleaning protocol applied.

In the analyses of the fouling phenomena, filterability and reversibility are two well distinct properties. Filterability is related to short term effects and reversibility to long term effects.

2.5 Concluding remarks

In this Chapter, the basics of membrane filtration have been introduced, to the extent that is relevant to this dissertation.

The performance of a membrane process depends on the occurrence of fouling, which is related to a number of factors. The most relevant aspects are the operating conditions (TMP, permeate flux, shear at the membrane surface, operating mode), the membrane characteristics (pore size, chemical properties) and the characteristics of the particles in the feed solution (size, charge, compressibility).

The ultrafiltration process is particularly affected by particulate and colloidal fouling. Raw sewage contains large amounts of both particles and colloids, of organic and inorganic origin; however, coagulation-flocculation and pre-treatments in general can modify the amount, the size and the charge characteristics of both particles and colloids.

The selection of appropriate operating conditions and pre-treatments will affect the performance of direct ultrafiltration of raw sewage, both in terms of filterability and reversibility.

Chapter 3

State of the Art

The State of the Art of direct membrane filtration is presented

3.1 Introduction

As said in Chapter 1, *direct membrane filtration* indicates a particular process where wastewater is filtrated over a membrane without being previously treated by a biological step.

This concept has mostly been related to reuse purposes, likely because of the produced water quality or because of the cost associated to membrane processes. Wastewaters of various strength have been used as feed water, and all membrane processes (MF, UF, NF and RO) have been at least tested.

Most of the researches have been limited to lab-scale whilst a few others have been run on pilot scale for duration until one year. The only example of commercial application concerns the treatment of pre-screened manure with VSEP technology (vibratory shear enhanced process). In this case the rapid vibratory movement creates a high shear-stress at the membrane surface and is capable of removing all the solids that deposit there. Although at the cost of relevant energy consumption, reusable water can be produced in one single step from raw manure, using RO membranes (Johnson *et al.*, 2004).

This system is hardly applicable in the treatment of domestic wastewater, as in this case the reference method is offered by the conventional activated sludge process, which is technically efficient and cheap. Indeed, most of the research

efforts focused on conventional membrane processes, such as tubular membrane and hollow fibres.

Among the previous researches, two categories can be distinguished: application for direct reuse and applications within a multi-steps reclamation concept.

3.2 Reuse concepts

3.2.1 Direct reuse concepts

MF, UF and NF of low-loaded wastewater for "secondary" reuse

An extended research was conducted in South Korea by Kyu-Hong Ahn and co-workers. In 1998 Kyu-Hong Ahn *et al.* treated pre-screened low loaded graywater from a resort and hotel complex with MF and UF tubular ceramic membranes (TiO_2 and ZrO_2). The permeate quality with respect to COD, TOC and turbidity "*satisfied the prevailing guidelines for secondary usage such as in toilet flushing*" [BOD $< 10\ mg/L$]. Surprisingly, the permeate quality was largely independent of the membrane cut-off, which was attributed to the peculiar particle size distribution of the influent, characterized by particles above the larger membrane pore size ($0.1\ \mu m$).

Lately, Kyu-Hong Ahn and Kyung-Guen Song investigated the use of hydrophilic PET, MF, submerged hollow fibres in the treatment of septic tank effluent (1999) and again in the treatment of graywater from a resort and hotel complex (2000). In both cases the permeate quality was sufficient for reuse as toilet flushing according to Korean norms. An important remark is that treating domestic wastewater about 60% of the TOC was removed by biodegradation in the membrane tank.

More recent research resulted in findings in contrast with the mentioned Korean experiences (Ramon et al., 2004). Testing UF and NF membranes for local reuse of graywater from a sport centre, the permeate quality improved with the molecular weight cut-off (MWCO) of the membrane, and only NF membranes guaranteed sufficient quality for the reuse applications (key parameter was the BOD in the permeate).

The different conclusions indicate that the quality of the permeate and the potential for reuse are strictly related to the feed water quality.

MF and UF of domestic wastewater for irrigation

Evenblij et al. (2002) tested the water quality produced by MF and UF of wastewaters from several treatment plants in the Netherlands. Surprisingly, the removals obtained with UF (0.03 μm) and MF (0.1 μm) membranes were rather similar: about 65% for COD, 15-20% for nitrogen and 30% for phosphorous. Calculations showed that if the wastewater flow of a 5000 p.e. village was treated with direct membrane ultrafiltration, the filtrate could be used to irrigate 10 hectares of wheat, soybeans or maize providing sufficient water and fertilizers (P, N and K). However, it was remarked that the storage system and distribution network should be handled carefully, in order to avoid bilological growth due to the high organics and nutrients concentrations.

The same principles were further tested in China (Hao *et al.*, 2005). High-strength wastewater from the university apartments was filtrated on MF tubular ceramic membranes (α-Al_2O_3/ZrO_2) and on MF and UF organic (PAN) hollow fibres membranes. The filtrate was used for irrigation of winter wheat in small laboratory test-fields. The membranes proved to remove 3-4 log of bacteria and 4-5 of coliforms, with better results for the tight UF membrane. The COD in the permeate ranged between 67–140 mg/L and total N was above 80 mg/L. The plants grew with no problems and in comparison to tap water enriched with fertilizers the wheat production increased of 7.5% in weight.

MF of primary effluent for ocean discharge

Aiming at ocean discharge, the focus is mainly on clarification and microbial removal. In California (USA), on account of the Orange County Water and Sanitation District, Sethi and Juby (2002) tested MF of primary clarifier effluent for one year. Using a crossflow, hollow fibres, outside-in pilot plant, results were defined "*promising*". Local requirements for BOD, COD and pathogens removal were respected and turbidity was constantly below 1 NTU.

3.2.2 Multi-steps reclamation concepts

Double membrane treatment

Sethi and Juby (2002) also introduced the concept of a complete treatment system without secondary biological treatment, based on membrane treatment. The concept was named IMANS (integrated membrane anaerobic stabilization

system), as high rate anaerobic stabilization of the RO concentrate was included.

A similar concept was actually investigated by Rulkens *et al.* (2005). The preliminary study concluded that the scheme has the potential to recover nutrients and effluent for reuse, producing substantially higher amounts of biogas than conventional systems and requiring very small footprint. With respect to conventional systems, the total costs were estimated "*higher but probably acceptable*".

MF and UF for advanced particles removal

Aiming at enhancing the treatment of municipal wastewater, van Nieuwenhuijzen (2000a; 2002) explored the potential of direct MF and UF of raw sewage. The application of tubular organic UF membranes (PVDF) seemed to be technically feasible to produce particle-free and bacteria-free filtrate. With respect to a reference scenario based on primary sedimentation followed by low loaded activated sludge, positive features were the savings on space requirements and reduced sludge production, although hindered by higher energy costs (van Nieuwenhuijzen, 2002). For the further treatment of the soluble contaminants of the filtrate, van Nieuwnhuijzen suggested biofilm systems and MBRs, in order to avoid particle recontamination.

3.3 Operational aspects

3.3.1 Overview

Table 3.1 summarizes the relevant operational aspects of the researches conducted so far on direct micro- and ultrafiltration of wastewater.

It is immediately visible that only crossflow systems have been applied, likely because of the high solids concentration of the feed water. The two applied configurations are tubular and hollow fibres, which are separately discussed in the following.

3.3.2 Tubular Membranes

Experimentation with tubular membranes has mostly focused on the effect of the operational parameters TMP and u_{cr}.

Table 3.1: *State of the Art of direct membrane filtration, operational aspects*

Membrane	material	feed	TMP $(m \cdot s^{-1})$	u_{cr} (bar)	ref.
Tubular					
MF, UF	ceramic	low strength	1.5-3.7	1-4	[1]
UF	PVDF	municipal	0.2-0.5	1-2.5	[2]
MF	ceramic	high strength	0.6-1.2	2-3.7	[3]
Hollow Fibre Outside-In					
MF	PET	septic tank eff.	0.2-0.8		[4]
MF	PET	low strength	0.2-0.9		[5]
MF	PP	primary eff.	0.13-1.3		[6]

[1] Kyu-Hong Ahn *et al.*, (1998); [2] van Nieuwenhuijzen *et al.*, (2000a), van Nieuwenhuijzen (2002); [3] Hao *et al.*, (2006); [4] Kyu-Hong Ahn and Kyung-Guen Song (1999); [5] Kyu-Hong Ahn and Kyung-Guen Song (2000); [6] Sethi and Juby, (2000).

Kyu-Hong Ahn *et al.* (1998, [1] in Table 3.1) compared the effect of crossflow velocity and TMP during continuous filtration of more than 10 hours. In all cases the overall resistance increased during the entire filtration run although a pseudo-stationary state was obtained after a few hours. The flux at pseudo-stationary state increased with crossflow velocity and a highly turbulent state (Re $>$ 20,000) was necessary to maintain the filtration stable. A unit increase of TMP caused the total resistance to double its value, which was explained as increased density of the cake layer. At the same crossflow velocity, approximately the same final flux value was obtained. Stable continuous operations could be maintained for 120 h at minimum TMP (1.5 bar) and maximum u_{cr} (4 $m \cdot s^{-1}$), producing a stable flux of about 100 LMH.

Hao *et al.*, (2006, [3]), operated in a very similar way, at elevated pressure and crossflow velocities. During continuous filtration runs of about 100 minutes at constant TMP, increasing crossflow velocity and TMP had a positive effect on the permeate flux at pseudo steady state. However, excessive TMP reduced

the flux and excessive u_{cr} appeared useless; optimal operating conditions were found at 1 bar and 3 $m \cdot s^{-1}$, with pseudo-steady flux at 140 LMH. The combination of forward flush and gas addition (N_2) proved that a loose cake is formed and can be actively reduced by proper cleaning. Operations at constant flux mode could maintain higher permeate flux at lower TMP than operations at constant TMP mode, and therefore are recommended.

Van Nieuwenhuijzen *et al.*, (2000a, [2]) operated at much lower applied TMP, inducing less fouling. The filtration mode was cyclic, alternating 10 minutes of production with a backflush of variable duration (between 30 and 120 s). At $TMP = 0.5$ bar, average permeate flux values of 70 LMH and 110 LMH were obtained at 1 and 2.5 $m \cdot s^{-1}$ respectively. Since a turbulent flow ($\mathrm{Re} > 4,000$) is reached already at 0.9 $m \cdot s^{-1}$, the highest permeation rate at higher u_{cr} was explained on the basis of the shear-stress at the membrane wall rather than on the turbulence criterion. An operating TMP interval of 0.2–0.4 bar was suggested, in order to reduce the density of the forming filter cake.

3.3.3 Hollow Fibres

Hollow fibre membranes are usually operated by suction, i.e. a certain permeate flux value is imposed by a pump. Some times the flux value is fixed and therefore a pure constant flux mode is used, some other times the flux value is manipulated to maintain the resistance and TMP values within thresholds. In both cases, the objective is to maintain a "sustainable" filtration and the main parameter to compare performances at different operating conditions is the duration before a "not-sustainable" acceleration in the resistance increase is observed.

Kyu-Hong Ahn and Kyung-Guen Song (1999, [4]) operated their plant with a productive cycle of 10 min filtration followed by 2 min idle, whilst an agitator with variable speed and direction was providing continuously the shear-stress necessary to remove the forming cake layer. Reducing the flux progressively from 20 to 10 LMH, the plant could run continuously for 120 days. At the end, also after chemical cleaning, a loss of 10-15 % permeability was observed.

It was noted that the agitation had the effect of reducing the mean particle size, and that about about 60% of the total TOC was removed by uncontrolled biodegradation. Furthermore, the decreased temperature of the feed reduced

the permeate flux not only because of changes in the water viscosity, but also by modification of the properties of the cake layer.

These results were confirmed in Kyu-Hong Ahn and Kyung-Guen Song (2000, [5]). Using the same system with different feed water, flux values higher than 20 LMH and Suction/Idle time ratio below 20% provoked rapid fouling.

It was suggested that 20 LMH is a sub-critical flux value because during operation it was possible to obtain a spontaneous cleaning once that the flux was reported at this value.

Sethi and Juby (2000) aimed principally at stable operations, which they obtained with intense cleaning. The plant was operated for one year at 18–20 LMH and 70-75% recovery. Backwash interval was 12-15 min. The feed was pre-screened over 600 microns mesh sieve and dosed with NaOCl to obtain chlorammine and avoid biofouling (i.e. the biological growth on the membrane surface). A complete chemical cleaning (citric acid at pH = 2, followed by alkalic solution) was performed every 3-4 days, which maintained the maximum TMP below 1 *bar*.

3.4 Coagulants addition

The addition of coagulants prior to membrane filtration aims at modifying particle characteristics and reducing contaminant loading. Both effect proved to play a role in improving membrane filtration, although the first effect is relevant already at low dosages and the second only at high dosages (Kim *et al.*, 2005; Shon *et al.*, 2005; De Carolis *et al.* 2001). The modification of particle characteristics can be related to increasing particle size, which affects the transport, and to the particle charge, which alters the cake properties (Lasshoud-Turcaud *et al.*, 1990; Visvanathan and Ben Aim, 1989). Filtering synthetic wastewater rich in organic matter, Shon *et al.* (2005) showed that at low dosages only large MW organics are removed.

Unfortunately, the available studies that focused on the fouling of coagulated (partially) untreated wastewater in combination with membrane filtration are limited.

Soffer *et al.* (2000) used a pressurized stirred test cell to test various organic membranes, both UF (cellulose, PA, PESU) and NF (PESU). In the first phase

coagulation was optimized with jar tests, in the second phase the effects of coagulation were studied by filtering three feed waters: the raw wastewater, the coagulated suspension without settling, and the supernatant after settling. Coagulation with $FeCl_3$ was executed at pH = 5.5. (charge neutralization zone) and pH = 7.8 (normal pH, sweep coagulation zone). The feed source was medium-strength sedimentated wastewater from a university campus.

Coagulant were dosed to a maximum of 300 mg/L. The stronger impact was on turbidity rather than on DOM (dissolved organic matter) and DOC (dissolved organic carbon) removal. Coagulation at acid pH was more efficient, in particular with respect to DOM (60% removal at 200 mg/L vs. 20% removal at 300 mg/L). Because of the higher efficiency, overdosing was observed at pH = 5.5 but not at pH = 7.8.

At pH = 7.8 and using a UF membrane with MWCO of 50 KDa, the addition of 25 and 75 mg/L of $FeCl_3$ increased the removal efficiency of DOC (dissolved organic carbon) of 10-30%. At the start of filtration the positive impact on the fouling rate can be summarized as follows: high dosage > coagulation with settling > coagulation without settling > no coagulation. Nevertheless, after 30 minutes of filtration the effect of coagulation become negligible.

The effects at pH = 7.8 and pH = 5.5 have been compared using a UF membrane with MWCO of 10 and 4 KDa, and a coagulant dosage of 150 mg/L. With the 10 KDa membrane, the acid pH reduces the fouling rate, but this effect is hardly detectable with the 4 KDa membrane. Again the various parameters can be ordered as follows with respect to improved permeate flux: coagulation with settling > coagulation without settling > no coagulation. It is interesting to note that with respect to DOC and DOM, the fraction retained by the membrane at the natural pH = 7.8 is more than double than at pH = 5.5, because of the less efficient coagulation.

The case of the NF membrane appears completely different: there is no difference of flux decline with and without settling, and fouling cannot be removed by flushing. This indicates that this fouling is caused by smaller particles insensitive to coagulation.

Abdessemed and Nezzal (2002) treated primary effluent by applying combinations of coagulation, adsorption and crossflow UF in lab-scale experiments. The experiments were conducted using two tubular inorganic membrane (ZrO_2) with MWCO of 10 and 15 KDa respectively; coagulation and adsorption were optimized based on turbidity removal only.

Coagulation in the range of 0–200 mg/L showed overdosing. The best turbidity removal was found at pH = 5.5 and 120 mg/L $FeCl_3$. Together with

40 mg/L of PAC (Powdered Activated Carbon), a final product with turbidity about 0 NTU and COD = 7 mg/L could be obtained, which might be suitable for industrial reuse. The presence of coagulant was more beneficial than the adsorbent for the improvement of the permeate flux. However, a substantial flux enhancement was obtained only at 40 mg/L.

Noteworthy, the COD removal with coagulation was about 50–60% higher than with the membrane alone.

3.5 Concluding remarks

The quality of the permeate obtained by direct membrane filtration depends mainly on the characteristics of the feed water and the membrane pore size. During micro- and ultrafiltration of municipal wastewater, the permeate can be expected to be reused for irrigation or further treated.

The membrane pore size affects also the fouling mechanisms and tight membranes are less prone to internal fouling. With respect to microfiltration, ultrafiltration should guarantee higher disinfection capability and lower internal fouling.

From an operational point of view, the pressure vessel configuration appears more flexible and suitable for discontinuous operations. In comparison to submerged systems, tubular membranes operate at high flux values and the manipulation of TMP and crossflow velocity allows for more extensive process control.
Additionally, submerged systems require bubble aeration, in order to control fouling. The addition of aeration to direct ultrafiltration would turn the system into an aerated MBR.

Previous researches mostly mention two fouling mechanisms: cake fouling and biofouling. The effects of cake fouling are perceivable in the short term, albeit biofouling becomes relevant in the long term.

Concerning short term fouling, little effort has been devoted to the description of fouling characteristics. Different authors express contracdictory opinions about the appropriate mode of operating micro- and ultrafiltration tubular membranes in the treatment of untreated wastewater: Kyu-Hong Ahn *et al.* (1998) and Hao *et al.* (2006) recommend operations at $TMP > 1$ bar and crossflow velocity > 2.5 $m \cdot s^{-1}$, whereas Van Nieuwenhuijzen tested crossflow

velocities below 2.5 $m \cdot s^{-1}$ and recommends operations below 0.4 bar. In all cases the effect of the operating conditions is evaluated based on the visual comparison of the trend of flux and resistance against time or volume. Differently, fouling characteristics should be described quantitatively and in such a way to be comparable among different systems.

The experience with coagulants, untreated wastewater and low pressure membranes is limited. Only one coagulant, $FeCl_3$, has been tested, and at very high dosages (up to 200 $mg \cdot L^{-1}$).

Results show that coagulation at acid pH (5.5) is more effective than coagulation at "natural" pH (7.8). Significant flux enhancement and significant removal of DOM (or DOC) are achieved only at very high dosage (above 40 $mg \cdot L^{-1}$).

The inclusion of organic substances in the coagulated flocs may results in less retention of organic matter by the membrane: apparently, this effect is more beneficial to the cake characteristics than the presence of coagulant flocs in the bulk feed solution. Nevertheless, the effects of coagulation tend to vanish with filtration time.

These findings should be tested using other kinds of coagulant and applying more dosages that may be "reasonable" in practice.

Chapter 4

Materials and Methods

Where the tools used during experimental investigations are described.

4.1 Filtration Set-up

The heart of the research presented in this Dissertation is based on filtration experiments. The characteristics of the set-up employed during the experiments affect the quality and the accuracy of the measurements, therefore they are of major importance.

The equipment in use includes the following elements:

- membrane;
- main circuit and control facilities ;
- data acquisition system;
- cleaning facilities.

Figure 4.1 presents a schematic drawing of the filtration set-up. The feed water is circulated from one of the the feed tanks to the membrane, where two streams are formed: the permeate and the retentate. The produced permeate is weighed on a balance, whereas the concentrate is returned to the feed tank. Alternatively, it can be discharged.

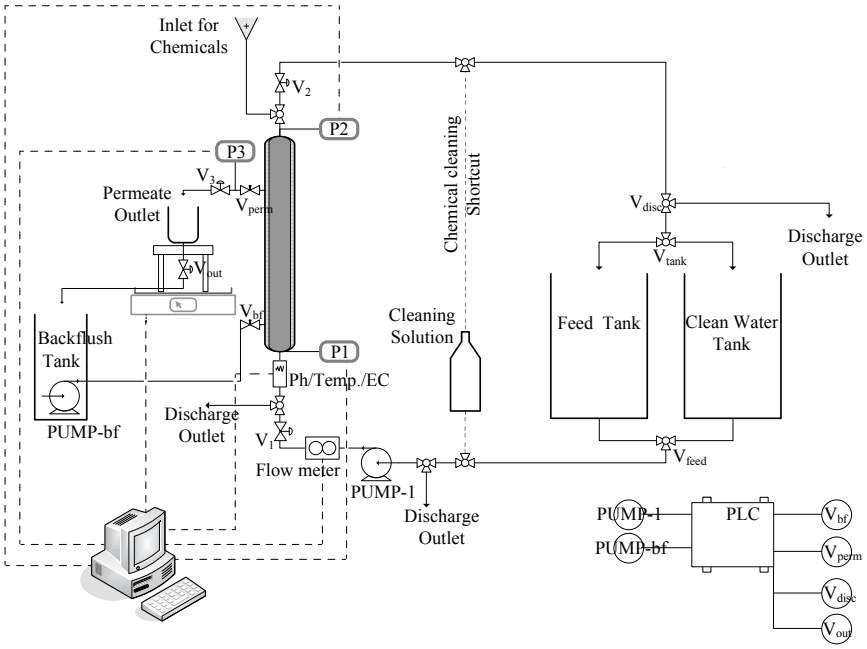

Figure 4.1: *Schematic drawing of the filtration set-up*

The membrane cleaning can be provided hydraulically or chemically. The filtration cycle is controlled by a PLC, whilst filtration data are acquired on a PC.

In the following, the main elements of the filtration set-up are described.

4.1.1 UF membrane

The membranes in use are X-flow F 4385. The mounted module consists of a PVC tube of 1 m length and 1 $inch$ diameter, containing 12 membrane tubes. The membranes have a diameter of 5.2 mm and are sealed with resin at both ends. The membrane material is polyvinyldenfluoride (PVDF) with nominal pore size of 30 nm. A picture of the module is presented in Figure 4.2

In the set-up, the membrane module is vertically placed. The feed water flows along its length inside the membrane tubes. The permeate side is con-

Figure 4.2: *The F 4385 membrane module in use*

nected to the backflush pump and to the atmosphere, for permeate extraction.

During the experiments, little variations are done to the membrane configuration. In a standard module the total membrane area is 0.176 m^2, but this is seldom used during testing (in practice, only during some of the long term tests of Chapter 5). Most of the time the membrane module is operated with 5 tubes and 7 tubes only, corresponding to a total membrane area of 0.073 and 0.103 m^2. The reasons are related to the overall set-up design and to "practical" problems:

- pressure and velocity along tubes are related, as expressed by the Bernoulli's equation. In order to maintain the ability to vary the crossflow velocity (u_{cr}) and the transmembrane pressure (TMP) within certain ranges, the number of membrane tubes inside the module needs to be reduced, which reduces the membrane area and the total cross section;

- larger filtrating membrane area requires larger feed water volumes, which have to be transported to the laboratory;

- the membrane area affects the permeate production rate, in terms of mass and volume. The permeate is collected and weighted on a balance, therefore the optimal measuring range must be respected.

The configuration with 5 tubes is realized by hand-casting spare tubes into

the PVC module, and is used during the short term test described in Chapter 5 and 7. This system has two negative drawbacks: 1) after several uses, because of the pressure or because of the chemical cleanings, the membranes tends to detach from the glue; 2) mounting 5 tubes only in the module implies that a large volume is left empty on the permeate side, which causes dilution of the permeate. This imposes to sample the permeate for analyses only when sufficient volume (to flush the permeate side volume) has been produced.

To overcome these limitations, during the tests described in Chapter 8 and during some of the the long term tests of Chapter 5, the membrane area is reduced using a different method. Starting from a standard 12-tube module, a few of them are filled with rubber cords provided by the manufacturer. This system allows to exclude the volume of the tubes completely, thus avoiding air and water stagnating into the tubes. At the same time, it maintains little the free volume at the permeate side.

This is done for 5 tubes, obtaining a 7 tubes configuration.

4.1.2 Main circuit

The main circuit is composed of two feed water tanks and a circulating loop made of PVC tubes and pipes. The flow through the loop is guaranteed by a centrifugal pump. Several valves, operated manually or via PLC, are used to control the flow and the pressure in the membrane module.

For any configuration of the membrane module, the circulation pump guarantees a minimum crossflow velocity of 2 $m \cdot s^{-1}$ at $TMP = 0.5\ bar$.

The control of the process is guaranteed by the following on-line measurements:

- Crossflow velocity: measured with an electromagnetic flow meter (Krohne, IFC 010K);
- Transmembrane pressure: the TMP is calculated based on the measurements of three pressure transmitters (Labom, type CB3010). The transmitters are located at the entrance of the membrane tube (P1), at the outlet of the membrane tube (P2) and at the outlet of the permeate stream (P3, see Figure 4.1). The transmembrane pressure is calculated as the difference between the average pressure at the permeate side and the pressure at the permeate side, as shown in equation 4.1

$$TMP = \frac{P1 + P2}{2} - P3 \tag{4.1}$$

- Permeate flux: out of the membrane module the permeate drips into a recipient placed on the top of a mass balance, connected to a PC. At a fixed time interval (mostly 10 sec., sometimes 5 sec.) the PC calculates the permeate volume, and hence the flux.

In some occasions other measurements are taken, such as temperature, conductivity (EC), pH and oxygen content, which are measured using standard electrodes from WTW. The electrodes are placed either in the feed tank or in a specific slot built on purpose just upstream the membrane module (see Figure 4.1).

The feed water can be wastewater or "clean" water. The wastewater is untreated municipal wastewater, pre-filtered at sampling on a 0.56 mm mesh sieve. The pre-filtration is meant to avoid clogging problems along the membrane tubes. As *clean water*, during the first experiments a mixture of about 2/3 demineralized water and 1/3 tap water is used. In the following, demineralized water is added with $MgSO_4$. This "conditioning" is necessary to the functioning of the electromagnetic flow meter.

The switch to select the feed water (V_{feed}) is manually operated, as well as the regulating valves to control the TMP, placed approximately in correspondence of the pressure meters (V_1, V_2, V_3). Differently, the circulating pump, the backflush pump and the on/off valves for the control of the filtration cycle are operated by a PLC (V_{bf} and V_{perm} according to filtration and backflush mode, V_{disc} to discharge the retentate).
The switch to direct the retentate flow is always operated manually (V_{tank}).

Initially, also the collected permeate is removed by hand when approaching the measuring limit of the balance. However, during cyclic operation, the discharge of the permeate is automated and synchronized with the backflush (V_{out}). The aim is that the filtration process can run autonomously for several hours. Unfortunately, the consequence is that the balance often operates in a weight range above the most accurate precision limit: when the total weight of 5 Kg is exceeded, the accuracy of the balance (Mettler PM34K) shifts from 0.1 g to 1 g.

4.1.3 Data acquisition

The information for process control (TMP and flux) and monitoring (Temperature, EC, pH, O_2 content) is conveyed to a PC. On the PC, a specific programme written with the software Testpoint handles this data-set for both online control and recording.

The programme has an input screen for the installation characteristics (number and diameter of membrane tubes), the filtration process (feed water, initial temperature, flow) and the recording process (time step, usually 10 *sec*).

At the start, it provides in real time the curves of TMP, permeate flux and resistance over time, calculated and displayed at each time step. The other parameters are recorded and displayed as simple values in windows refreshed every 10 *sec*.

4.1.4 Cleaning facilities

Hydraulic cleaning of the membrane occurs in two ways. The first is by circulating clean water at high velocity, in order to produce a scouring effect on the membrane walls (forward flush). The second is to operate a backwash (or backflush).

To this purpose, a dedicated centrifugal pump is immersed in a tank filled with demineralized water, where also the permeate flows during long term experiments. The pump provides a TMP of 0.8 *bar*, in the opposite direction of the usual permeation flow, and is actuated by the PLC.

Also the chemical cleaning is practiced in two different ways. The first is statical, by pouring alkaline (NaOCl) or acid (citric acid or HCl) solution from the top of the membrane module.

The second, dynamical, makes use of the usual circulation pump to convey an alkaline detergent (Divos 109). A 10 L f vessel of solution is connected with a shortcut to the membrane module and the solution is circulated at high crossflow velocity. A little volume is forced to permeate the membrane, in order to obtain a deeper cleaning of the pores.

4.2 Feed water

The feed water used during the experiment is untreated wastewater or effluent of the primary sedimentation from the wastewater treatment plant (WWTP)

"De Groote Lucht"(Vlaardingen, NL). The WWTP treats the wastewater from three different sewer networks, belonging to the areas of Vlaardingen, Maasluis and Schiedam. All sewer systems collect wastewater of household and industrial origin.

Table 4.1 summarizes the yearly average quality (2005) of the mentioned feed wastewaters. In all cases, values correspond to a common medium-strength municipal wastewater.

Table 4.1: *Yearly average of feed wastewater streams (2005)*

Parameter		Vlaardingen	Maasluis	Schiedam	Pr.Effl.
TSS	$(mg \cdot L^{-1})$	190	188	148	65
BOD_5	$(mgO_2 \cdot L^{-1})$	129	115	99	54
COD	$(mgO_2 \cdot L^{-1})$	388	350	295	158
N-Kjeldhal	$(mg \cdot L^{-1})$	32	34	39	25
P-tot	$(mg \cdot L^{-1})$	5.5	5.5	6.7	4.8

The sampling point used for untreated wastewater is placed downstream the preliminary rough screen, but upstream the merging point of the three pipelines that reach the WWTP. Therefore, the three wastewaters are sampled separately and mixed afterwards.

During the tests of July-August 2004, which compare the filtration results of untreated wastewater and primary effluent (see Chapter 5 and 7), the three wastewater are mixed in a fixed ratio that approximately reproduce the yearly average of the three flows: 40L:25L:35L (Schiedam:Maasluis:Vlaardingen). During the other tests, the ratio is more simply $40L$:$30L$:$30L$.

The effluent of the primary sedimentation tank (herafter: "primary effluent"), is sampled just upstream the common aeration tank. At this stage, the three streams are already mixed.

4.3 Filterability tests

4.3.1 Wastewater sampling

During each testing day, the total volume of the wastewater sample is about 100–120 L. As mentioned earlier, at the moment of sampling the wastewater is filtrated over a 0.56 mm mesh sieve, in order to retain paper and other debris. The wastewater is collected in jerry canes and transported to the laboratory of the Delft University of technology, which takes approximately 30 $min.$ by car. In the laboratory the jerry canes are stored in a fresh room, located underground. This is supposed to alter the characteristics of the wastewater as little as possible. In any case, the samples are used within the day of collection, and are never stored overnight.

At the start of the research (March 2004), a few experiments are also conducted directly on-site. However, since the results appear comparable and the logistic more difficult, it is decided to continue the experimentations in the laboratory of the University.

4.3.2 General test procedure

The filtration tests are batch tests conducted at constant TMP. Results of tests at constant flux are not reported in this dissertation and can be found in Ravazzini *et al.*, (2005a).

Although various kinds of filtration test are performed, there is a general standard procedure that can be summarized as follows:

- Measurement of membrane resistance (R_{mem}) filtrating clean water at TMP=0.5 bar and u_{cr}=1.5 $m \cdot s^{-1}$. The corresponding flux value is later referred to as Clean Water Flux (CWF);

- Setting of desired operating conditions: during filtration of clean water, TMP and u_{cr} are regulated to the desired values;

- Filtration test with wastewater;

- Cleaning.

The initial measurement of the membrane resistance is of major importance, because membrane resistance determines the starting flux value, which may affect the following course of filtration. This theme is debated in Paragraph 4.3.5.

The regulation of the operating parameter TMP and u_{cr} is executed manually. Nevertheless, values can be set with good accuracy and variations at the start are within 5%.

The start of the filtration test remains a very delicate moment. Switching the feed from clean water to wastewater causes turbulence in the flow, which sometimes provokes the loss of one or two measurement points, corresponding to 20 to 30 *sec.* of delay from the start of filtration and the recording of "good" measurements. When the flux decline is rapid, this reflects in a substantial difference of the starting value of flux and resistance. Consequently, the initial measurements of the CWF and R_{mem} become even more important.

During filtration, TMP and u_{cr} are monitored. Corrections to the regulations, applied when a variation of the initial settings $\geq 10\%$ occurs, are barely necessary. The activities are usually limited to the sampling of permeate and the preparation of the solution for chemical cleaning.

At the end of the filtration tests the cleaning protocol consists of three steps:

- Membrane rinsing: 1–2 *min.* of backflush with contemporary circulation of clean water at the maximum u_{cr};
- Application of the cleaning solution: Divos 109, at 0.4% w/w, is circulated for 40 minutes at 2 $m \cdot s^{-1}$, with slow permeation;
- Rinsing of cleaning solution and measurement of the achieved CWF.

When the membrane is left overnight or unused for long period, it is stored in a NaOCl solution poured from the top of the membrane module. The concentration of NaOCl is varied considering the occurrence of diffusion to the permeate side, in order to obtain a final concentration around 200 ppm.

When the membrane is soaked for too long in an alkaline solution, it is found that it loses permeability, i.e. the R_{mem} is higher than normal. In most cases, the application of citric acid or HCl solution at pH = 3 is sufficient to restore the original permeability. In some other cases, the permeability is restored by simply filtrating wastewater and cleaning as usual.

4.3.3 Elaboration of results

Calculation of fundamental process parameters

As mentioned in paragraph 4.1.3, the filtration set-up sends to the PC the pressure and weight data that are used to calculate the TMP and the permeate flux. The following equation is used:

$$J_{meas} = \frac{dM}{dt}\frac{3600}{A_m \cdot \rho} \tag{4.2}$$

where:
M = mass of produced permeate (g)
t = time (s)
A_m = membrane area (m^2)
ρ = permeate density (kg/m^3), and
J_{meas} = measured flux value (LMH)

Based on the measured flux and TMP values, the filtration resistance can be calculated at each step measurement by applying Darcy's Law (Equation 2.1):

$$R_t = \frac{TMP_t}{J_{meas(t)} \cdot \eta_t} \tag{4.3}$$

where t indicates the time dependency.

The permeate viscosity η_t is clearly a key parameter to calculate R_t. However, the viscosity is a function of temperature, and during circulation through the pump the temperature of the feed water increases. Therefore, experimental data must be corrected for the temperature increase during the filtration period.
In practice, the measured filtration data are treated as follows.

Assuming the permeate viscosity equal to that of pure water, the relation with temperature has been expressed in Equation 2.2 (Huisman, 1996):

$$\eta_p = \frac{479 \cdot 10^{-3}}{(T + 42.5)^{1.5}} \tag{4.4}$$

where:
η_p = permeate viscosity ($Pa \cdot s$); and
T = Temperature (°C).

At the start of filtration the temperature value is measured in the feed tank and inserted in the measuring programme, which calculates η_{start} (permeate viscosity at the start). This value is used by the programme during the entire duration of the experiment, calculating and displying R'_t:

$$R'_t = \frac{TMP_t}{J_{meas(t)} \cdot \eta_{start}} \tag{4.5}$$

During post-processing of the recorded data, the flux values are corrected on the basis of the feed water temperature measurements executed during the filtration test. For each time step, the permeate viscosity η_t is calculated and applied. The "corrected" flux values $J_{corr(t)}$ correspond to an hypothetical experiment at constant temperature equal to the feed water temperature at the start:

$$J_{corr(t)} = J_{meas(t)} \cdot \frac{\eta_t}{\eta_{start}} \tag{4.6}$$

From the corrected flux values, corrected resistance R_t values are obtained:

$$R_t = \frac{TMP_t}{J_{corr(t)} \cdot \eta_{start}} = R'_t \cdot \frac{\eta_{start}}{\eta_t} = \frac{TMP_t}{J_{meas(t)} \cdot \eta_t} \tag{4.7}$$

It must be noted that most of the literature about membrane filtration reports filtration data as referred to a reference temperature (usually 15 °C or 20 °C). This is meant to improve the comparability of data obtained at different temperature, but is voluntarily avoided in this dissertation.

The standardization to a reference temperature is usually done accounting for the change in permeate viscosity only, i.e. in the same way as described above. However, some works have shown that the effect of temperature variation on the filtration rate include modifications to the membrane properties (Te Poele, 2002) and to the filter cake as well (Ahn, 1999; Chiemchaisri and Yamamoto, 1994). Consequently the correction for permeate viscosity is only partial.

In this dissertation, the flux and resistance results of the filtration tests are presented as referred to the temperature at the start of filtration, calculated as explained above. The correction of the filtration data for the temperature

increase during the single test is deemed necessary for the interpretation of fouling development, however, the correction is little since the temperature increase during 30 *min* tests is within 1.5 °C and during long term tests within 3.0 °C.

With respect to the entire set of tests presented, the feed water temperature varies in a rather broad range (about 10 °C). Therefore, it is preferred to provide the observed flux and resistance values and the feed water temperature value rather than applying a "partial" standardization.

Filtration Curves

During filtration at constant TMP, the development of fouling over time results in an increase of resistance and in the corresponding decline of flux, as described by Equation 2.1. Since the transport of foulants towards the membrane decreases with time, the curves of flux and resistance tend to a "plateau" that represent the approaching to a condition of equilibrium between the concentration/accumulation of material and the scouring process.

An example with duration of 30 *min* is shown in Figure 4.3.

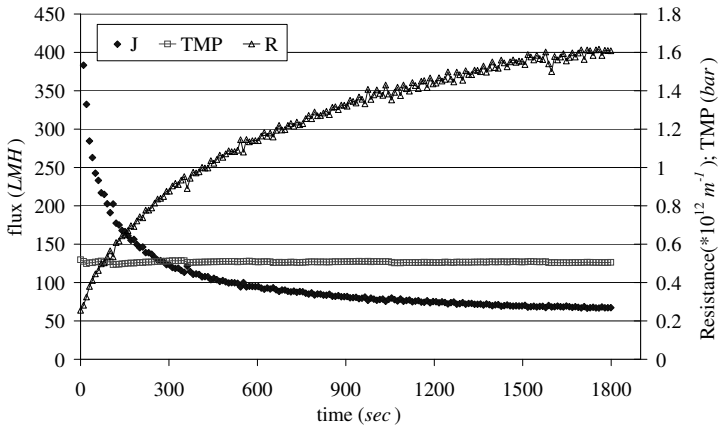

Figure 4.3: *Example plot of J, R and TMP curves vs. time*

The representation of the filtration curves over time $J(t)$ and $R(t)$ communicates the general "feeling" of the way the filtration process develops over time.

However, the occurrence of fouling certainly relates to the transport of material towards the membrane, which is function of the permeate flux. Therefore, investigating filtration characteristics, the filtration curves over volume $J(vol)$ and $R(vol)$ are preferred.

In Figure 4.4, the results of the same filtration tests of Figure 4.3 are plotted as a function of volume.

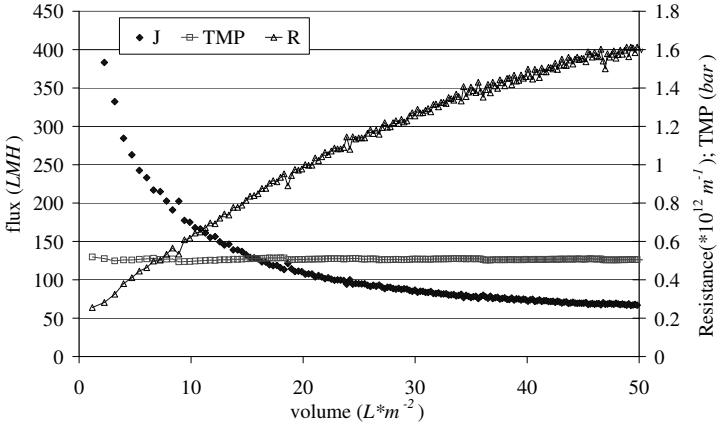

Figure 4.4: *Example plot of J, R and TMP curves vs. produced volume*

It is important to remark that the permeate flux, more than the permeate volume, affects the transport of material. This is especially true for a crossflow system, where a fraction of the material in the bulk solution is carried away in the retentate. The permeate volume results from the integration in time of the permeate flux, but the total resistance at equal produced volume depends on the way that this volume has been produced. This is the reason why $R(vol)$ curve are used to determine what operating conditions produce higher permeate volumes with less fouling.

During filtration at constant TMP, there is no fixed relation between filtration time and produced volume, as it is during constant flux filtration. Therefore, the plot of $R(vol)$ and $(R(t)$ present slightly different information and are both used in this dissertation.

Lump parameters for performance evaluation: ΔR and ΔJ

During the standard test duration of this research, 30 minutes, the development of fouling results in the overall resistance increase $\Delta R_{30} = R_{end} - R_{start}$ and in the corresponding flux drop $\Delta J = J_{end} - J_{start}$. At equal filtrated volume, the overall resistance increase is $\Delta R_{vol} = R_{vol} - R_{start}$. These values could be used to present and compare the filtration data in a summarized form.

Obviously, ΔR_{30}, ΔR_{vol} and ΔJ are strongly affected by the initial resistance value R_{start}. The first two directly, the latest because of the relation between J and R (see Equation 2.1).

Two factors have a major impact on R_{start}, the membrane resistance R_{mem} and the accuracy of the experimental measurements at the start of filtration.

The variations of R_{mem} during the testing session are analyzed in Paragraph 4.3.5.

Concerning the experimental inaccuracy, it has already been said that the un-steady flow at the start of the filtration causes the loss of a couple of measuring points. The effect of such loss is bigger when the fouling is more rapid. It should also be mentioned that this problem increases when the filtration procedure is completely automated via PLC (2005), probably because of unsatisfactory synchronization of the actuated valves.

However, during the short term tests with raw wastewater and primary effluent, R_{end} and the resistance increase ΔR_{30} show the same trend. This indicates that the variations in the membrane resistance at the start of filtration are small when compared to the overall resistance increase, and ΔR_{30} can be used to describe the resistance increase. The same can be said for ΔR_{vol}, also when a little produced permeate volume is considered.

On the opposite, J_{start} values are strongly affected by the inaccuracy of the start of the measurement. For instance, J_{start} values cannot be proportionally related to the applied TMP, as they should according to the Darcy's law (before fouling builds-up). Consequently, also ΔJ values are largely inaccurate.

Throughout the whole dissertation, ΔR_{30} and ΔR_{vol} are profusely applied, whereas J_{start} and ΔJ are used with caution.

Shear stress at membrane wall

During crossflow filtration the major process parameters are TMP and u_{cr}, both responsible of changing the flow velocity field of the transported solution.

The effect of TMP is by definition applicable to any membrane configuration, but the effect of u_{cr} depends on the hydraulic of the system in use. A way to make the effect of u_{cr} comparable throughout different membrane systems, is to express filtration results as a function of the shear stress at the wall τ. The shear stress is indeed the actual "force" acting on the deposing particles as a consequence of u_{cr}.

For tubular membranes, the shear stress can be calculated according to the following Equation (Elmaleh and Abdelmoumni, 1998):

$$\tau = \frac{f}{2} \cdot \rho \cdot u_{cr}^2 \tag{4.8}$$

where:
τ = shear stress (Pa);
ρ = liquid density $(kg \cdot m^{-3})$;
f = friction factor $(-)$.

The friction factor depends on the Reynolds number (Re), as follows:

- Re≤2,500–4,000 : $\frac{f}{2} = 8/\mathrm{Re}$;

- 5,000≤Re≤200,000 : $\frac{f}{2} = 0.023 \cdot Re^{-0.2}$

The Reynolds number is an adimensional number that is to determine whether a flow is turbulent or laminar. Turbulence is achieved when Re≥4,000 The Reynolds number can be calculated as follows:

$$Re = \frac{u_{cr} \cdot d}{\nu} \tag{4.9}$$

where:
d = tube diameter (m); and
ν = kinematic viscosity (m^2/s).

Table 4.2 summarizes turbulence and shear stress data for the filtration set-up at the reference temperature of 15°C and 20°C.

Table 4.2: *Turbulence and shear stress values for the filtration set-up*

u_{cr} $(m \cdot s^{-1})$	Re (-)	Turbulence	$\frac{f}{2}$ (-)	τ (15°C) (Pa)	τ (20°C) (Pa)
1	5,200	Yes	0.00415	4.3	4.2
1.5	7,800	Yes	0.00383	8.9	8.6
2	10,400	Yes	0.00362	14.9	14.4

In Chapter 5 and 7 the resistance values at equal filtrated volume $R(vol)$ are presented as a function of TMP and τ as well.

4.3.4 Reproducibility of results

The reproducibility of results is essential to any experimental activity. Obviously, in practice identical experiments give equivalent result only to a certain extent. What matters is that the accuracy of the result (measured for instance as standard deviation) is little with respect to the differences to be measured.

Treating "real" raw wastewater several factors can impact the reproducibility of results; among others: the variability of the feed water quality with days, the stability of the feed water during storage periods, and the experimental conditions (status of the membrane, status of the entire set-up, disturbance to the measurements).

An additional factor is the test procedure itself. In facts, in some cases it is not possible to avoid/exclude modifications of the sample.

For instance, during the short term experiment of Chapter 5 and Chapter 7, the same sample of 100 L is filtrated repetitively during the three tests of the day. During one test the permeate is extracted continuously for 30 $min.$, and at the end it is returned to the feed tank. This is done to avoid the increase of suspended solids concentration in the feed water and control the temperature increase, which could modify the filtration characteristics. In facts, using a sample of 100 L, the extracted permeate volume is 4–8% of the total and the feed water temperature rises up to 1.5°C. Additionally, it can be calculated that with the 5 membrane tubes configuration, at 1 and 2 $m \cdot s^{-1}$, the total volume of the feed water is recirculated 9 and 18 times respectively. All these factors pose the question whether the feed water is modified significantly by the passage

through the circulation pump or not.

On the opposite, during the tests of Chapter 5 and Chapter 8, the procedure is different and a certain amount of feed waters (30, 60 or 120 L) is used for one test only. This method avoids the modifications eventually induced by the circulation pump, however the comparison is made among feed waters from different jerry canes, although all sampled within a few minutes. This poses the question whether the compared results originate from exactly identical or only similar wastewaters.

An answer is found empirically. Figure 4.5 compares filtration curves $R(t)$ obtained on the same day with the same wastewater sample filtrated twice (Day-1A and Day-1B) with filtration curves obtained from other samples (Day-2 and Day-3).

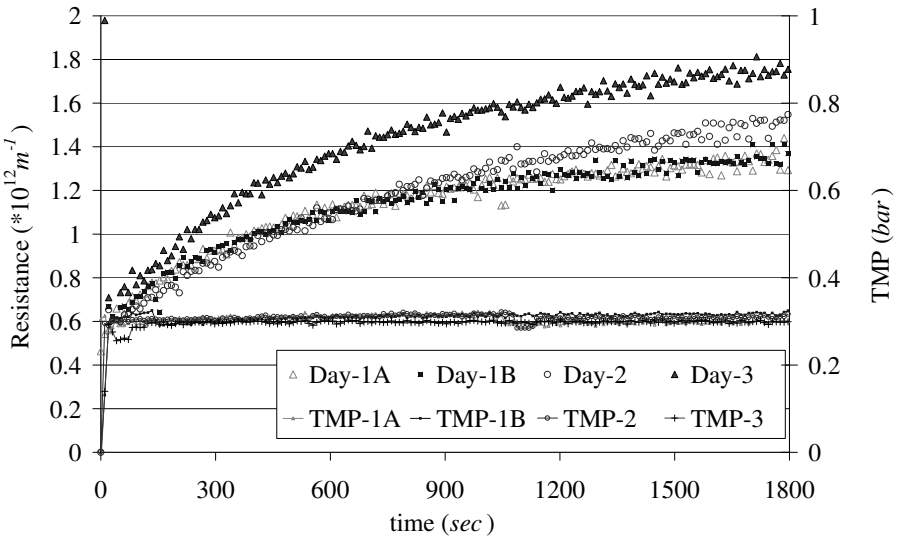

Figure 4.5: *Repeatability filtrating twice the same sample (Day-1A and Day-1B) and filtrating two different samples (Day-2 and Day-3)*

Filtrating twice the same sample seems to have negligible effects on the filterability of wastewater, and the repeatability is high. Differently, when samples from different days are compared the repeatability is low.

This indicates that the variability of the feed water quality with days affects the filterability relevantly. Only results obtained on the same sample can be strictly compared. This obliges to use short term experiments that can be repeated during the same day as major tools of investigation.

4.3.5 Membrane Resistance

The membrane resistance R_{mem} is the resistance to filtration caused by the membrane itself, i.e. is the resistance of a *clean* membrane. However, during the experiments, R_{mem} is more often the resistance of a *cleaned* membrane, which of course is different and varies with use.

During constant TMP experiments the value of the membrane resistance R_{mem} is a key element. It determines the starting flux value, i.e. the transport of material toward the membrane, and hence the starting of the building up of fouling. Keeping R_{mem} value as constant as possible is fundamental for the repeatability of results.

Unfortunately, despite the application of efficient cleaning products, for a number of practical reasons it is not always possible to start the experiments at the same R_{mem} value.

The manufacturer indicates for the membranes in use a value of permeability $\geq$ 1000 LMH at 25°C, which has been confirmed experimentally for all the tested membranes. This value corresponds to a clean membrane resistance R_{mem} of approximately $0.4 \cdot 10^{12} m^{-1}$ at 25°C.

Figure 4.6 compares the average, the standard deviation and the extreme observed values of the membrane resistance R_{mem} during the main test sessions described in this dissertation. Temperature range is 17–25 $°C$; "RS" indicates Raw Sewage and "PE" primary effluent.

R_{mem} exhibits a rather large range of variation, both in terms of average values and standard deviation.

The differences in average values can be explained by two facts: small differences from the manufacturing process, and membrane aging. During "RS short term" an old membrane is used; during the other sessions, each time a brand new one. The " aged" membrane may have a lower average R_{mem} in

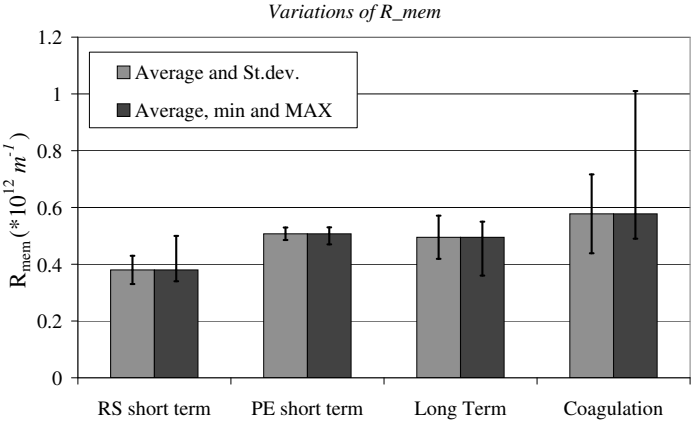

Figure 4.6: *Average, standard deviation, minimum and maximum values of R_{mem} during testing sessions*

consequence of the numerous chemical cleaning.

The standard deviation in the R_{mem} value is within 4 and 15%, except the case of the coagulation tests (24%, discussed in Chapter 8). Obviously, single measurements exhibit a greater variability.

As mentioned earlier, the variations in membrane resistance impact strongly the value of J_{start}, whereas the effect on the following course of filtration appears more limited. Two facts can explain this finding.

The first is that the variations in the R_{mem} value are little with respect to the total increase during the filtration experiments. The second is that varying the operating conditions changes the development of R more evidently than the variations of R_{mem}.

The effect of different R_{mem} values is more relevant when comparing filtration data obtained at the same applied conditions. This is the case in Chapter 8.

4.4 Jar Tests set-up

4.4.1 Small scale set-up

The jar tests is a standard test developed for testing the effects of coagulation. Consequently, the equipment consists of small units where the coagulation process can be simulated in well controlled conditions.

In this research a standard device developed by KIWA is used (KIWA, 1974). The device consists of six beakers of 2 L volume, provided with stirrers. The rotational velocity is the same for all the stirrers, so that the effect of different dosages can be compared. The *mean velocity gradient* G, i.e. the power input to fluid volume, is related to the rotational velocity of the blades via a known relation, reported in Appendix A.
A picture of the apparatus is shown in Figure 4.7.

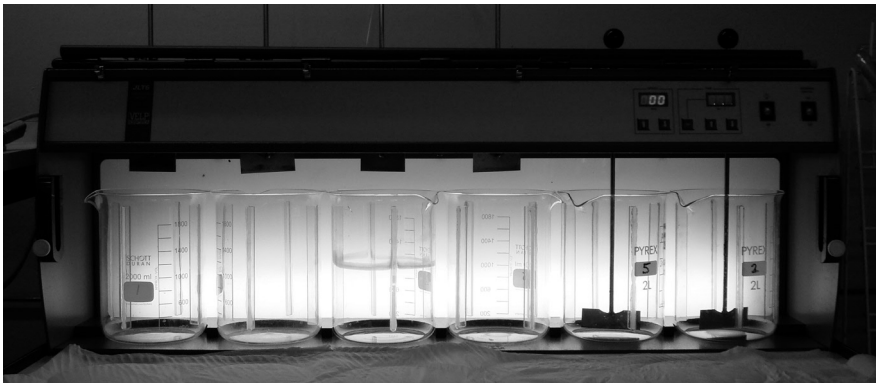

Figure 4.7: *KIWA Jar Test set-up*

4.4.2 50 L mixing chamber

In order to upscale the coagulation-flocculation process to the 50 L required for the filtration test, it is necessary to realize a specific mixing chamber of appropriate volume. This is done using a plastic tank of analogous shape (including added-in deflectors) and a rotating shaft with accurate speed control. The shape

of the propeller is different, being simply rectangular. The relation between the rotational velocity and the mean velocity gradient G is calculated based on the equations presented in the following (Metcalf & Eddy, 2003).

G, (s^{-1}), is defined as a function of P:

$$G = (\frac{P}{\eta \cdot V})^{0.5} \tag{4.10}$$

where:
η is the dynamic viscosity of the fluid $(Pa \cdot s^{-1})$;
V is the tank volume (m^3); and
P is the power $(N \cdot m \cdot s^{-1})$.

P is calculated differently during fast mixing ("coagulation"):

$$P = (N_p \cdot \rho \cdot n \cdot D^3) \tag{4.11}$$

and during slow stirring ("flocculation"):

$$P = \frac{(C_d \cdot A \cdot \rho \cdot v_p^3)}{2} \tag{4.12}$$

where:
N_p = power number for impeller (unitless);
ρ = liquid density $(kg \cdot m^{-3})$;
n = revolution per second (rps);
D = diameter (m);
C_d = coefficient of drag of paddle moving perpendicular to fluid (unitless);
A = blade "orthogonal" area (m^2); and
v_p = relative velocity of paddles with respect to the fluid $(m \cdot s^{-1})$ usually assumed 0.6–0.75 times paddle-tip speed.

The efficiency of the hand-made equipment and the application of the Formulas are validated by the results. In facts, similar turbidity removal are obtained at small and large scale at the same operating conditions (see Chapter 8).

4.5 Physical-Chemical analyses

Every filtration measurement is accompanied by physical-chemical analyses, whether for characterizing feed water and permeate (TSS, COD, TOC, NH_4^+

and dissolved phosphates), for process control (temperature, turbidity, conductivity and pH), or for assessing the fouling potential (Colour, Humic substances, Proteins and Polysaccharides).

Since the wastewater is filtrated over a 0.56 mm mesh sieve at sampling, all the analyses must be intended operated on such pre-treated wastewater.

Additionally, the analyses presented in Chapter 5 and 7, are executed on the filtrate of a paper filter for suspended solids analyses (Schleicher&Schuell 589^2, nominal pore size 7–12 μm). In this case, the values of the measured components refers to the colloidal and dissolved fraction only.

TSS

The analysis of total suspended solids (mg/L) is executed filtrating a 100 mL sample over a paper filter (Schleicher&Schuell 589^2), and weighting the retained dried mass. The procedure is according to NEN.

Cuvette tests

The chemical analyses of the feed water and permeate are executed using standard cuvette tests from Merck read by a XXXXX photometer. Results are expressed in mg/L.

The methods in use are reported in Table 4.3.

Table 4.3: *Cuvette tests analyses*

Parameter	Method
COD	Spectroquant 14541; 14540
TOC	Spectroquant 14878
NH_4^+	Spectroquant 14559; 00683
Phosphates	Spectroquant 14729; 14848; 00798

In the case of feed water, the TOC and phosphates measurement are conducted on the filtrate over a 0.45 μm cellulose acetate filter (Sartorius). Therefore, the measured values correspond to dissolved organic carbon (DOC) and dissolved phosphates.

Light absorption

A set of four components with high potential fouling rate is measured through light absorption measurements, whether directly (Colour and Humic substances) or after colorimetry (proteins and polysaccharides). In order to avoid the interference of turbidity, all the samples are pre-filtered over a 0.45 μm cellulose acetate filter (Sartorius).

The main instrument used for these mesurements is a photospectrometer Milton roy spectromic 401. Only for the humic substances, the UV-VIS photo spectrophotometer Perkin-elmer Lambda 16 is used.

In details:

- COLOUR is measured as UV-absorption at 455 nm, in a 4 cm cell (Standard Methods, 1998). Results are given in terms of absorbance (cm^{-1})

- HUMIC SUBSTANCES are measured as UV-absorption at 254 nm, in a 1 cm quartz glass cuvette. The UV-absorption at this wavelength is typical of several compounds found in water and wastewater, such as lignin, tannic humic substances and various aromatic compounds, whereas other organics (e.g. carboxylic acids and carbohydrates) do not absorb significantly at this wavelength. For this reason, UV_{254} is often used as bulk indication of NOM or TOC in surface waters or reclaimed water (Lee *et al.*, 2004; Yuan *et al.*, 2002; Levine *et al.*, 1999), and as indication of humic substances in wastewater and effluent (Soffer *et al.*, 2000; Te Poele, 2006). Results are expressed in terms of absorbance (cm^{-1}).

- PROTEINS are measured according to the improved method of Te Poele, (2006). This method is a variant of the method of Rosenberg (2003), also a modified form of the method of Lowry *et al.* (1951) (see Appendix B). Absorption of the formed colour is measured at 750 nm in a 4 cm glass cuvette. The amount of proteins is expressed in mg/L.

- POLYSACCHARIDES: Also polysaccharides are measured according to the variation of Te Poele (2006) on the Rosenberg's method (Rosenberg, 2003) (Appendix B). The colorimetric method is based on Dubois *et al.*, (1956). The absorption of the formed colour is measured at 487 nm in a 4 cm glass cuvette. The amount of polysaccharides is expressed in mg/L.

Others

A few other common parameters are measured, for various purposes, using standard probes. A brief list is presented in Table 4.4.

Table 4.4: *Other monitored parameters measured by standard probes*

Parameter	Units	Probe
Turbidity	(NTU)	Turbidimeter Hach 2100 N
Conductivity	$(\mu S \cdot cm^{-1})$	WTW Cond 197i
pH	(-)	WTW pH 197i
Temperature	(°C)	contemporary reading from WTW Cond 197i and WTW pH 197i

Chapter 5

Filtration of raw wastewater

Several combinations of TMP, u_{cr} and backflush frequency are tested during filtration experiments of various durations. The effects on flux decline, fouling and permeate production are noted and discussed.

5.1 Short-term filterability at constant TMP

5.1.1 Short term filtration tests

Short-term filtration tests are conducted to investigate the role of the crossflow velocity u_{cr} and the transmembrane pressure TMP on the filterability of raw wastewater. Crossflow velocity and TMP are the main parameters to control the filtration process.

The standard test consists of 30 minutes of un-disturbed batch filtration at constant TMP. The duration is chosen for two reasons. The first is that this duration allows to conduct more experiments on the same wastewater sample during one day, which is deemed to obtain comparable results (see Paragraph 4.3.4). The second is that the the duration of a filtration run during UF of wastewater is usually shorter than 30 minutes; therefore this duration is sufficient to acquire information on the effect of u_{cr} and TMP in practice.

TMP values are set at 0.3, 0.5 and 1.0 bar; u_{cr} at 1.0, 1.5 and 2.0 $m \cdot s^{-1}$. During one day, 3 tests are performed on the same sample. One parameter (TMP or u_{cr}) is kept constant and the other is varied, which results in the two

series of test summarised in Table 5.1. The same membrane is used throughout both test series. Further details on the general procedure can be found in Paragraph 4.3.2.

Table 5.1: *Short term filterability tests at constant TMP, (July–August, 2004)*

Series	Testing day	u_{cr} $(m \cdot s^{-1})$	TMP (bar)
A	1	1.0	0.3 - 0.5 - 1.0
	2	1.5	0.3 - 0.5 - 1.0
	3	2.0	0.3 - 0.5 - 1.0
B	4	1.0 - 1.5 - 2.0	0.3
	5	1.0 - 1.5 - 2.0	0.5
	6	1.0 - 1.5 - 2.0	1.0

5.1.2 Water Quality

The quality of the feed water and the permeate during short-term experiments is shown in Table 5.2. The feed water is sampled at the start, the permeate at the end of the 30 min, in order to avoid dilution phenomena on the permeate side of the membrane module (see Paragraph 4.1.1).

Ortophosphates are measured in the filtrate of a 0.45 μm cellulose acetate membrane. The other parameters are analysed after filtration over a standard paper filter for suspended solids analyses, as described in Paragraph 4.5.

Table 5.2: *Quality of the feed water (soluble fraction) and permeate during short-term tests with raw sewage*

		Turbidity NTU	TSS mg/L	EC $\mu S/cm$	COD mg/L	NH_4^+ mgN/L	PO_4^{3-} mgP/L
Raw	mean	110.7	84.0	1328	222	39.5	4.7
	st.dev.	41.0	47.3	213	46	3.3	0.8
Perm.	mean	0.15	n.d	1276	138	39.4	4.0
	st.dev.	0.13	-	207	26	11.6	0.8

The wastewater can be qualified as typical medium-strength urban wastewater. Although the procedure for the analysis of the feed water is somewhat different, results are in agreement with the measurements of Evenblij *et al.* (2002) at the same location. It is noted that, as expected, the membrane guarantees a clear filtrate and is permeable to organics (COD) and nutrients (dissolved ortophosphates and ammonia).

Each day, during the first test, the EPS content is measured in the feed water and in the permeate. The permeate is sampled at the end of the 30 minutes filtration, to avoid dilution phenomena. Results for proteins and polysaccharides are shown in Figure 5.1.

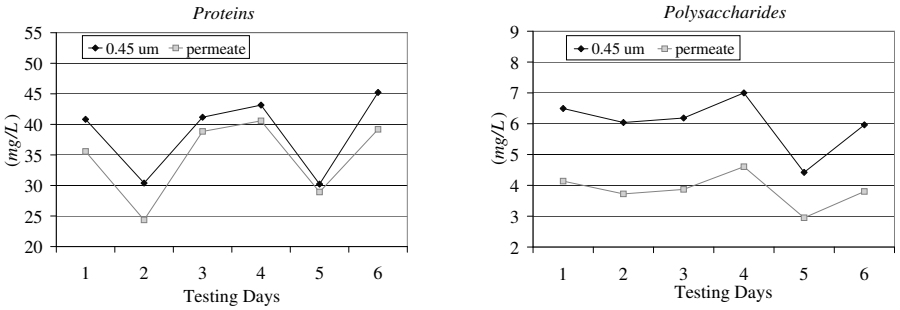

Figure 5.1: *EPS concentrations in the feed water and in the permeate during short-term tests with raw sewage*

A large fraction of the total EPS permeates the membrane, whereas the rest is rejected or involved in fouling. Retention varies in the range 7–22% for proteins and 33–38% for polysaccharides.

5.1.3 Flux decline

During 30 minutes of continuous filtration, the flux decreases strongly. The flux decline takes place for the major part during the first minutes and slows down in the following. This happens at all the applied combinations of TMP and crossflow velocity, but the amount of the flux drop and the final flux value depend on the applied conditions.

In Figure 5.2 three exemplary curves from series A are plotted.

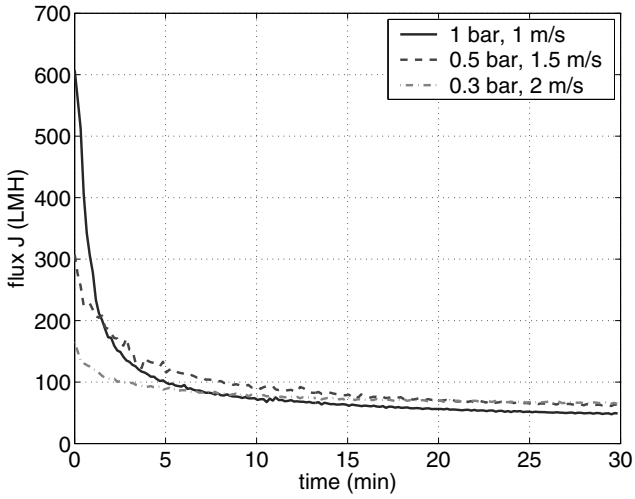

Figure 5.2: *Example curves of flux decline at the variation of* u_{cr} *and* TMP

The curves of Figure 5.2 represent the whole tested range of variations, as they correspond to the applied combinations that produce the most, the medium and the least fouling (1 *bar* & 1 $m \cdot s^{-1}$; 0.5 *bar* & 1,5 $m \cdot s^{-1}$; 0.3 *bar* & 2 $m \cdot s^{-1}$ respectively).

It can be noted that the differences originated by the imposed operating conditions are remarkable.

The specific effects of TMP and crossflow velocity are made visible in Figure 5.3 and Figure 5.4. Figure 5.3 shows curves obtained at constant u_{cr} during one day of test series A, whereas Figure 5.4 shows curves obtained at constant TMP during one day of test series B. In both cases, the three curves are obtained filtrating the same sample. "Middle" operating conditions are chosen to give an "average" visible quantification of the respective effects.

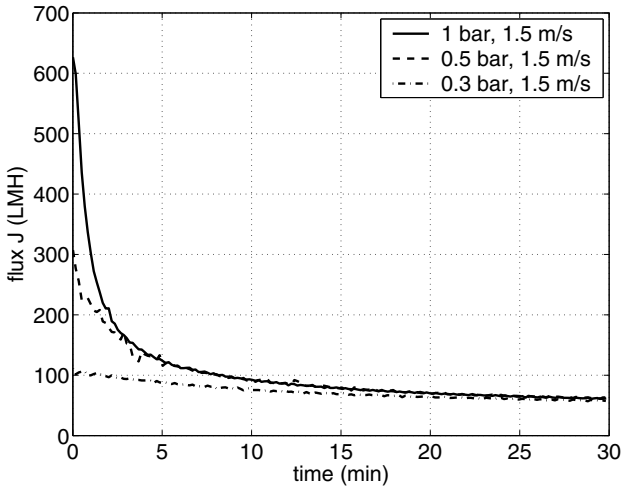

Figure 5.3: *Flux decline varying TMP when $u_{cr} = 1.5\ m \cdot s^{-1}$*

In Figure 5.3 it is visible that the applied TMP is responsible for the starting value of flux. For instance, the starting flux value at 1 bar is 627 LMH and at 0.3 bar is 111 LMH. This is an obvious consequence of the Darcy's Law (Equation 2.1), that dictates that the flux of non-fouled membranes is proportional to the applied TMP. Measured starting flux values do not exactly show this proportionality because of the influence of the membrane permeability and the inaccurate measurements at the very first instants of the filtration tests (see Paragraphs 4.3.2).

Flux values after 30 minutes are very similar.

Figure 5.4 shows the effect of crossflow velocity at equal TMP. The starting flux value is independent from the crossflow velocity, but after 30 minutes,

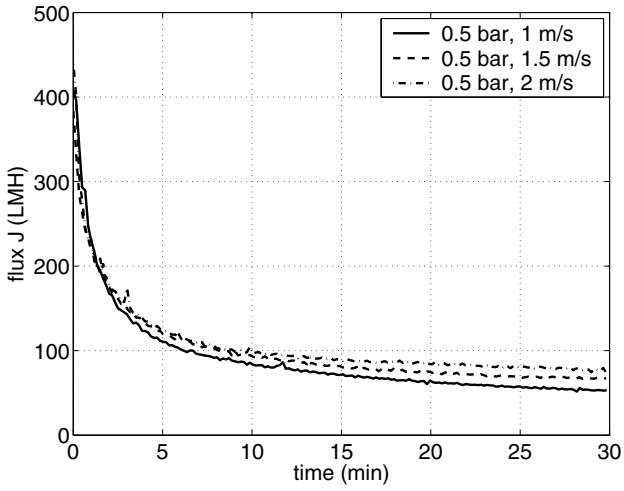

Figure 5.4: *Flux decline varying* u_{cr} *when* $TMP = 0.5$ *bar*

higher u_{cr} result in higher flux values.

The entire set of flux decline data from test series A and B is summarized in Table 5.3. The presented values are the starting flux J_{start} (i.e. the flux measured 10 seconds after switching the feed to wastewater) the final flux J_{end} and the flux drop ΔJ.

The reproducibility of the data seems acceptable, in the sense that the effect of the investigated parameters is clearly visible on the results.
Data confirm that:

- J_{start} is determined by the TMP;
- J_{end} is mainly influenced by u_{cr};
- at equal TMP increasing crossflow velocity increases J_{end};
- at equal u_{cr} a higher TMP produces a larger flux drop.

Table 5.3: *Overview of flux decline data during short-term filterability tests with raw sewage (July–August, 2004)*

Testing day	Series	TMP	u_{cr}	T	J_{start}	J_{end}	ΔJ
		(bar)	$(m \cdot s^{-1})$	$(^{\circ}C)$	(LMH)		
	A	1.0	1.0	21	607	46	561
a	A	0.5	1.0	21	343	40	303
	A	0.3	1.0	20	194	43	151
	A	1.0	1.5	21	627	55	572
b	A	0.5	1.5	21	307	49	258
	A	0.3	1.5	20	111	57	53
	A	1.0	2.0	21	668	64	604
c	A	0.5	2.0	20	227	72	150
	A	0.3	2.0	20	165	67	98
	B	1.0	1.0	21	646	51	595
d	B	1.0	1.5	21	782	66	716
	B	1.0	2.0	21	1054	74	979
	B	0.5	1.0	21	408	53	355
e	B	0.5	1.5	21	383	67	316
	B	0.5	2.0	20	439	73	366
	B	0.3	1.0	20	296	52	244
f	B	0.3	1.5	20	291	68	223
	B	0.3	2.0	20	248	81	167

5.1.4 Resistance increase

During the 30 minutes of filtration resistance increases continuously. Symmetrically to what was done with flux curves, the effect of TMP and u_{cr} on the resistance increase is clarified with the help of three figures.

Figure 5.5 gives an overview of the range of variations by plotting the curves with the most, the medium and the least fouling during series A. Figure 5.6 shows the separate effect TMP and u_{cr} at $u_{cr} = 1{,}5\ m \cdot s^{-1}$ and $TMP = 0,5$ *bar* respectively.

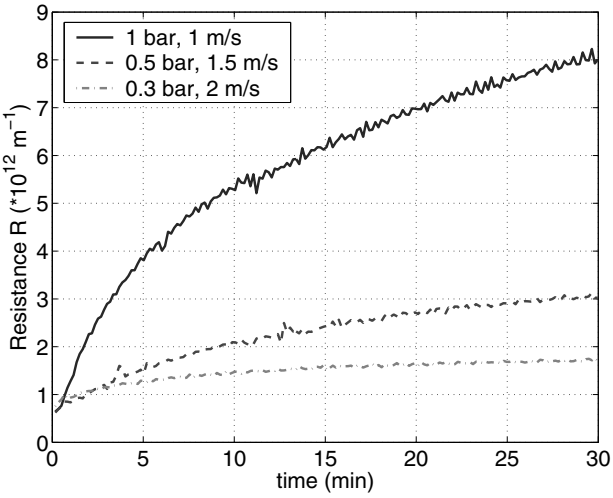

Figure 5.5: *Resistance increase with time: exemplary curves at various u_{cr} and TMP*

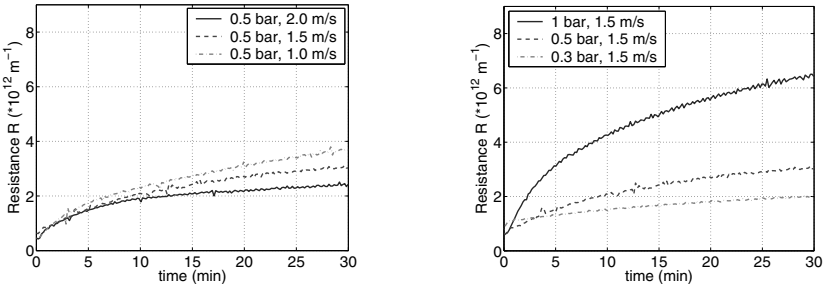

Figure 5.6: *Specific effect of variation of u_{cr} (left) and TMP (right)*

All the curves show a concavity downwards during the entire filtration period: the slope of $R(t)$ slows down with time. The variations of operating conditions affect both the overall resistance increase ΔR_{30} and the slope of $R(t)$. In details, increasing TMP increases both ΔR_{30} and the initial slope of $R(t)$, whereas increasing crossflow velocity reduces them.

Figure 5.7 summarizes the results from the whole test series A and B in terms of ΔR_{30}. ΔR_{30} values are plotted vs. the applied TMP, and values at the same crossflow velocity are linearly interpolated.

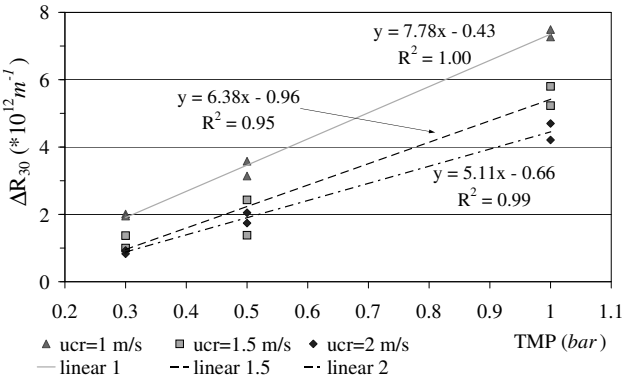

Figure 5.7: *Overall ΔR_{30} for all the tested combinations of u_{cr} and TMP*

Data show a good correlation with both TMP and u_{cr}. At a given crossflow velocity, the values of ΔR_{30} are proportional to the applied TMP. At a given TMP, ΔR_{30} values at higher u_{cr} are smaller. The slope of the trend line decreases with the applied u_{cr}, which indicates that sufficient crossflow velocity can reduce the fouling formation caused by TMP.

Data also show a good replicability of the experiments throughout the two series. Only one value of series B (0.5 *bar* & 1.5 $m \cdot s^{-1}$) lies outside the general trend. This fact could not be explained, the only hypothesis is that some experimental error occurred during the preparation of the feed solution.

5.1.5 Permeate production

The production of permeate is the aim of membrane filtration. The produced permeate volume results from the integration of flux with time; nevertheless, the analysis of the produced volume may provide additional information to what can be understood from flux curves.

A brief comparison among the effect of different operating conditions can be done considering the global production during the entire filtration period. This is shown in Figure 5.8, where the values of *specific produced volume* (SPV) of both test series A and B are presented. The SPV is the produced volume per square meter membrane ($L \cdot m^{-2}$). Values are grouped in triplets measured on the same sample.

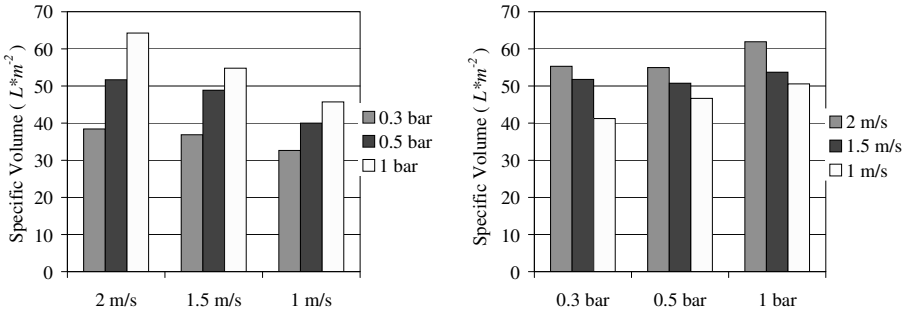

Figure 5.8: *Comparison of specific produced volume SPV at applied combinations of u_{cr} and TMP. Series A (left) and B (right)*

The SPV during 30 minutes varies between 33 and 64 $L \cdot m^{-2}$. Higher volumes are obtained with increasing values of TMP and u_{cr}. More precisely, at equal TMP, increasing u_{cr} increases SPV; at equal u_{cr}, increasing TMP increases SPV.

Further details are revealed in details in Figure 5.9, where the plots of cumulative permeate volume *vs.* time are shown.

At the beginning of the filtration interval, the curves at the same TMP are

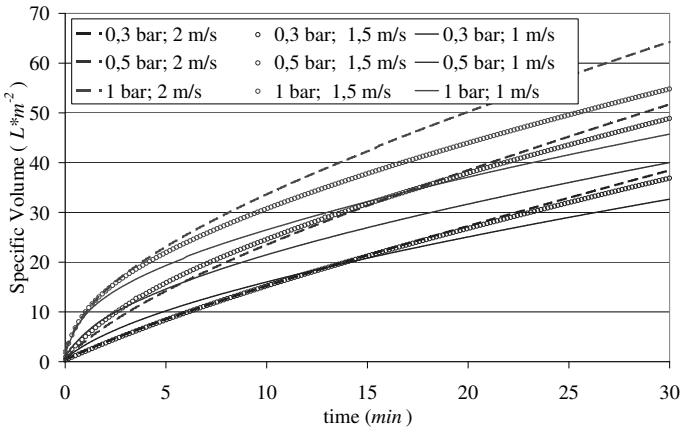

Figure 5.9: *Cumulative permeate volumes during test-series A*

grouped, independently from the crossflow velocity. In the last minutes, curves at the same u_{cr} tend to become parallel regardless of TMP values.

This means that the TMP value affects mainly the first minutes of filtration, as seen from flux decline curves when it was noted that the TMP determines J_{start}. On the opposite, the crossflow velocity has a stronger influence on J_{end} and affects permeate production only after a few minutes from the start.

5.1.6 Fouling development

As seen from flux and resistance curves, fouling is substantial and is affected by TMP and crossflow velocity. A further insight on fouling development is given by plotting filtration data in terms of *filtrated volume* and *shear stress*.

Resistance and filtrated volume

Plotting the resistance increase in terms of filtrated volume means to describe the fouling per produced unit permeate volume. Results are summarised using the usual three plots: Figure 5.10 shows the $R(vol)$ curves with the least, middle and most fouling from test-series A. Figure 5.11 shows the effects of crossflow velocity and TMP separately.

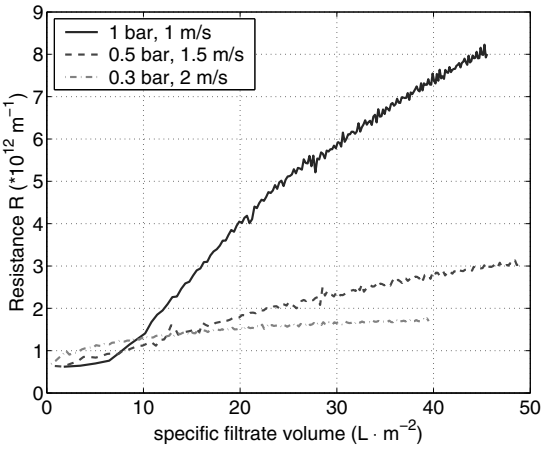

Figure 5.10: *Example curves $R(vol)$ at various u_{cr} and TMP*

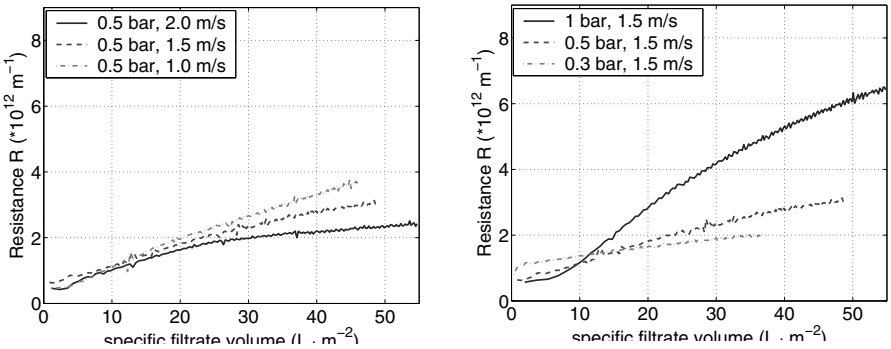

Figure 5.11: *Resistance increase at equal filtrated volume: effect of variation of u_{cr} (left) and effect of variation of TMP (right)*

The developments of the resistance increase per unit filtrated volume in the three cases of Figure 5.10 are different, which indicates that the larger ΔR_{30}'s observed at higher TMP values are not simply a consequence of the higher amount of filtrated volume. The fouling is quantitatively and maybe qualitatively affected by the applied values of TMP and u_{cr}.

The *filterability* depends on the applied conditions.

Figure 5.11 (left) shows that the crossflow velocity has two positive effects: to reduce the resistance increase at equal filtrated volume, and to increase the overall permeate production over the 30 minutes.

Figure 5.11 (right) reveals that the effect of increasing TMP is more complex. At the start, higher TMP values apparently produce less fouling per unit permeate volume. This is mainly a consequence of the larger volume filtrated before the membrane fouls. In the long term, higher TMP values produce bigger total volume but at the cost of a larger increase of resistance per unit volume produced.

Resistance vs. shear stress

During crossflow ultrafiltration the relation between permeate volume and deposited material is not obvious and is influenced by back-transport mechanisms. Back-transport depends on the feed water characteristics, the membrane characteristics and the flow velocity field of the solution (see Paragraph 2.4).

In a defined system like the one applied here, the velocity field results from the flux value and the crossflow velocity. More correctly, the crossflow velocity produces a shear stress "τ" at the membrane wall, through a non-linear relation.

For the set-up in use, the shear stress values corresponding to the applied crossflow velocity values have been calculated in Paragraph 4.3.3.

In Figure 5.12 the values of resistance increase at equal extracted volume ($30\ L \cdot m^{-2}$) are plotted versus the applied shear stress. Data originates from test-series A, and tests from series B yield analogous results.

Figure 5.12 shows that:

- the increase of shear stress τ reduces the resistance increase at equal filtrated volume consistently ;

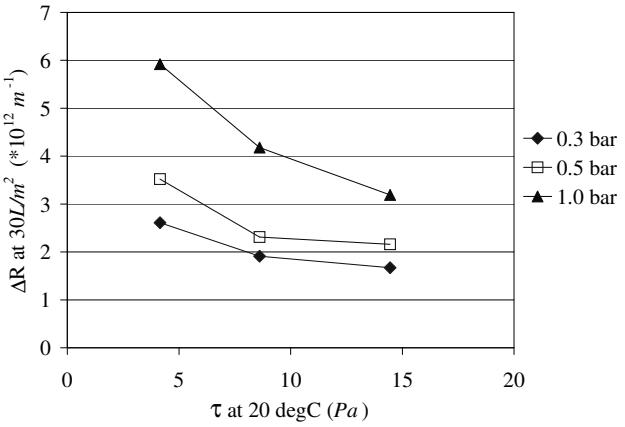

Figure 5.12: *Resistance increase vs. shear stress for different applied TMP at equal filtrated volume (30 L/m^2)*

- such positive effect becomes smaller at increasing values of τ: shifting from 4.2 Pa to 8.6 Pa, the reduction in ΔR_{30} is at least two fold than shifting from 8.6 to 14.5 Pa.;
- the effect is bigger at higher fouling conditions, i.e. at higher applied TMP.

5.1.7 Discussion of results

The extensive analysis of filtration data shows the fundamental influence of the operating conditions during ultrafiltration of untreated sewage. Despite the use of six different samples of wastewater, the course of filtration is mainly determined by the applied TMP and u_{cr}. This emerges from data about flux decline (Table 5.3) and resistance increase (Figure 5.7).

The trend of resistance R appears the most appropriate indicator to describe the filtration process. In fact, although the effects of TMP and u_{cr} are clearly

visible from flux data as well, the trend of resistance shows a smaller "dispersion" of results. The explanation is two fold:

- at the applied conditions, the initial membrane permeability has little effect on the development of resistance during 30 minutes, whereas it strongly affects the initial values of flux;
- when an experimental disturbance produces small oscillations in the TMP value, the flux value is affected directly, whereas the resistance is calculated from the ratio of TMP and flux and is therefore less sensitive to them.

The influence of the operating parameters on the course of filtration can be summarised as follows.

Increasing u_{cr} reduces fouling and therefore increases productivity, with effects visible a few minutes after the start of filtration. Differently, increasing TMP increases productivity and fouling as well. Therefore, the gain in productivity is obtained during the first minutes of filtration and decreases with time.

Such results are in agreement with previous researches on membrane filtration of untreated wastewater. Hao *et al.* (2006), found that during crossflow microfiltration increasing values of crossflow velocity from 2 to 3.7 $m \cdot s^{-1}$ always resulted in higher fluxes. However, they suggested a maximum value of TMP to maximize permeate production and avoid excessive fouling (1 bar at $u_{cr} = 3$ $m \cdot s^{-1}$). Ahn *et al.*,(1998) conducted 10 hours experiments again with crossflow ceramic membranes. They stated that: a) as the crossflow velocity increases, at pseudo steady-state the permeate flux increases and the total resistance decreases; b) at constant u_{cr} the highest TMP produces the highest initial flux, but soon the flux drops drastically and as time progresses it tends to converge.

The observed behaviours are also in agreement with theory. The crossflow velocity helps to reduce the fouling phenomena, because:

- it increases the turbulence of the flow, enhancing back-transport phenomenons;
- it produces a scouring effect on the wall of the membrane tubes, thus changing the equilibrium in the deposition and removal of particles

The effect of the applied TMP can be summarized as follows:

- higher TMP results in higher starting flux value J_{start} ;
- high flux values enhance the transfer of material toward the membrane;
- both internal and external fouling are increased. Higher permeation rate may enhance internal fouling because the drag force may overcome the double layer rejection (Song and Elimelech, 1995). Superficial fouling (filter cake) is enhanced as direct consequence of increased convection. Since wastewater filter cakes are typically compressible (Lojkine 1992; Roorda, 2003), increasing TMP has the double effect of increasing the mass of the deposit and its resistance.

The plots of resistance increase versus filtrated volume show that the occurrence of fouling is not a mere consequence of the filtrated volume: filterability and fouling characteristics depend on TMP and u_{cr} values.

In this case, knowing what fouling mechanisms occur would help to understand how to modify TMP and u_{cr} in order to reduce fouling effectively.

A first issue is whether fouling is internal or external, or both. Untreated wastewater can be expected to be rich in particles bigger than the membrane pore size (0.03 μm), as can be derived from particle size distribution data from other researches (see Table 5.4). In these conditions a thick cake layer will rapidly form, and the observed effect of crossflow velocity and TMP can probably be referred to changes in the characteristics of the filter cake. In particular, increasing crossflow velocity could be responsible for a thinner filter cake, whereas increasing TMP for increasing cake density.

However, the presence of a cake layer does not exclude the occurrence of other contemporary mechanisms. The presence of organic load in the permeate, indicated by the high COD and EPS concentrations, is a proof that organic macromolecules present in the feed water permeate through the pores and eventually originate internal fouling.

Fouling mechanisms will be further discussed through Paragraphs 6.5.2, 6.5.3 and 6.5.4.

A second issue concerns the selection of optimal operating conditions (TMP and u_{cr}) with respect to permeate production and fouling formation.

Table 5.4: *Example references of particle size distribution in raw wastewater*

Feed origin	Particles range	Remarks	Reference
resort	0.5-6.39 μm	no toilet-flushing	Ahn *et al.*, (1998)
septic tank	> 0.1 μm	up to 500 μm	Ahn and Song, (1999)
apartments	mainly $20 - 30$ μm	little < 0.2 μm	Hao *et al.*, (2005)
grey-water	mean size 0.1 μm	95 % volume particles > 5 μm	Ramon *et al.*,(2004)

The positive effect of TMP on productivity is mainly limited to the first minutes. At fixed crossflow velocity, after 5 minutes of filtration the fluxes generated at 1 or 0.5 *bar* are about the same. After 10 minutes, there is no more difference also with the flux generated at 0.3 *bar* (see for instance Figure 5.3). The corresponding resistance increase at 1 *bar* is double than at 0.5 *bar* and triple than at 0.3 *bar* (see Figure 5.5). The effect of crossflow velocity on productivity is almost negligible during the first 5 minutes (see Figure 5.9). Additionally, the reduction in resistance increase due to u_{cr} is less important at low TMP and decreases for increasing values of " τ " (see Figure 5.12).

From these observations it is concluded that the optimal operating conditions could be filtration runs a few minutes long, at not-too-high values of TMP. At these conditions a crossflow velocity of about 1.5 $m \cdot s^{-1}$ could be sufficient to control fouling. Obviously, these considerations will be subject to the efficiency of the cleaning procedure (backflush) to remove the generated fouling after each filtration run.

This issue will be investigated in Paragraph 5.2.

Finally, it is remarked that the flux decline observed at the chosen operating conditions is severe but not dramatic. 30 minutes of unstopped filtration resulted in final flux values of 40–81 LMH. During ultrafiltration of secondary effluent gross-flux values are in the range 25–60 LMH in case of hollow fibres and around 100 LMH in case of tubular membranes (Te Poele, 2006; Broens *et al.*, 2004; Roorda, 2004; Chalmers *et al.*, 2000; Van Houtte *et al.*, 1998).

Results appear encouraging, although with respect to the feasibility of direct ultrafiltration of raw sewage other issues need to be considered as well. First of all, the reversibility of fouling during long-term operation and the energy cost associated to crossflow velocity have to be investigated.

5.2 Extended filtration at constant TMP

Extended filtration tests are conducted to evaluate the feasibility of continuous operations, where "continuous operations" indicates the typical operating mode during ultrafiltration: productive runs are interrupted by short backflush periods.

The short-term tests of Paragraph 5.1 do not provide information about the reversibility of the fouling formed during the filtration period, therefore it is necessary to test how eventual residual fouling builds up cycle after cycle.

5.2.1 Aim and test series

A series of tests with duration of some hours is conducted at various values of TMP and u_{cr}. The duration of the filtration period and backflush period are varied, with the duration of the backflush always maintained approximately as 10 % of the filtration period. The aim is multifold:

- to investigate if continuous operations are sustainable in time;
- to investigate if productivity can be increased by selecting an appropriate filtration/backflush cycle.
- to investigate what is the minimum necessary crossflow velocity, as crossflow velocity affects the energy expenditure and hence the operational costs.

Initial conditions are set at low TMP (0.3 bar) and high crossflow velocity (2 $m \cdot s^{-1}$). The filtrating cycle is 10 minutes of filtration alternated to 1 minute of backflush, and the duration is progressively extended from 1 to 7 hours. In the following of the test series, the effect of operational parameters is investigated through daily comparative tests. Each day two tests of 3 hours are performed on the same sample, modifying only one parameter per time (TMP, u_{cr} and filtration cycle).

A summary of the investigated operating conditions is reported in Table 5.5.

Two different membrane modules are used. At the start of filtration, the membrane resistance R_{mem} is typically in the range 0.38–0.54 $\cdot 10^{12}$ m^{-1} for the

Table 5.5: *Overview of operating conditions during extended filterability tests at constant TMP (Testing Period: November 2004 - July 2005)*

TMP (bar)	u_{cr} $(m \cdot s^{-1})$	duration (h)	filtration time	backflush time
0.3	2	3-7	10 (min)	1 (min)
0.2; 0.3; 0.4	1; 1.5; 2	3	3 (min)	18 (s)
0.2; 0.3	2	3	1 (min)	5 (s)
0.3	2	3	1 (min)	5 (s) *idle*

first membrane module and 0.52–0.62 $\cdot 10^{12}$ m^{-1} for the second (corresponding CWF are approximately in the range 900-500 LMH/bar).

As the testing period extends from winter (November 2004) to summer (July 2005), the feed water temperature at the start of the tests varies from 14 to 23 °C. The corresponding variation in dynamic viscosity is about 30% (calculated using Formula 4.4), which impacts strongly over flux values. Considering also the variability of feed water quality, productivity results must be considered with caution.

5.2.2 Results

Sustainability of continuous operations

Relevant fouling occurs during each test, but operations sustainable in time appear possible. Apparently, at the proper conditions, fouling formation is substantial at the start but stops after 30-50 min of filtration.

Differences in the initial membrane resistance R_{mem} seem to have negligible effect already a few minutes after the start. At the applied conditions the total resistance R increases until 0.8–1.4 $\cdot 10^{12}$ m^{-1}, then stabilizes. Apparently, the additional resistance that builds up during each cycle is reversible and a stable gross-flux is achieved (hereafter, *pseudo-steady* flux).

In Figure 5.13 results of the test of 7 hours at $TMP = 0.3$ bar and $u_{cr} = 2$ $m \cdot s^{-1}$ are shown. The pseudo-steady flux is reached rapidly, within 30 minutes. The average resistance is below $0.8 \cdot 10^{12}$ m^{-1} and the gross-flux oscillates

between 125 and 105 LMH, decreasing during each filtration interval.

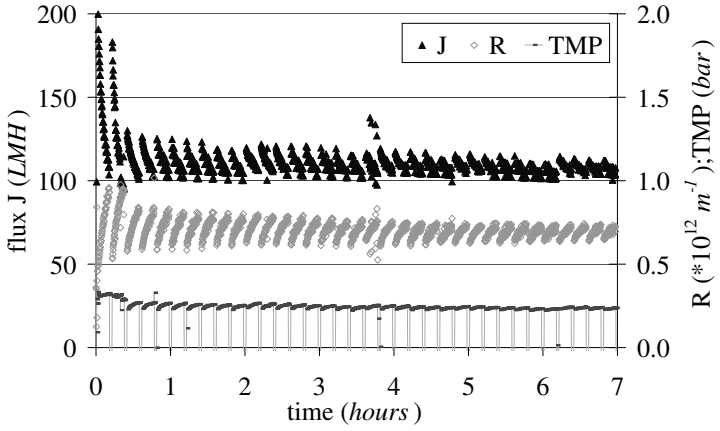

Figure 5.13: *Filtration of untreated sewage at 0.3 bar and 2 $m \cdot s^{-1}$ (10 min filtration - 1 min backflush)*

Figures from 5.14 to 5.16 show some plots of the comparative filtration tests of 3 hours (compared graphics are from the same day). The following findings are summarised:

- decreasing crossflow velocity increases fouling formation during each run; operations at $u_{cr} = 1.5\ m \cdot s^{-1}$ appear equally stable as at $u_{cr} = 2\ m \cdot s^{-1}$ (Figure 5.14), but not at $u_{cr} = 1\ m \cdot s^{-1}$;
- increasing TMP increases fouling formation at every crossflow velocity (Figure 5.15);
- increasing backflush frequency may help to reduce fouling (Figure 5.16);
- backflushing is strictly necessary to control fouling (Figure 5.16).

Productivity

The comparative tests show that the production of permeate varies with the operating conditions. As mentioned earlier, when data from different days are

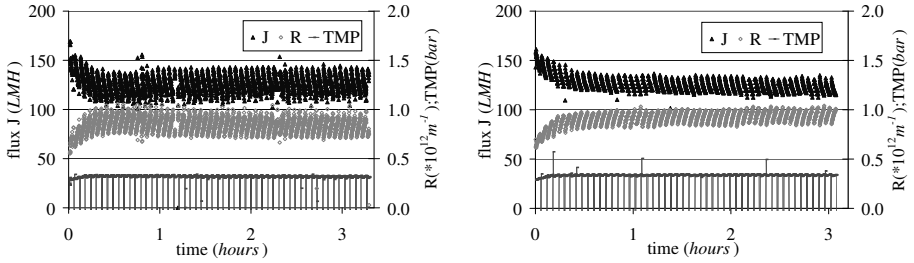

Figure 5.14: *Effect of crossflow velocity: filtration at 1.5 $m \cdot s^{-1}$ (left) and 2 $m \cdot s^{-1}$ (right) (0.3 bar; 3 min filtration + 18 sec backflush)*

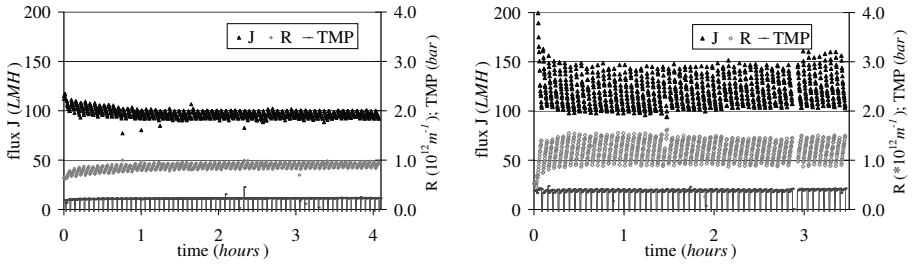

Figure 5.15: *Effect of TMP: filtration at 0.2 bar (left) and 0.4 bar (right) (1 $m \cdot s^{-1}$; 3 min filtration + 18 sec backflush)*

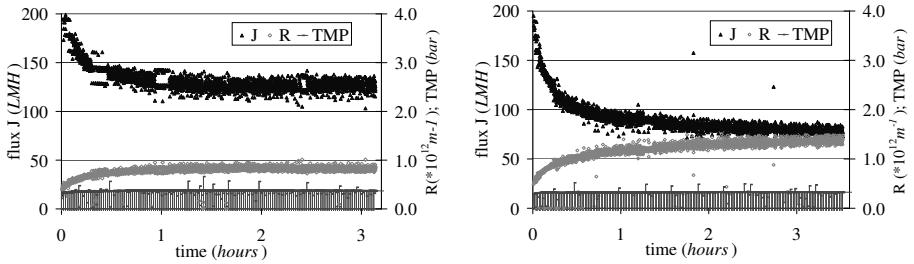

Figure 5.16: *Effect of backflush frequency: 1 min filtration + 5 sec backflush (left) and 1 min filtration + 5 sec idle (right) (0.3 bar, 2 $m \cdot s^{-1}$)*

considered, it is difficult to quantify the effect of varying crossflow velocity and backflush frequency, because of the variations in feed water temperature and filterability. Nevertheless, changes in TMP result in clearly appreciable variations of productivity.

The pseudo-steady gross flux values observed during the filtration period are in the range 70–80 LMH at $TMP = 0.2$ bar and 115–125 LMH at $TMP = 0.3$ and 0.4 bar. Therefore, increasing TMP from 0.2 to 0.3 bar is favourable to permeate production, whereas increasing TMP from 0.3 to 0.4 bar is not.

From the measured gross-flux, the net-flux can be calculated by considering the loss of permeate during backflush. Net-flux values are found around 40 LMH at $TMP = 0.2$ bar and 70–85 LMH at $TMP = 0.3$ and 0.4 bar. In particular, the highest value (85 LMH) is measured at $TMP = 0.3$ bar and 2 $m \cdot s^{-1}$ alternating 1 min of filtration and 5 sec of backflush.

5.2.3 Discussion

Sustainable operations are possible, not because fouling is avoided but because it is "controlled". Crossflow velocity and backflush play a fundamental role.

The development of resistance with time shows two distinct trends: an increase at the beginning, and a "*plateau*" with pseudo-steady flux at longer times. The initial fouling is irreversible with respect to backflush cleaning. On the opposite, at pseudo-steady state, the fouling that forms during the filtration period is constant and is entirely removed by the subsequent backflush. The hypothesis is that at this phase a dynamic balance is reached in the deposition and removal of fouling materials. In other words, for the considered time frame, the main fouling mechanism is a weak cake layer formed on the top of a more tenacious fouling.

The hypothesis of a weak reversible cake layer is supported by the observations on the effect of crossflow velocity and TMP. Higher crossflow velocity corresponds to lower fouling during the filtration interval because the shear stress would determine cake thickness and composition. Higher TMP would rapidly increase the resistance because of a higher specific cake resistance, although at the tested conditions the filter cake remains equally reversible.

It is interesting to remark that the characteristics of the dynamic cake layer and the consequent filtration performance are strongly dependent on the applied operating conditions:

- the pseudo-steady state at $TMP = 0.2\ bar$ has always lower gross-flux values and lower resistance values than pseudo-steady state at $0.3\ bar$. Since the transport of material to the membrane can be reasonably related to the permeate flux, and the resistance to the cake characteristics, it is evident that the cake characteristics do not depend on the permeate flux only but also on the applied TMP;

- during comparative tests, when the second test is conducted on the same wastewater sample of the first, similar results are obtained. This indicates that eventual modifications of feed water characteristics induced by recirculation (as mentioned by Hlavacek and Boucet, 1993; Visvanathan and Ben Aim, 1989; Ahn *et al.*, 1998; Rulkens *et al.*, 2005), are of minor importance with respect to operating conditions.

The best operating conditions with respect to productivity are found at $TMP = 0.3\ bar$ and $u_{cr} = 2\ m \cdot s^{-1}$, alternating 1 min of production to 5 sec of backflush. In terms of gross-flux, $TMP = 0.3\ bar$ seems the most appropriate because $0.2\ bar$ causes a loss in productivity and $0.4\ bar$ produces consistently more fouling during the filtration period. Although also this fouling appears reversible, the lack of gain in productivity suggests to prefer the lower TMP value.

In membrane processes the energy expenditure strongly affects the production cost per volume of produced permeate. In particular, in crossflow systems, the energy for recirculation is a large part of the total (see Chapter 9). Since filtration at $u_{cr} = 1.5\ m \cdot s^{-1}$ appears as stable as filtration at $2\ m \cdot s^{-1}$ with negligible decrease in productivity, $TMP = 0.3\ bar$ and $u_{cr} = 1.5\ m \cdot s^{-1}$ is suggested as the optimal filtrating conditions with respect to cost.

Sustainable operations with net-fluxes in the range 70–85 LMH are observed. When compared with the usual operating fluxes during ultrafiltration of municipal wastewater of secondary effluent (25–60 LMH in case of hollow

fibers and around 100 LMH in case of tubular membranes), these values appear noteworthy.

Additionally, when net-fluxes are considered, it must be remembered that the filtration procedure is not optimised. On the opposite, it gives a disadvantage to the less fouling operating conditions, as it overestimates the backflush requirements.

The loss of permeate volume during backflush ($Volume_{bf}$) is estimated on the basis of the resistance value at the end of the backflush (R_{bf}), as if this value was maintained during the entire duration of the backflush Δt. Equation 5.1 clarifies the calculation.

$$Volume_{bf} = J_{bf} \cdot \Delta t = \frac{TMP_{bf}}{\eta_p \cdot R_{bf}} \cdot \Delta t \tag{5.1}$$

The estimated $Volume_{bf}$ is larger when the resistance increase after backflush is smaller, i.e. when the irreversible fouling is smaller. This is the case at low TMP and high u_{cr}, which would likely require a "lighter" backflush.

Consequently, in this case the net-fluxes could be higher than calculated.

5.3 Conclusions

Ultrafiltration of untreated wastewater with tubular organic membranes is investigated through filtration tests at constant TMP with duration from 30 minutes to some hours. Aim of the experiments is to evaluate the influence of the operating conditions on filterability, and eventually to identify an adequate mode of operation. The parameters object of study are transmembrane pressure TMP, crossflow velocity u_{cr} and backflush frequency.

Continuous filtration experiments of 30 minutes reveal that the development of fouling with time, as well as the amount of fouling per unit volume produced, are strictly related to the applied conditions (u_{cr} and TMP).

The crossflow velocity clearly contributes to reduce the fouling. Increasing values of TMP increases the total permeate production during 30 minutes, but also the fouling.

When the same crossflow velocity is applied, the total resistance increase during 30 minutes is proportional to the TMP but not to the filtrated volume,

which may indicate the accumulation of a compressible layer at the membrane surface.

Longer tests, mostly of 3 hours duration, are conducted to asses the feasibility of continuous filtration using regular backflushing. Based on the observations of short-term tests, the TMP is set below 0.4 bar whereas u_{cr} values at 1, 1.5 and 2 $m \cdot s^{-1}$. Applied filtration periods are 10 minutes maximum.

Stable operations, sustainable in time, are obtained with a net permeate production in the range 70–85 LMH.

Fouling cannot be avoided but can be controlled thanks to the backflush and crossflow velocity. The resistance increases initially and reaches a pseudo-steady value after 30-50 minutes of filtration, according to the applied conditions and the feed water characteristics. Backflush appears strictly necessary to guarantee the reversibility of fouling at pseudo-steady state.

The optimal value of TMP, with respect to productivity and fouling increase, seems to be 0.3 bar. Apparently, operations at 1.5 $m \cdot s^{-1}$ guarantee the same process stability than at 2 $m \cdot s^{-1}$, without relevant loss in permeate production.

The reversibility of the fouling at the pseudo-steady state reinforces the hypothesis that shortly after the start the dominant fouling mechanism is cake filtration.

Chapter 6

Filtration Characteristics

Filtration curves obtained at different combinations of TMP and crossflow velocity are interpolated using traditional models for low pressure filtration adapted to crossflow systems. When accounted for the inaccuracy of the measurements, the cake filtration model most accurately describes the trend of flux decline and can be used to compare fouling behavior at different operating conditions.

6.1 Analysis of filtration curves

6.1.1 Introduction

The following analysis of filtration curves aims at evaluating the efficiency of classical filtration models to describe the fouling characteristics of crossflow ultrafiltration of raw wastewater.
For such a rich mixture as raw wastewater, the actual fouling mechanism is expected to be complex. Untreated wastewater transports particles, colloids and dissolved macromolecules, which interact with each other and with the membrane surface. Single molecules and aggregates may penetrate into the pores or adsorb or accumulate on the membrane surface. The transport and the aggregation of materials is also affected by the operating conditions,i.e. the transmembrane pressure, the hydrodynamic of the system and the temperature. Finally, the variability of the feed water may impact filtration performance.

The application of simple models may help to understand the characteristics of flux decline or at least to quantify it in comparable form. If relations within flux decline and the operating conditions can be established, this may

contribute to the development of an appropriate strategy to control fouling and optimise process performances.

6.1.2 Blocking Laws for constant TMP filtration

The expression "blocking laws" (or "classical model") refers to a group of models derived by the theory of filtration through porous media. These models disregard the actual mechanisms that originate or hamper the fouling, such us transport and chemical-physical interactions, and focus on the description of flux decline in relation to the changes around and on the membrane. They are typically used to interpret fouling development from a macroscopic point of view.

The set of blocking laws includes four different models: pore blocking (or complete blocking), intermediate blocking, pore constriction (or standard blocking) and cake filtration.
Complete pore blocking assumes that particles reaching the membrane singularly produce pore sealing, i.e. that each particle blocks one pore (internally or at the membrane surface) and that particles do not superimpose one over another. The number of "free" membrane pores is proportional to the convective transport of solute to the membrane surface. Also during *intermediate blocking* the single particle entering a pore is responsible for complete sealing, but superimposition of particles is allowed. Therefore, multi-layer deposit may occur. *Pore constriction* assumes that particles would penetrate the pores and depose internally, reducing the volume available for the flux flow. The overall available pore volume is proportional to the convection of solute to the membrane, which is proportional to the permeating volume. Finally, during *cake filtration*, a "cake" deposit forms on the membrane surface. This cake layer offers an additional resistance to the flux flow, proportionally to the cake mass and specific resistance. The overall cake mass is again proportional to the transport of particles to the membrane.

Historically, each model has been derived independently, as described in Bowen and Jenner (1995a). In the frame of power-law non-newtonian fluids, a general and compact analytical expression for dead-end filtration at constant pressure was firstly given by Hermia (1982).

Hermia's expression applies to constant pressure dead-end ultrafiltration, with the hypothesis that the permeation through the membrane can be de-

scribed by the Hagen-Poeiuseuille equation for laminar flow in cylindrical pores. In this case the application of Darcy's Law leads to the following general equation for flux decline:

$$\frac{dJ}{dt} = -kJ(J)^{2-n} \tag{6.1}$$

The coefficient "n" is a dimensionless constant that depends upon the occurring fouling mechanism. Correspondingly to the four classical models its value is as follows:

- $n = 2$: for pore blocking;
- $n = 1,5$: for pore constriction;
- $n = 1$: for standard blocking; and
- $n = 0$: for cake filtration.

A detailed description on how to derive these numbers from Equation 6.1 can be easily found in literature (Hermia, 1982; Van der Berg and Smolders, 1990; Lojkine, 1992; Roorda, 2004).

The constant "k" is known as *fouling coefficient* and its unit depends on the value of n. For each of the four models, k can also be written as the product of various parameters, accordingly to the physical interpretation of the involved fouling mechanism. This is explained in details in Paragraph 6.3.2.

6.1.3 Extension to crossflow filtration

Hermia's equation for dead-end filtration can be adapted to crossflow filtration as well. It is known that the positive effect of crossflow filtration on fouling is due to the enhancement of solute back-transport mechanisms, which reduce the net convection and thus the accumulation of foulants on the membrane surface. Therefore, a back-transport term J^* can be introduced in equation 6.1 to account for it. The result is the unifying equation for crossflow filtration, presented by Field *et al.* (1995):

$$\frac{dJ}{dt} = -k(J - J^*)(J)^{2-n} \tag{6.2}$$

The term J^* relates to the overall back-transport flux from the membrane, due to the crossflow velocity. However, its interpretation slightly differs in different works.

From Equation 6.1, when $J = J^*$, $dJ/dt = 0$. In the work of Field *et al.* (1995), this provides theoretical explanation for the concept of *critical flux*: at $J = J^*$, the velocity of the foulants toward and away from the membrane is equal and no fouling is formed, therefore J^* is the critical flux.

During constant flux operation, it is sufficient to maintain the extracted flux below this threshold to avoid fouling. During constant TMP operation, the starting flux value is normally higher than the "critical" value and the concept of a limiting threshold does not apply. Starting from a not-sustainable value the flux declines until a "terminal" value is reached, corresponding to a dynamical equilibrium between the fouling formation and removal rates. The flux decline ends because, at that flux value, the velocity of the foulants toward and away from the membrane are finally equal. Therefore J^* can be interpreted as the "terminal" flux at steady-state (Arnot *et al.*, 2000).

Whether J^* is viewed as limiting condition or as asymptotic terminal value, it is likely related to the effective velocity of solute mass transfer away from the membrane (Zeeman and Zydney, 1996; Hong and Elimelech, 1997; Yuan *et al.*, 2002).

6.2 Review on the application of blocking laws

6.2.1 Use of blocking laws

The blocking laws have been applied to a very broad range of feed waters. The highest number of studies considered protein fouling of synthetic water, prepared using Bovine Serum Albumin solutions (BSA). Other types of fouling that have been investigated include fouling by inorganic colloids, by NOM (synthetic or from surface waters), by oily-water emulsions and finally by wastewater (secondary effluent). Although the fouling mechanisms may differ strongly from case to case, the most of the listed components can be found in the raw wastewater; therefore all the findings of these studies should be considered.
Some example references are indicated in Table 6.1.

Table 6.1: *Application of blocking laws: example references*

Feed	Configuration	Membrane	References
BSA solution	dead-end	MF	Bowen *et al.*,(1995b)
	dead-end	MF	Ho and Zidney, (2000)
	dead-end	MF/UF	Iritani *et al.*,(1995)
	dead-end	MF	Jacob *et al.*,(1998)
	dead-end	MF	Hlavacek and Bouchet, (1993)
	dead-end	MF/UF	Tracey and Davis, (1999)
Whey proteins	dead-end	MF	Mourouzidis-Mourouzis and Karabelas,(2006)
Inorganic	dead-end	MF/UF	Kim *et al.*, (1993)
Colloids	crossflow	MF	Visvanathan and Ben Aim (1989)
	dead end	MF	Madaeni, (1998)
NOM solution	crossflow	NF	Kilduff *et al.*,(2002)
	dead end	MF	Yuan *et al.*,(2002)
	crossflow	NF	Hong et Elimelech,1997
	dead-end	UF	Katsoufidou *et al.*,(2006)
Oily-water emulsion	dead-end/ crossflow	MF	Arnot *et al.*, (2000)
Secondary effluent	dead end	MF	Fratila-Apachitei *et al.*,(2001)
	dead end	MF/UF	Laabs (2001)
	dead end	MF/UF	Roorda (2004)

The typical application of blocking laws is to fit a set of filtration data obtained in a small, well controlled environment (test-cells). Both dead-end and crossflow configuration are used, with a net prevalence for dead-end. The reason probably lies into two positive features of the dead-end system: a) it allows for a closed mass balance; and b) the process parameters can be estimated easily by linearized plot functions of volume V and time t (see for instance: Hermia, 1982; Bowen *et al.*, 1995b; Ho and Zidney, 2000; Arnot *et al.*, 2000). Using crossflow systems results in more uncertainties due to the variable feed concentration and characteristics over time, the less defined hydraulic conditions, the longer piping and the passage of the feed through the circulating pump.

Equation 6.1 and 6.2 can be exploited in the two following ways:

- "n" is assigned the value of one of the four models (0; 1; 1.5; 2) and the model is fitted to experimental data. The model that provides the highest fitting performance, usually in terms of correlation coefficient (R^2), indicates the occurring filtration mechanism.

- the general Equation 6.1 is fitted to filtration data and "n" is calculated; the value obtained is compared to the typical values of the four models.

The use of the first approach assumes that one single fouling mechanism is predominant during the entire filtration period. On the opposite, the second approach often shows that "n" is not constant but evolves during the filtration period, i.e. the predominant fouling mechanism varies with time and produced volume. Typically "n" moves from high to low values, corresponding to a shift from pore blocking or pore constriction to cake filtration. This has been observed for proteins (Bowen *et al.*, 1995b; Ho and Zidney, 2000), for colloids (Madaeni, 1998), for secondary effluent (Fratila Apatichei et al., 2001) and for NOM (Yuan et al., 2002).

Some authors advise that the use of the blocking laws alone is insufficient to determine the occurring fouling mechanism.
The first approach would be incomplete because a succession or a mixture of fouling mechanism may occur (Kim *et al.*, 1992; Jacob *et al.*, 1998; Katsoufidou *et al.*, 2005). The second approach may lead to dubious results: Iritani *et al.* (1995) report that in the case of deeply internally fouled membranes "n" can decrease to negative values, theoretically unexplained. Hlavacek and Bouchet (1993) affirm that in general the overlapping of different fouling mechanisms may originate the same flux declining curve and consequently a good fit does not necessarily identify the fouling mechanism.

Despite these warnings, nowadays the blocking laws and the derived models (e.g. the "Ho and Zidney" model), are considered "well grounded" knowledge and represent the preferential tool for the interpretation of filtration data.

The aim of the application of blocking laws has turned two-fold: supporting the identification of the predominant fouling mechanisms and quantifying the fouling in a comparable way (Arnot, 2000; Laabs, 2001; Kilduff, 2002; Roorda, 2004; Katsoufidou *et al.*, 2005). In order to improve the reliability of conclusions, the results of the modeling are usually accompanied by side analyses like

foulants permeation rate, membrane autopsy and SEM (Scanning Electron Microscopy).

6.2.2 Main Findings

With respect to the study presented here, the relevant findings from the articles of Table 6.1 are summarized in the following:

- the *relative size* of the membrane pores with respect to possible fouling materials (particle, colloids, macromolecules or solutes), is essential to determine whether fouling will occur internally or externally. The wider the pore size distribution of the membrane and the particle size distribution of the feed water, the higher the possibility of coexisting or successive fouling mechanisms (Madaeni 1998, Kim *et al.*, 1993; Iritani *et al.*, 1995; Yuan and Zidney, 2000).

- the *particles size distribution* of transported solutes can vary because of shear conditions. Proteins aggregates can be modified by shear through feeding pumps or pores (Hlavacek and Boucet, 1993); shear can induce aggregation of inorganic colloids which may form "bridges" around membrane pores (Visvanathan and Ben Aim, 1989).

- *permeation drag and shear* affect fouling characteristics. High initial permeation rate increases flux drop substantially, as reported for inorganic colloids (Kim *et al.*, 1993; Madaeni, 1998), NOM (Hong and Elimelech, 1997; Yuan *et al.*, 2002), domestic wastewater (Ahn *et al.*, 1998), and proteins (Iritani *et al.*, 1995; Ho and Zidney, 2000). Song and Elimelech (1995) explain that the permeation drag may overcome the electrostatic repulsion between particles and membrane. Iritani *et al.* (1995) show that the transition from initial pore blocking to cake filtration is accelerated at higher pressure. Velasco *et al.* (2003), note that during dead-end MF of BSA, increasing pressure changes the value of "n", thus the occurring fouling mechanism.

  Kim *et al.*(1993) noted that in the case of silver colloids, reducing concentration polarization may promote the transport of fine particles into the membrane pores. During ultrafiltration of paper mill wastewater and activated sludge, Choi *et al.*(2005) observed that higher tangential flow caused slightly higher irreversible fouling due to higher permeation drag.

- a simple *analysis of the curves R vs. time* is a valid tool to evaluate the fouling coefficient "n" (Koltuniewicz, *et al.*, 1995; Arnot *et al.*, 2000; and Ho and Zidney, 2000). When dR/dt is > 0 with decreasing slope with time, the equation of Field's general model (equation 6.2) requires that "n" is strictly < 1. This excludes pore blocking and pore constriction as dominant fouling mechanisms when the plot of R *vs. time* is concave downwards.

6.3 Fitting of Flux Curves

6.3.1 Aim and methodology

The object of the work is to investigate if any of the blocking laws can satisfactorily describe the observed curves of flux decline, and eventually clarify or quantify the effect of the operating conditions (u_{cr} and TMP) emerged in Chapter 5.

This work follows the approach of assigning to "n" the value of one of the models and fitting the corresponding equation to the experimental data. Three of the blocking laws are applied: pore blocking, pore constriction and cake filtration. These three models are chosen because they correspond to clearly distinct fouling mechanisms: at the pores entrance (pore blocking), on the membrane surface (cake) or internally (pore constriction). If one model appeared prevailing, this may help to improve strategies for fouling control.

The source data are the time, volume and flux values of the filtration tests presented in Chapter 5. Between series A and B, only one set of data is used per each couple of operating conditions: the set with the more accurate measurements. All measured values are used, without any preliminary smoothing of the datasets; only a few very "obvious" outliers have been removed.

The fitting is conducted on three time intervals: the entire filtration period of 30 minutes, the first 5 minutes and the last 20 minutes. This is done to account for the findings that the fouling mechanism may vary while the filtration process is ongoing: splitting the rapid flux drop of the first 5 minutes from the pseudo-steady final part may help to emphasize this variation.

It is remarked that the quality of the feed water during the filtration experiments is not constant, because the tests were conducted using wastewater sampled in different days.

6.3.2 Fitting Procedure

The three classical models for cross-flow filtration are used in the forms presented by Kilduff *et al.* (2002), reported in Table 6.2.

Table 6.2: *Equations for models fitting, from Kilduff et al. (2002)*

Model	Fitting equation
Pore blocking	$J = (J_0 - J^*) \cdot exp\left(-\frac{J_0 \alpha_{pb} C_b}{N_0 \pi r_p^2} t\right) + J^*$
Pore Constriction	$J = J^* \left(\frac{\left[1 + \frac{\sqrt{J_0} - \sqrt{J^*}}{\sqrt{J_0} + \sqrt{J^*}} exp\left(-\frac{2\sqrt{J_0 J^*}}{r_0^2} \frac{\alpha_{pc} C_b A_m}{\pi \delta_m}\right)\right]}{\left[1 - \frac{\sqrt{J_0} - \sqrt{J^*}}{\sqrt{J_0} + \sqrt{J^*}} exp\left(-\frac{2\sqrt{J_0 J^*}}{r_0^2} \frac{\alpha_{pc} C_b A_m}{\pi \delta_m}\right)\right]} \right)^2$
Cake filtration	$J = \left[\frac{\alpha_c C_b A_m}{J_0 R_m}\left(\frac{V}{A_m} - J^* t\right) + \frac{1}{J_0}\right]^{-1}$

In Table 6.2:

- α_c : average specific cake resistance $(m \cdot kg)^{-1}$;
- α_{pb} : average pore blocking parameter, i.e. number of pores blocked per unit mass of solute transferred to the membrane surface $(m^2 \cdot kg^{-1})$;
- α_{pc} : average pore constriction parameter, i.e. volume of pores blocked per unit mass of solute transferred to the membrane surface $(m^3 \cdot kg^{-1})$;
- A_m : permeable membrane area (m^2);
- C_b: bulk solution concentration $(kg \cdot m^{-3})$;
- δ_m : membrane thickness (m^{-1});
- J_0 : starting flux at $t = 0$ (LMH);
- N_0 : number of cylindrical pores per unit membrane area $(pores \cdot m^{-2})$;

- r_p : equivalent pore radius (m);
- R_m : membrane resistance (m^{-1}); and
- V : produced permeate volume (m^3).

Since not all the parameters indicated in Table 6.2 are known, they are aggregate into the *fouling rate constant* "k_i", as indicated in Table 6.3. Consequently, the equations actually used for the fitting are as reported in Table 6.4.

Table 6.3: *Aggregate constants α_i as used during curves fitting*

	Pore Blocking	Pore Constriction	Cake filtration
Constant	$k_{pb} = \frac{\alpha_{pb} \cdot C_b}{N_0 \pi r_p^2}$	$k_{pc} = \frac{\alpha_{pc} \cdot C_b}{(r_p^2 \pi \delta_m)}$	$k_c = a_c \cdot C_b$
Units	m^{-1}	m^{-3}	m^{-4}

Table 6.4: *Equations in use during models fitting*

Model	Fitting equation
Pore blocking	$J = (J_0 - J^*) \cdot exp\left(-J_0 * k_{pb} * t\right) + J^*$
Pore Constriction	$J = J^* \left(\frac{\left[1 + \frac{\sqrt{J_0} - \sqrt{J^*}}{\sqrt{J_0} + \sqrt{J^*}} exp\left(-\frac{2\sqrt{J_0 J^*}}{r_0^2} * k_{pc}\right)\right]}{\left[1 - \frac{\sqrt{J_0} - \sqrt{J^*}}{\sqrt{J_0} + \sqrt{J^*}} exp\left(-\frac{2\sqrt{J_0 J^*}}{r_0^2} * k_{pc}\right)\right]} \right)^2$
Cake filtration	$J = \left[k_c * \frac{A_m}{J_0 R_m}\left(\frac{V}{A_m} - J^* t\right) + \frac{1}{J_0}\right]^{-1}$

The fitting is realized by minimising the squared residuals between the measured flux values and the model estimations. Because of the characteristics of the equations, non-linear least square methods are used. To this purpose, a specific *Excel*© spreadsheet has been prepared for each model. Using the function

"solver" a preliminary estimation of the model parameters is obtained. This estimation is used as input values for a *Matlab*© function for more accurate evaluation. One example of the *Matlab*© functions is available in Appendix C.

Differently from Arnot *et al.* 2000, during fitting the starting value of flux J_0 is not free to oscillates but is fixed equal to the CWF value measured before the filtration test. This is done because J_0 has a strong influence on the results of the fitting. Since occasional errors may occur also during CWF measurements, when the CWF value results lower than the actual measured flux at the start of filtration J_{start} this procedure is disregarded and J_{start} is taken as J_0. This happened only in one case (0.3 bar, 2 $m \cdot s^{-1}$.

The procedure resolves into the estimation of 2 parameters: "k_i" and J^*. The first is the *fouling rate constant* reported in Table 6.3, the second represents the global back-transport mechanism(s). Since k_i is the product of some constants for the model-specific parameter α_i (see Table 6.3), hopefully it can be related to the fouling development and to the operating conditions. The same is valid for J^*, that is expected to relate to the crossflow velocity and eventually to the final flux value.

6.3.3 Presentation of results

The results of the fitting are presented in graphical and numerical form.

The graphical representation is limited to three Figures, corresponding to the operating conditions that produce the maximum, the "middle" and the minimum fouling (1 bar & 1 $m \cdot s^{-1}$; 0.5 bar & 1.5 $m \cdot s^{-1}$; and 0.3 bar & 2 $m \cdot s^{-1}$ respectively).

Hereafter, these operating conditions will be referred to as "high fouling" "middle fouling" and "low fouling".

The numerical results are summarized in one Table that includes the estimated parameters J^* and k_i, the correlation coefficient R^2 and the Sum of Squared Residuals SSe.

6.4 Fitting results

6.4.1 Overall fitting

In Figure 6.1, Figure 6.2 and Figure 6.3, the plots resulting from the fitting of the three fouling models are shown. Starting from the same point J_0 , the three fitting curves show remarkably different slopes and curvatures.

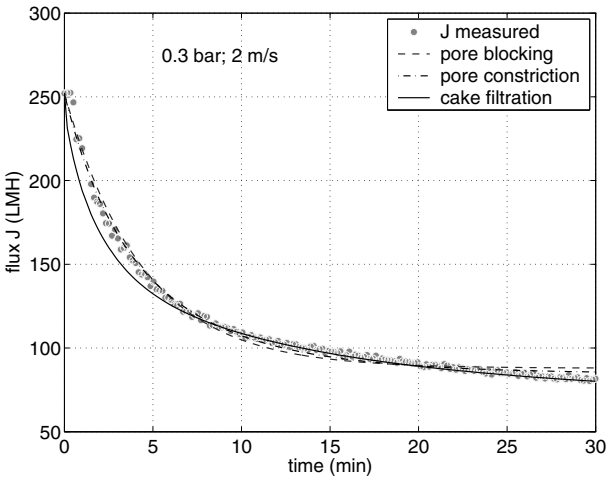

Figure 6.1: *Fitting of filtration data with blocking laws, TMP = 0.3 bar and* $u_{cr} = 2m \cdot s^{-1}$

At low fouling conditions (Figure 6.1), the pore narrowing and the pore blocking curves adapt to the measured points better during the first minutes of filtration, whereas the cake model is the only one that "catches" the trend of flux decline at longer times.

At middle fouling conditions (Figure 6.2), the cake model suits the flux decline very well during the entire period, whereas the other two show a delayed decline at the beginning and an unrealistic horizontal asymptotes during the second half of the filtration test.

At high fouling conditions (Figure 6.3), the pore blocking model performs

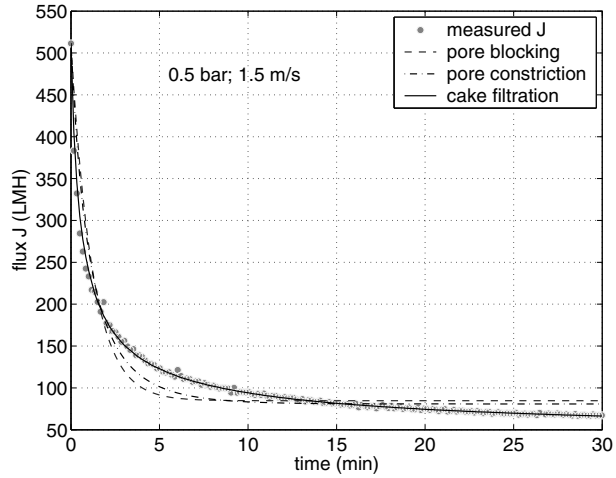

Figure 6.2: *Fitting of filtration data with blocking laws, TMP = 0.5 bar and* u_{cr} *= 1.5* $m \cdot s^{-1}$

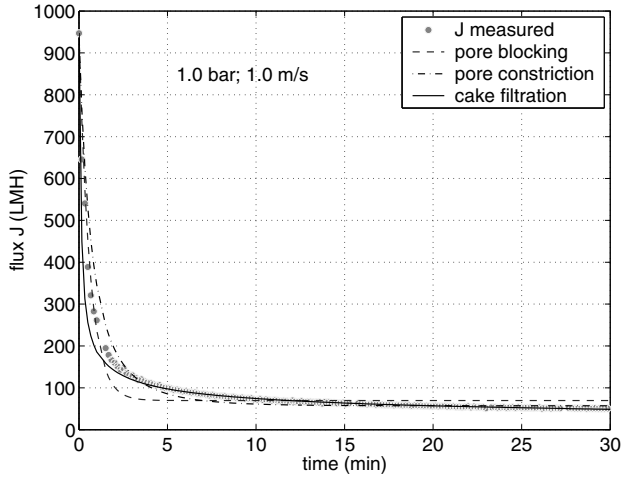

Figure 6.3: *Fitting of filtration data with blocking laws, TMP = 1.0 bar and* u_{cr} *=1* $m \cdot s^{-1}$

better during the first rapid flux drop (duration about 1 min). However, after minute 10, the pore blocking and the pore constriction curves have a horizontal trend again, whereas the cake curve reproduces the measured points adequately.

It appears that for the first minutes of filtration fitting results are contradictory. Concerning the second half of the filtration run, experimental values are well matched by the cake model, whereas pore constriction and pore blocking fail to predict the endless decline of flux and estimate constant flux values.

From a mathematical point of view, the results of the fitting are presented in Table 6.5.

The pore constriction model shows the highest average value for R^2: 0.962 vs. 0.940 of the pore blocking and 0.920 of the cake model. The squared residuals are in the order of 10^3–10^5 LMH^2 for all models.

The best fitting is obtained 3 times by the cake model, 5 times by the pore narrowing model and 2 times by the pore constriction model (pore narrowing and pore blocking are first ex-equo at $TMP = 1\ bar$, $u_{cr} = 1\ m \cdot s^{-1}$).

Results are difficult to interpret, as no model fits all the filtration curves better. Additionally, the fitting results of the models appear independent from the operating conditions.

Also the estimated model parameters J^* and k_i show little relation to the applied operating conditions.

The values of J^* vary within the interval 20–92 LMH, except in one case (cake filtration at $TMP = 0.3\ bar$, $u_{cr} = 1.5\ \ m \cdot s^{-1}$, but this value originates from a relatively bad set of measurements). J^* are generally higher at high crossflow velocity, but not always.

k_i, relates rather to the applied TMP than to the crossflow velocity. For the cake filtration model, k_i always increases with TMP. For the pore narrowing and pore blocking model, the same trend is valid at $u_{cr} = 1\ m \cdot s^{-1}$ and $1.5\ m \cdot s^{-1}$ but not at $2\ m \cdot s^{-1}$.

Table 6.5: *Estimated model parameters and statistics during 30 min filtration*

	u_{cr}	TMP	J^*	k_i [(a)]	R^2	SSe
Cake	$(m \cdot s^{-1})$	(bar)	(LMH)	$\cdot 10^{10}$ (m^{-4})	(-)	$\cdot 10^3$ $(LMH)^2$
	1	0.3	26.2	88	0.956	17
	1	0.5	20.9	120	0.986	10
	1	1.0	27.3	340	0.918	130
	1.5	0.3	3.1	35	0.842	110
	1.5	0.5	52.2	140	0.996	2.2
	1.5	1.0	50.5	280	0.895	180
	2.0	0.3	63.5	5.4	0.983	3.9
	2.0	0.5	71.8	150	0.980	12
	2.0	1.0	52.5	200	0.724	840
Pore Constrict.	$(m \cdot s^{-1})$	(bar)	(LMH)	(m^{-3})	(-)	$\cdot 10^3$ $(LMH)^2$
	1	0.3	57.2	0.63	0.986	5.5
	1	0.5	67.0	0.71	0.968	23
	1	1.0	64.6	0.89	0.977	37
	1.5	0.3	57.8	0.31	0.932	45
	1.5	0.5	80.9	0.81	0.926	43
	1.5	1.0	81.4	0.85	0.967	56
	2.0	0.3	84.7	0.42	0.989	2.4
	2.0	0.5	89.0	0.81	0.961	24
	2.0	1.0	85.9	0.59	0.950	150
Pore Blocking	$(m \cdot s^{-1})$	(bar)	(LMH)	(m^{-1})	(-)	$\cdot 10^3$ $(LMH)^2$
	1	0.3	61.0	0.076	0.971	11
	1	0.5	71.6	0.084	0.932	51
	1	1.0	69.8	0.104	0.943	92
	1.5	0.3	66.7	0.040	0.942	39
	1.5	0.5	84.7	0.097	0.871	75
	1.5	1.0	86.2	0.099	0.945	93
	2.0	0.3	87.9	0.054	0.982	4.1
	2.0	0.5	92.2	0.097	0.972	45
	2.0	1.0	92.4	0.068	0.950	150

[(a)] $= \alpha_c$ for cake model, α_{pb} for pore blocking, α_{pc} for pore constriction

6.4.2 Fitting during minutes 0-5

When the initial part of filtration is considered, the worse part of the data set is used. At the start of filtration, the permeate flux is high and readily transports fouling material to the membrane surface. At the same time, the flow inside the membrane module is unsteady because the feeding has just been switched from one tank (clean water) to another (raw sewage) and the TMP may oscillate. This leads to the not desirable situation that the initial points have high absolute values and sometimes are also very dispersed, as for example in Figure 6.4. For this reason, the algorithm used for the fitting showed some problems to converge, and a more robust function had to be written to fit the data with the cake model.

The fitting results are presented in Figure 6.4, Figure 6.5, Figure 6.6 and Table (6.6).

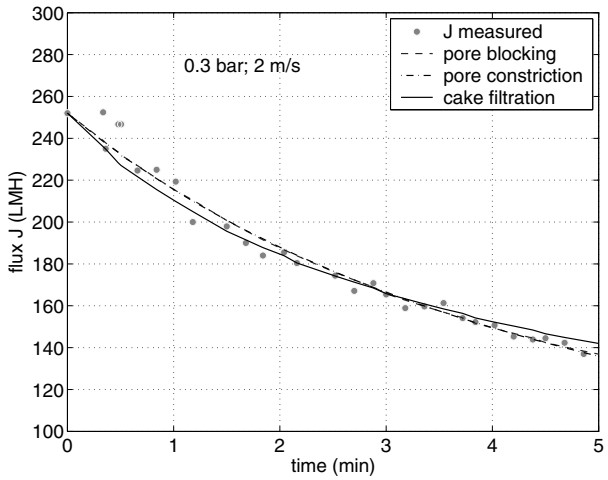

Figure 6.4: *Fitting of filtration data with blocking laws, minute 0–5, TMP = 0.3 bar and* $u_{cr} = 2\ m \cdot s^{-1}$ *(two curves almost overlapping)*

At low fouling conditions, the curves obtained with the three models are very similar, although the cake model exhibits a slightly more pronounced bending (Figure 6.4) and pore blocking and pore constriction almost overlap. At middle and high fouling conditions, the pore blocking and pore constriction model

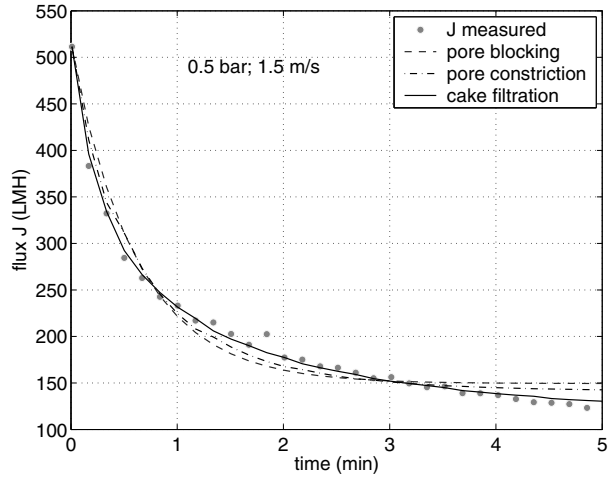

Figure 6.5: *Fitting of filtration data with blocking laws, minute 0–5, TMP = 0.5 bar and* $u_{cr} = 1.5\ m \cdot s^{-1}$ *with blocking laws*

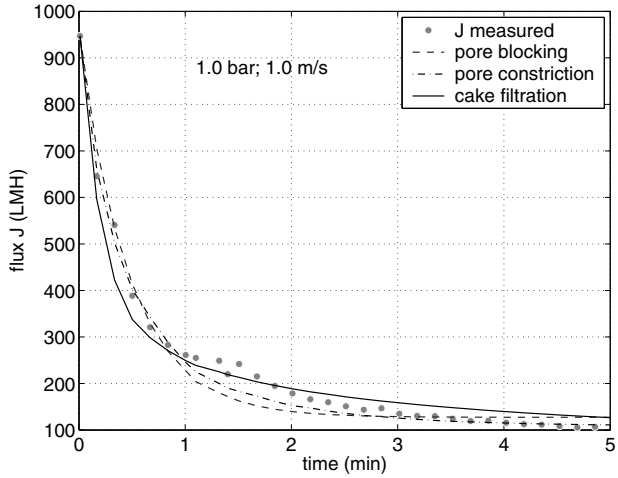

Figure 6.6: *Fitting of filtration data with blocking laws, minute 0–5, TMP = 1.0 bar and* $u_{cr} = 1\ m \cdot s^{-1}$

exhibit a peculiar trend (Figure 6.5 and Figure 6.6). The modelled curves compromise between the rapid flux decline of the first points, "heavy" in terms of fitting, and the last points of the fitting interval. Consequently the last data points are fitted with a non-realistic horizontal asymptote, similarly to the results obtained when fitting the entire data set (Paragraph 6.4.1).

The pore constriction and the the pore blocking model have a clearly higher average value for R^2: 0.975 and 0.974 vs 0.938 of the cake model. However, when considering the single plots, results are scattered: the highest R^2 is obtained 4 times by the pore constriction, 3 times by the pore blocking and twice by the cake model.
Despite only one sixth of the entire data set being considered, the squared residuals are in the order of 10^3 - 10^5 LMH^2. This is the same range for the fitting of the entire filtration run, which indicates that most of the "unexplained" residuals belongs to the initial phase.

Concerning the estimated parameters, it is difficult to recognize any trend. It can be noted that in the case of the cake model J^* is almost always zero, which indicates that the application of the model is troublesome. Values of k_i usually increase with TMP.

Table 6.6: *Estimated model parameters and statistics during min 0–5*

	u_{cr}	TMP	J^*	k_i [(a)]	R^2	SSe
Cake	$(m \cdot s^{-1})$	(bar)	(LMH)	$\cdot 10^{11}$ (m^{-4})	(-)	$\cdot 10^3$ $(LMH)^2$
	1	0.3	0.0	6.1	0.926	7.7
	1	0.5	0.0	10	0.981	5.1
	1	1.0	0.0	22	0.955	49
	1.5	0.3	0.0	1.7	0.901	7.1
	1.5	0.5	87.1	17	0.995	1.0
	1.5	1.0	0.0	18	0.909	94
	2.0	0.3	0.0	2.0	0.968	0.9
	2.0	0.5	0.0	9.5	0.987	4.9
	2.0	1.0	0.0	11	0.821	250
Pore Constrict.	$(m \cdot s^{-1})$	(bar)	(LMH)	(m^{-3})	(-)	$\cdot 10^3$ $(LMH)^2$
	1	0.3	42.2	0.603	0.974	2.7
	1	0.5	110.0	1.000	0.993	1.8
	1	1.0	107.9	1.090	0.996	4.6
	1.5	0.3	57.3	0.366	0.928	5.2
	1.5	0.5	141.3	1.480	0.978	4.7
	1.5	1.0	121.3	1.030	0.980	21
	2.0	0.3	76.6	0.408	0.984	4.1
	2.0	0.5	133.9	1.202	0.9983	4.3
	2.0	1.0	105.3	0.685	0.960	53
Pore Blocking	$(m \cdot s^{-1})$	(bar)	(LMH)	(m^{-1})	(-)	$\cdot 10^3$ $(LMH)^2$
	1	0.3	78.0	0.097	0.977	2.4
	1	0.5	126.0	0.130	0.988	3.4
	1	1.0	127.2	1.132	0.989	12
	1.5	0.3	101.0	0.059	0.925	5.4
	1.5	0.5	149.3	0.188	0.957	4.9
	1.5	1.0	141.8	0.125	0.986	1.4
	2.0	0.3	102.5	0.069	0.957	1.3
	2.0	0.5	145.1	0.016	0.981	4.9
	2.0	1.0	152.5	0.102	0.995	4.0

[(a)] $= \alpha_c$ for cake model, α_{pb} for pore blocking, α_{pc} for pore constriction

6.4.3 Fitting during minutes 10-30

When only the results of the last 20 *min* (10–30) are used, the more stable part of the data set is considered for the fitting. Results are shown in the usual three plots (Figure 6.7, 6.8 and 6.8) and in Table 6.7.

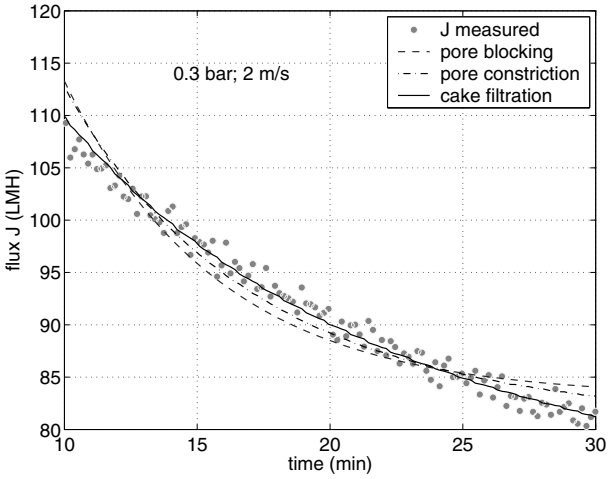

Figure 6.7: *Fitting of filtration data with blocking laws, minute 10–30, TMP = 0.3 bar and* $u_{cr} = 2\ m \cdot s^{-1}$

From visual inspection, the cake filtration model is the only suitable to describe the flux curves during minutes 10–30. This model reproduces the trend of the measured points satisfactorily whereas the pore constriction and pore blocking model show an excessive curvature.

One of the hypothesis of the non-linear Least Square methods is that residuals are distributed as "white noise" and do not present any "unexplained" meaningful trend or bias. Among all the fitting procedure effectuated, this hypothesis is respected at its best by the cake model and for this time interval, always under the condition that the initial flux equals J_0. An example is given in Figure 6.10.

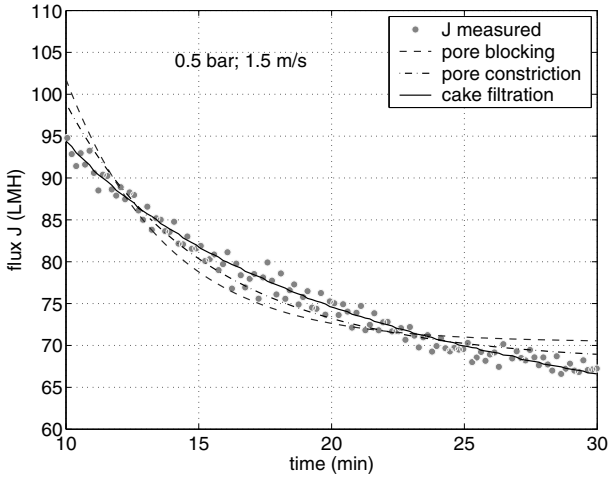

Figure 6.8: *Fitting of filtration data with blocking laws, minute 10–30, TMP = 0.5 bar and* $u_{cr} = 1.5\ m \cdot s^{-1}$ *with blocking laws*

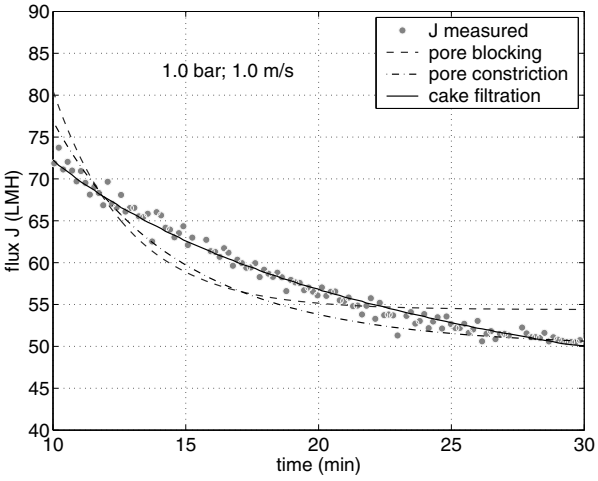

Figure 6.9: *Fitting of filtration data with blocking laws, minute 10–30, TMP = 1.0 bar and* $u_{cr} = 1\ m \cdot s^{-1}$ *with blocking laws*

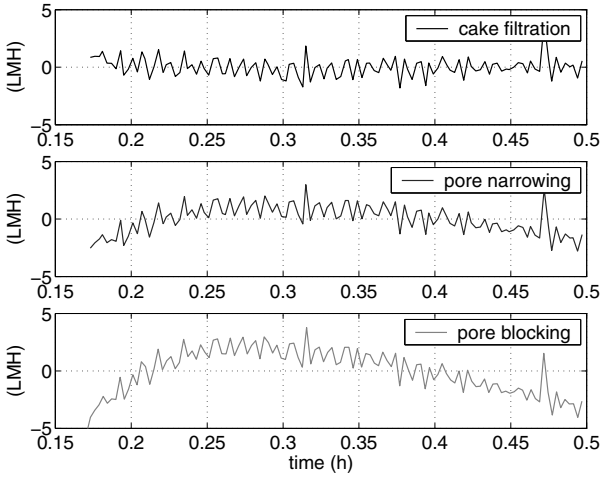

Figure 6.10: *Residuals of optimal fitting of filtration data with blocking laws during minutes 10–30,* $TMP = 0.3bar$ *and* $u_{cr} = 1\ m \cdot s^{-1}$

The results from the fitting process are improved regarding both the correlation coefficient and the estimated model parameters.

The average correlation coefficient is 0.945 for the pore constriction model, 0.867 for the pore blocking model and 0.977 for the cake model. The latest is the highest average value obtained with our set of data. The cake filtration model is the one that fits the data best in all cases except $TMP = 0.3\ bar$ and $u_{cr} = 1.5\ m \cdot s^{-1}$. However, as noted before, this set of measurements is of bad quality.

The amount of squared residuals, which is of the order 10^3–$10^5\ LMH^2$ for the entire filtration period, for the cake model reduces to 79–210 LMH^2. The other models show definitively lower fitting performances (see Table 6.7).

For each of the three models, the estimation of the back-transport J^* is strictly depending on the cross flow velocity. Remarkably, given a certain u_{cr}, J^* varies in a small range and the ranges from different crossflow velocities do not overlap (see Figure 6.7).
The estimated fouling rate constants nicely relate to the applied TMP. Increas-

Table 6.7: *Estimated model parameters and statistics during min 10–30*

	u_{cr}	TMP	J^*	k_i^*	R^2	SSe
Cake	$(m \cdot s^{-1})$	(bar)	(LMH)	$\cdot 10^{11}$ (m^{-4})	(-)	$(LMH)^2$
	1	0.3	31.2	9.5	0.984	79
	1	0.5	18.2	12	0.990	86
	1	1.0	32.9	37	0.982	75
	1.5	0.3	38.9	5.1	0.952	210
	1.5	0.5	52.8	14	0.983	98
	1.5	1.0	53.2	29	0.983	96
	2.0	0.3	65.4	5.1	0.983	120
	2.0	0.5	73.0	15	0.945	95
	2.0	1.0	60.9	22	0.974	130
Pore Constrict.	$(m \cdot s^{-1})$	(bar)	(LMH)	(m^{-3})	(-)	$\cdot 10^2$ $(LMH)^2$
	1	0.3	51.6	0.443	0.965	1.7
	1	0.5	53.6	0.334	0.949	4.2
	1	1.0	51.8	0.331	0.928	3.1
	1.5	0.3	65.8	0.388	0.969	1.2
	1.5	0.5	67.9	0.351	0.953	2.9
	1.5	1.0	67.7	0.302	0.944	3.1
	2.0	0.3	80.7	0.344	0.954	3.1
	2.0	0.5	80.0	0.386	0.881	4.4
	2.0	1.0	76.0	0.282	0.945	2.9
Pore Blocking	$(m \cdot s^{-1})$	(bar)	(LMH)	(m^{-1})	(-)	$\cdot 10^2$ $(LMH)^2$
	1	0.3	54.1	0.044	0.918	4.3
	1	0.5	57.7	0.029	0.859	12
	1	1.0	54.3	0.022	0.797	9.2
	1.5	0.3	68.2	0.041	0.953	2.2
	1.5	0.5	70.4	0.031	0.884	7.5
	1.5	1.0	70.2	0.022	0.827	1.0
	2.0	0.3	83.1	0.041	0.922	5.4
	2.0	0.5	81.5	0.034	0.795	7.8
	2.0	1.0	78.3	0.020	0.836	9.1

ing TMP implies increasing k_c for the cake model and decreasing k_{st} and k_{pb} for pore narrowing and pore blocking respectively (data in Table 6.7).

6.5 Discussion and interpretation of results

6.5.1 Discussion of fitting results

The results of the fitting show that there is no single blocking law that fully catches the flux decline during the entire 30 minutes of filtration.

As reported in Paragraph 6.2, several authors interpreted similar findings as a proof of varying fouling mechanism. For instance so did Kilduff *et al.* (2002) during the unsatisfactory fitting of 10 h filtration curves. However, with respect to the tests presented here, other issues should be considered before drawing the same conclusion.

The analysis of the squared residuals indicates that almost all the variations unexplained by the models belong to the initial phase. Indeed, when the first five minutes of filtration are considered separately, the results of the fitting are very poor. The reason can be found in the the unsteady flow conditions at the start of the experiments (Paragraph 6.4.2).

In order to verify the influence of this experimental inaccuracy, the first minutes of some sets of data have been filtered and smoothed in various ways and fitting results have been compared to the results from the original sets of measurements (not shown). Results confirms that completely different fitting results can be obtained by little manipulation of data, and a single "unrealistic" data point may affect the overall outcome.

Consequently, the fitting results obtained by the initial phase only must be disregarded.

Unfortunately, the effects of the inaccuracy at the start of filtration extends to the fitting of the 30 minutes curve, as the absolute flux values from the initial phase are very large when compared to values of the second phase. Since the fitting algorithm compromises between the two phases, results from the first five minutes tend to be overweighted in importance, which results in the horizontal asymptotes of Figure 6.2 and Figure 6.3.

A particular remark is also made for the importance of J_0. This parameter has such a strong impact on the fitting results that its value should be chosen always on the basis of some physically meaningful value, such as CWF. If J_0 is let free to vary in order to optimise fitting performances, it is always possible to obtain excellent fitting values, but of questionable meaning.

As shown from R^2 and SSe values, the results from the fitting during minutes 10–30 seem to be the most reliable. In this case the flux curves are fitted at best by the cake model.

If the values of J^* and k_c estimated by fitting minutes 10-30 are used to plot the flux decline during the entire filtration period Figure 6.11, Figure 6.12 and Figure 6.13 are obtained.

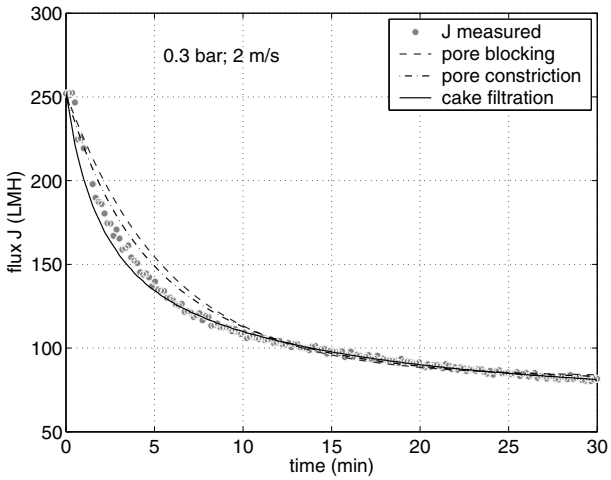

Figure 6.11: *Fitting curves calibrated with blocking laws during minutes 10–30¡ TMP = 0.3 bar and* $u_{cr} = 2\ m \cdot s^{-1}$

The cake model reproduces reasonably also the data outside the interval

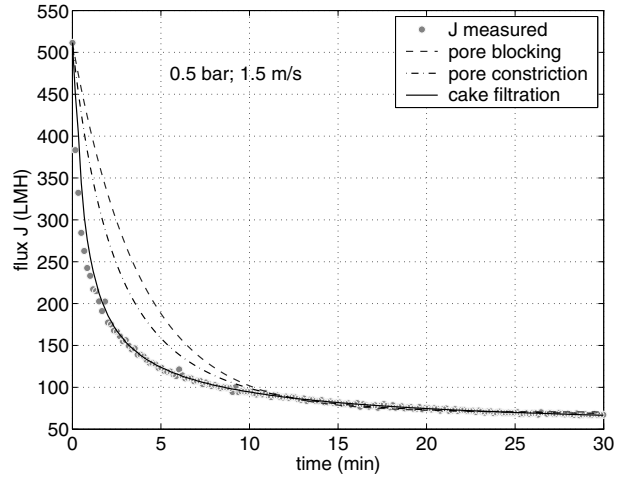

Figure 6.12: *Fitting curves calibrated during minutes 10–30 at TMP = 0.5 bar and* $u_{cr} = 1.5\ m \cdot s^{-1}$ *with blocking laws*

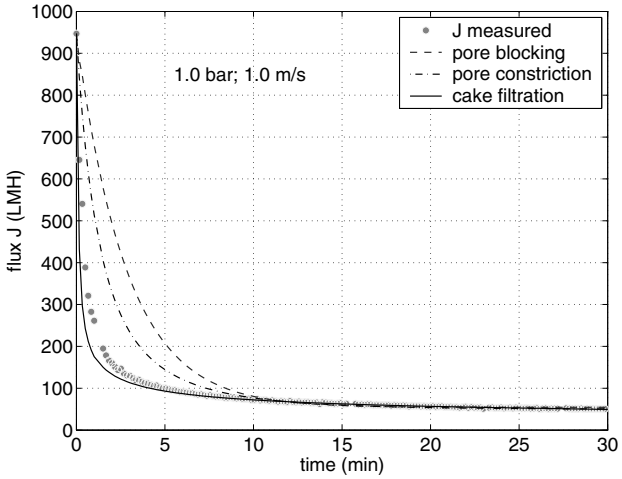

Figure 6.13: *Fitting curves calibrated during minutes 10–30 at TMP = 1.0 bar and* $u_{cr} = 1\ m \cdot s^{-1}$ *with blocking laws*

used for the estimation of J^* and k_c (only at $TMP = 0.1$ *bar* the flux drop during the first 5 minutes is slightly overestimated, see Figure 6.13). This is in opposition to what observed applying the other two models.

It is concluded that the cake model can be used to describe qualitatively and quantitatively the flux decline with good accuracy. However, the model parameters must be estimated using the most reliable sub-group of measurements, corresponding to minutes 10–30 of the filtration period.

6.5.2 Fouling mechanisms

The fitting results show that the cake model interpolates filtration data best. However, in Paragraph 6.2.1 it was noted that fitting results alone should not be used to draw conclusions about the occurring fouling mechanisms. This issue is discussed in the following.

Raw sewage always transports substantial amounts of large particles, colloids and dissolved organic, as visible from Table 5.2. The presence of large particles is favourable to cake formation, but other circumstances are favourable to internal fouling: the presence of dissolved organic matter, the high permeation drag and the enhanced back-transport induced by the crossflow velocity. Therefore, both internal and external fouling are expected to occur.

According to Koltuniewicz *et al.*, (1995), the concavity of the filtration curves $R(t)$ provides indication over the fouling mechanisms (see Paragraph 6.2.2). Studying d^2R/dt^2 in details would require heavy manipulation of the experimental data, in order to obtain a derivable function from discontinuous and dispersed values. Here, filtration data are simply interpolated with a 6^{th} order polynomius, from which dR/dt values are calculated. Afterwards, dR/dt values are plotted *vs.* time in order to study their "positivity" (see Figure 6.14).

Differently from expectations, for all the curves dR/dt is > 0 and with decreasing slope. This corresponds to a concavity downwards and is evidence for surface fouling. Therefore, cake filtration would be the major fouling mechanism during the entire filtration period.

At the light of this observation, the little discrepancies between modelled curve and observed flux values during the first minutes can be interpreted in

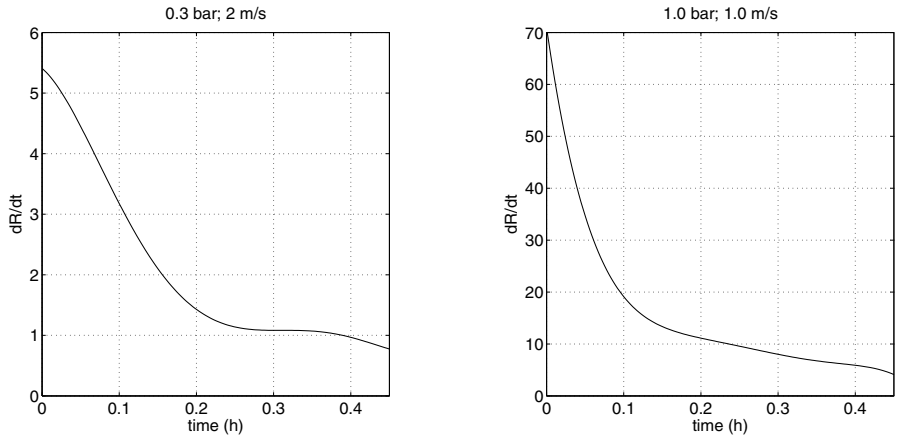

Figure 6.14: *Example plots of dR/dt vs. time*

terms of cake characteristics. The largest discrepancies were seen at $TMP = 1\ bar$ (Figure 6.13). The modeled curves are obtained based on the flux measurements during minutes 10–30, when an extensive cake layer is already formed. During the first minutes the cake layer is still building up and the specific cake resistance is smaller. Therefore, the flux drop in the initial phase results overestimated.

In Figure 6.14 it is visible that the decrease is not steady and after a while some oscillations are observed. In terms of surface fouling, the changes in slope could be explained by cake "disruption" and compaction. However, there is no reason to deny that it corresponds to the visible effect of other fouling mechanisms. One possibility is that despite the prevalent effect of cake formation, smaller particles can still permeate through the porosities of the cake and foul the membrane pores.

In conclusion, the trend of resistance with time is in agreement with the results of the fitting and indicates that surface fouling is quantitatively the dominant fouling mechanism, especially but not only after a few minutes from the filtration start. However, it cannot be excluded that other fouling mechanisms occur as well.

A further step is to verify if the cake model parameters allow further inter-

pretation of the fouling characteristics in relation to the operating conditions.

6.5.3 Characteristics of cake filtration of raw sewage

In Table 6.8 the values of J^* and k_c estimated by the cake filtration model using the data from minutes 10–30 are presented again. The Table emphasizes the relations among model parameters and operating conditions.

Table 6.8: *Estimated parameters for cake filtration model, minutes 10–30*

	$J^*\,(LMH)$			$k_c\ (m^{-4})$		
u_{cr}	$1m \cdot s^{-1}$	$1.5m \cdot s^{-1}$	$2m \cdot s^{-1}$	$1m \cdot s^{-1}$	$1.5m \cdot s^{-1}$	$2m \cdot s^{-1}$
$0.3\,bar$	31.2	38.9	65.4	$9.5 \cdot 10^{11}$	$5.1 \cdot 10^{11}$	$5.6 \cdot 10^{11}$
$0.5\,bar$	18.2	52.8	73.0	$1.2 \cdot 10^{12}$	$1.4 \cdot 10^{12}$	$1.5 \cdot 10^{12}$
$1.0\,bar$	32.9	53.2	60.9	$3.7 \cdot 10^{12}$	$2.9 \cdot 10^{12}$	$2.2 \cdot 10^{12}$

Despite the variation of the feed water quality during the tests, it seems that J^* and k_c, representative of fouling characteristics, can be related to the operating conditions and their physical meaning.

The values of J^* are homogeneously distributed in three non contiguous groups, increasing with the applied crossflow velocities. In agreement with the results of Chapter 5, this emphasizes the effect of crossflow velocity in the reduction of fouling, as promoter of back-transport flux.

J^* varies between 18 LMH and 73 LMH. Under the various conditions that are tested, this appears a reasonable interval for the identification with both the critical flux or the steady state flux. The J^* values can be compared with the final values of flux J_{end} of the filtration test. Estimated J^* are slightly lower than observed J_{end}, which suits the observation that in the last minutes of the filtration tests the rate of flux decline is little, as if approaching a steady-state not reached yet.
Unfortunately, there is no literature available on crossflow ultrafiltration of raw wastewater to compare these values. During crossflow nanofiltration of NOM from surface water at $u_{cr} = 0.1\ m \cdot s^{-1}$, Kilduff *et al.* (2000) estimated $J^* = 17\ LMH$; whereas during dead-end MF of humic acid solutions, Yuan *et al.* (2002), introduced J^* in the Ho-Zidney's model obtaining values between 8

and 33 LMH at different stirring velocities. It seems reasonable that a crossflow system with $u_{cr} > 1\ m \cdot s^{-1}$ shows higher J^*.

The fouling rate constant k_c is the product of the specific resistance of the cake layer α_c and the bulk solute concentration C_b. The data used here originates from different samples and C_b is unknown and variable.

At a certain crossflow velocity, k_c increases with increasing TMP. In the worst case, k_c is even six times bigger than the minimum value. This indicates the predominant role of the TMP to determine the resistance of the filter cake, and suggests the hypothesis that the cake is compressible. This is further investigated in Paragraph 6.5.4.

On the other hand, the effect of the crossflow velocity on the cake resistance is not clear.

It would be interesting to compare the estimated values of the specific cake resistance with others found in literature. However, in Kilduff's formulation of the blocking laws the specific cake resistance α_c is defined as average cake specific resistance *per deposited mass* (in $m^{-1}kg^{-1}$) and not *per thickness of cake deposit* (in $m \cdot kg^{-1}$) as in all the dead-end filtration literature. Given that the density of the cake layer is unknown, values are not comparable except with the ones in Kilduff *et al.*, 2000. In that case, α_c was found of the order of 10^{16} $m^{-1}kg^{-1}$. Here, in the hypothesis that C_b is in the order of $10^{-1}kg \cdot m^{-3}$, α_c is significantly lower: in the order of 10^{12}–10^{13} $m^{-1}kg^{-1}$. This can be explained by the smaller particle size of the foulants (NOM) and the higher applied TMP (2–6 bar) during Kilduff experimentations, which likely results in a less porous and permeable cake.

6.5.4 Compressibility of filter cake

During micro- and ultrafiltration, the forming filter cakes are often found to be compressible. This has been observed for bacterial cells (Lojkine, 1992), proteins (Ho and Zidney, 2000), NOM (Yuan *et al.*, 2002) and inorganic colloids Kim *et al.*, 1993). Concerning secondary effluent of municipal wastewater, during ultrafiltration Roorda (2004) found a high degree of compressibility for filter cake, as it was hypothesized by Boerlage *et al.* (2003, 2004), to explain their experimental results with the MFI.

The same can be expected for untreated wastewater, as many transported components are similar in the two wastewaters and the concentration is at least 10

fold higher for the latter ($> 100\ mg/L$ vs. $< 10\ mg/L$).

A compressible cake would explain the dependence of k_c from TMP, as the degree of compaction is dependent on the applied pressure and translates into a higher resistance to filtration.
The relationship between the resistance of a compressible filter media and the applied pressure is usually expressed by the following power law (see Paragraph 2.4.4):

$$\alpha_{cake} = \alpha_0 \cdot \Delta P^s \tag{6.3}$$

where α_{cake} is the specific cake resistance (in $m \cdot kg^{-1}$) and α_0 is a constant related to size and shape of the particles within the deposit.

The exponent "s" is the *compressibility coefficient*, $= 0$ for incompressible layer and near 1 for highly compressible cakes. For BSA solution, different values of "s" have been reported: 0.43 by Opong and Zidney (1991), 0.82 by Ho and Zidney (2000), between 0.28 and 0.41 by Yuan *et al.*, (2002). For secondary effluent, Roorda (2004) found values between 0.61 and 0.75.

In order to study cake compressibility, the value of increased resistance at equal filtrated volume ΔR can be used:

$$\Delta R = R_{tot} - R_{mem} \tag{6.4}$$

where R_mem is the resistance of the clean membrane.

In the hypothesis that the resistance increase is due to the cake:

$$\Delta R = \alpha_{cake} \cdot \delta_c \tag{6.5}$$

where δ_c is the thickness of the forming cake.

During dead-end filtration δ_c can be easily calculated because the deposited mass of cake is proportional to the filtrated volume. In the case of crossflow filtration, it is more difficult to estimate the cake mass and calculate its thickness. However, in the hypothesis that the crossflow velocity is the dominant factor to determine the thickness of the filter cake (regardless of TMP and C_b), in first approximation δ_c can be assumed to be more or less constant.

From Equations 6.3 and 6.5, the compressibility coefficient can be calculated as the slope of a log-log plot of ΔR vs. TMP. Figure 6.15 show the results for

the three tested crossfow velocities at equal filtrated volume = 40 $L \cdot m^{-2}$ (note that the value at $u_{cr} = 1.5\ m \cdot s^{-1}$, unrealistic as explained before, is removed). The observed slope is always above 1.

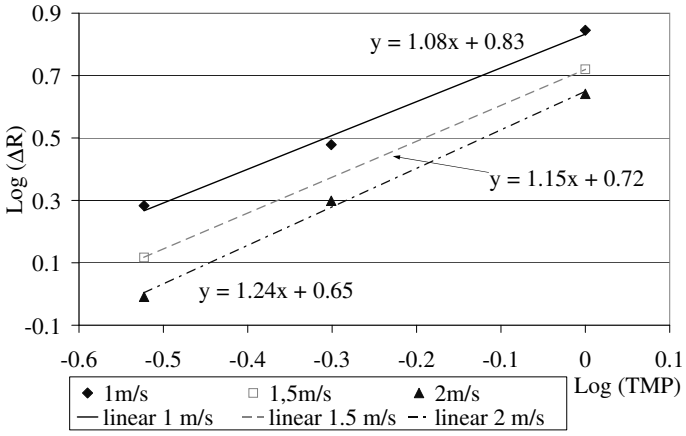

Figure 6.15: *Log-log plot of measured increased resistance ΔR vs. operating TMP at different crossflow velocities.*

On one hand, this indicates that the cake is probably highly compressible. On the other hand, compressibility alone is not sufficient to explain the results. In the absence of additional information, this observation can impact the hypotheses that cake fouling is quantitatively dominant and that δ_c is approximately constant with u_{cr} when TMP and C_b vary.

A further check is to evaluate cake compressibility using the estimated values of k_c. As previously seen, $k_c = \alpha_c \cdot C_b$, where α_c is the average cake specific resistance *per deposited mass* and not *per thickness of cake deposit* as α_{cake}. However, the two parameters should be proportional through the (function of) density of the deposit. With this limitation, the same procedure as for ΔR can be applied.
Since k_c is calculated over the entire fitting period, the hypothesis is that the cake specific resistance during minutes 10–30 is approximately stable at each

filtrating conditions. The log-log plot of k_c vs. TMP is shown in Figure 6.16, together with linear trend lines (note that in this case the value at $u_{cr} = 1.5\ m \cdot s^{-1}$ is not removed).

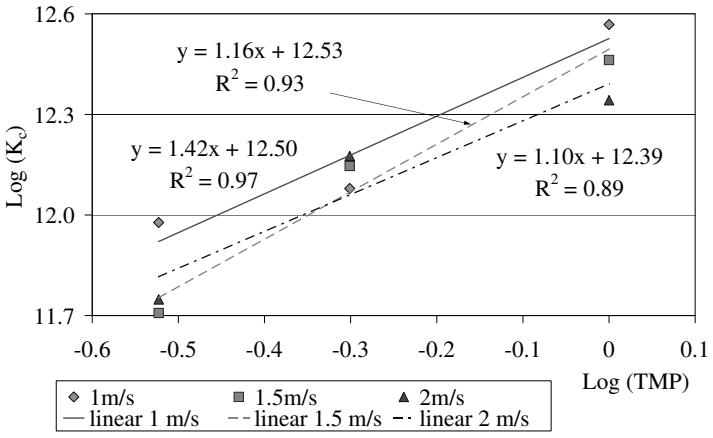

Figure 6.16: *Log-log plot of estimated k_c's vs. operating TMP at different crossflow velocities.*

The increasing rate of k_c with TMP is again > 1, which confirms the trend obtained using ΔR.

In order to explain the result in term of cake layer, an hypothesis can be made that the influence of TMP is not limited to cake compression and extends to cake morphology or cake thickness. This is one possibility because the value of TMP may change the characteristics of foulant transport to and from the membrane.

However, the "unexplained" increase of resistance could be generated by other fouling mechanisms than cake formation. Song and Elimelech, (1995) and Velasco *et al.* (2003) report that the permeation drag increases with TMP and affects foulants penetration into membrane pores. Therefore, another potential explanation is that varying TMP causes different rates of internal fouling, whether during the first phase or the entire filtration period.

6.6 Conclusions and recommendations

Three filtration models are applied to the constant TMP tests presented in Chapter 5. The main objective is to describe the observed flux curves in an improved form, i.e. to be able to quantify the fouling and describe the flux decline through well defined parameters of the applied models (J^* and k_i).

Next to this, the relations between model parameters and operating conditions are investigated.

The applied models are pore blocking, pore constriction and cake filtration, as preliminary considerations about the feed water composition and the relative particles-pore size distributions suggest that both internal and external fouling may occur. In particular, the highest content of suspended solids may result in thick cake formation.

The results of the overall fitting show that no single model can satisfactorily describe the flux decline curves during the entire filtration period. However, a more detailed analysis indicates that results are biased by the inaccuracy of the measurements during the first minutes of filtration. When only measurements from minutes 10–30 are used to calibrate the models, the cake filtration model describes satisfactorily the overall flux decline.

The estimated parameters of the cake filtration model, J^* and k_c, allow a clear comparison of the fouling behavior under different operating conditions. They reproduce the influence of crossflow velocity and TMP on flux decline decribed in Chapter 5, and provide a more robust theoretical interpretation of results.
In the model:

- J^* represents the back-transport flux or the expected final value of flux at steady state, and its value should increase with the crossflow velocity. The estimated J^* values increase with the crossflow velocity as well as the pseudo-steady state flux;

- k_c is the product of the cake specific resistance α_c and the bulk concentration C_b, and its value should depend on both the shear and the applied TMP. Varying operating conditions, the value of k_c can increase up to six times, and the largest effect can be appointed to the applied TMP. This suggests the formation of a highly compressible cake.

Both the analysis of dR/dt and the successful fitting of the cake model suggest that cake fouling is quantitatively dominant. However, the overall resistance increase cannot be modelled as depending on the cake compressibility only. Most likely, a highly compressible cake is formed but this is not the exclusive fouling mechanism, and internal and external fouling coexist.

Finally, it is recommended to validate the observations about the occurring fouling mechanisms using an improved well-defined filtration system and membrane inspection methods, such as membrane autopsy. Particular attention should be devoted to the accuracy of the measurements during the initial transient phase and to the determination of the cake mass. A major point is to determine whether internal fouling is relevant and if it occurs during the beginning phase only, or it continues when the filter cake is formed. The last aspect might improve the strategies to control irreversible fouling.

Chapter 7

Filtration of primary effluent

The short-term filterability of the effluent of a primary clarifier is tested with the same procedure used for raw sewage. The results are compared and the effect of primary sedimentation is evaluated.

7.1 Procedure

7.1.1 Short-term filterability tests

The filterability of primary effluent is studied looking at the effect of variations of the applied TMP and u_{cr}.

The procedure and the test scheme are the same as the ones described in Chapter 5 for raw sewage: during one day 3 tests are executed on the same sample, varying one of the two parameters. The experiments are repeated twice, in different order: during test series A the tests are executed daily at equal crossflow velocity, during test series B the tests are executed daily at equal TMP. The testing session followed shortly after the tests with raw sewage (August 2004). Table 7.1 reports the test schedule and the temperature of the feed water.

The membrane module in use is the same used during the tests with raw sewage. Details can be found in Paragraph 4.3.5.

Table 7.1: *Short term filterability tests with primary effluent: applied operating conditions and feed water temperature (August-September 2004)*

Series	Testing day	u_{cr} $(m \cdot s^{-1})$	TMP (bar)	T $(°C)$
A	1	1.0	0.3 - 0.5 - 1.0	22 - 23 - 24
	2	1.5	0.3 - 0.5 - 1.0	23 - 25 - 25
	3	2.0	0.3 - 0.5 - 1.0	23 - 24 - 24
B	4	1.0 - 1.5 - 2.0	0.3	22 - 23 - 24
	5	1.0 - 1.5 - 2.0	0.5	22 - 22 - 22
	6	1.0 - 1.5 - 2.0	1.0	21 - 21 - 22

7.1.2 Water quality

The main objective is to evaluate the effect of primary sedimentation on filterability; therefore the effluent of the primary sedimentation tank of " De Groote Lucht" is used. Raw sewage and primary effluent are tested on different days, consequently the feed water in the two cases is *not* the same water that has undergone a settling process. Nevertheless, it is supposed that results can be equally significant.

Some physical-chemical characteristics of the feed primary effluent (soluble fraction) and the permeate during the testing period are summarized in Table 7.2.

Table 7.2: *Quality of the feed water (soluble fraction) and permeate during short-term tests with primary effluent*

		Turbidity NTU	TSS mg/L	EC $\mu S/cm$	COD mg/L	NH_4^+ mgN/L	PO_4^{3-} mgP/L
Pr.Eff.	mean	55.6	48.1	1067.2	126	31.8	4.5
	st.dev.	26.8	20.7	338	42.9	10.3	2.4
Perm.	mean	n.d.	0.10	1036	78	30.3	3.4
	st.dev.	-	0.02	300	30	9.5	1.6

As done for raw sewage, each day of the testing session also the EPS are measured. The measurement takes place during the first test of the day, in the

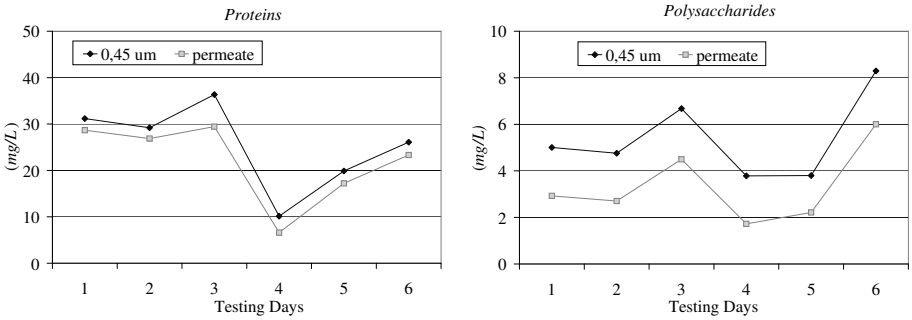

Figure 7.1: *Measured proteins ans polysaccharides concentration in the primary effluent and in the permeate during the testing period*

feed wastewater and in the permeate (the permeate is sampled at the end of the 30 minutes filtration). Figure 7.1 shows the daily values of proteins and polysaccharides in the feed water and in the permeate. Values range within 5–35 mg/L for proteins and 2–8 mg/L for polysaccharides.

7.2 Results of filtration tests

7.2.1 Flux and permeate production

During 30 minutes of continuous filtration the flux declines strongly, although the overall drop depends on the applied operating conditions. An overview of the results is given in Figure 7.2, which presents the measured curves $J(t)$ of the most fouling, the average and the least fouling applied combination of TMP and u_{cr} (test series A).

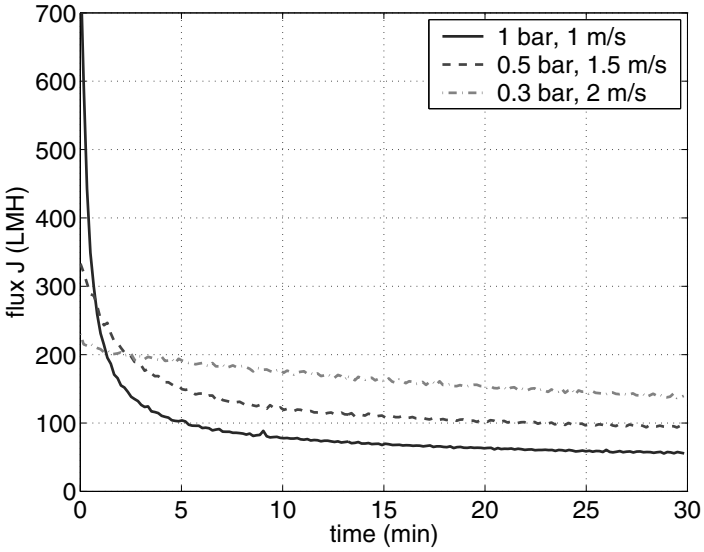

Figure 7.2: *Example curves of flux decline at the variation of* u_{cr} *and* TMP

Figure 7.2 shows how the overall flux drop and the curvature of the declining curves are strictly related to the applied conditions. In particular:

- higher TMP values produce higher initial fluxes but result in lower flux values already after a few minutes;

- at the least fouling condition the typical trend of a sudden drop of flux followed by slow decline is not visible. Apparently, in this case the flux

declines continuously and almost constantly during the entire filtration period.

Detailed results from both test series A and B are presented with the help of three figures.

Figure 7.3 shows the starting values J_{start}.

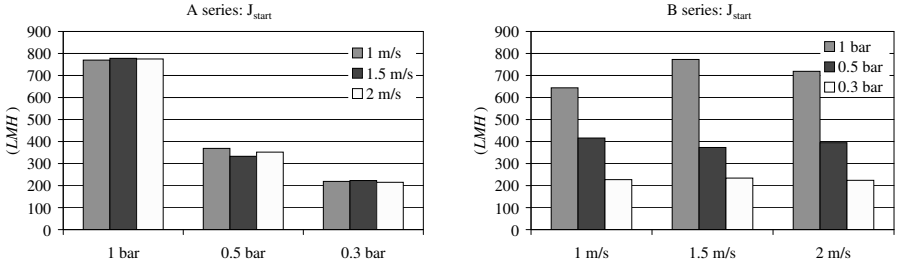

Figure 7.3: *Initial flux J_{start} during A and B test series with primary effluent*

J_{start} is dependent on the applied TMP regardless the value of crossflow velocity. Values are rather constant throughout both test series, which indicates good accuracy in the experimental conditions.

Figure 7.4 emphasizes the effect of TMP and u_{cr} on the final value of flux J_{end}.

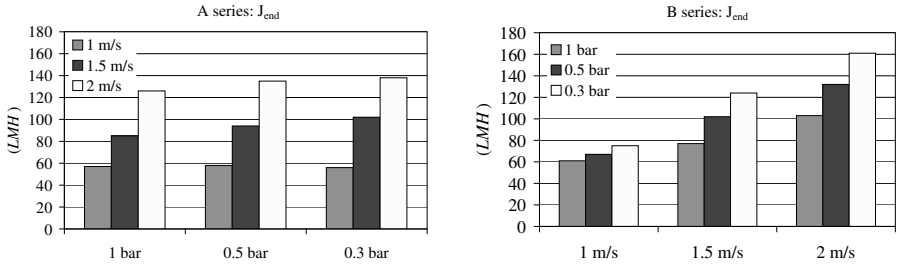

Figure 7.4: *Final flux J_{end} during A and B test series with primary effluent*

During test-series A, at $u_{cr} = 1\ m \cdot s^{-1}$, J_{end} is about the same independently from the applied TMP. Differently, in all other cases J_{end} increases for decreasing applied TMP.

The effect of the crossflow velocity is always to increase J_{end}.

The consequences of the trend observed for J_{end} reflects in the total permeate production, depicted in Figure 7.5.

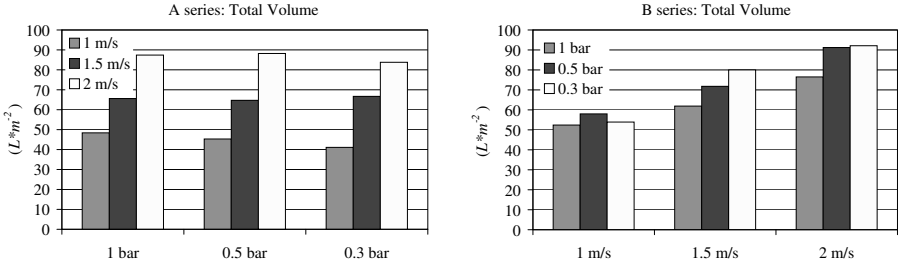

Figure 7.5: *Total produced specific volume during A and B test series with primary effluent*

At $u_{cr} = 1\ m \cdot s^{-1}$ increasing values of TMP correspond to larger produced volumes during test-series A, but not during test-series B. At crossflow velocity equal to 1.5 and 2 $m \cdot s^{-1}$, during test series A increasing TMP does not lead to any relevant variation in produced volume; on the opposite, during test-series B, larger volumes are obtained decreasing the applied TMP.

Again, the crossflow velocity has always a positive effect increasing the total produced volume.

7.2.2 Resistance and fouling development

The plots of resistance with time, useful to provide an intuitive impression of the filtration results, are exemplified in Figure 7.6. The figure shows the usual three curves from series A.

A summary of the overall results from both test series is presented in Figure 7.7, which shows the overall resistance increase during 30 minutes.

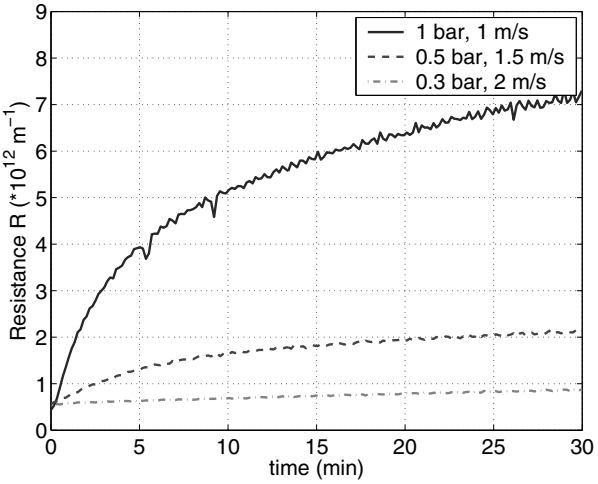

Figure 7.6: *Example curves $R(t)$ at various u_{cr} and TMP*

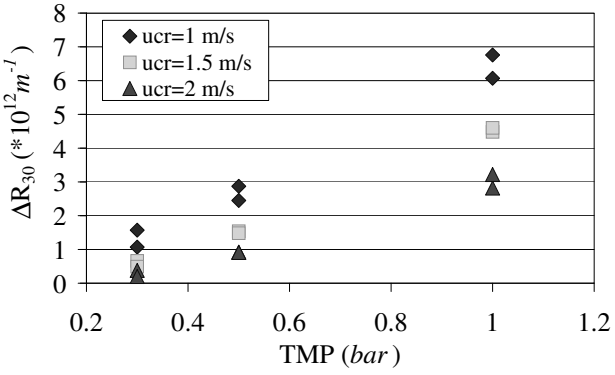

Figure 7.7: *Overall resistance increase values during test series A and B filtrating primary effluent*

From both Figures it is visible that the total resistance increase after 30 minutes varies in a wide range (between $0.5 \cdot 10^{12}$ and $7 \cdot 10^{12}$ m^{-1}). The increase is more rapid at high applied TMP and low crossflow velocity.

Figure 7.6 shows that this is the case since the first instants of filtration, whereas Figure 7.7 confirms that data show a good replicability of the experiments throughout the two series. The little scattering of results is probably due to the variable feed water characteristics.

The development of resistance over filtrated volume $R(vol)$ can reveal the fouling characteristics. To this purpose, the usual three exemplary curves are plotted in Figure 7.8.

The results from all the performed tests are summarized in Figure 7.9, where ΔR values at 40 $L \cdot m^{-2}$ filtrated volume are plotted versus the shear stress.

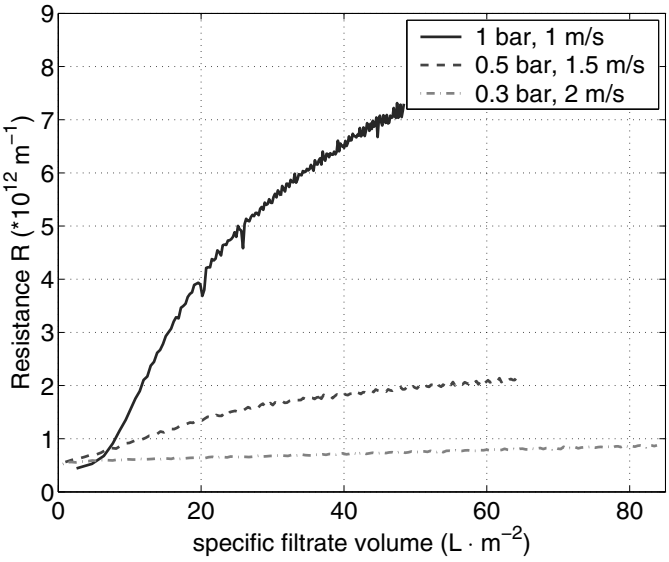

Figure 7.8: *Example curves $R(vol)$ at various u_{cr} and TMP*

Figure 7.8 confirms that fouling development is strictly a function of the op-

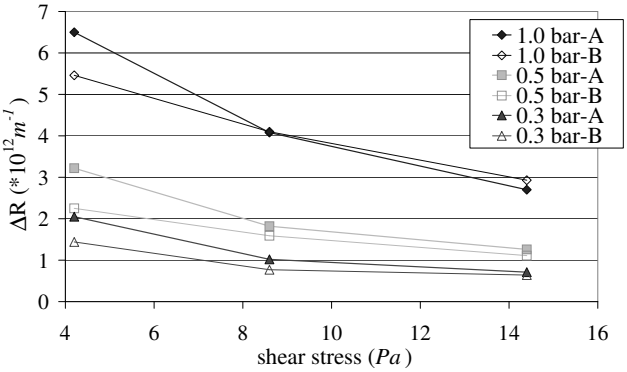

Figure 7.9: *Resistance increase vs. shear stress for different applied TMP at equal filtrated volume (40 $L \cdot m^{-2}$)*

erating parameters: at equal filtrated volume, the resistance increase is bigger when the TMP is high and/or u_{cr} is small.

Figure 7.9, shows that τ has the effect of reducing the resistance increase. The effect is stronger when fouling is higher, i.e. ΔR are more significantly reduced at high applied TMP and shifting from 4.2 to 8.6 Pa rather than from 8.6 to 14.5 Pa.

7.2.3 Analysis of filtration curves

Similarly to what done in Chapter 6 with raw sewage, the flux curves $J(t)$ from test series A are interpolated with three classical models for crossflow ultrafiltration: pore blocking, pore constriction and cake filtration. The fitting is realized using the same non-linear Least Square method (see Paragraph 6.3.2).

On the basis of the results with raw sewage, the fitting exercise is performed on the entire curve of 30 minutes and separately to the last 20 minutes.

The complete overview of the results of the fitting is presented in Appendix D, whereas the following Paragraphs provide a brief summary of the major points.

Overall fitting

When the entire 30 minutes of filtration are considered the highest fitting performances are obtained by the pore constriction model. Among the 9 combinations of TMP and u_{cr} that have been analysed, the pore constriction model presents 6 times the highest correlation coefficient (R^2), whereas the cake model 3 times. The average R^2 is 0.979 for the pore constriction, 0.966 for the pore blocking and 0.935 for the cake filtration model.

However, these values are misleading and the fitting must be considered unsatisfactory. The modelled curves obtained with the pore constriction and pore blocking model often present a stationary flux value starting already at minute 10 (see Figure 7.10). As explained in Paragraph 6.1.3, this stationary value is calculated mathematically as final asymptote at steady conditions; therefore, it is not acceptable that the estimated final flux value is higher than observed flux values. This failure is due to the big difference between the starting and the final flux values, which causes the fitting algorithm to overweight the importance of the first minutes of filtration, as explained in Paragraph 6.4.1 and Paragraph 6.4.2.

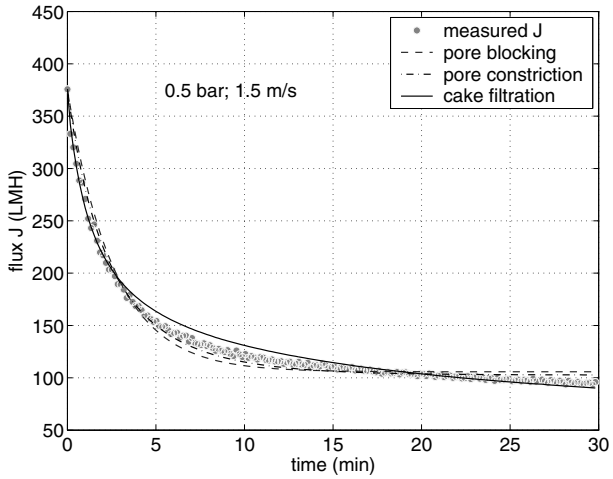

Figure 7.10: *Example of fitting applying 3 models to filtration of primary effluent at* $TMP = 0.5\ bar$ *and* $u_{cr} = 1.5m \cdot s^{-1}$

Fitting during minutes 10-30

When only data from minutes 10–30 are fitted, the cake model obtains the highest R^2 eight out of nine times, with an average value of 0.977. The validity of this superior fitting is confirmed by the analysis of the residuals, which appear to be the most "randomly" dispersed (see Figure 7.11).

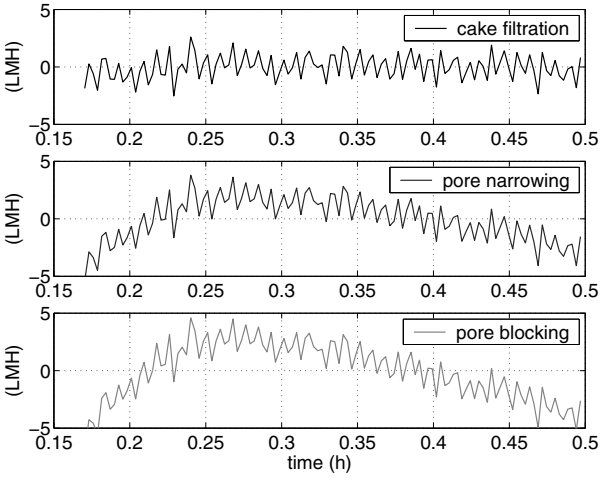

Figure 7.11: *Residuals of optimal fitting of filtration data during minutes 10-30 at* $TMP = 0.5bar$ *and* $u_{cr} = 1.5m \cdot s^{-1}$ *using blocking laws*

The estimated J^* strictly depends on the crossflow velocity. Values are in the range 41–45, 71–85 and 100–132 LMH at $u_{cr} = 1$, 1.5 and 2 $m \cdot s^{-1}$ respectively. It is noted that these values can be considerably lower than the observed final flux values J_{end}, which indicate that the model actually formulates a prediction of an asymptotic value yet to be reached outside the investigated interval.

Concerning the estimated k_c [1], values depend on both TMP and u_{cr}.

When high TMP (= 1 bar) or low u_{cr} (= 1 $m \cdot s^{-1}$) are applied, k_c is in the range 11–34 $\cdot 10^{11}$ m^{-4}). At 0.3 bar and 2 $m \cdot s^{-1}$, k_c can be as little as 1.4 $\cdot 10^{11}$ (m^{-4}). Therefore, highly fouling conditions can produce a specific

[1] k_c is the product of the specific cake resistance per unit mass α_c with the bulk solution concentration C_b, see Table 6.3

resistance more than 20 times higher than little fouling conditions.

Finally, when the values of k_c and J^* estimated during minutes 10–30 are used to plot the entire flux curve, it is found that the cake model reproduces the observed flux decline rather satisfactorily also during the first minutes (see Figure 7.12, Figure 7.13, and Figure 7.14). On the opposite, the pore blocking and the pore constriction models do not.

The curve estimated by the cake model is seven out of nine times slightly below the measured points, which indicates that the model overestimates the fouling (see Figure 7.13, and Figure 7.14). The two exceptions are represented by the least fouling combination of operating conditions: $u_{cr} = 1.5$ and $2\ m \cdot s^{-1}$ at $0.3\ bar$. In the first case the fitting is satisfactory (see Figure 7.13), and in the second the flux decline is poorly reproduced by all the models.

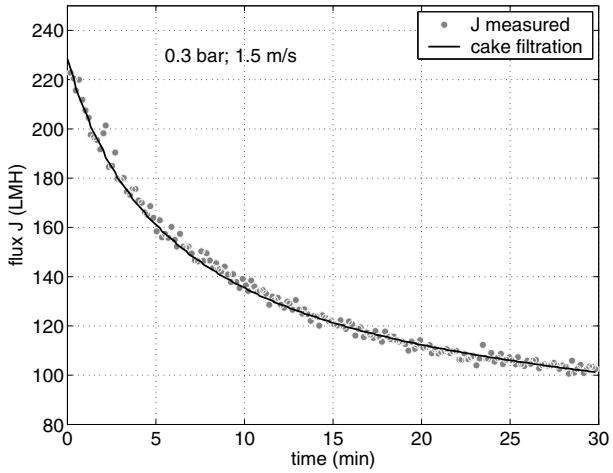

Figure 7.12: *Modelling filtration at 0.3 bar and 1.5 $m \cdot s^{-1}$ on minutes 10–30 according to cake model*

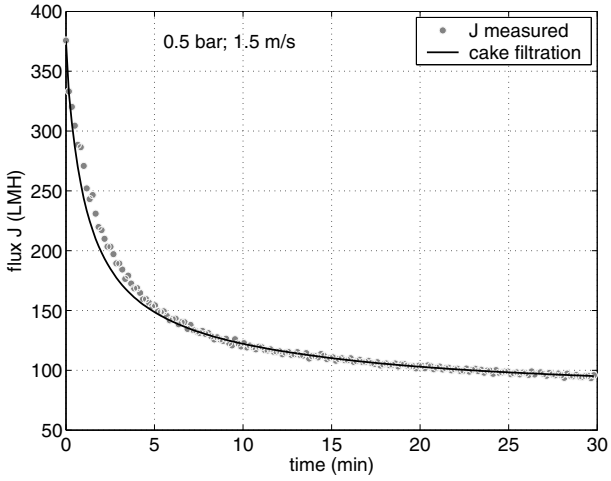

Figure 7.13: *Modelling filtration at 0.5 bar and 1.5 $m \cdot s^{-1}$ on minutes 10–30 according to cake model*

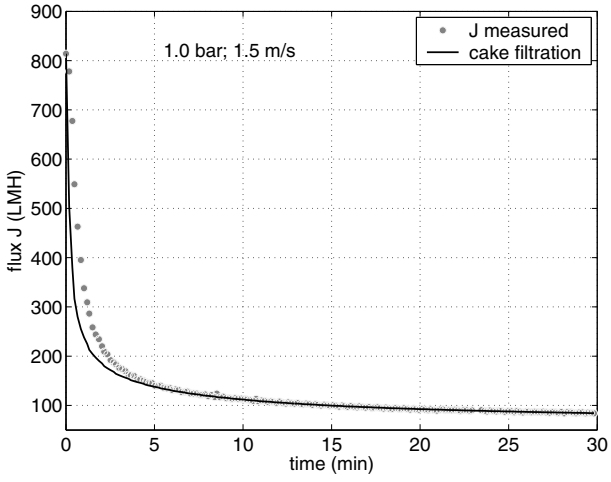

Figure 7.14: *Modelling filtration at 1.0 bar and 1.5 $m \cdot s^{-1}$ on minutes 10–30 according to cake model*

7.2.4 Characteristics of filter cake

Although not shown here, the curves dR/dt have been studied as in Paragraph 6.5.2. The results indicate that cake formation is the predominant fouling mechanism during ultrafiltration of primary effluent at all the tested conditions. Coupling this finding to the fact that the cake model calibrated on minutes 10-30 reproduces more satisfactorily the observed flux decline, it can be assumed that a cake layer is actually formed, and it is worth investigating its characteristics. In particular, it is interesting to verify if the compressibility of the filter cake could explain the influence of TMP on the resistance increase.

As in Paragraph 6.5.4, two methods are applied. The first exploits the ΔR values at equal filtrated volume and the second the k_c values obtained by the modelling. In both cases (and under similar hypotheses), the data are interpolated according to the power law in Formula 6.3.

Results are presented in Figure 7.15 and Figure 7.16.

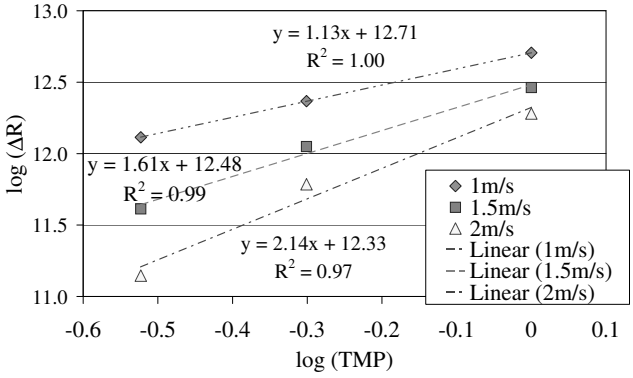

Figure 7.15: *Cake compressibility as a function of TMP and u_{cr}; filtration of primary effluent, ΔRs measured at 30 $L \cdot m^{-2}$*

The results are very similar. The values of the cake compressibility factor "s" are all above 1 and increase with increasing crossflow velocity. This indicates that compressibility alone cannot account for the observed resistance increase at different applied TMP, and that the unexplained portion increases with the crossflow velocity.

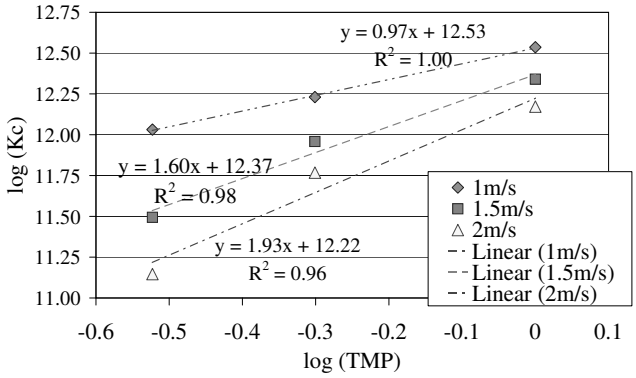

Figure 7.16: *Cake compressibility as a function of TMP and u_{cr}; filtration of primary effluent, estimated k_c values*

7.3 Comparison with raw waste-water

7.3.1 Water quality

Table 7.3 compares the feed water quality during short-term tests with raw sewage and primary effluent.

Table 7.3: *Quality of the feed water (soluble fraction) during short-term tests with raw sewage and primary effluent*

	Turbidity NTU	TSS mg/L	EC $\mu S/cm$	COD mg/L	NH_4^+ mgN/L	PO_4^{3-} mgP/L	Av.T $°C$
Raw Sewage							
mean	110.7	84.0	1328	222	39.5	4.7	20.6
st.dev.	41.0	47.3	213	46	3.3	0.8	0.5
Primary Effluent							
mean	55.6	48.1	1067.2	126	31.8	4.5	22.9
st.dev.	26.8	20.7	338	43	10.3	2.4	1.2

From the data in Table 7.3, it is visible that the strength of the wastewater reaching the WWTP during the testing of primary effluent is lower. This can be easily concluded by the average concentrations of conductivity and ammonium, which are both insensitive to the sedimentation step, and both decrease of about 20%.

Because of the combined effect of the sewage originally more "diluted" and the effect of sedimentation, the primary effluent presents a lower content of suspended solids (48 $mg \cdot L^{-1}$ vs. 84 $mg \cdot L^{-1}$), a lower content of fine particles (average turbidity values are 56 NTU vs. 110 NTU) and a lower COD (126 vs. 222 $mg \cdot L^{-1}$, sum of colloidal and dissolved COD only, see Paragraph 4.5).

The primary effluent exhibits also lower average EPS content. From Figure 5.1 and 7.1 the average EPS concentration is 25.5 vs 38.5 $mg \cdot L^{-1}$ for proteins and 5.4 vs 6.0 $mg \cdot L^{-1}$ for polysaccharides.

Finally, the average temperature of the feed water during testing of primary effluent is 2.3 $°C$ higher, which corresponds to 5.3% decrease in permeate viscosity.

7.3.2 Results of filtration tests

The filterability of primary effluent is strongly affected by the operating parameters TMP and u_{cr}, i.e. increasing crossflow velocity reduces fouling formation whereas increasing TMP increases it.

From a qualitative point of view, the same behavior was observed during short-term tests with raw sewage. However, the filterability of primary effluent is superior because the resistance increase is smaller at every tested combination of TMP and u_{cr}. Figure 7.17 compares the resistance increase at equal filtrated volume (the same is observed at equal filtration time).

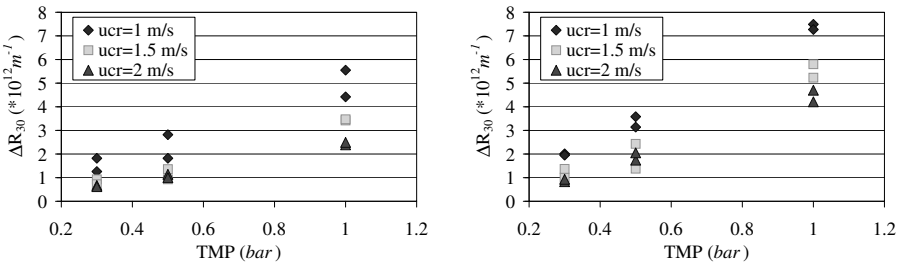

Figure 7.17: *Comparison of resistance increase at equal filtrated volume (30 $L \cdot m^{-2}$) with primary effluent (left) and raw sewage (right)*

Concerning flux values, as previously noted the starting value of flux J_{start} is a mere consequence of the applied TMP, for both feed waters.

On the opposite, the final value of flux J_{end} is heavily influenced by both the operating parameters (TMP and u_{cr}) and the feed water characteristics. Results from the two feed waters are compared in Figure 7.18.

Figure 7.18 shows that J_{end} is in the range 60–140 $L \cdot m^{-2}h^{-1}$ for primary effluent and 45–75 $L \cdot m^{-2}h^{-1}$ for raw sewage. Therefore, the flux decline filtrating primary effluent is remarkably smaller. Additionally, in the case of primary effluent increasing TMP usually reduces J_{end} and increasing u_{cr} increases it. In

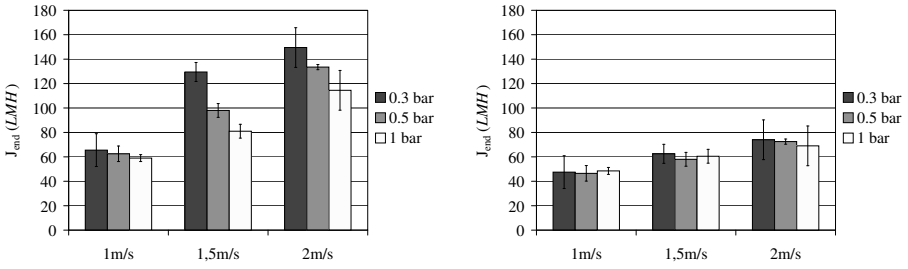

Figure 7.18: *Comparison of average J_{end} values filtrating primary effluent (left) and raw sewage (right)*

the case of raw sewage, J_{end} is almost insensitive to TMP and little differences are obtained at equal u_{cr}.

Figure 7.19, compares the specific volumes produced with the two wastewater (average on the two series).

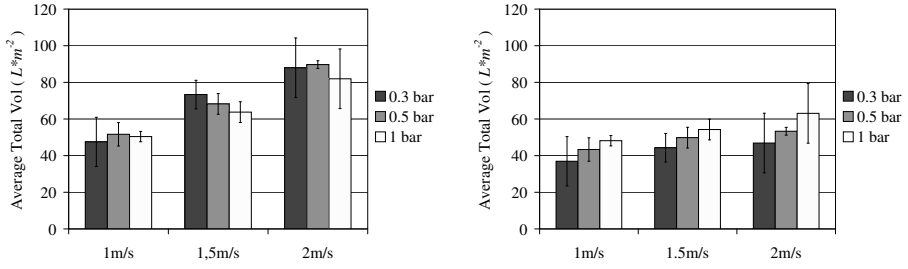

Figure 7.19: *Comparison of average produced volumes filtrating primary effluent (left) and raw sewage (right)*

The average volume produced with primary effluent is in the range 47–87 $L \cdot m^{-2}$, whereas it is 37–62 $L \cdot m^{-2}$ with raw sewage. Therefore, primary effluent produces about 30–40% higher volumes than raw sewage.

In both cases the volume increases with u_{cr}, whereas the effect of TMP is different. During filtration of primary effluent the permeate production is maximised at high u_{cr} (1.5 - 2 $m \cdot s^{-1}$) and moderate-low TMP (0.3 - 0.5 bar). On

the opposite, during filtration of raw sewage the permeate production increases with TMP.

The explanation for such difference lies in the rate of the flux decline (i.e. of the building up of fouling).

During filtration of raw sewage, the rate of flux decline is dramatic in all cases and after a few minutes the flux values are well below 100 LMH. Consequently, the larger volume produced in the initial phase at higher TMP cannot be counterbalanced by the production during the rest of the time.

On the opposite, during filtration of primary effluent, fouling formation slows down remarkably when the proper operating conditions are applied. At moderate-low TMP and high crossflow velocity fluxes are well above 100 LMH for the entire duration of filtration, so that a relevant part of the permeate production is produced also in the second half of the filtration test.

7.3.3 Results of modelling

The results of the modelling show that for both feed waters the fitting of the entire filtration period is biased and the highest fitting performances are given by the cake model calibrated during minutes 10–30. In that case, the sensitivity of the estimated fitting parameters to the operating conditions is very similar for both feed waters.

Results for J^* are displayed in Figure 7.20.

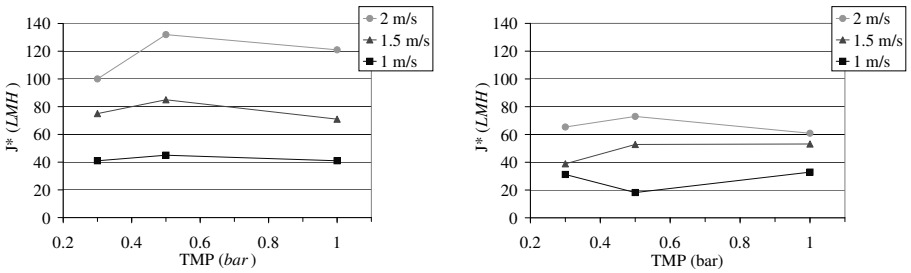

Figure 7.20: *Comparison of average J^* values filtrating primary effluent (left) and raw sewage (right)*

The estimated J^* values depend mainly on the crossflow velocity, and values with primary effluent are about 30% higher than with raw sewage (Figure 7.20).

Results for k_c are shown in Figure 7.21.

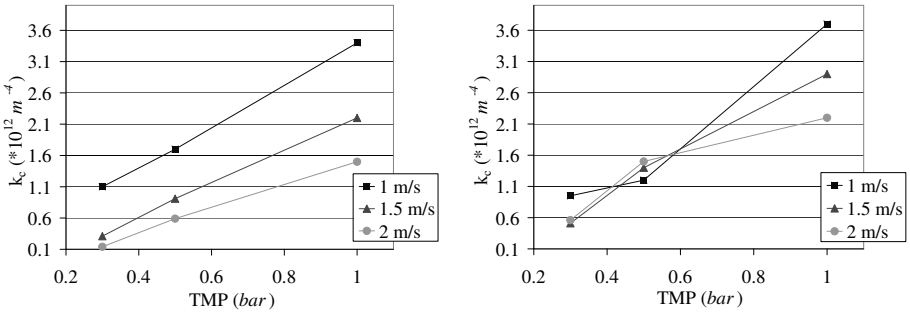

Figure 7.21: *Comparison of k_c values filtrating primary effluent (left) and raw sewage (right)*

Although results with raw sewage are slightly more confused, it is clear that k_c values increase with increasing TMP and decreasing crossflow velocity. Surprisingly, the order of magnitude of k_c is the same for both feed waters (Figure 7.21.

7.3.4 Compressibility of filter cake

Table 7.4 summarizes the values of the compressibility coefficient "s" estimated at various crossflow velocities. Results are displayed for both raw sewage and primary effluent, using both the ΔR and the k_c method.

The compressibility factor s assumes bigger values in the case of primary

effluent. Also the increase with the increasing crossflow velocity is more evident in the case of primary effluent.

Table 7.4: *Comparison of estimated compressibility coefficient s at various crossflow velocities*

u_{cr}	raw sewage		primary effluent	
	$s(\Delta R)$	$s(k_c)$	$s(\Delta R)$	$s(k_c)$
1.0 $(m \cdot s^{-1})$	1.08	1.15	1.13	0.97
1.5 $(m \cdot s^{-1})$	1.15	1.10	1.61	1.60
2.0 $(m \cdot s^{-1})$	1.24	1.42	2.14	1.93

7.4 Discussion of results

From all the investigated issues, the ultrafiltration of sedimentated wastewater with respect to the ultrafiltration of untreated wastewater shows two contradictory faces.

On one side, primary effluent has a higher filterability. Flux values, produced permeate volumes and observed resistance increase are usually 20-30% better during filtration of primary effluent.

On the other side, the fouling characteristics of the two feed waters are really similar. The development of resistance over time and volume, the effect of the operating parameters (TMP and shear stress) and also the modelling with the blocking laws show that essentially the same type of fouling occurs with the two feed waters.

Obviously, the origin of the observed difference and similarity lies in the characteristics of the two feed waters.

The difference in temperature of the feed water, corresponding to about 5% improvement in viscosity, may contribute to the increased filterability of primary effluent but cannot explain it completely.

Chemical-physical analyses indicate that during the testing of primary effluent the wastewater reaching the WWTP had a lower average strength. Nevertheless, the daily concentrations of foulants such as COD and EPS fluctuate, and values in the primary effluent are sometimes higher than in the raw sewage. Additionally, for proteins and polysaccharides retention was about the same for both wastewaters, as shown in Figure 7.22.

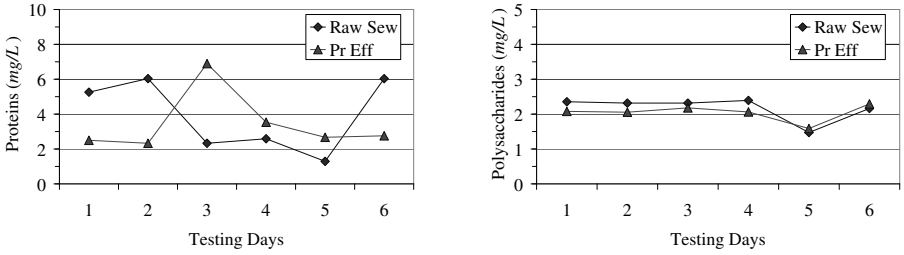

Figure 7.22: *Retained proteins and polysaccharides filtrating primary effluent and raw sewage*

Based on these observations (comparable concentrations of some specific foulants, lower overall strength of primary effluent), a simple hypothesis can be made to explain the findings: the difference in filterability and the similarity in fouling characteristics originate from the fact that the wastewater matrix is the same but primary effluent transports less materials.

The results of modelling (cake model calibrated on minutes 10–30) reproduce the findings discussed above. The superior filterability is expressed by J^* values, that are 20–30% higher for primary effluent. The similar fouling characteristics are indicated by the k_c values, that are almost identical.

A further insight on the comprehension of fouling is obtained studying the characteristics of the filter cake at the various applied operating conditions.

Short and long term tests have shown that at least a part of fouling is due to cake formation. This cake is compressible, but Table 7.4 shows that compressibility alone is not sufficient to explain the increase of fouling with TMP,

neither for raw sewage nor for primary effluent. Fouling is indicated by an increase in resistance ΔR, which in the case of cake filtration has been written as $\Delta R = \alpha_c \cdot m_c$. Therefore, fouling may originate from an increased amount of deposited solids (m_c) or from a higher specific cake resistance (α_c).

Table 7.4 shows that the compressibility coefficient is little above 1 (or even below it) at u_{cr} equal to 1 $m \cdot s^{-1}$, and increases with increasing crossflow velocity. The increase is bigger for primary effluent rather than raw sewage. This means that the fraction of fouling that cannot be explained with compressibility is larger at high crossflow velocity and for primary effluent.

It follows that the trend shown by "s" depends upon the efficiency of the crossflow velocity to prevent the accumulation of material on the membrane, which is higher for more filterable waters (primary effluent) and high u_{cr}. When high strength feed water and little crossflow velocity are applied, a similar amount of foulants reaches the membrane independently from the applied TMP. Increasing the crossflow velocity, the quantity or the characteristics of the material that can accumulate in the filter cake are changed.

An hypothetical mechanism, based on selection of particles size, cake thickness and internal fouling rate, is sketched in Figure 7.23.

On the left, raw sewage is filtrated at low crossflow velocity. At any applied TMP, the high initial permeation flux is not counteracted by an effective back transport and large particles are transported to the membrane. In the following course of filtration these particles shield the cake layer from the scouring effect of u_{cr}, favouring the accumulation of material in a thick compressible layer. In conclusion , more or less the same amount of compressible filter cake is formed, independently form the applied TMP.

On the right, primary effluent is filtrated at high crossflow velocity. Because of the smaller average particle size in the feed and the effective back transport, the accumulated material result in a thinner and more dense cake. Small foulants can more easily reach the membrane pores, because they need to go through a thinner filter cake. Increasing the value of TMP, the permeation flux may exceed the back-transport, increasing the deposited mass, or even increasing the internal fouling. In both cases, the observed increase of fouling cannot be explained by compressibility only.

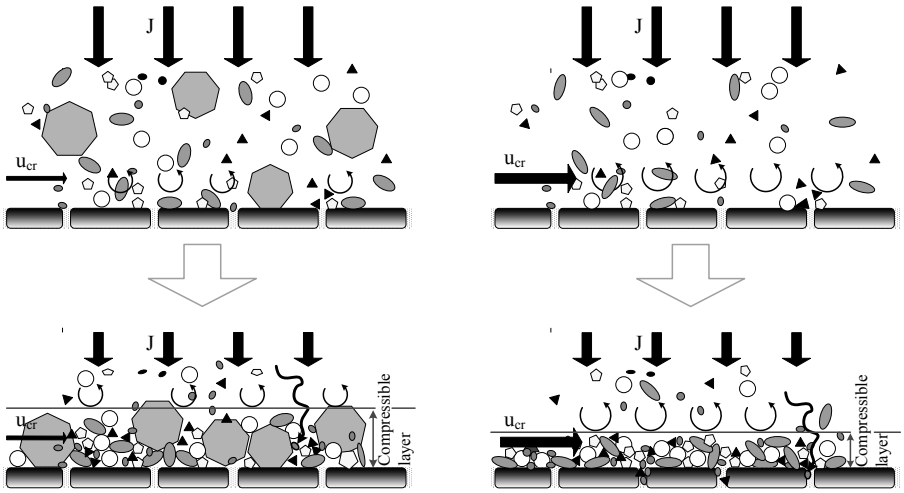

Figure 7.23: *How to explain the more compressible cake at lower u_{cr} and using raw sewage (see text).*

7.5 Conclusions

Short-term filtration experiments show that primary effluent and raw sewage have similar filtration characteristics, although the filterability of primary effluent is superior at all the applied combinations of TMP and u_{cr}.

A simple explanation for these findings is that both feedwaters contain comparable amounts of dissolved foulants (e.g., EPS) but during the days of testing primary effluent was particularly diluted.

During 30 minutes of continuous filtration, the superior filterability of primary effluent produces a limited difference on the observed resistance increase but it leads to remarkably higher produced volume (+ 25–50%).

The maximum difference between the two feed waters is observed at low

fouling conditions: in the case of primary effluent, at $u_{cr} = 2\ m \cdot s^{-1}$ the flux value at $TMP = 0.3$ and $0.5\ bar$ is remarkably higher than at $TMP = 1\ bar$, in opposition to the findings during ultrafiltration of raw sewage.

The fouling mechanisms appear to be the same during filtration of both feed waters; or at least, the trend of resistance with volume $R(vol)$ and the modelling with blocking laws give very similar results with respect to varying operating conditions (TMP and u_{cr}).

Cake filtration is certainly occurring, although other mechanisms may exists as well.

In both cases the major fouling observe at high TMP cannot be accounted to cake compressibility only. Operating at high TMP produces *more* fouling, whether by modifying the cake properties (thickness and density), or by increasing the internal fouling rate.

The application of the blocking laws appears satisfactory to provide indications about the filterability of different feed waters at different operating conditions.

For both feed waters, the best results from modelling are obtained by the cake model calibrated on minutes 10–30 of the filtration test. Consequently, primary effluent and raw sewage could be compared through the estimated parameters k_c and J^*.

The estimated J^* values for primary effluent are about 20–30% higher than in the case of raw sewage, which indicates the higher filterability of primary effluent. k_c values are almost identical in the two cases. The effects of the operating conditions on k_c and J^* is similar for both feed waters.

Chapter 8

Coagulants Addition

Several coagulants are tested to evaluate their effects on filterability and reversibility. The selection of the appropriate coagulants and mixing conditions is made through standard jar tests whereas the filtration tests are conducted at TMP = 0.3 bar and 1.5 $m \cdot s^{-1}$. The filtration and the cleaning procedures are specifically designed to asses reversibility.

8.1 Introduction

In wastewater treatment coagulants are traditionally applied for two purposes: to enhance the removal of particulate and colloids during primary and secondary sedimentation and to improve sludge dewaterability.

The use of coagulants in combination with membrane filtration is reported to be either successful or detrimental. However, in recent years, coagulant addition is becoming a consolidated practice especially during ultrafiltration of effluent (De Carolis *et al.*, 2001; Te Poele, 2002, Qin *et al.*, 2004). The positive effects of the coagulation-flocculation process during membrane filtration can be summarized as follows:

- it aggregates fine particles and colloids reducing the fractions of foulants capable of entering membrane pores;

- it creates large flocs, which can enhance back-transport mechanisms;

- it modifies the physical-chemical characteristics of the deposing materials, changing the properties of the cake layer (i.e. porosity and charge).

The main aims of adding coagulants during ultrafiltration of raw sewage, are to positively impact the filterability of the feed water and the reversibility of the fouling layer. Positive side-effects could be improvements in permeate quality and sludge dewaterability, wherease negative side-effects could be to increase the complexity of the system and to contaminate the sludge chemically.

According to literature coagulation is more efficient at low pH and filtrating only supernatant (see Paragraph 3.4). Nevertheless here:

- the coagulation flocculation step is added as in-line process, aiming at preserving the compact size of the process. This implies that after coagulation the entire coagulated suspension is conveyed to the membrane, and not only the supernatant. The produced flocs take part to the forming filter cake, hopefully improving its characteristics in terms of increased porosity, reversibility and retention of foulants;

- pH is not modified. This is in favour of the concept of a compact simple treatment unit, and enables the immediate reuse of the permeate (reuse laws require the pH to be in the range 6.4–9; Lazarova and Bahri, 2005; Metcalf and Eddy, 2003; Aquarec, 2006).

The choice of the applied coagulant dosages requires compromise between different issues. On one hand, the dosing range should be sufficiently high to investigate the potential effect of coagulants addition. On the other hand, aiming at developing a compact process, the dosage should be not too high, in consideration of the additional sludge production. Applied dosages should also be within the common application range for primary sedimentation, otherwise it would probably be wiser to set up a separate chemically enhanced sedimentation step in front of the ultrafiltration. Finally, the dosing range for the different coagulants should be reasonably comparable.

To cope with these needs, a wide dosing range is investigated during jar tests and smaller dosages are applied during ultrafiltration tests. The maximum dosage of each coagulant that is applied to the membrane (d_{max}), is the one that has given 70% turbidity removal during jar test.

8.1.1 Test series

The investigation proceeded as successive steps, and it is presented in the same form.

Paragraph 8.2 presents the procedure used for the selection of coagulants and the results .

Paragraph 8.3 presents the first ultrafiltration experiments (Test series I), aiming at investigating contemporary filterability and reversibility with coagulant dosage.

Given the (partially) unsatisfactory results of Test series I, Test series II and III are performed, where filterability and reversibility are studied separetely (Paragraph 8.4 and Paragraph 8.5 respectively).

8.2 Selection of coagulants

8.2.1 Approach

The selection of the coagulants to use in combination with the ultrafiltration unit is made through standard jar tests.

The jar test is a method to evaluate the effect of dosages and mixing conditions during coagulation flocculation, and *not* to evaluate the effect of coagulant addition with respect to membrane filtration. In facts, there is no clear relation between the modifications obtained by coagulation-flocculation and wastewater filterability. Here the assumption is that an efficient coagulation-flocculation removes a higher amount of compounds that could contribute to membrane fouling and produces flocs that can take part to the building up of the cake layer.

8.2.2 Description of tested coagulants

During Jar tests six different coagulants are used: three metallic salts and three organic cationic polymers.

The metallic coagulants are chosen among the ones of common use in wastewater treatment: $FeCl_3$, $Al_2(SO_4)_3$, $PACl$ (Poly- Aluminium- Chloride). Two different aluminum salts are tested because $Al_2(SO_4)_3$ is often cheaper, but $PACl$ has been reported to produce stronger flocs and higher performances in association with membrane filtration (Te Poele *et al.*, 2006).

The organic polymers are provided by Cytec Industries Inc. . The selection covers the most common chemical types of organic cationic polymers used in

water clarification and filtration. All the polymers are suitable for application at a wide pH range. Only *C*-592 is certified by NSF International with respect to application in drinking water production and environmental risk (visit *http://www.nsf.org* for details). The products are listed in Table 8.1, whereas extracts from the Data Sheets can be found in Appendix E.

Table 8.1: *Tested cationic organic polymers*

Product	Type	Relative molecular weight	Appearance
Superfloc®*C*-592	polyDADMAC[a]	Medium	Liquid
Superfloc®*C*-581	polyamine	High	Liquid
Superfloc®*C*-492	PAM[b]	High	Powder

[a] poly-diallyl, dimethil ammonium chloride
[b] polyacrylamide

8.2.3 Description of Jar tests

The jar tests are conducted using a standard apparatus with six beakers, described in Paragraph 4.4.1.
A typical jar test consists of three successive phase: rapid mixing, slow mixing and settling (Metcalf & Eddy, 2003). After the coagulation-flocculation process has taken place, the suspension is left to settle before the supernatant is sampled and analysed. In order to account for the sedimentation effect, one of the beakers always contains an unmodified wastewater sample (blank).

The variables considered for mixing are the G-values and the time interval during the rapid mixing and the slow mixing phase. The efficiency of the process is evaluated differently during the preliminary and the complete tests, as explained in the following.

All the tests are executed at room temperature, in the range 17–21 °C . The measured variation of temperature during comparative tests is negligible (1 °C maximum).

The results of the jar tests are not extensively shown here but can be found in Varela Pinto (2006).

Preliminary tests

During preliminary tests one sample is used for several tests during one day, varying coagulant types, dosages and mixing conditions. The performances are evaluated based on turbidity removal only. The applied conditions are summarized in Table 8.2.

Table 8.2: *Summary of tested dosages and mixing conditions during preliminary jar tests (October 2005 - March 2006)*

Coagulant	Dosage	Rapid Mixing		Slow Mixing		Settling time
		G	time	G	time	
	(mg/L)	(s^{-1})	$(min.)$	(s^{-1})	$(min.)$	$(min.)$
C-592	5-15	520-750	20-120	30-65	3-10	20
C-581	10-30	520-750	20-120	30-65	3-10	20
C-492	0.1-0.8	520-750	20-120	30-65	3-10	20
$FeCl_3$	2-50	150-750	30-60	30-65	1-20	30
PACl	1-15	750	30-60	30-65	5-15	20
$Al_2(SO_4)_3$	2-50	150-750	30-60	30-65	20	30

Complete tests

The "complete" tests are executed twice on the same water sample and on the same day. The optimal conditions emerged from the preliminary tests are applied in two identical experiments, except a few cases when one parameter (mostly the dosage) is slightly changed. A summary is reported in Table 8.3.

The process is evaluated based on an extensive set of chemical-physical analyses: pH, conductivity, COD, TOC, NH_4^+, ortophosphates, turbidity, colour and UV_{254} (see Paragraph 4.5 for details).

COD, NH_4^+ and ortophosphates are indicators of the removal performances with respect to traditional pollution parameters. pH and conductivity measure

Table 8.3: *Summary of tested dosages and mixing conditions during "complete" jar tests (October 2005 - March 2006)*

Coagulant	Test	Dosage	Rapid Mixing		Slow Mixing	
			G	time	G	time
		(mg/L)	(s^{-1})	$(min.)$	(s^{-1})	$(min.)$
C-592	I/II	0;2;4;6;8;20	750	120	50	10/15
C-581	I/II	0;2;4;6;8;20	750	120	50	10/15
C-492	I	0;0.05;0.1;0.2;0.3;0.4	750	120	50	10
	II	0;0.025;0.05;0.1;0.2	750	120	50	15
$FeCl_3$	I	0;2;5;10;20;50	750	60	30	20
	II	0;2;4;6;12;30	750	60	30	20
PACl	I/II	0;1;2;4;8;15	750	60	65	15

the modifications induced by the coagulants on the feed water in terms of acidity and salinity. Finally, the light-absorption measurements (turbidity, colour and UV_{254}) and partially the TOC are used to assess the efficiency of the coagulant to confine fine particles and organics into the flocs. A consistent removal is supposed to reflect on positive improvements in filterability.

Combination of metallic and polymeric coagulants

Four combinations of the best performing metallic coagulants and polymers are tested to assess if the addition of small dosages of polymers can improve the efficiency of the metallic coagulants. Therefore, $FeCl_3$ and $PACl$ are mixed with *C*-592 and *C*-581 at the optimal conditions for the metal salts in use (see Table 8.3). Results are evaluated based on turbidity removal only. Table 8.4 reports the tested dosages.

8.2.4 Results and discussion

Polymers and metallic salts have different effects on the wastewater.

As expected, metallic salts decrease the pH and increase the conductivity, whereas organic polymers do not. However, the effect is modest. Dosing 15

Table 8.4: *Combination of metallic coagulants and polymers: dosages during jar tests*

Metallic Coagulant ($FeCl_3$ or $PACl$) (mg/L)	Polymer (C-592 or C-581) (mg/L)
0	0
1	0; 0.1; 0.2; 0.5; 1.0; 2.0
3	0; 0.1; 0.2; 0.5; 1.0; 2.0

mg/L of $FeCl_3$ or $PACl$, the pH of the wastewater remain above neutrality (pH=7) and the conductivity increases of 1.5–3% only.

As also expected, ammonia is insensitive to the dosage of both metallic coagulants and polymers, On the opposite, orthophosphates can be removed with metallic coagulants. At pH 7–7.5, the positively charged ammonium ions are not attracted into the flocs originated by cationic polymers or Al[III] and Fe[III] species. On the opposite, ortophosphates can easily precipitate as metallic salts of both Al[III] and Fe[III], from which the observed removal.

In the tested range polymers exhibit overdosing effect. Metallic coagulants do not, and removal performances always increase with dosage. The overdosage occurs at different coagulant concentration in different days, which indicates that the optimal dosage of polymers depends on the quality of the wastewater.

The specificity of the polymer type and dosage to a given wastewater is reinforced from the observation that the optimal mixing conditions reported by Nieuwenhuijzen (2002) during similar studies with high molecular weight cationic polymers yielded poor results (15–49% turbidity removal, varying with dosages and coagulants).

Concerning the combination of metallic and polymeric coagulants, in all cases the addition of polymer increases the turbidity removal with respect to the initial metallic coagulant dosage. However, the gain is comparable with the results obtained adding an equivalent amount of metallic coagulants.

One example is given in Figure 8.1. In the Figure, also the removals obtained with $PACl$ only during “complete” tests are plotted, for comparison purposes.

Although they are obtained on a different sample, results are really similar, as it can be seen for dosage = 1 mg/L.

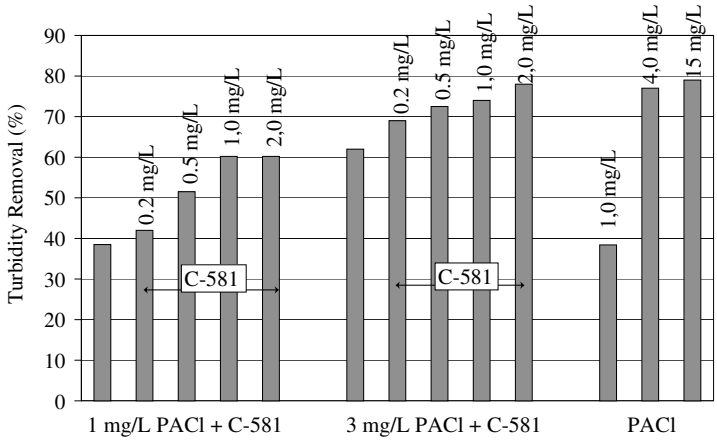

Figure 8.1: *Turbidity removal mixing metallic coagulants and polymers (example: $PACl$ + C-581)*

With respect to turbidity, colour and UV_{254}, higher removal percentages are observed with the use of metallic coagulants. At the optimal conditions, turbidity removal is up to 95% for metallic coagulants and about 70% for polymers. However, it must be remarked that the applied dosages of polymers have been smaller, because of the threshold imposed by the mentioned environmental regulation. When applied to the ultrafiltration process, coagulation will necessary be limited to smaller dosages, because of consideration about sludge production and coagulant costs.

The best COD removals are found around 50% for both polymers and metallic coagulants. In Nieuwenhuijzen (2002) it is reported that the average particles-related COD in the Netherlands is 64% and that only this fraction can be entrapped by coagulation-flocculation. Consequently, during our experiments, only particulate and supracolloidal COD have been removed.

It is noted that if the finest particles are not removed from the wastewater, they are still available to contribute to membrane fouling.

Except that at the maximum applied dosages, the TOC removal percentages are usually lower than COD removal percentages. Since the TOC is more likely than COD an indicator of organic matter, and the organic matter is often related to fouling, again coagulation-flocculation seems to have a limited impact on fouling compounds.

COD and TOC removals shows the same trend of the light absorption measurements, also during the occurrence of overdosing (Figure 8.2). This confirms that the results correspond to the efficiency of flocs formation. Overdosing means excess of available cations, which causes the diffuse layer of suspended particles to be positively charged. Consequently, particles remain stable in suspension instead of flocculating (see Chapter 2). These particles adsorb UV light and also correspond to the measured TOC and COD increase.

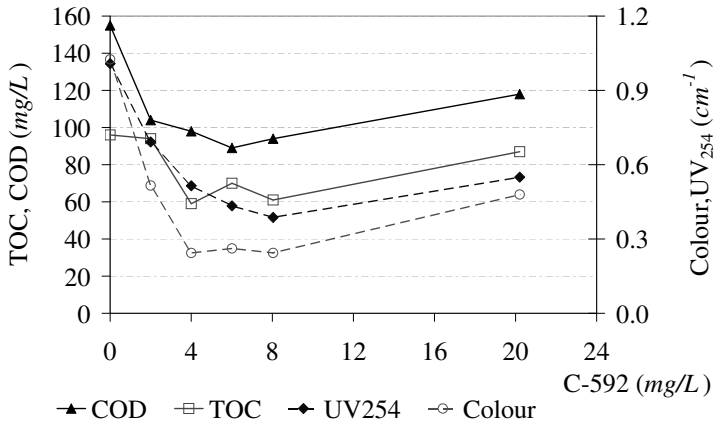

Figure 8.2: *Effect of coagulant dosage on COD, TOC, UV_{254} and Colour (0.45 µm filtrate, shows overdosing)*

Final selection of coagulants

The final selection of the coagulants to apply in combination with ultrafiltration is made on the basis of removal performances and other observations:

- among metallic coagulants, $FeCl_3$ is the cheapest and largely diffuse coagulant at wastewater treatment plant whereas Aluminum salts are emerging for the high performances (Te Poele, 2002, Qin *et al.*, 2004). Since $PACl$ performs better than $Al_2(SO_4)_3$ and produces stronger flocs (Te Poele, 2006), $FeCl_3$ and $PACl$ will be tested during ultrafiltration;
- among organic polymers, C-492 produces high removal at very low dosages. Nevertheless, flocs are sticky and attach to every surface, therefore the use in combination with membrane appears detrimental;
- C-592 exhibits higher performances at low dosages than C-581.

In conclusion, $FeCl_3$, $PACl$ and C-592 are selected for testing with the membrane. $PACl$ and C-592, will be mixed for testing the effect of combined coagulants.

8.3 Ultrafiltration tests, series I

8.3.1 Tests procedure

Each ultrafiltration test makes use of 50 L of fresh wastewater. The coagulation flocculation takes place in the mixing chamber described in Paragraph 4.4.2, at the optimal conditions emerged during jar tests (Table 8.3). After settling, the entire coagulated suspension is conveyed to the ultrafiltration unit.

The maximum dosage per each coagulant (d_{max}) is set to the one that has given 70% turbidity removal during jar test. One blank and 3 different dosages are tested: 1/4 d_{max}, 1/2 d_{max} and d_{max}. Since the test procedure takes more than 3 h, during one day only two tests can be performed and the four dosages must be tested in two different days. This poses the problem of the comparability of results when the same operating conditions (TMP and u_{cr}) are applied to different sample.

Dosages and test schedule are summarized in Table 8.5

The filtration test is composed by two distinct phases, aiming at evaluating the effects of coagulant dosage on the short-term filterability and on the reversibility of fouling during cyclic operations. The operating conditions are fixed at $TMP = 0.3\ bar$ and $u_{cr} = 1.5\ m \cdot s^{-1}$.

Table 8.5: *Coagulant dosages and test schedule during test series I (March-May 2006)*

Coagulant	Day I		Day II	
	I - blank (mg/L)	II - $\frac{1}{4}d_{max}$ (mg/L)	III - $\frac{1}{2}d_{max}$ (mg/L)	IV - d_{max} (mg/L)
$FeCl_3$	0	2	6	12
$PACl$	0	1	2	4
C-592	0	2	4	8
$PACl$ + C-592	0 + 0	3 + 0.2	3 + 0.5	3 + 1

Initially, the coagulated wastewater is filtered continuously for 30 minutes. The observed increase of resistance ΔR_{30} is used to indicate the filterability.

After a backflush of 1 minute, the evaluation of the reversibility is carried on. The procedure is made of a cycle of 7 runs of 10 minutes filtration interrupted by 30 seconds backflush. The reversibility is assessed by studying the drop of resistance after each backflush (see Figure 8.3).

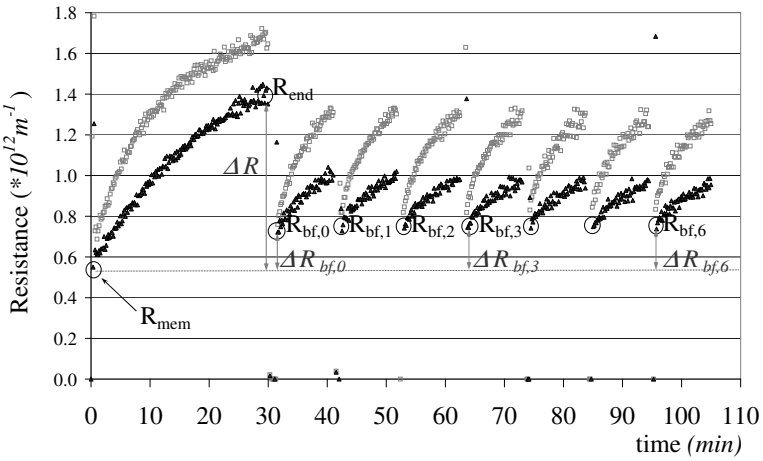

Figure 8.3: *Combined filterability-reversibility test, with and without coagulant*

The duration of the backflush interval is half of the value during the tests of Paragraph 5.2, because that value could achieve full reversibility of produced fouling also without coagulants.

After each test the membrane is cleaned according to the usual procedure and is used for the following tests.

It is noted that the executing the cyclic filtration starting from a "*fouled*" membrane allows to simulate the effect during normal operation.

8.3.2 Filterability and Reversibility parameters

With respect to Figure 8.3, filterability is evaluated as $\Delta R_{30} = R_{end}$ - R_{mem}.

R_{end} is the average of last 5 values of resistance (i.e. 50 *sec.*) and R_{mem} is the clean membrane permeability measured prior to filtration.

Reversibility is evaluated by mean of the resistance values after each backflush period: $R_{bf,i}$. Each $R_{bf,i}$ value is the average of the first 5 resistance measurements after the backflush, corresponding to approximately 50 *sec.*.

In first place, $R_{bf,0}$ is calculated after the first backflush with 1 minute duration. $\Delta R_{bf,0} = R_{bf,0}$ - R_{mem} is the fraction of ΔR_{30} that can be removed by the backflush itself.

Secondarily, the series of $R_{bf,i}$ values is used to calculate $\Delta R_{bf,i} = R_{bf,i}$ - R_{mem}. The series of $\Delta R_{bf,i}$ gives indications about the trend of the reversible fouling after each filtration period.

Temperature effects can be neglected: the temperature variation among Day I and Day II is always smaller than 2 $°C$, and the temperature increase during cyclic filtration less than 1 $°C$.

8.3.3 Results

Filterability

Figure 8.4 summarizes the results of the filterability tests by showing ΔR_{30} values.

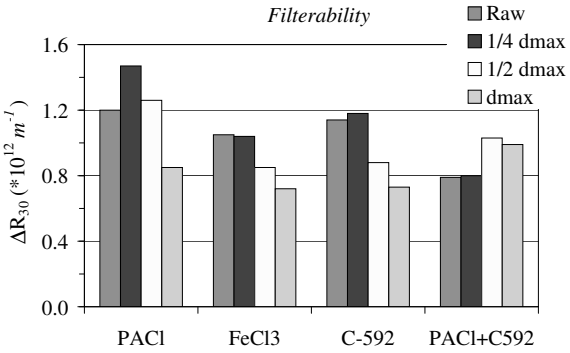

Figure 8.4: *Effect of coagulant dosages on short-term filterability*

All coagulants show similar results, except the case $PACl$ + C-592, which is biased by unusual membrane conditions, as explained in the following.

Despite the use of different samples during test I - II and tests III - IV, a clear trend is visible with increasing coagulant dosage. The addition of $\frac{1}{4}d_{max}$ appears useless or even detrimental to the filterability of raw wastewater. On the opposite, $\frac{1}{2}d_{max}$ and d_{max} always produce an increase in filterability. The decrease in ΔR_{30} when d_{max} is applied is about 30-35% .

The exception represented by the combination of $PACl$ and C-592 can be explained on the basis of the unusual conditions of the membrane during the day of test I and II, which biases the calculation of ΔR_{30}. R_{mem} values were rather constant during the testing period, oscillating in the interval 0.49 - 0.57 $\cdot 10^{12} m^{-1}$. Differently, on the first day of test with $PACl$ + C-592, R_{mem} values were 1.01 and 0.82 $*10^{12} m^{-1}$ during test I and II respectively. The reason can be found in the long storage period prior to that tests, during which the membrane was in contact with an alkaline preservative solution that caused "swelling". However, when R_{end} is considered, results are in agreement with the general trend.

Reversibility

The results of reversibility tests are displayed in detail in Figure 8.5, which shows the series of calculated values $\Delta R_{bf,i}$.

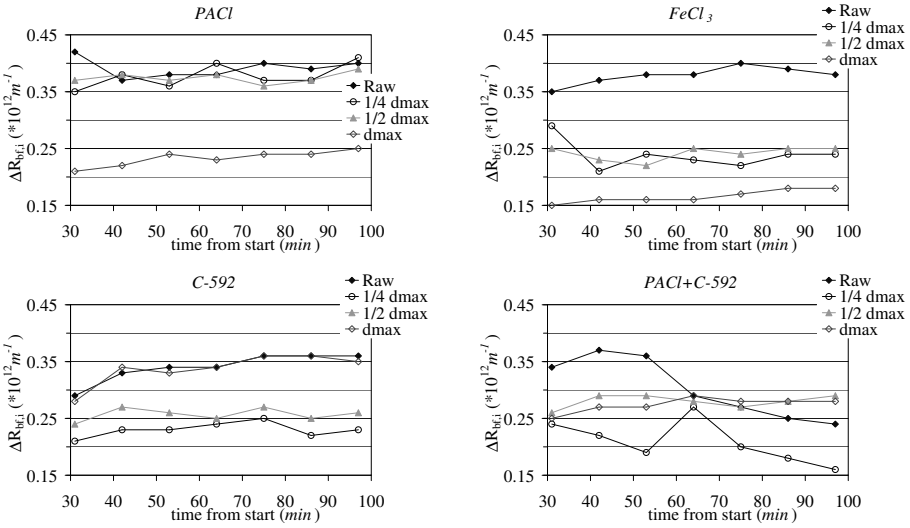

Figure 8.5: *Trends of resistance increase with and without coagulants, as* $\Delta R_{bf,i}$

At the end of the 30 *min* filtration, the reversibility of fouling after 1 *min.* backflush is not complete. The irreversible fouling is not negligible; $\Delta R_{bf,0}$ is in the range 0.15–0.35 $\cdot 10^{12} m^{-1}$.

Results from the cyclic filtration are not very clear. In general, $\Delta R_{bf,i}$ values seem to increase with time, with the exception of the biased test with $PACl + C$-592. Nevertheless, the growth is slow and the expected differences due to the coagulant dosages are hardly appreciable (the latter may also depend on the variability of wastewater between testing day I and II).

Additionally, in some cases the final value of resistance after the cycle is lower than $\Delta R_{bf,0}$.

It is concluded that the method is not suitable to quantify the effect of coagulant type and dosage on reversibility.

8.4 Ultrafiltration tests, series II

8.4.1 Test Procedure

Test series II is meant to assess filterability and reversibility during a single 30 *min.* continuous run. The aim is to reduce the impact of the variation of wastewater quality, by testing different dosages on the same wastewater.

The operating conditions are fixed at 0.3 bar and 1.5 $m \cdot s^{-1}$.

The continuous tests are executed in group of 3 during the same day, using one sample of 150 L (each experiments consumes 50 L). The tested coagulant dosages are blank, $\frac{1}{2}d_{max}$ and d_{max}. Filterability is quantified as ΔR_{30} and reversibility as $\Delta R_{rev} = R_{end} - R_{bf}$.

R_{bf} is the residual resistance after 1 *min.* backflush. Differently from test series I, R_{bf} is measured using clean water.

An example of the procedure is given in Figure 8.6. After 30 minutes of filtration the feeding is interrupted and the permeate bucket emptied. The filtration of wastewater starts again for 5 minutes, during which the permeate is collected for analyses. Finally, after 1 *min* backflush, tap water is fed to the installation in order to measure the residual resistance R_{bf}.

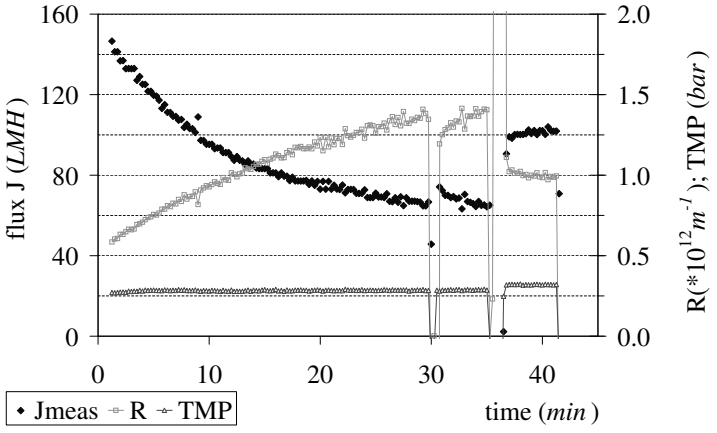

Figure 8.6: *Filterability test, series II, June–September 2006*

8.4.2 Results

Filterability

Figure 8.7 summarizes the effect of coagulant dosing on filterability by showing the resistance increase ΔR_{30}'s for all the applied coagulants (or combination).

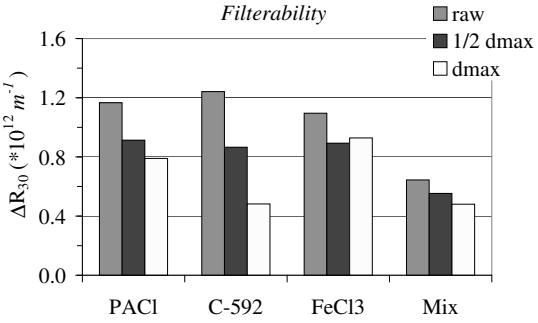

Figure 8.7: Effect of coagulant dosages on short-term filterability

In consequence of coagulants addition the ΔR_{30} values decrease substantially. At the maximum dosage applied, the reduction is 32% for $PACl$, 18% for $FeCl_3$, 61% for C-592 and 25% for the combination $PACl$ + C-592. Therefore, it is confirmed that filterability can be improved by coagulants addition.

Reversibility after 30 *min* of continuous filtration

In Figure 8.8, the total ΔR_{30} values are split into the reversible and irreversible parts.

The effect of coagulant addition on the reversible fraction varies from case to case. In the case of $PACl$ and $FeCl_3$ the addition of coagulant seems to increase the amount of reversible fouling, whereas this decreases with C-592.

On the opposite, the irreversible fouling decreases with coagulant addition in all the cases. It can be noted d_{max} produces only a little improvement compared to $\frac{1}{2}d_{max}$.

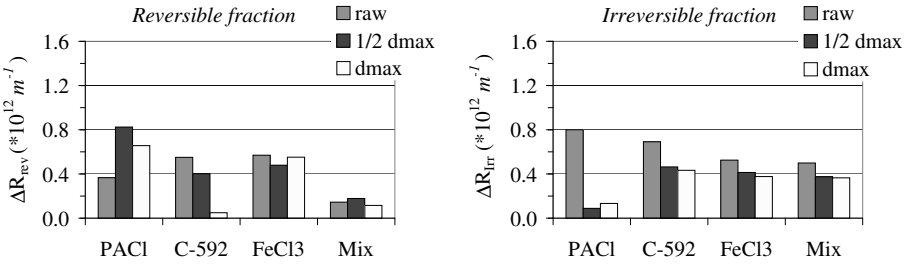

Figure 8.8: *Effect of coagulant dosing on fouling: reversible (left) and irreversible (right) fraction of resistance increase*

8.5 Ultrafiltration tests, series III

8.5.1 Test Procedure

For each coagulant, the tests of Series III are executed one day after the corresponding test of Series II, using a different wastewater sample.

An example of the procedure is given in Figure 8.9.

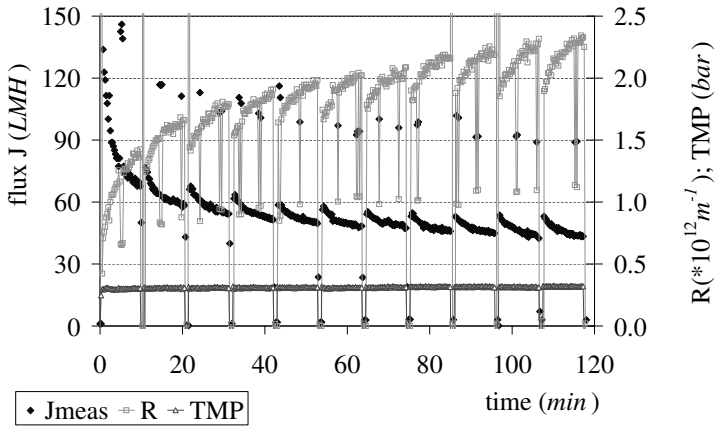

Figure 8.9: *Long term reversibility test, series III, June–September 2006*

Starting from a clean membrane, 10 *min* of filtration are alternated to 30 *sec* of backflush for a total duration of 2 *h* (11 cycles). With respect to Test Series I, the use of a clean membrane and the extended duration are meant to to emphasize the effect of coagulant addition with respect to reversibility.

The same sample (two times 50 *L*) is used to compare raw wastewater and wastewater added with d_{max}. Reversibility is assessed through the series of $\Delta R_{bf,i} = R_{bf,i}$ - R_{mem}, as in Test Series I.

8.5.2 Results

For each coagulant, results are shown in Figure 8.10.

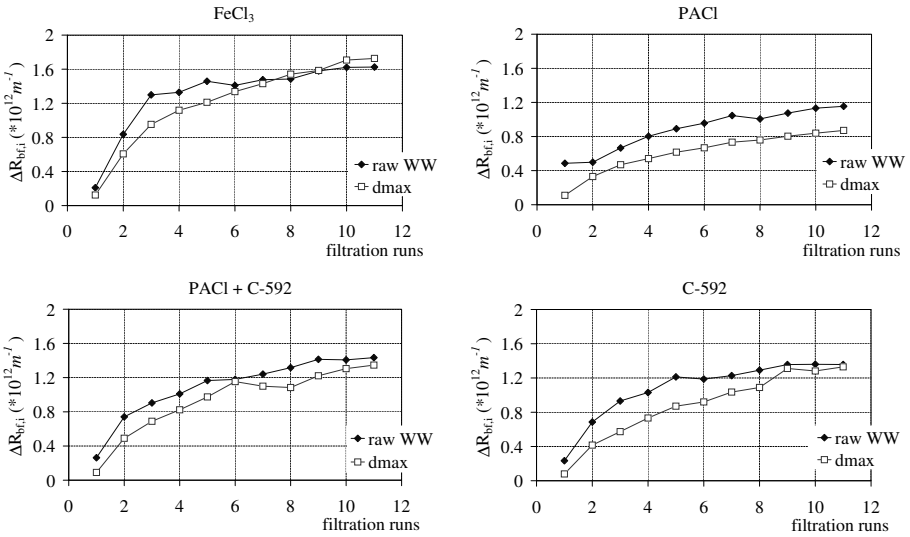

Figure 8.10: *Trends of resistance increase with and without coagulants, as* $\Delta R_{bf,i}$

For both coagulated and raw wastewater 30 *sec* of backflush are not sufficient to remove the building up of fouling. A fraction of irreversible fouling is produced during each filtration period and the resistance increases continuously run after run.

It can be noted that:

- during the first runs the resistance increase is slower for the coagulated water, indicating a higher reversibility. However, with the exception of $PACl$, this is only a temporary effect and after 2 h similar total resistance increase is observed;
- the overall resistance increase is much higher than it was during tests series I, when the same cyclic filtration was started from a not completely cleaned membrane. Comparing the results at the start of cycle 7, the total resistance increase was $0.18–0.41 \cdot 10^{12} m^{-1}$ during test series I and is $0.7–1.4 \cdot 10^{12} m^{-1}$ during test series II.

8.6 Fitting of filtration curves

8.6.1 Procedure

The method developed in Chapter 6 is applied to the short-term filterability tests of Series II. The cake model, the pore constriction model and the pore blocking model are fitted to the filtration curves of Test series II (raw wastewater, $\frac{1}{2}d_{max}$ and d_{max}). The fitting is calculated for the entire filtration interval and for minutes 10–30.

In agreement with the findings of Chapter 6 and 7, the best fitting results are obtained by the cake model calibrated on minutes 10–30, which are presented here.

8.6.2 Results of cake model fitting during minutes 10–30

A visual impression of the results of the fitting is given in Figure 8.11 and 8.12. The estimated parameters and the usual statistics are presented in Table 8.6.

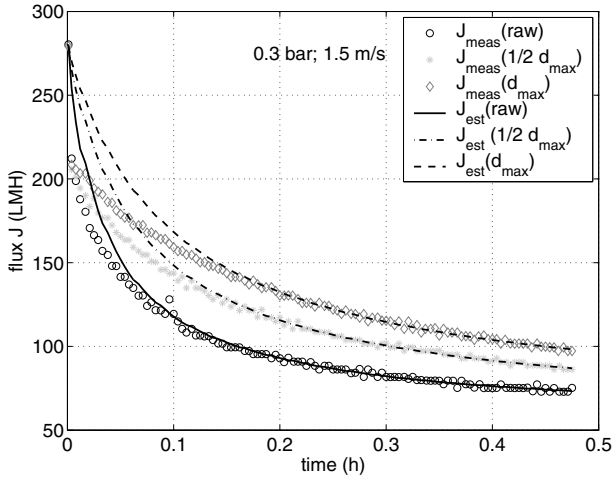

Figure 8.11: *Results of modeling curves during PACl addition*

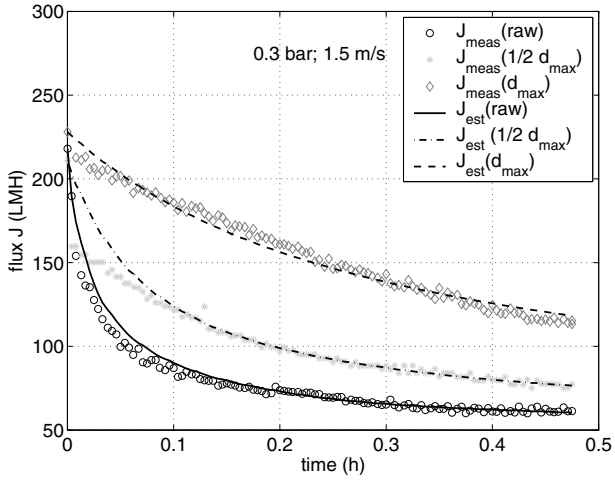

Figure 8.12: *Results of modeling curves during C592 addition*

Table 8.6: *Estimated parameters and statistics with cake model calibrated on minutes 10–30 (TMP = 0.3 bar, u_{cr} = 2.0 $m \cdot s^{-1}$)*

	dosage	J^* (LMH)	k_i^* $\cdot 10^{11}$ (m^{-4})	R^2 (-)	SSe $(LMH)^2$
$PACl$	raw	62.6	6.1	0.971	103
	$\frac{1}{2}d_{max}$	63.4	3.1	0.986	101
	d_{max}	64.1	2.1	0.988	113
Mix	raw	92.0	8.1	0.905	222
	$\frac{1}{2}d_{max}$	91.6	4.1	0.713	1170
	d_{max}	89.2	2.9	0.975	124
$FeCl_3$	raw	69.3	9.1	0.939	155
	$\frac{1}{2}d_{max}$	64.9	4.9	0.907	238
	d_{max}	62.3	6.6	0.961	110
C−592	raw	57.3	12.0	0.911	142
	$\frac{1}{2}d_{max}$	58.9	4.2	0.971	130
	d_{max}	0.0	0.6	0.944	1101

From Figure 8.11 and Figure 8.12 it is visible that the measured flux values at the start are well below the modeled starting value, corresponding to the J_0 values measured with clean water prior to filtration. Consequently, the first part of the flux curve is badly modeled.

When coagulant is dosed, the flux decline is smooth and after 30 minutes still continues. This is the hardest trend for the model to fit: in an extreme case the rate of flux decline seems almost linear and the fitting is definitively not satisfactory (Figure 8.12, C-592, d_{max}).

The difference between the observed and estimated curves increases with the dosage of coagulant.

The poor modeling results are confirmed by the statistics in Table 8.6.

The average correlation coefficient (R^2) is 0.931, rather low when compared with results from Chapter 6 and 7.

Looking at the estimated parameters, the main remark concerning J^* values is that the dosage of coagulant has little effect.

Other general comments are hardly possible. J^* has a slight increase with

dosage for $PACl$ and a slight decreases with the Mix. The value $J^* = 0$ obtained with C-592 d_{max} indicates the failure of the fitting when the flux declines with very little curvature (without inserting the constriction $J^* > 0$ in the code, the model would estimate a negative value).

The effect of the dosage on k_c is more obvious. Excluding the *failed* case of C-592 d_{max}, the values of k_c follows the same trend of ΔR_{30} in Figure 8.7: increasing coagulant dosage reduces k_c. The only exception is represented by $\frac{1}{2}d_{max}$ for $FeCl_3$.

However, it can be noted that the variation is small compared to the variations provoked varying TMP and u_{cr} during the filtration of raw sewage (Paragraph 6.5.3) and primary effluent (Paragraph 7.2.3).

8.7 Physical-chemical analyses

8.7.1 Procedure

A large set of chemical-physical analyses is executed during both test series I and II. Since results are similar, the values from the filterability tests of series II, more homogeneous because executed on the same sample, are described in the following.

The analyses are performed on the feed and on the permeate. The feed can be raw wastewater or supernatant, filtrated over a 0.45 μm membrane when necessary. Table 8.7 reports the list of the analyses.

Table 8.7: List of performed analyses

	Raw	**0.45 μm filtrate**	**Permeate**
Turbidity	*	*	*
pH	*	*	*
EC	*	*	*
Colour		*	*
UV		*	*
EPS		*	*
COD	*	*	*
Metals[a]			*

[a] metals analysis only when using a metallic coagulant

With respect to the definition given in Paragraph 2.1.1, a different classification of of particle size is used. The aim is to adapt the classification to the applied fractionation procedure. Consequently: "suspended solids" is the materials above 7–12 μm, "colloids" is the material between 0.45 μm and 7–12 μm, "supra-dissolved solids" is the material between 0.03 μm and 0.45 μm, "dissolved matter" the material below 0.03 μm.

8.7.2 Results

Concerning pH and conductivity (EC), the results confirm the observations of the jar tests: the metallic coagulants decrease pH and increase conductivity. However, at the applied dosages changes are small: pH remains above neutrality and EC varies less than 3%.

The COD and the turbidity in the supernatant indicate that a good coagulation is achieved also in the 50 L coagulation set-up: COD and Turbidity removals are comparable with the ones obtained during jar tests (36-43% for COD, about 70% for turbidity).

Figure 8.13 reports the values of COD in the various fractions during filtration of raw wastewater and d_{max}. In agreement with the approach of Paragraph 8.2.4, by comparing the COD concentration in the different fractions it is possible to draw some conclusions about the effect of coagulation on the particles of different size.

For both raw and coagulated water, the COD content decreases progressively from the feed water, to the 0.45 μm filtrate and the permeate. The gap between feed water and 0.45 μm filtrate, is much smaller in the case of coagulated water.

The COD values in the supernatant of the coagulated water are considerably lower than in the raw wastewater. Except for $FeCl_3$, also the COD values in the 0.45 μm filtrate are higher in the case of raw wastewater. On the opposite, the comparison of COD values in the two pemeates show that they are equal in the case of PACl, lower for coagulated water with C-592, higher for the coagulated water with $FeCl_3$ and with the Mix.

Apparently, coagulation enhances the removal of particulate and colloidal COD, but also of the supra-dissolved fraction. This last finding is in disagreement with experience (van Nieuwenhuijzen, 2002; Soffer *et al.*, (2000); Shon *et*

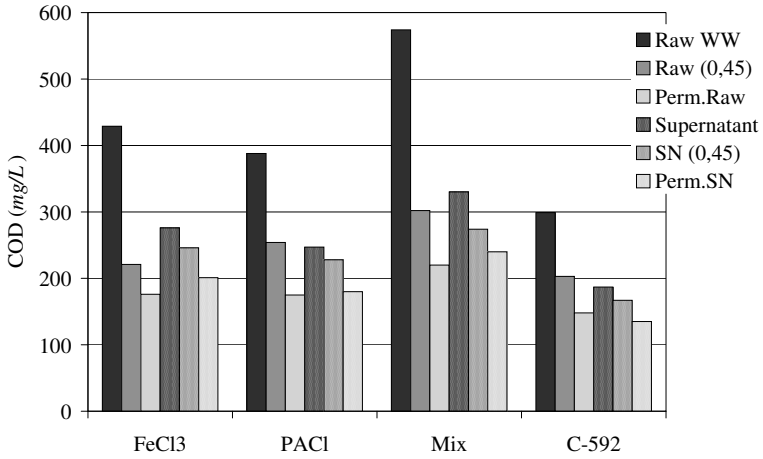

Figure 8.13: *COD values in the feed water fractions during filtration of raw wastewater and* d_{max}

al., 2005); it may be suggested that coagulation or hydrolysis phenomena of organic matter may occur during the storage period of the sample.

Finally, the COD values in the permeate can be said insensitive to coagulation.

The effect of coagulation on the fine constituents of the feed identified as foulants (UV_{254}, Colour, Proteins and Polysaccharides), is similar for all test series. Results for raw wastewater, $\frac{1}{2}d_{max}$ and d_{max} are shown in Figure 8.14.

In the left column, results from the 0.45 μm filtrate are shown. Results are consistent, as all the measured parameters decrease with increasing coagulant dosage (colour result from test SN2 with $PACl$ is probably a measurement error).

On the right column, the corresponding values in the permeate are shown. In this case the measured values can hardly be related to the applied coagulant dosage. In most cases values in the permeate are below values in the 0.45 μm filtrate, but there are two exceptions with Proteins (Mix; C-592) and one with Polysaccharides (C-592).

Finally, it is remarked that at the highest applied dosage traces of metals are found in the permeate, which must be considered in case of reuse options.

8.8 Discussion of ultrafiltration results

8.8.1 General

The filtration tests essentially demonstrate that the addition of coagulants, at the dosages and conditions applied, has sensible effects on filterability and fouling characteristics, but not on reversibility.

In order to explain such dichotomy, the main findings are discussed in detail in the following.

8.8.2 Foulants removal by coagulation

From literature, coagulation-flocculation at natural pH is expected to have limited efficiency in aggregating into flocs dissolved foulants (see Paragraph 3.4).

In agreement with that, the COD concentration in the various fractions (raw feed, supernatant,) indicates that the addition of coagulants mostly involves particles and colloids.

Nevertheless, from the values in the $0.45\mu m$ filtrates of raw and coagulated feed water, it appears that also a little of the supra-dissolved fraction is removed. This result is confirmed by the measurements of UV_{245}, colour and EPS in the supernatant, which show decreasing values with increasing coagulant dosage (see Figure 8.14, left column).

In conclusion, at the start of filtration the coagulated water contains less "free" colloids and supra-dissolved foulants than the feed water.

8.8.3 Flux decline and fouling mechanisms

With respect to raw wastewater, during the filterability tests the coagulated water shows a "slower" flux decline.

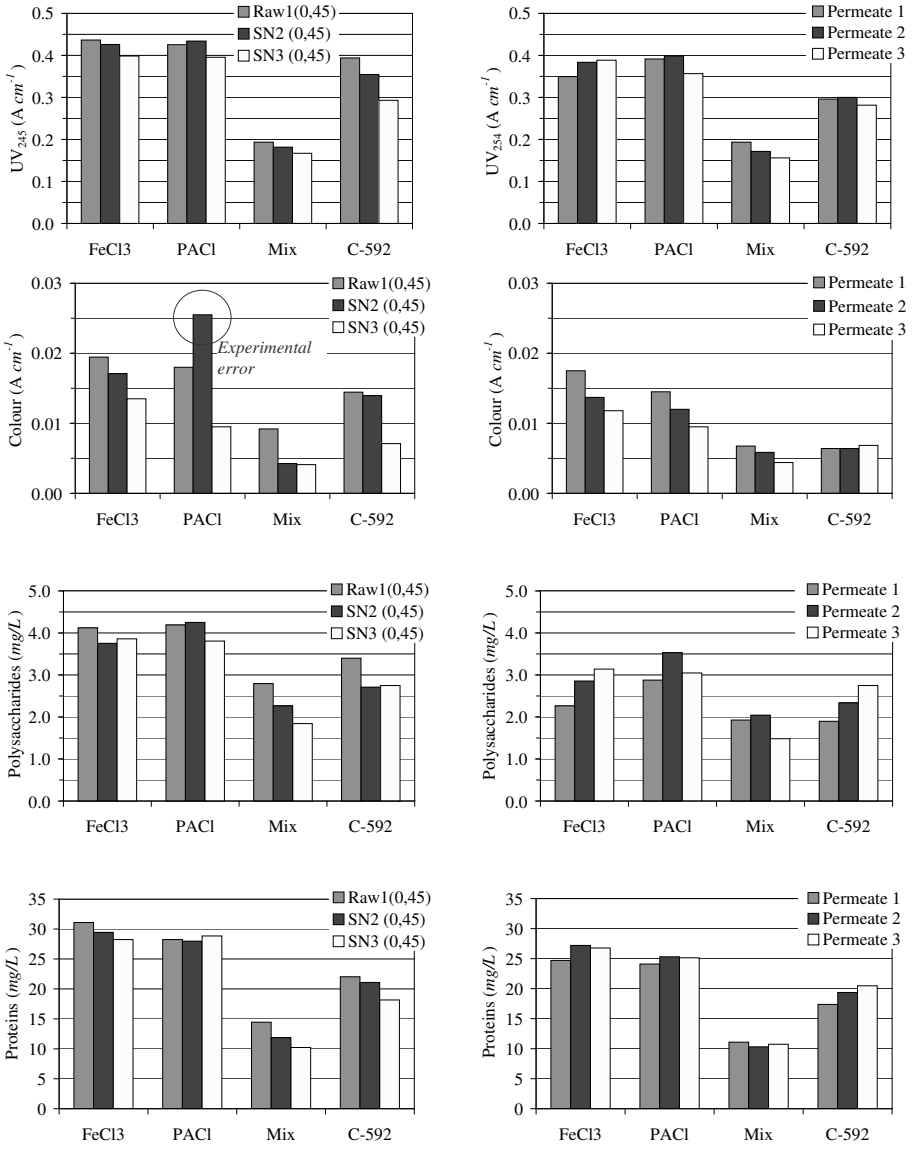

Figure 8.14: *Foulants in the 0.45 μm filtrate (left) and in the permeate (right). SN2 = SuperNatant $\frac{1}{2}d_{max}$ and SN3 = SuperNatant d_{max}*

The delayed decline could be caused by several mechanisms, such as entrapment of foulants in the flocs, enhanced back-transports, erosion of the filter cake, enhanced porosity of the filter cake and entrapment of dissolved foulants in the cake layer, that could act as additional filter on top of the membrane.

Obviously, none of the formulated hypothesis can be fully proved on the basis of the available data. Nevertheless, the following two remarks seem possible.

1) The coagulated water contains less foulants in a "free" form, and therefore colloidal fouling and internal fouling could be reduced.

2) The rapid formation of a cake layer on the membrane surface can protect it from more dramatic types of fouling. This hypothesis finds confirmation in the comparison of the reversibility results during test series I and II (note that the results of the filterability tests in the two periods are similar, therefore overall results are likely comparable):

- during test series I, 70 minutes of cyclic filtration were executed starting from a "fouled" membrane and produced a resistance increase always below $0.1 * 10^{12} m^{-1}$. During test series II, starting from a clean membrane, the increase after 70 minutes was several times higher, between 0.7 and $1.4 \cdot 10^{12} m^{-1}$;

- during test series I, the total increase of resistance after the last backflush (about 100 *min* from start) is in the range $0.24–0.40 \cdot 10^{12} m^{-1}$. After the same filtration time, for series II the irreversible fouling is in the range $1.1–1.6 * 10^{12} m^{-1}$.

In conclusion, the filtration procedure impacts on fouling formation and reversibility, and in particular the rapid accumulation of material obtained by 30 *min* of unstopped filtration protects the membrane from irreversible fouling.

It can be suggested that the delay in flux decline caused by coagulant addition is somewhat similar. The volume of flocs covers the membrane surface rapidly and hinders the transport of smaller foulants to the membrane surface and pores.

8.8.4 The effect of time and shear

The modifications induced by coagulation are transient, i.e. after two hours of filtration the resistance increase is the same whether the coagulant is dosed to the feed water or not.

This fact was already reported in literature (Al Malack, 1996; Soffer *et al.*, 2000; Kim, *et al.*, 2001) and the chemical analyses can help interpreting this finding.

Differently from the values in the 0.45 μm filtrate, the values of UV_{254}, colour and EPS in the permeate do not decrease with the coagulant dosage. In three cases, EPS are even higher in the permeate than in the 0.45 μm filtrate, although the membrane nominal pore size is more than 10 times smaller.

Excluding measurement errors, this can be explained supposing that during the recirculation in the filtration set-up the coagulated flocs break.

During the static filtration over the 0.45 μm membrane, the flocs are preserved and coagulants retain the foulants "proportionally" to the dosage. During the filtration in the crossflow set-up, the total feed volume is recirculated more than 100 times in 2 h, and the plenty of passages through the pump produce the rupture of flocs and the release of foulants.

The fact that these foulants are found in the permeate, also reveals that the filter cake is not capable of retaining them.

$PACl$ is the only coagulant that maintain an appreciable effect after 2 h. This result is in agreement with the information from literature, where $PACl$ is reported to produce stronger flocs than $FeCl_3$ (Te Poele, 2006) and the flocs of C-592 have been reported to have a limited resistance to shear (Kim et al, 2001).

8.8.5 Modelling

The overall fitting with the method developed in Chapter 6 and 7 is not very effective and some flux decline rates of coagulated water can be hardly modeled.

This is first of all a consequence of the automated measurement procedure, which causes the loss of some initial measurement points, so that J_0 is remarkable higher than the initial flux values. When the last 20 min of filtration are used for fitting, the impact of this problem should be limited but fitting results

are still low. This may depend on the slow continuous flux decline. Since a pseudo-stationary flux is not reached, there is not a stable sub-set of data that prevails in the calculation of model parameters.

However, there is also a positive note. The fitting with the cake model calibrated on minutes 10–30 estimates minimal differences in J^*, i.e. that the addition of coagulant has negligible effect. The "prediction" is in agreement with the general results of the 2 h reversibility tests and is obtained on the basis of a 30 minutes filterability test. Looking at Figures 8.11 and 8.12, the final flux values after 30 minutes appear rather distinct; therefore, when the accuracy of the data is sufficient, the method is capable of extrapolating information that is hardly visible.

8.9 Conclusions and recommendations

Two metallic coagulants ($FeCl_3$, $PACl$) and one cationic organic polymers (C-592) are tested in combination with crossflow ultrafiltration of raw municipal wastewater. The aim is the development of a compact purely physical-chemical hybrid system for wastewater treatment.

At natural pH (7.5-7.8), metallic coagulants and cationic organic polymers successfully aggregate in the flocs a minor fraction of colloidal and supra-dissolved COD and organics. However, the shear forces during recirculation induce the ruptures of the flocs and the release of foulants, which become available to permeate or foul the membrane.

During crossflow ultrafiltration, when sufficient dosage is applied, coagulant addition results in a moderate increase of short-term filterability (20-35%).

On one hand, the positive effect of coagulants addition on filterability might be related to the observed entrapment of foulants. On the other hand, the overall resistance increase is affected by the filtration procedure and a positive contribution is given by the formation of a protective cake layer on the membrane surface, enhanced by coagulant flocs.

The effect of coagulant addition is only temporary and looking at the reversibility the improvements becomes rapidly negligible. After 2 h, among the tested coagulants only $PACl$ seems to enhance flux value stably. The stability

of the flocs with respect to shear forces appear a key issue for the effectiveness of coagulants addition prior to filtration.

The fitting of flux curves with blocking laws is somewhat difficult. Nevertheless, by using the data from 30 *min* filtration, the estimated model parameters predict (or reproduce) the limited effect of coagulation observed from the flux values after 2 *h*.

Chapter 9

Application

Concepts and results from previous chapters are integrated with data from existing ultrafiltration and MBR plants to attempt estimating the cost of water production with direct ultrafiltration.

9.1 Method and boundaries

In the following, the cost of crossflow direct ultrafiltration with tubular membranes is estimated. The exercise is based on the configuration of the filtration rig used in this research, i.e. batch single-stage. Only water production costs are considered, whereas sludge costs, land costs, and all the other items not strictly related to the process itself are excluded (e.g. staff, insurances, etc...).

With respect to the potential applications listed in the Introduction, the estimate may apply to the case of water extraction by "sewer mining" (see Paragraph 1.3.3). In order to evaluate the economics of direct ultrafiltration for preliminary treatment or complete treatment information about sludge treatment would be required. This is out of the scope of this dissertation and is not discussed here.

The cost estimation is based on a hypothetical plant design, presented in the following Paragraph 9.2. The operating figures of Paragraph 5.2.2 are combined with general figures of existing crossflow UF and MBR plants, chosen among industrial and civil applications, in consideration of similarities and differences with the hypothetical design.

The calculation is made for two different plant sizes: 300 P.E. and 5000 P.E. (1 P.E. = 200 m^3/day). Ideally, the two sizes correspond to a tourist resort and a small treatment plant, where water extraction by direct ultrafiltration could be applied for irrigation purposes or to reduce peak loads.

The calculation proposed assumes that operations are run continuously for 24 $h \cdot day^{-1}$, all year long.

9.2 Description of hypothetical plant

A plant for direct ultrafiltration would be composed essentially by a membrane filtration unit and a buffer tank, as it was already presented in Figure 1.4. Figure 9.1 reproduces that concept adding a few details for the technical implementation.

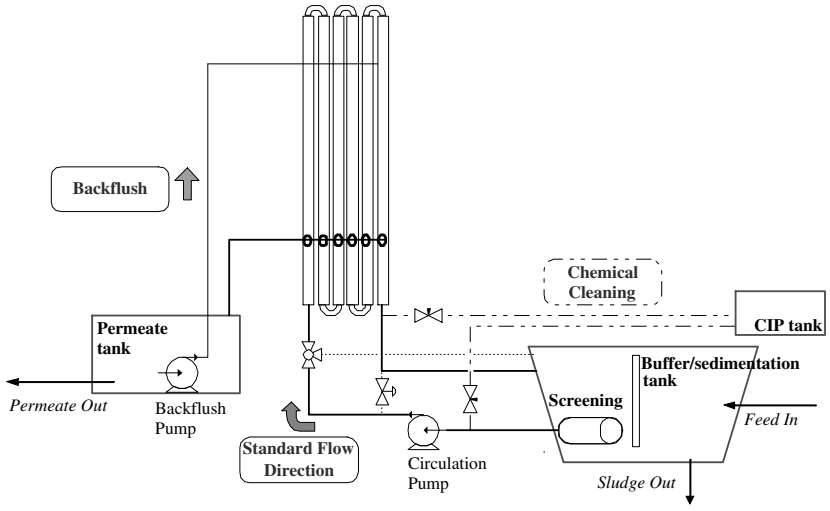

Figure 9.1: *Schematic layout of direct ultrafiltration*

The stream of raw wastewater enters a collection tank which acts both as a buffer for the flow and as a sedimentator to separate settleable solids. From

the buffer tank, the wastewater is pumped into the membrane system, which produces two streams: the concentrate (returned to the buffer tank), and the permeate. A (partially) separated pipe system is provided for the cleaning in place (CIP) procedure, which is a robust cleaning procedure for recovering membrane permeability. It can be noted that:

- in the buffer tank, sedimentation prior to the intake of the membrane circuit is enhanced by means of a simple flow deflector;
- the intake of the membrane circuit is further protected by a fine screen, to avoid introducing into the circuit undesired big particles. When this screen has a mesh dimension of about 0.56 mm mesh, the circulated water will have the same characteristics as during the testing of the previous Chapters;
- the membrane system can be operated in two directions, in order to avoid excess fouling of one module due to the order in the train (the first modules operate at higher TMP whereas the last modules filter a more concentrated wastewater).
- to reduce costs the circuit for the CIP procedure makes use of the circulating pump of the main membrane system. Alternatively, being seldom practiced, the CIP can be realized on single module in a separate system, using a spare pump of the main membrane system.

However, Figure 9.1 is merely a visualization of a general concept. Several other issues remain open before a general design can be attempted:

- *membrane configuration*: the membrane unit of Figure 9.1 represents six modules in series, according to the typical configuration of high-pressure crossflow filtration. In practice, two different configurations are possible, as explained in the following Paragraph 9.5.1. The number and type of membrane modules obviously differ according to the required membrane area and conversion factor;
- *piping*: more complicated piping and instrumentation could be added to allow the exclusion of some modules from operation during maintenance practice or because they are temporary not necessary;
- *sludge extraction*: for the sake of simplicity, the sketch of the buffer tank does not include a sludge-extraction system. This could be realized by gravity (cheaper) or with a pump (for more accurate process control,

specifically the sludge concentration). The proper choice is probably dependent on the application and on the global management of the produced permeate and waste stream, therefore it is not discussed here;

- *pre-screening*: in practical applications the buffer tank design is anticipated to be a key element. Indeed, in MBR's (STOWA, 2002; De Wilde *et al.*, 2005) and in UF systems (Te Poele, 2006; Judd and Jefferson, 2003) the pre-screening is of fundamental importance. Additionally, some authors report that during filtration of untreated wastewater the permanence of the rejected organic matter in the loop lead to reduction in the soluble COD, most likely because of uncontrolled biological degradation or biological flocs formation (Ahn *et al.*, 2001; Rulkens *et al.*, 2005). This phenomenon is not taken into account here but it could turn into a major point because of the beneficial effect on the organic content of the permeate.

Although the discussion above includes several ideas for implementing the process, it also confirms that the overall design of a direct ultrafiltration plant is far to be completed. Consequently, cost estimates will find support on comparison with similar existing plants rather than calculating in detail the components of an hypothetical plant.

9.3 Data of calculation exercise

9.3.1 Operating conditions

In Paragraph 5.2.2 it was demonstrated that at certain operating conditions direct ultrafiltration of raw sewage can be run stably for several hours. Table 9.1 reports the specifications of the experiments corresponding to the three highest calculated net-flux values.

It is remarked that the operating conditions have not been optimized, neither in terms of permeate production, nor of energy consumption.

The three conditions that yielded the highest productivity are pretty similar. Since pre-treatments such as sedimentation and coagulation have shown little effect on improving the filterability of raw wastewater (see Chapter 7 and Chapter 8), the values of Table 9.1 are assumed as design basis. The exact values,

Table 9.1: *Maximum calculated net-flux values (long-term tests, Paragraph 5.2.2)*

TMP *bar*	u_{cr} $m \cdot s^{-1}$	Filtration time *min.*	BF time *sec.*	Av.gross-flux LMH	Net-flux LMH
0.3	2	3	18	125	83
0.3	1.5	3	18	125	79
0.3	2	1	5	122	86

slightly more conservatives than the observed ones, are summarized in Table 9.2.

Table 9.2: *Design operating values for cost estimation*

TMP	0.3	*bar*
BF Pressure	0.8	*bar*
u_{cr}	1.5 - 2	$m \cdot s^{-1}$
Gross-flux	120	LMH
BF flux	350	LMH
Net-flux	70	LMH

9.3.2 Design Inputs

For the two proposed plant-size, the starting point is the daily flow. The goal is to convert at least the 75% of it into permeate within the same day, so that it could be reused or further treated. Consequently, it is supposed that the ultra-filtration plant is connected to a traditional wastewater treatment system where the untreated flow/sludge is delivered (it could be a septic tank, the sewer, or even a sludge treatment line).
Using the operating conditions of Table 9.2, the minimum required membrane area is calculated and a reasonable design is made for the membrane units and necessary pumps, considering commercially available products.

Table 9.3 reports the design values used in cost estimate.

Table 9.3: *Summary of design data for the two estimates*

	Resort	Small Plant
Daily feed flow	60 $m^3 \cdot d^{-1}$	1000 $m^3 \cdot d^{-1}$
Daily permeate flow	48 $m^3 \cdot d^{-1}$	877 $m^3 \cdot d^{-1}$
Membrane module	3 m; 8 $inch$	3 m; 8 $inch$
Number of modules	1	18
Membrane area	29 m^2	522 m^2
Max Conversion Factor	81%	88%
Independent street	1	3
Circulation pump(s)	2–5 ($m^3 \cdot h^{-1}$); 1 (bar)	2–5 ($m^3 \cdot h^{-1}$); 3.5 (bar)
Backflush pump(s)	10 ($m^3 \cdot h^{-1}$); 1 (bar)	60 ($m^3 \cdot h^{-1}$); 1 (bar)

9.3.3 Cost data from existing plants

The ultrafiltration process is used in a variety of industrial applications, water treatment and wastewater treatment. Although the general principles are the same, each application is characterized by very specific features, *in primis* the feed water matrix. Also the economic boundaries change from case to case, e.g. there are enormous differences while processing highly valuable products, or drinking water, or wastewater. This background reflects in the existing variety of membrane geometry, material, configuration and mode of operation. Applications are often specifically tailored and consequently figures are very scattered. Caution must be taken while generalizing over cost data and references should be chosen appropriately.

For calculation purposes, the membrane filtration unit is assumed to be identical to the units of existing MF/UF crossflow plants and MBRs that mount the same type of membrane module.

Cost figures for MBR systems often include the attached biological treatment, and the corresponding internal recirculation and aeration systems. Since these are not present in direct ultrafiltration, the capital costs will be compared only to the data of membrane filtration of WWTP effluent.

Differently, energy costs for membrane filtration will be taken from industrial MBRs, where multitubes crossflow membranes are largely applied (municipal wastewater MBRs typically use hollow fibres and flat sheet in immersed configuration, whereas effluent filtration offers several examples of capillary filtration).

The information available in literature is often not homogeneous also in the way it is presented. In the following, comparisons are made based on specific costs, i.e. on the cost per m^3 of produced permeate. Sometimes figures were provided in this form in literature, in other cases values have been recalculated according to the following assumptions: inflation rate 2.5%, interest rate 6%, depreciation period of 15 years for the entire plant, exchange rate 1 €= 1.33 US$ (dated 2006).

9.4 Estimate of Capital Costs

9.4.1 Literature Data

For ultrafiltration plants, Baker (2004) reports the purchase-cost figures reproduced in Figure 9.2 . The suggested bandwidth is rather large; however for typical plants of 10,000-100,000 $gal \cdot d^{-1}$ (38–380 $m^3 \cdot d^{-1}$) the capital costs are in the range 2-5 US$ $\cdot gal \cdot d^{-1}$ capacity.
These values can be re-calculated according to the assumptions above, yielding specific capital costs of approximately 0.1–0.3 € $\cdot m^{-3}$.

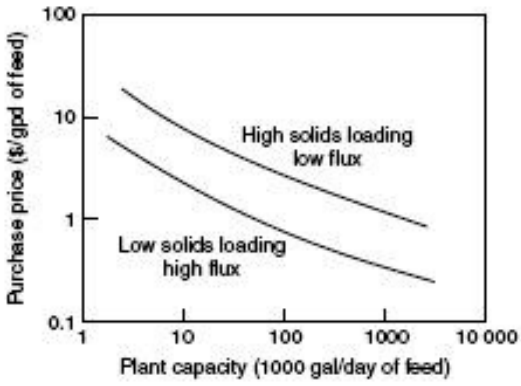

Figure 9.2: *Purchase price of ultrafiltration plants (from Baker, 2004)*

Baker (2004) provides also a useful indicative break down of the the total

capital costs, reproduced in Table 9.4.

Table 9.4: *tab:UF plants capital cost break down (from Baker, 2004)*

Pumps	30 %
Membrane Modules	20 %
Module housings	10 %
Pipes, valves, frames	20 %
Controls/other	20 %
Total	100 %

Concerning example applications in municipal wastewater treatment, two famous cases are the MF systems of the"West Basin", sized 19,000 $m^3 \cdot d^{-1}$, and the Groundwater Replenishment System (GWRS) sized 300,000 $m^3 \cdot d^{-1}$. Both systems treat secondary clarified effluent prior to RO filtration, the first using a "pressure" crossflow system and the second a submerged system. Actual cost figure from the "West Basin" can be found in Dhuram *et al.*, (2001), whereas Chalmers *et al.* (2000) provide a "typical" cost estimate that summarizes the preliminary estimations by candidate manufacturers. These cost figures are compared in Table 9.5.

Table 9.5: *Capital cost comparison MF/UF plants*

		Baker	West Basin	GWRS
Plant Cost	$\cdot 10^3$ US$	20–50		59400
Daily Flow	$\cdot 10^6$ *gal*	0.01–0.1	5	80
Specific Cost	€$\cdot m^{-3}$	0.1–0.3	0.1	0.04

The size of the two example-applications is relevantly larger than the typical plants from Baker. Capital costs from the West Basin plant meet the bandwidth provided by Baker, whereas the GWRS are well below the minimum. This may indicate a large effect of the economy of scale, as it appears in Figure 9.2. However it may also depend on the different applied technology or on different total

cost calculation methods.

9.4.2 Application to Direct UF

Capital costs are calculated based on the foreseen costs of the principal equipment components: pumps, membrane modules, membrane skids (assumed equivalent to frames, housing and valves). The components specifically found in the direct ultrafiltration set up, i.e. the buffer tank and the 0.5 mm sieve, are not computed; however similar equipments (buffer tank, pre-screening) are normally installed at ultrafiltration plants and therefore their value is included in the overall estimate.

Table 9.6 reports the estimated cost for the principal equipment (without spare parts). Budget prices are considered, with a 10 % discount for membranes and skids components for the case "Small Plant". The specific capital cost ($€ \cdot m^{-3}$) is calculated using the Net Present Value (NPV) divided by the expected permeate production.

Table 9.6: *Estimation of capital costs for direct UF*

	Resort			Small Plant		
	n.	€(tot)	$€ \cdot m^{-3}$	n.	€(*tot*)	$€ \cdot m^{-3}$
Circulation Pumps	1	400		3	9000	
Backflush pump	1	800		3	3000	
Membrane modules	1	3500		18	57000	
Skids		1700			28000	
TOTAL		6400			97000	
NPV (15 years)		10200	**0.04**		154000	**0.03**

According to Baker (2004), the items included in Table 9.6 correspond to about the 80% of the total capital costs. This yelds total specific capital costs equal to about 0.05 and 0.04 $€ \cdot m^{-3}$ respectively. Adding an approximate 30% to account for uncertanties, a final estimate of 0.06 and 0.05 $€ \cdot m^{-3}$ is obtained.

Compared to the example references in Table 9.5, these estimates are within the range provided by Baker. More accurately, they are in the medium -low

bandwidth of Baker, in agreement with the trend shown by the two more recent reference installations.

The result can be partially explained by the fact that direct ultrafiltration operates at flux = 70 LMH, whereas GWRS at 15–20 LMH. By working at high fluxes, direct ultrafiltration reduces the demand for membrane surface, which in the calculation is the most costly item.

For the calculated values the influence of the plant size on the specific capital costs is little.

9.5 Estimate of Operational Costs

9.5.1 Literature Data

Table 9.7 compares the O&M costs of the previous literature references, with the exclusion of sludge treatment costs.

The historical values from the West Basin are in good agreement with the breakdown proposed in Baker (2004). Differently, the estimated values for the GWRS indicate lower power and cleaning requirements, although the absolute cost figure for membrane replacement is similar.

Table 9.7: *tab:UF plant O&M cost break down (from Baker, 2004)*

	Baker	West Basin		GWRS	
	%	€$\cdot m^{-3}$	%	€$\cdot m^{-3}$	%
Replacement	30-50	0.02	22	0.018	74
Cleaning	10-30	0.03	32	0.003	13
Power	20-30	0.02	22	0.003	13
Labour	15	0.02	22		
Total	100	**0.1**	100	**0.02**	100

In all cases, membrane replacement, cleaning (i.e. chemicals) and power are the most important items in O&M, accounting for at least the 60% of the total, more likely for the 70–80%.

Membrane replacement and cleaning requirements depend on the membranes in use and the feed water quality, whilst the energy demand is strongly related to the configuration and the operating conditions.

Details on the energy demand are provided in the following.

Energy demand

As mentioned before, the application of multi-tube membranes operated in crossflow side-stream systems is almost exclusively practiced in the MBR treatment of industrial and high-strength wastewater. There exist essentially two possible configurations: *pumped* and *airlift*.

Pumped systems usually operate horizontally mounted membranes at high pressure and high crossflow velocity. Most of the times, to exploit the energy consumed to achieved the proper operating conditions, a variable number of modules (from 2 to 8) is connected in series.
Airlift systems make use of vertically mounted membranes, and modules are connected in parallel. Exploiting the addition of air bubbles for hydraulic and cleaning purposes, they are operated at lower pressure and flow rates. Permeate is extracted by suction pressure.

The two configurations clearly involve different operational parameters and result in different Specific Energy Demand (SED, $kWh \cdot m^{-3}$). Table 9.8 summarizes the operational data and the energy demand for different MBR systems (adapted from Judd, 2006).

Compared to the data in Table 9.8, the design of the direct ultrafiltration plant is a bit "unique", being a pressurized system with vertically mounted membranes, operating at moderate crossflow velocity and low pressure.

9.5.2 Application to direct UF

Operating costs are estimated based on the triplet power-chemicals-membrane replacement.

With respect to the estimate of capital costs, the estimate of the operating costs is less straightforward, as it requires to formulate some assumptions for aspects that have not been tested. This is especially true for the cleaning protocol and for the membrane replacements, whereas the energy consumption can

Table 9.8: *Summary of side-stream multi-tube MBR plants, adapted from Judd,2006*

Application	TSS g/L	TMP bar	u_{cr} $m \cdot s^{-1}$	Flux LMH	SED$^{(a)}$ $kWh \cdot m^{-3}$
Norit "pumped" (industrial WW)	12-30	1-5		80-200	1.5-4
Norit "airlift" (municipal WW)	8-12	0.05-0.3		30-60	0.5-0.7
Wehrle "pumped" (low energy; pilot)			1-2	55	1.5
Werhle "airlift" (landfill lechate)	12-15			50-60	2-3
Wehrle "pumped" (landfill lechate)		3		107	5
Wehrle "pumped" (food/dairy)				87-129	2-4
Milleniumpore (black& greywater)	12-15	0.8	2	16.5	1.8

$^{(a)}$ = includes membrane + biology + civil, except the case of Milleniumpore, where the value is for the membrane system only

be estimated quiet well from the information of Paragraph 9.5.1. All the formulated assumptions are with "conservative" approach: the cleaning requirements and the membrane deterioration during direct ultrafiltration are supposed to be higher than values reported for ultrafiltration of effluent in Aquarec (2006), Daugherty *et al.* (2005), EPRF (2002).

Assumptions

Cleaning Protocol
Additionally to the backflush practice, the cleaning requirements include a chemically enhanced backflush (CEB) and a Cleaning-In-Place (CIP) procedure. The supposed schedule is as follows:

- CEB: every 6 hours, with duration of 1 minute, using 200 ppm NaOCl;

- CIP: every 2 weeks, composed by an acid cleaning followed by an alkaline cleaning. The acid wash uses a solution of HCl at pH = 3, the alkaline Divos 109 is applied at the same concentration as during filtration experiments.

Calculations are made for a volume consumption of chemicals double than during laboratory activities, to account for uncertainties. Prices are based on the practice in The Netherlands, and vary according to the yearly purchased quantities. The result is an overall estimated expenditure of 0.023 and 0.030 $€ \cdot m^3$ produced permeate, for the "resort" ad the "small plant" respectively.

Despite the abundance of chemical cleaning event scheduled for direct ultrafiltration with respect to reference microfiltration systems, the overall cleaning costs are similar. This can be explained by the fact that during double membrane filtration, as at West Basin and GWRS, a few mg/L of chlorine are dosed *in continuous* to the MF feed, in order to prevent biofouling especially on the following RO system (Aquarec, 2006; Thompson, 2003; EPRF, 2002; Lazarova, 2003; Van Houtte 1998). Because of the high content of organics and ammonia in the raw sewage, discontinuous "shock" chlorination with the CEB is preferred.

Membrane Replacement
In Judd and Jefferson (2003) there is a comprehensive list of cases of industrial application where polymeric membranes have a replacement time of 3–7 years. During effluent treatment, it is usual to assume a replacement time of 4 or 5 years (Aquarec, 2006). For our calculation, we assume a life time of 1 year for the single module of the "resort" case and <4 years for the small plant, calculating to replace an average of five modules per year.

Energy Demand
The operating conditions of direct ultrafiltration are in between the two typical "pumped" and "airlift" systems, although closer to the values of the 'airlift" configuration: low solid concentration, $TMP = 0.3\ bar$, $u_{cr} = 1.5$ - $2\ m \cdot s^{-1}$, net-fluxes = 70 LMH. However, compared to the SED values in table, during direct ultrafiltration there is no consumption for biological aeration, which is a relevant fraction of the total (about 40% in submerged systems, Garces *et al.*, 2007). From these considerations it could be expected that direct ultrafiltration has a energy demand close, and probably below, to the lower limit of the "airlift" configuration, i.e. 0.5 $kWh \cdot m^{-3}$.

This value finds confirmation in Rulkens *et al.*, 2005. They conducted experiments of direct ultrafiltration of raw wastewater using the same membrane modules as this research, only at slightly different operating conditions. At $TMP = 0.8$ bar and $u_{cr} = 1.5\ m \cdot s^{-1}$, they obtained stable flux-values at 50 LMH, for which they estimated a specific energy demand of 0.5 $kWh \cdot m^{-3}$.

Another confirmation is found in the Milleniumpore "Eden Project" case study (Judd, 2006). This is a small MBR (40 $m^3 \cdot day^{-1}$) that recycles water in a touristic park, using crossflow multitubes configuration. The treated wastewater includes discharges from toilets and washrooms of the tourist park, the biocomposter effluent, storm water and run-off water. The permeate is reused for the irrigation of the gardens that constitute the main attraction of the park. This plant has a layout pretty similar to the hypothetical direct ultrafiltration plant, as shown in Figure 9.3.

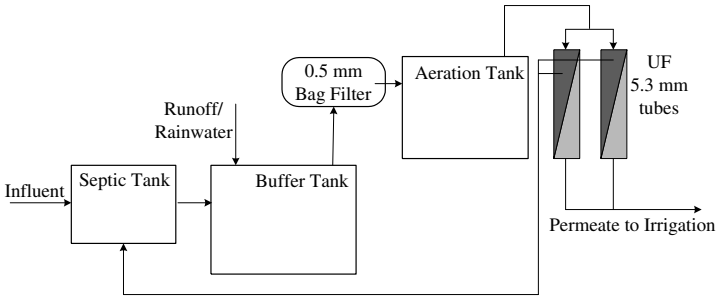

Figure 9.3: *"Eden Project" MBR, the flow scheme*

The specific energy demand of the membrane system is 1.8 $kWh \cdot m^{-3}$ at $TMP = 0.8$ bar and $u_{cr} = 2\ m \cdot s^{-1}$; the permeation rate is 16.5 LMH. In a sidestream (MBR) system the energy demand per liquid pumping relates to pressure and conversion according to Formula 9.1 (Judd and Jefferson, 2003):

$$W_h = \frac{1}{\rho\, \xi\, \Theta} \cdot \Sigma \Delta P \tag{9.1}$$

When the density (ρ) and the pump efficiency (ξ) are assumed to be the same, the specific energy demand depends on the conversion achieved by a single passage of fluid (Θ) and on the total headloss ΔP, sum of the headloss in

the feed/retentate channel (ΔP_r) and in the membrane modules (ΔP_m).
In the case of direct ultrafiltration, Θ is $70/16.5 = 4.2$ times higher than for the "Eden" MBR, therefore the energy demand can be calculated as $(1.8\ /4.2) = 0.42\ kWh \cdot m^{-3}$.
Additionally, direct ultrafiltration operates at $TMP = 0.3\ bar$ instead of 0.8 *bar*, therefore ΔP_r will be smaller, further reducing the energy demand.

In conclusion, it seems acceptable and conservative with respect to uncertainties to assume for the entire direct ultrafiltration system (circulating pump, backflush pump, valves and actuators) an energy consumption of 0.5 $kWh \cdot m^{-3}$.

Summary of Operating Costs

Table 9.9 summarises the estimated operating costs.

Table 9.9: *Estimate of operating costs for direct UF*

	Resort			Small Plant		
	n.	€(tot)	$€ \cdot m^{-3}$	n.	€(tot)	$€ \cdot m^{-3}$
Replacements		1750	0.08		17500	0.05
Cleaning			0.04			0.03
Power*			0.04			0.04
TOTAL			**0.16**			**0.12**

* = energy cost: $0.07\ € \cdot kWh^{-1}$.

The totals of Table 9.9 should correspond to approximately 70–80% of the overall operating costs, yelding total O&M costs of 0.20 and 0.15 $€ \cdot m^{-3}$ respectively. Accounting an additional 30% for uncertanties, the final estimate amounts to 0.3 and 0.2 $€ \cdot m^{-3}$.

This value is well above the operating costs at West Basin (2–3 times higher) and at GWRS (10–15 times higher). Although an important role is played by the higher energy consumption of the tubular membranes configuration, the most of the increased costs can be accounted to membrane replacement, the rate of which is actually unknown and has been assumed rather conservatively.

9.6 Total Costs

Table 9.10 summarises the calculated capital and operating cost estimates, and compares them with the references.

Table 9.10: *Summary of total costs*

	West Basin $€ \cdot m^{-3}$	GWRS $€ \cdot m^{-3}$	Resort $€ \cdot m^{-3}$	Small Plant $€ \cdot m^{-3}$
Capital	0.1	0.04	0.06	0.05
O&M	0.1	0.02	0.30	0.20
Total	0.2	0.06	0.36	0.25

The estimated total price for the produced permeate is approximately in the range 0.20–0.40$€ \cdot m^{-3}$, where 0.25$€ \cdot m^{-3}$ is the calculated value for the small plant case and 0.36$€ \cdot m^{-3}$ the calculated value for the resort case.

Considering the uncertainties and approximations, this range is in agreement with the 0.24 $€ \cdot m^{-3}$ proposed for a similar application in Rulkens *et al.* (2005).

With respect to the literature data from existing membrane plants, the estimated range is 50% higher than the data from the microfiltration units of West Basin (0.19$€ \cdot m^{-3}$) and several times higher than the one of GWRS (0.06$€ \cdot m^{-3}$).

These differences mainly originate from the operating costs and especially from the membrane replacement costs. However, it should be considered that the West Basin and GWRS plants are additional ultrafiltration steps that follow a complete biological treatment, whereas the direct ultrafiltration plant is stand alone.

9.7 Discussion and conclusions

Direct membrane filtration seems to be an applicable treatment process for raw and primary wastewater. This conclusion is drawn upon technological, operational and economical basis; the estimated price for the produced permeate is approximately 0.20–0.40 $€ \cdot m^{-3}$.

The cost estimate provided here is only a general indication of the order of magnitude of the costs. More reliable figures will be possible only after long-term pilot testing, filtrating various feed wastewaters.

Nevertheless, the following outcomes of the calculation exercise deserve a special remark:

- the capital costs of direct ultrafiltration with (crossflow) multi-tubular membranes are close to the capital costs of (submerged) micro- and ultrafiltration post treatment step using capillary membranes;

- the calculated high operational costs are an obvious consequence of the "conservative" approach during the calculation. The adoption of a conservative approach originates from the fact that the reference figures concern filtration of clarified WWTP effluent, whereas direct ultrafiltration concerns raw wastewater. The proposed chemicals consumption and membrane deterioration need to be verified in practice and may result lower than estimated. At least this is the general impression obtained by the long term fouling observed during four years of non-continuous testing.

- the energy expenditure for the crossflow system is approximately the same as for submerged MBR's. The energy consumption for direct ultrafiltration is estimated around 0.5 $kWh \cdot m^{-3}$; for MBR Schilde, Garces *et al.* (2007) report 0.6 $kWh \cdot m^{-3}$, and for the MBR Nordkanal Engelhardt and Lindner (2006) report 0.4–0.8 $kWh \cdot m^{-3}$;

Notwithstanding the differences in the scenarios of application and the quality of the product water, the estimated cost figure can be compared to the cost of conventional treatment of municipal wastewater in The Netherlands.

In UNIE (2003), the overall cost of wastewater treatment (inclusive of water collection, land costs and sludge handling) is indicated in the range 0.25–0.45 € per "hydraulic pollution equivalent (*vervuilingseenheden*[1])". This corresponds to 0.50–0.90 € $\cdot m^{-3}$, i.e. 0.57–1.02 € $\cdot m^{-3}$ after actualization for the inflation rate.

[1] vervuilingseenheden = amount of wastewater corresponding to total oxygen demand of 136 $mg \cdot d^{-1}$. For design purposes it is usually converted into 50 $m^3 \cdot year^{-1}$, dry weather flow

The application of direct ultrafiltration within the existing system would not require additional infrastructure, the plant has little footprint [2] and can be highly automated. Therefore, at the price of 0.20–0.40 €$\cdot m^{-3}$, the application of direct ultrafiltration within the Dutch wastewater system may result economically attractive.

Furthermore, the possible benefits from use of the produced permeate could be incorporated in a cost-benefit analysis. In case that disinfected nutrient-enriched permeate could be applied as fertilising irrigation water for crop farming, the benefit would be the saving of extra artificial fertiliser (Evenblij and Van Nieuwenhuijzen, 2002). Other gains could be the production of biomass from permeate, via algae farming, or the production of biogas by anaerobic digestion of the concentrate (sludge): the energy recovered from the algae-biomass or the biogas could be of economical benefit and balance the energy use of the direct ultrafiltration plant.

Finally, next to economical cost-benefit analysis, also social cost-benefit analysis (Ruijrok, 2001) could be carried out.

In conclusion, being demonstrated the technical feasibility and a preliminary economical attractiveness, more research and investigations into the reuse of permeate could be carried out to determine the advantages and applicative scenarios of the process. Direct ultrafiltration appears attractive for typical situations, such as sanitized irrigation water, and eventually for industrial application; the development of applicable treatments and production schemes is connected to the determination of reuse options for the permeate.

[2] in the typical configurations eight 3 m x 8 *inch.* modules can be mounted in 4 m^2 area per 4 m height (Judd, 2006; Futselaar, 2005). Based on Table 9.3 this configuration yields an output of about 96 $m^3 \cdot d^{-1}$ permeate per m^2 footprint area, i.e. about 480 $p.e. \cdot m^{-2}$.

Chapter 10

Epilogue

Where the major achievements, problems, unsolved questions, interesting points of this extensive Dissertation are recalled and briefly dscussed

10.1 Object of the performed work

The main aim of the work presented in this Dissertation was to test experimentally a novel membrane process, direct ultrafiltration of raw sewage, by mean of tubular polymeric membranes.

In a newly built facility, systematic data sets have been generated while varying feed wastewater (untreated sewage, effluent of primary clarifier, coagulated sewage) and fundamental operating parameters (TMP, crossflow velocity, backflush cycle). The effects have been evaluated in terms of filtration characteristics (flux decline and resistance increase), with respect to elapsed time and produced volume. In addition, mathematical modelling has been applied (blocking laws). The purpose of the latter was to support the interpretation of results by generating comparable parameters.

A frame to the experimental work was provided by reviewing other contributions to the same subject, discussing potential applications and conducting a basic cost estimate of the process.

10.2 Review of earlier work

A review of earlier works show that membrane filtration of untreated (or partially treated) wastewater is still at preliminary development stage.

Previous experiments focused on crossflow systems only. Various membrane configurations and materials have been tested in combination with a variety of feed water. Nevertheless, results appear scattered and there is a lack of standardisation in the description of fouling characteristics. Consequently, it is not possible to compose a unique picture from all the different experiences.

Concerning operational aspects with tubular membranes, main object of this dissertation, previous experiences showed the relevance of turbulence and shear stress at the membrane wall in reducing flux decline and fouling occurrence. This was normally achieved by mean of increasing crossflow velocity; suggested values for stable filtration performances were 4 $m \cdot s^{-1}$ (Kyu-Hong Ahn *et al.*, 1998), 2.4 $m \cdot s^{-1}$ (van Nieuwebhuijzen, 2002) and 3 $m \cdot s^{-1}$ (Hao *et al.*, 2006).

Increasing TMP produced more rapid fouling, which was explained suggesting the occurrence of cake formation: the density of the filter cake would increase when higher TMP is applied. However, there is no agreement on optimal operating values, and suggested TMP values varied between 0.2 *bar* (van Nieuwenhuijzen, 2002) to 1.5 *bar* (Kyu-Hong Ahn *et al.*, 1998).

The effect of physical-chemical pre-treatment has been seldom investigated. In literature, only two papers were found concerning the coagulation and adsorption of primary clarifier effluent prior to micro- ultrafiltration (Soffer *et al.*, 2000; Abdessemed and Nezzal, 2002). In both cases the selected coagulant was $FeCl_3$. At natural pH dosages above 25 mg/L were necessary to obtain significant removal of DOM (or DOC); significant flux enhancement required a minimum of 40 mg/L. Soffer *et al.*, 2000 noted that the impact of coagulant addition on filtration performance was only temporary.

10.3 New results and discussion

10.3.1 Raw Sewage

The filtration tests with raw sewage confirmed the impact of the principal operating parameters on filtration characteristics.

During continuous filtration the fouling development is a function of the applied TMP and crossflow velocity. Figure 5.5 shows that, after 30 min, in all tested conditions the resistance to filtration due to fouling exceeded of several times the initial membrane resistance. However, the increase may differ of more than one order of magnitude.

Figure (5.10) shows that shortly after the start of filtration the increase of resistance per permeate volume produced is more favourable operating at low TMP (0.3 bar) and high crossflow velocity (2 $m \cdot s^{-1}$). However, Figure 5.12 clarifies that when TMP is ≤ 0.5 bar the additional advantage of increasing the shear stress at the wall from 8.6 to 14.5 Pa (corresponding to $u_{cr} = 1.5$ and 2 $m \cdot s^{-1}$) is little.

This is a relevant finding because previous researches always suggested the application of higher shear values. For stable filtration Elmaleh and Abdelmoumni (1998) suggested a range of 20–30 Pa, which is confirmed by Bourgeous *et al.* (2001), van Nieuwenhuijzen (2002) and Hao *et al.*(2006). Kyu-Hong Ahn *et al.* (1998) even applied 51 Pa[1].

The impact of TMP on fouling formation is substantial. In agreement with the suggestions of previous researches, the relation between resistance increase and TMP (Figure 5.7) may indicate the formation of a compressible cake layer. However, during crossflow filtration the increase of TMP may also modify the quantity and quality of the material transported to the membrane or its penetration through the pores.

The results from mathematical analysis of the filtration curves supports the understanding that cake formation is quantitatively the prevalent fouling mechanisms (Figure 6.14). Nevertheless, both filtration and modelling data show that the increase of cake density (specific resistance) is not sufficient to fully explain the effect of TMP (Figure 6.15 and Figure 6.16). It is concluded that the applied TMP value affects in visible manner the mass transport and eventually promotes other fouling mechanisms than cake formation.

The combination of the effects of TMP and crossflow velocity suggested to select low TMP (0.2–0.4 bar) during extended testing of cyclic operation (alternation of filtration periods and backflush). Applied crossflow velocity values were 1, 1.5 and 2 $m \cdot s^{-1}$.

It is found that during cyclic operations backflush is necessary and sufficient

[1] for Hao *et al.*(2006) and Kyu-Hong Ahn *et al.* (1998) shear stress values at the wall have been recalculated at 20°C, according to Equation 4.8

to maintain fouling formation at acceptable level. For the tested duration (4–7 h) stable filtration was obtained both at 1.5 and 2 $m \cdot s^{-1}$, with gross flux values above 100 LMH and net flux values around 70–85 LMH (5.2.2).

Apparently, a dynamic cake layer is created on the top of the membrane surface, which is partially removed at backflush. The irreversible fouling layer formed during the first 30 min protects the membrane from further irreversible forms of fouling, and the resistance values stabilizes during the entire filtration period. Experiments with coagulant addition supported this interpretation (8.8.3).

Two final remarks conclude the discussion over direct filtration of raw sewage:

- the fact that operations are sustainable in time also at $u_{cr} = 1.5\ m \cdot s^{-1}$ is of major importance for the economics of the process. When compared with values from MBRs, the estimated Specific Energy Demand for direct ultrafiltration is at the bottom of the bandwith of side-stream crossflow technology (Table 9.8) and is comparable to submerged technology (Paragraph 9.7). According to Baker (2004) the energy consumption of a standard ultrafiltration plant represents 20-30 % of the operating costs, and it is outstanding that the same impact is calculated for energy consumption during the treatment of raw sewage (Table 9.9);

- the applied chemical cleaning was able to restore membrane permeability under all circumstances. This is a strong indication that the process can find application both for continuous and intermittent operations. The bottom line, although eventually not economical, is that excessive fouling can be removed with frequent chemical cleaning.

10.3.2 Modelling

The general outcome of the modelling with blocking laws is that the cake model, calibrated on the stable part of the 30 min filtration test, interpolates satisfactorily the entire flux decline curve (Paragraph 6.4.3, Figures 6.7, 6.8 and 6.9).

The model is based on two parameters, one concerning the cake specific resistance (k_c, in m^{-4}) and one concerning the final asymptotic flux value (J^*, in LMH).

According to the results presented throughout the whole Dissertation, k_c should not be interpreted as strictly representing the cake resistance only. Differently, it represents the (main) contribution of the cake and of other forms of fouling (6.5.4).

The use of k_c allows to compare fouling formation at different operating conditions, providing a global value obtained by an extensive set of measurement, and therefore likely more significant than punctual values of resistance at given filtration time or filtrated volume (ΔR's). However, throughout the entire Dissertation the findings from k_c values could be backed by ΔR's.

In theory, J^* values correspond to the asymptotic values that can be approximated at pseudo-stationary state. Operating at constant TMP, J^* represents a sort of final flux value that is sustainable in time, whereas at constant flux it coincides with the *critical flux* (see Paragraph 6.1.3). A unifying approach is that if J^* is the flux at the dynamic equilibrium, when equal transport of foulants to and from the membrane occurrs, it can also be interpreted as the backtransport flux. Starting the filtration from a clean membrane, this would be the maximum flux that does not produce fouling, i.e. the critical flux.

Two observations support the hypothesis that the estimated J^* values reasonably satisfy these physical interpretations:

- within the limitations of a mathematical fitting, the estimated J^* values are often well below the observed J_{end}, especially at low u_{cr} (see Figure 10.1). This supports the idea that J^* is the estimation of an actual asymptotic value based on the curvature of flux decline during the observed 30 minutes interval;

- during critical flux measurements with the same equipment and feed water, sustainable values were found in the same range of calculated J^* (Ravazzini *et al.*, 2005a; 2005b). The critical flux at $u_{cr} = 2\ m \cdot s^{-1}$ was 90–105 LMH for raw sewage and 100–150 LMH for primary effluent respectively. Raw sewage was also tested at $u_{cr} = 1\ m \cdot s^{-1}$, resulting in critical flux values in the range 18–35 LMH. These numbers must be considered with caution, because they are based on a few experiments and the procedure made use of a step-up method with increasing step of 15–20 LMH. Nevertheless, constant flux filtration for raw sewage could be repetitively maintained with negligible fouling formation for 4–7 h, at about 70 LMH, which is approximately the estimated J^* of Figure 7.20.

The application of the cake model to the filtration curves obtained with co-

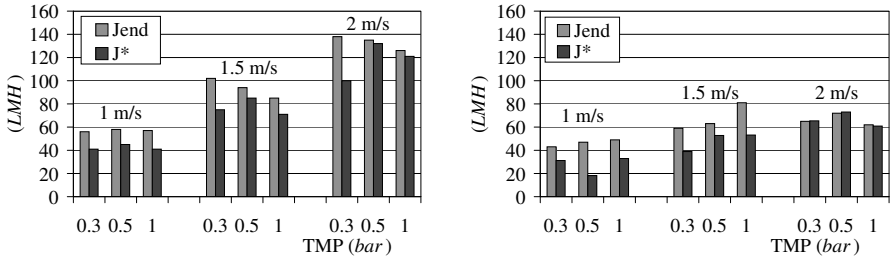

Figure 10.1: *Observed J_{end} vs. estimated J^* values, Primary Effluent (left) and Raw Sewage (right)*

agulated water proved more difficult. This depended on increased experimental inaccuracy and eventually on the fact that the flux curves were more similar to each other, as they were generated at fixed operating conditions. Yet J^* values anticipated that the effect of coagulant dosing (and dosage) is negligible in the long term.

10.3.3 Primary Clarifier Effluent

The filtration characteristics of primary effluent and raw sewage at the variation of operating conditions (TMP and u_{cr}) appeared really similar. However, primary effluent showed significantly higher filterability (20-30 %).

These features were visible both in terms of resistance increase (Figure 7.17), produced filtrate volume (Figure 7.19) and estimated model parameters (Figures 7.20 and 7.21).

On the basis of the concentration values of some parameters invariant by sedimentation (conductivity and ammonium), it was argued that the higher filterability could depend on a lower average strength of the feed wastewater during the testing period with primary effluent. The similar filtration characteristics could be explained considering that with respect to other components often related to fouling (i.e. EPS), the two feed waters had the same matrix ("footprint").

The major difference concerns the trend of additional fouling induced by

increasing TMP: the portion that cannot be explained by cake compressibility is bigger in the case of primary effluent. Since this unexplained portion is bigger also at high crossflow velocity, a physical interpretation can be proposed. The high crossflow velocity is more selective than low crossflow velocity in retaining away from the membrane surface the transported matter, and especially large particles. Likewise, a similar effect is produced by the smaller amount of transported particles and the smaller average particles size of primary effluent with respect to raw sewage (see Figure 7.23).

On the basis of the collected data it is not possible to conclude whether these selective mechanisms affect the amount of deposited foulants, their characteristics or their penetration into the membrane pores. However, it is reasonable to expect that at high crossflow velocity and during filtration of primary effluent the fraction (of the total) of smaller foulants that reaches the membrane is higher. This may induce more dense filter cakes, or more tenacious interactions foulants-membrane surface, or higher internal fouling rate. During ultrafiltration of WWTP effluent, (Roorda, 2002) noted that filterability is mainly affected by particles 5–20 times larger than the pore size (0.1–0.2 μm in his case), which participate to cake formation. Te Poele (2006) noted that irreversible fouling is influenced by macro-molecules and dissolved material below 0.1 μm, indicating proteins adsorption as major fouling mechanism.

Therefore, it can be concluded that large particles somehow shield the membrane by the formation of a superficial cake.

From an operational point of view, sedimentation of raw sewage prior to ultrafiltration had a positive effect on filterability. Nevertheless, it may prove not relevant in practice. In facts, the class of particles that this process can remove has the lower potential for fouling irreversibly the membrane.

In practical applications sedimentation is recommended; however it is speculated that the main aim is the separation of fiber and debris, in order to avoid clogging of pipes and screens. A rough settlement can be sufficient to the scope (e.g. imhoff or septic tank, as suggested in Chapter 9).

10.3.4 Addition of Coagulants

The experimentations with coagulants concerned the application of various coagulant types (metal salts, polymers, combinations of both) at natural pH (7.8). The feed wastewater was first coagulated and than filtrated over the membrane. Maximum applied dosages were chosen “comparable” with usual practice in primary sedimentation.

During jar tests $FeCl_3$, $PACl$ and C-592 were found the best performing coagulants. As expected, coagulation removed mainly particulate and colloidal matter. However, from the analyses conducted on coagulated water fractionated over various filters, it appeared that also a little of supra-dissolved fraction was removed (Figure COD).

Measurable effects were produced also on light absorption parameters, corresponding to the measurements of UV-absorption, colour, proteins and polysaccharides in the filtrate over 0.45 μm membrane. These effects were interpreted as effective binding of organic fouling matter.

The filterability of coagulated water improved with coagulant dosages (Figures 8.4 and 8.7). On the opposite, reversibility did not: apparently, the positive effect of coagulant addition vanishes in less than 2 h, except for $PACl$ (Figure 8.10).

The transient effect of coagulant addition is in agreement with previous researches. From the comparison of supernatant and permeate it is supposed that during recirculation the turbulence of the flow breaks the flocs (especially in the pump) and releases previously bounded foulants. However, it could also be speculated that the entrapment of large particles in back-transported flocs allows the small unbound particles to reach the membrane more easily and foul it. From the comparison of irreversibility tests executed on a fouled and cleaned membrane, it is argued that the rapid formation of a cake layer covering the membrane surface has a positive effect on reversibility (Paragraph 8.8.3).

Summarising, the effect of coagulant addition is to slow down the building up of fouling, whereas the theoretical final equilibrium values of resistance and flux are unchanged.

With respect to the practical implementation of the process, it seems that in-line pre-treatment with coagulation does not lead to significant advantages. Different could be the case of filtrating only the supernatant, eventually increasing the coagulant dosage.

10.4 Overall conclusions

The answer to the main question at the basis of this dissertation is that crossflow ultrafiltration of untreated sewage is technically, operationally and economically feasible.

A detailed analysis of the filtration characteristics has shown that:

- Sustainable operating conditions are $TMP = 0.3\ bar$ and $u_{cr} = 1.5$–$2\ m \cdot s^{-1}$. These conditions lead to the formation of a loose (dynamic) cake which allows gross flux values above 100 LMH and protects the membrane from other irreversible forms of fouling;

- Cake filtration dominates quantitatively the formation of fouling but is not the exclusive occurring mechanism;

The cost of direct ultrafiltration is estimated around 0.2–0.4 €$\cdot m^{-3}$. This is an approximate value for the production of water excluding wastewater collection and treatment of rejected concentrate. In the Dutch market such cost may result attractive. Its attractiveness could further improve when accounting for the possible benefits from use or reuse of the produced permeate, not included in the calculated values.

At the light of the previous remarks, it seems that the practical application of direct ultrafiltration may likely concern typical cases where the permeate characteristics are of particular value. The permeate of municipal wastewater is characterised by a high level of sanitation, nutrients and organic content; therefore, it appears suitable for the fertilisation of crops or other vegetations (e.g. algae-biomass). Additional post-treatments of the permeate would increase the overall cost but could enable nutrients recovery or industrial reuse. Other feed waters may present other advantages.

Additional findings of this research are the following:

- Primary sedimentation and coagulation-flocculation impact short-term filterability but have limited impact on fouling reversibility. Therefore, the application seems irrelevant to process performance;

- Fouling decline can be interpolated satisfactorily using the cake filtration model. In particular, the model parameters allow a meaningful comparison of the filterability results among curves obtained at different operating conditions. This tool may be of support in the selection of appropriate operating conditions, as well as in the further development of the process, by allowing the comparison of data obtained warying feed waters, membranes, etc. ...

10.5 Future work

The work presented in this Dissertation aimed at contributing to the development of direct ultrafiltration of raw sewage using tubular membranes. After it is finished, a lot of work remains to be done.

A list of relevant issue is proposed in the following.

From an operational point of view, the presented results should be validate for continuous operations, eventually with an upscaled Pilot Plant. This particularly applies to the assumptions of Chapter 9 (sustainable net-flux, energy and chemical consumption) with respect to long term fouling and biological fouling. Additionally, it would be important to determine the practicable concentration factors, as they affect the applicability of the process and especially the treatment of the waste stream (in Ravazzini *et al.* (2005), concentration values up to 85% were achieved).

The findings about filterability and filtration characteristics could be extended with an improved understanding of the fouling mechanisms. This could be done by integrating accurate filtration data with advanced physical-chemical analyses. A useful tool could be time-related measurements of foulants retention and permeation data, another one membrane autopsy. More in general, this issue can be investigated by means of qualitative and quantitative analyses of foulants concentration in the feed water (fresh and recirculated), in the cake layer, on the membrane surface and in the permeate.

Other example areas of research are:

- operations at constant flux (the quoted preliminary measurements of critical flux value have shown comparable performances with constant TMP operations);

- coagulation with other products and dosages (eventually filtrating the supernatant only);

- refinement techniques and reuse possibilities for the produced permeate.

The last item is of particular relevance. At the actual stage the permeate that can be produced by direct ultrafiltration of raw municipal wastewater is indeed an interesting but unusual resource.

In Paragraph 1.3.3 a list of potential applications has been discussed, mainly water extraction for agricultural reuse, advanced pre-treatment for overloaded systems, complete physical-chemical treatment of wastewater. In addition to these, the technique might be applicable to a variety of feed waters similar to municipal wastewater, such as surface run-off, combined sewer overflow, wastewaters from animal farms etc.... The selection of specific target applications will drive the development and set the boundaries for further development and research.

Bibliography

Abdessemed, D., G. Nezzal (2002). Treatment of Primary Effluent by Coagulation-Adsorption-Ultrafiltration for Reuse. Desalination 152: 367-373.

Ahn, K.-H., J.-H. Song, and Ho-Young Cha (1998). Application of Tubular Ceramic Membranes for Reuse of Wastewater from Buildings. Water Science and Technology 38: 373-382.

Ahn, K.-H., K.-G. Song (1999). Treatment of Domestic Wastewater Using Microfiltration for Reuse of Wastewater. Desalination 126: 7-14.

Ahn, K.-H. , K.-G. Song (2000). Application of Microfiltration with a Novel Fouling Control Method for Reuse of Wastewater from a Large Scale Resort Complex. Desalination 129: 207-216.

Ahn, K.-H., K.-G. Song, Yeom, I.T. and Park K.Y. (2001). Performance Comparison of Direct Membrane Separation and Membrane Bioreactor for Domestic Wastewater Treatment and Reuse Water Science and technology: Water Supply 1(5-6): 315-323.

Altena, F.W., G. Belfort (1984). Lateral Migration of Spherical Particles in Porous Flow Channels: Application to Membrane Filtration. Chemical Engineering Science 39: 343-355.

Altena, F.W. et al., G. Belfort, Otis, J., Fiessinger F., Rovel, J. M., Nicoletti, J. (1983). Particle Flow in a Laminar Silt Flow: A Fundamental Fouling Study. Desalination 43: 221-232.

AQUAREC (2006). Water Reuse System Management Manual. European Commission Technical Series, Editors Bixio, D. and Wintgens, T. ISBN: 9279019341. Bruxelles, BE.

Arnot, T.C., A. B. Koltuniewicz, Field, R.W. (2000). Cross-Flow and Dead-End Microfiltration of Oily-Water Emulsions Part II. Mechanisms and Modelling of Flux Decline. Journal of Membrane Science 169: 1-15.

AWWA (American Water Works Association) (1998). Standard Methods for the Examination of Water and Wastewater, 20th Edition. ISBN: 0875532357. Editors: American Public Health Association, American Water Works Association and Water Environment Federation.

Bacchin, P., Si-Hassen, D., Starov, V., Clifton, M.M., and Aimar, P. (2002). A unifying model for concentration polarization, gel layer formation and particle deposition in cross-flow membrane filtration of colloidal suspensions. Chemical Engineering Science 57(1): 77-91.

Baker, R.W. (2004). Membrane Technology and Applications 2nd Edition. Chichester (UK), John Wiley & Sons, Ltd.

Belter, P.A., Cussler, E.L., and Hu, W. S. (1988). Bioseparations-Downstream Process for Biotechnology. New York, Wiley.

Bixio, D., B. De Heyder, Joksimovic, D., Cikurel, H., Miska, V., Muston, M., Schfer, A.I., Ravazzini, A.M., Aharoni, A., Savic, D. and Thoeye C. (2005). Municipal Wastewater Reclamation: Where Do We Stand? An Overview of Treatment Technology and Management Practice. Water Science & Technology: Water Supply 5(1): 77-85.

Bixio, D. and T. Wintgens, Editors (2006). Water Reuse System Management Manual Aquarec. ISBN: 9279019341. European Commission Technical Series, Bruxelles, BE.

Bixio, D. , C. Thoeye, Wintgens, T., Ravazzini, A., Miska, V., Muston, M., Chikurel, H., Joksimovic, D. and Melin T. (2008). Water Reclamation and Reuse: Implementation and Management Issues. Desalination 218(1-3): 13-23.

Blatt, W. (1970). A. Dravid, Michaels, A.S., Nelsen, L. and J.E. FlinnSolute

Polarisation and Cake Formation in Membrane Ultrafiltration: Causes, Consequences and Control Techniques. Membrane Science and Technology. New York, Plenum: 47-91.

Boerlage, S.F.E., Kennedy, M.D., Aniye, M.P., Abogrean, E., Tarawneh, Z.S. and Schippers, J.C. (2003). The MFI-UF as a Water Quality Test and Monitor. Journal of Membrane Science 211: 271-289.

Boerlage, S.F.E., Kennedy, M.D., Tarawneh, Z.S. De Faber, R. and Schippers, J.C. (2004). Development of the MFI-UF in constant flux filtration. Desalination 161: 103-113.

Bouregeous, K.N., J. L. Darby, and Tchobanoglous, G. (2001). Ultrafiltration of Wastewater: Effects of Particles, Mode of Operation, and Backflush Effectiveness. . Water Research 35(1): 77-90.

Bowen, W.R. and Jenner, F. (1995a). Dynamic Ultrafiltration Model for Charged Colloidal Dispersions: A Wigner-Seitz Cell Approach. Chemical Engineering Science 50(11): 1707-1736.

Bowen, W. R., J. I. Calvo, Hernandez, A. (1995b). Steps of Membrane Blocking in Flux Decline During Protein Microfiltration. Journal of Membrane Science 101(1-2): 153-165.

Brant, J. A., A. E. Childress (2002). Membrane-Colloid Interactions: Comparison of Extended DLVO Predictions with AFM Force Measurements. Environmental Engineering Science 19: 413-427.

Bratby, J. (2006). Coagulation and Flocculation in Water and Wastewater Treatment, 2nd Edition. IWA Publishing, ISBN: 1843391066.

Broseliske, G.H., Verkerk, J.M. (2004). De Europese Kaderrichtljin Water. 23th Vakantiecursus in Riolering en Afvalwaterbehandeling, Delft, NL.

Butler, R. and Mac Cormick, T. (1995). Opportunities for Decentralized Treatment, Sewer Mining and Effluent Re-Use Desalination 106: 273-283.

Chalmers, B., Leslie, G., Sudak, D., Alexander, K. (2000). Selection of a Microfiltration Process for the Groundwater Replenishment System, the Largest

Advanced Recycled Water Treatment Plan in the World. AWWA Annual Conference, Denver, Colorado.

Chellam, S., Wiesner, M.R. (1998). Evaluation of Crossflow Filtration Models Based on Shear-Induced Diffusion and Particle Adhesion: Complications Induced by Feed Suspension Poldispersity. Journal of Membrane Science 138(1): 83-97.

Chen, V., A. G. Fane, Madaeni, S., Wenten, I.G. (1997). Particle Deposition During Membrane Filtration of Colloids: Transition between Concentration Polarization and Cake Formation. Journal of Membrane Science 125: 109-122.

Chiemchaisri, C. and Kazuo Yamamoto (1994). Performance of Membrane Separation Bioreactor at Various Temperatures for Domestic Wastewater Treatment. Journal of Membrane Science 87(1-2): 119-129.

Cho, B.D., and Fane A.G. (2002). Fouling transients in nominally subcritical flux operation of a membrane biioreactor. Journal of Membrane Science 209(2): 391-403.

Choi, H. , K. Zhang, Dionysiou, D.D., Oerther, D.B., Sorial, G.A. (2005). Effect of Permeate Flux and Tangential Flow on Membrane Fouling for Wastewater Treatment. Separation and Purification Technology 45: 68-78.

Daughtery, J. L., Deshmukh, S. S., Patel, M. V. Markus M., R. (2005). Employing Advanced Technology for Water Reuse in Orange County. Water Recycling 2005. S. Diego, Ca.

Davis R.H., Leighton D.T. (1987). Shear-Induced Transport of a Particle Layer Along a Porous Wall. Chemical Engineering Science 42: 275-281.

De Wilde, W., Thoeye, C. and De Gueldre, G. (2005). Operational Experiences and Optimisations Two Years after Start-up of the First Full-Scale Mbr for Domestic Wastewater Treatment in the Benelux. 6th AACHENER TAGUNG Sieldlungswasserwirtschaft und Verfahrenstechnik. Eurogress Aachen, Germany.

Decarolis J., Hong S. Taylor J. (2001). Fouling Behaviour of a Pilot Scale inside-out Hollwo Fiber Uf Membrane During Dead-End Filtration of Tertiary Wastewater. Journal of Membrane Science 191: 165-178.

Defrance L., Jaffrin M.Y. (1999). Comparison between Filtrations at Fixed Transmembrane Pressure and Fixed Permeate Flux: Application to a Membrane Bioreactor Used for Wastewater Treatment. Journal of Membrane Science 152: 203-210.

Dubois, M., Gilles, K.A., Hamilton, J.K., Rebers, P.A., Smith,F. (1956). Colorimetric Method for the Determination of Sugars and Related Substances. Analytical Chemistry 28: 350-356.

Ebner H. (1981). Die Kontinuierliche Mikrofiltration. Essig. Chem. Eng. 53: 25-31.

Elmaleh, S., L. Abdelmoumni (1998). Experimental Test to Evaluate Performance of Anaerobic Reactor Provided with an External Membrane Unit. Water Science and Technology 38(8-9): 385-392.

Engelhardt, N. and Lindner, W (2006). Experiences with the World's Largest Municipal Waste Water Treatment Plant Using Membrane Technology. Water Practice & Technology 1(4).

EPA (2001). Low Pressure Membrane Filtration for Pathogen Removal: Application, Implementation and Regulatory Issues.

EPRF, Expert Panel Review and Findings (2002). Singapore Water Reclamation Study. Singapore, Public Utility Board, Ministry of Environment Singapore.

EU Council (1976) Bathing Water Directive. 76/160/EEC.

EU Council (1991). Eu Urban Wastewater Treatment Directive. 91/271/EEC.

EU Council (2000). Eu Council Directive Establishing a Framework for Community Action in the Field of Water Policy. 2000/60/Ec of 23 October 2000.

EU Council (2001) European Priority Substances Decision. 2455/2001/EEC.

EU Council (2002) European Bathing Water Communication. 581/2002/EEC.

EUROSTAT (2003) Water use and waste water treatment in the EU and in Candidate Countries. Statistics in Focus 8/2003. Available at *www.europa.eu.int/comm/eurostat*.

Evenblij, H. (1999). Preliminary Study into Membrane Filtration of Raw Wastewater at Wwtp Bennekom. Master thesis, Delft University of Technology, CiTG, Section of Sanitary Engineering. Delft, NL.

Evenblij, H., Van Nieuwenhuijzen, A.F. and Van der Graaf, J.H.J.M. (2002). Direct Reuse of Membrane Filtrated Raw Wastewater. International Conference From Nutrient Removal to Recovery. Amsterdam, The Netherlands. Proceedings: 51-60.

Evenblij, H. (2006). Filtration Characteristics in Membrane Bioreactors. PhD Thesis, Delft University of Technology, CiTG, Section Sanitary Engineering. Delft, NL.

Fane, A. (2005). Sustainability and Membrane Processing of Wastewater for Reuse. IWA Specialty conference on Wastewater Reclamation and Reuse for Sustainability (WRRS 2005). Jeju-Do, Korea.

Field, R. W., D. Wu, Howell, J. A., Gupta, B. B. (1995). Critical Flux Concept for Microfiltration Fouling. Journal of Membrane Science 100: 295-272.

Flemming, H.-C., W. J. (2001). Rilevance of Microbial Extracellular Polymeric Substances (EPS) - Part I: Structural and Ecological Aspects. Water Science and Technology 43(6): 1-8.

Flemming, H.-C., W. J. (2001). Rilevance of Microbial Extracellular Polymeric Substances (EPS) - Part Ii: Technical Aspects. Water Science and Technology 43(6): 9-16.

Foley, G., Mc Carthy, A.A., Walsh, P.K. (2005). Evidence for Shape-Dependent Deposition in Crossflow Microfiltration of Microbial Cells. Journal of Membrane Science 250: 311-313.

Fratila-Apachitei, L.E., Kennedy, M.D., Linton, J.D., Blumed, I. and Schippers, J.C. (2001). Influence of Membrane Morphology on the Flux Decline During Dead-End Ultrafiltration of Refinery and Petrochemical Waste Water. Journal of Membrane Science 182: 151-159.

Fred Fu, L., Dempsey, B. A. (1998). Modeling the Effect of Particle Size and Charge on the Structure of the Filter Cake in Ultrafiltration. Journal of Membrane Science 149: 221-240.

Futselaar, H., Schoenviwille, H., van't Oever, R. (2005). The Side-Stream Mbr-System for Municipal Wastewater Treatment. WRRS 2005. Jeju-Do, Korea.

Garces, A.,W. De Wilde, Thoeye, C. and G. De Gueldre (2007). Operational Cost Optimisation of Mbr Schilde. 4th IWA International Membranes Conference - Membranes for Water and Wastewater Treatment. Harrogate, UK.

Green, G., Belfort, G. (1980). Fouling on Ultrafiltration Membranes: Lateral Migration and the Particle Trajectory Model. Desalination 35: 129-147.

Gregory, J. (2006). Particles in Water, Properties and Processes. ISBN: 1843391023. IWA Publishing.

Guglielmi, G., Chiarani, D., Saroj, D.P. and G. Andreottola (2007). Impact of Chemical Cleaning and Air-Sparging on the Critical and Sustainable Flux in a Flat Sheet Membrane Bioreactor for Municipal Wastewater Treatment. 4th IWA International Membranes Conference - Membranes for Water and Wastewater Treatment. Harrogate, UK.

Hao, X.-D., Li, H.-H., Cao, X.-Q. (2005). Reuse of Wastewater for Irrigation after Pathogens and Viruses Trapped with Membranes. ASPIRE 2005, the 1st International Water Association - Asia Pacific Regional Group (IWA-ASPIRE) Conference & Exhibition. Singapore, 10–15 July 2005.

Hao, X.-D. , Li, H.-H. , X.-H., Chen (2006). Effect of Operational Modes on Filtrate Flux with Direct Membrane Filtration of Wastewater. IWA World Water Congress and Exhibition. 12–15 September, Beijing, China.

Harmant, P., Aimar, P. (1998). Coagulation of Colloids in a Boundary

Layer During Cross-Flow Filtration. Colloids and Surfaces A: Physicochemical and Engineering Aspects 38(2-3): 217-230.

Henze, M. (1992). Characterization of Wastewater for Modeling Activate Sludge Processes. Water Science and Technology 25(6): 1-15.

Hermia, J. (1982). Constant Pressure Blocking Filtration Laws - Application to Power-law non Newtonian Fluids. Transactions of the Institution of Chemical Engineers 60:183-187.

Hlavacek, M., and Bouchet, F. (1993). Constant Flowrate Blocking Laws and an Example of Their Application to Dead-End Microfiltration of Protein Solutions. Journal of Membrane Science 82: 285-295.

Ho, C.C., Zydney, A.L. (1999). Effect of Membrane Morphology on the Initial Rate of Protein Fouling During Microfiltration. Journal of Membrane Science 155(2): 261-275.

Ho, C.C., Zydney, A.L. (2000). A Combined Pore Blockage and Cake Filtration Model for Protein Fouling During Microfiltration. Journal of Colloid and Interface Science 232: 389-399.

Ho, C.C., Zydney, A.L. (2001). Protein Fouling of Asymmetric and Composite Microfiltration Membrane. Industrial and Engineering Chemistry Research 40: 1412.

Ho, C.C., Zydney, A.L. (2002). Transmembrane Pressure Profiles During Constant Flux Microfiltration of Bovine Serum Albumin. Journal of Membrane Science 209: 363-377.

Hochstrat, R., Wintgens, T., Melin, T., and P.J. Jeffrey (2006). Assessing the European Wastewater Reclamation and Reuse Potential - a Scenario Analysis. Desalination 188: 1-8.

Hong, S., and Elimelech, M. (1997). Chemical and Physical Aspects of Natural Organic Matter (Nom) Fouling of Nanofiltration Membranes. Journal of membrane science 132(1-2): 159-181.

Huisman, I. H., Dutrk, B., Persson, K.M., Tragfirdh, G. (1997). Water

Permeability in Ultrafiltration and Microfiltration: Viscous and Electroviscous Effects. Desalination 113: 95-103.

Huisman, I.H., Trgrdh, G., Trgrdh, C. (1999). Particle Transport in Crossflow Microfiltration - Ii. Effects of Particle-Particle Interactions. Chemical Engineering Science 54(2): 281-289.

Huisman, I. H., Prdanos, P., Hernndez, A. (2000). The Effect of Protein-Protein and Protein-Membrane Interactions on Membrane Fouling in Ultrafiltration. Journal of Membrane Science 179: 79-90.

Huisman, L., Ed. (1996). Rapid Filtration - Lecture Notes Watermanagement, Section Sanitary Engineering, Delft University of Technology.

Iritani, E., Mukai, Y., Tanaka, Y. and Murase, T. (1995). Flux Decline Behaviour in Dead-End Microfiltration of Protein Solutions. Journal of membrane science 103: 181-191.

Jacob, J., Pradanos, P., Calvo, J.I., Hernandez, A., Jonsson, G. (1998). Fouling Kinetics and Associated Dynamics of Structural Modifications. Colloids and Surfaces A: Physicochemical and Engineering Aspects 138: 173-183.

Jarusutthirak, C., Amy, G., Croue', J.-P. (2002). Fouling Characteristics of Wastewater Effluent Organic Matter (Efom) Isolates on NF and UF Membranes. Desalination 145: 247-255.

Johnson, G., Culkin, B., Stowell, L. (2004). Membrane Filtration of Manure Wastewater.
$http://www.vsep.com/pdf/Membrane\_filtration\_of\_manure.pdf$.

Judd, S. (2006). The MBR Book - Principles and Applications of Membrane Bioreactors in Water and Wastewater Treatment. ISBN:1856174816, Elsevier.

Judd, S. and Jefferson, B. (2003). Membranes for Industrial Wastewater Recovery and Re-Use. ISBN: 9781856173896, Elsevier.

Katsoufidou, K., Yiantsios, S.G. , Karabelas, A.J. (2005). A Study of Ultrafiltration Membrane Fouling by Humic Acids and Flux Recovery by Backwashing: Experiments and Modeling. Journal of Membrane Science 266: 40-50.

Kilduff, J.E., Supatpong Mattaraj, Sensibaugh, J., Pieracci J.P., Yanxiao, Y. and Belfort, G. (2002). Modeling Flux Decline During Nanofiltration of Nom with Poly(Arylsulfone) Membranes Modified Using Uv-Assisted Graft Polymerization. Environmental Engineering Science 19(6): 477-495.

Kim, J.K., Chen, V., Fane, A.G. (1993). Ultrafiltration of Colloidal Silver Particles: Flux, Rejection and Fouling. Journal of colloid and interface science 155: 347-359.

Kim, J.-S., Akeprathumchai, S., Wickramasinghe, S.R. (2001a). Flocculation to Enhance Microfiltration. Journal of Membrane Science 182: 161-172.

Kim, J.-S., Lee, C.-H., Chang, S. (2001b). Effect of Pump Shear on the Performance of a Crossflow Membrane Bioreactor. Water Research 35(9): 2137-2144.

Kim, S.H., Moon, S.Y., Yoon, C.H., Yim, S.K., Cho J.W. (2005). Role of Coagulation in Membrane Filtration of Wastewater for Reuse. Desalination 173: 301-307.

KIWA (1974) Theorie vlokvorming (in Dutch). Report number 34.
http://www.kiwawaterresearch.eu/

Knoppert, P.L., van der Heide, J., Ed. (1990). Chemical Water Treatment, Desinfection and Oxidation, Coagulation and Flocculation. Lecture Notes Watermanagement, Section Sanitary Engineering, Delft University of Technology.

Koltuniewicz, A.B., Field, R.W., Arnot, T.C. (1995). Cross-Flow and Dead-End Microfiltration of Oily-Water Emulsion. Part I: Experimental Study and Analysis of Flux Decline. Journal of Membrane Science 102: 193-207.

Koros, W., J., Y.H. Ma and T., Shimidzyu T. (1996). Terminology for Membranes and Membrane Processes; IUPAC Recommendations 1996. Journal of membrane science 120: 149-159.

Kroiss, H. (2004). What Is the Potential for Utilizing the Resources in Sludge? Water Science and Technology 49(10): 1-10.

Laabs, C., Amy, G., Jekel, M., Buisson, H. (2003). Fouling of Low-Pressure (MF and UF) Membranes by Wastewater Effluent Organic Matter (EfOM): Characterization of EfOM Foulants in Relation to Membrane Properties. Water Science and Technology: Water Supply 3(5-6): 229-235.

Laabs, C. (2004). Fouling of Low-Pressure Membranes by Municipal Wastewater: Identification of Principal Foulants and Underlaying Fouling Mechanisms. PhD Thesis, Technical University of Berlin, Process Technology. Berlin, D.

Lahoussine-Turcaud, V., Wiesner, M. R., Bottero J.Y. (1990). Fouling in Tangential-Flow Ultrafiltration: The Effect of Colloid Size and Coagulation Pretreatment. Journal of Membrane Science 52: 173-190.

Laspidou, C.S., Rittmann, B.E. (2002). A Unified Theory for Extracellular Polymeric Substances, Soluble Microbial Products, and Ative and Inert Biomass. Water Research 36: 2711-2720.

Lazarova, V., Sheilds, P., Levine B., Savoye P., Hranisavljevic D., Renaud P. (2003). Production of High Quality Water for Reuse Purposes: The West Absin Experience. Water Science & Technology: Water Supply 3(3): 167-175.

Lazarova, V. and Bahri, A. (2005). Water Reuse for Irrigation. Boca Raton, Florida (USA), CRC press.

Lee, A., Amy, G., Croue, J.P., Buisson, H. (2004). Identification and Understanding of Fouling in Low-Pressure Membrane (MF/UF) Filtration by Natural Organic Matter (NOM). Water Research 38: 4511-4523.

Lee, N., Amy, G., Croue, J.P. (2006). Low-Pressure Membrane (Mf/Uf) Fouling Associated with Allochthonous Versus Autochthonous Natural Organic Matter. Water Resesarch 40: 2357-2368.

Levine, B.B., Madireddi, K., Lazarova, V., Stenstrom, M.K., Sufflet, M. (1999). Treatment of Trace Organic Compounds by Membrane Processes: At the Lake Arrowhead Water Reuse Pilot Plant. Water Science and Technology 40(4-5): 293-301.

Lojkine, M.H., R.W. Field and J.A. Howell (1992). Crossflow Microfiltration

of Cell Suspension: A Review of Models with Emphasis on Particle Size Effects. Transition Inst. Chemical Eng. 70(149-164).

Lowry, O.H., Rosenbrough, N.J, Farr, A.L., Randall. R.J. (1951). Protein Measurement with the Folin Phenol Reagent. Journal of Biological Chemistry 193:265-275.

Madaeni, SS. (1999). The Application of Memmbrane Technology for Water Disinfection. Water Research 33(2): 301-308.

Madaeni, S.S., Fane, A.G., Grohmann, G.S. (1995). Virus Removal from Water and Wastewater Using Membranes. Journal of Membrane Science 102: 65-75.

Madaeni, S.S. (1998). Ultrafiltration of Very Dilute Colloidal Mixtures. Colloids and Surfaces A: Physicochemical and Engineering Aspects 131: 109-118.

Madsen, R. (1977). Hyperfiltration and Ultrafiltration in Plate and Frame Systems. New York, Elsevier.

Mc Donogh, R.M., Fell, C.J.D., A.G., Fane (1989). Charge Effects in the Crossflow Filtration of Collodis and Particulates. Journal of Membrane Science 43: 69-85.

Meireles, M., Clifton, M. Aimar, P. (2002). Filtration of Yeast Suspensions: Experimental Observations and Modelling of Dead-End Filtration with a Compressible Cake. Desalination 147(1-3): 19-23.

Metcalf & Eddy (2003). Wastewater Engineering: Treatment and Reuse (4th Intenational Edition). New York, Mc-Graw Hill.

Michaels, A.S. (1968). Chemical Engineering Progress 64: 31-44.

Mourouzidis-Mourouzis, S.A., and Karabelas, A.J. (2006). Whey Protein Fouling of Microfiltration Ceramic Membranes - Pressure Effect. Journal of membrane science 282: 124-132.

Mulder, M. (1996). Basic Prinicples of Membrane Technology. Dordrecht, NL, Kluver Academic Publisher.

Nagaoka, H., Ueda, S., Miya, A. (1996). Influence of Bacterial Extracellular Polymers on the Membrane Separation Activated Sludge Process. Water Science and Technology 34(9): 165-172.

Nieuwenhuijzen, A. F. van, Evenblij, H., and J.H.J.M. van der Graaf (2000a). Direct Wastewater Membrane Filtration for Advanced Particle Removal from Raw Wastewater. 9th Gothenburg Symposium. Istanbul, Turkey.

Nieuwenhuijzen, A. F. van, Evenblij, H., and J.H.J.M. van der Graaf (2000b). Direct Wastewater Membrane Filtration for Advanced Particle Removal from Raw Wastewater. Chemical Water and Wastewater Treatment VI, Eds. Hahn H.H., Hoffmann, E., Ødegaard H.

Nieuwenhuijzen, A. F. van (2002). Scenario Studies into Advanced Particle Removal in the Physical-Chemical Treatment of Wastewater. Water Management. Delft, NL, Delft University of Technology. Doctorate.

Opong, S.W., and Zydney, A.L. (1991). Hydraulic permeability of protein layers deposited during ultrafiltration. Journal of Colloid and Interface Science 142(1): 41-60.

Porter, M.C. (1972). Concentration Polarization with Membrane Ultrafiltration. Industrial & Engineering Chemistry Product Research and Development 11: 234-248.

Qin, J.J., Htun Oo, M., Lee, H. and Kolkman, R. (2004). Dead-End Ultrafiltration for Pre-Treatment of RO in Reclamation of Municipal Wastewater Effluent. Journal of Membrane Science 243: 107-113.

Ramon G., Green M., Semia R., Dosoretz C. (2004). Low Strength Graywater Characterization and Treatment by Direct Membrane Filtration.

Ravazzini, A.M., van Nieuwenhuijzen, A.F., and J.H.J.M. van der Graaf (2005) Ultrafiltration of raw municipal wastewater: sustainable conditions for constant transmembrane pressure and constant flux operations. WRRS 2005 - Wastewater Reclamation and Reuse for Sustainability, Jeju (Korea) 8-11 November 2005 (Proceedings).

Rautenbach, R. and Vossenkaul, K. (2001). Pressure Driven Membrane Processes - the Answer to the Need of a Growing World Population for Quality Water Supply and Waste Water Disposal. Separation and Purification Technology 22-23: 193-208.

Ripperger, S., Altmann, J. (2002). Crossflow Microfiltration - State of the Art. Separation and Purification Technology 26: 19-31.

Rogers, A.N. (1984). Economics of the Application of Membrane Processes. Orlando, FL, Academic Press.

Romero, C.A., and R.H. Davis (1998). Global model of crossflow microfiltration based on hydrodynamic particle diffusion. Journal of Membrane Science 39: 157-185.

Roorda, J. (2002). Filtration Characteristics in Dead-End Ultrafiltration of Wwtp-Effluent. PhD Thesis, Delft University of Technology, CiTG, Water Management. Delft, NL.

Rosenberger, S. (2003). Charakterisierung va belebtem Schlamm in Memranbelebungsreaktoren zur Abwasserreinigung (in German). PhD Thesis, University of Berlin, Germany.

Rosenberg, S.K., Evenblij, H., Te Poele, S., Wintgens, T., Laabs C. (2005). The Importance of Liquid Phase Analyses to Understand Fouling in Membrane Assisted Activated Slude Process - Six Case Studies of Different European Research Groups. Journal of Membrane Science 263: 113-126.

Ruijgrok, E. (2001). Transferring economic values on the basis of an ecological classification of nature. Ecological Economics 39(3): 399-408.

Rulkens, Wim H., Houten, van R.T., Futselaar H., Temmink H., Bruning, H., Grolle, K., Bisselink, R. and Brouwer H (2005). Innovative Concept for Sustainable Treatment of Municipal Wastewater. Wastewater Reclamation and Reuse for Sustainability, Jeju Do, Korea.

Salgot, M., Huertas, E. (2003). Milestone Report Aquarec M2.1: Regulations and Guidelines on Wasteater Reuse.

Sethi, S., Juby, G. (2002). Microfiltration of Primary Effluent for Clarification and Microbial Removal. Environmental Engineering Science 19: 467-475.

Shon, H.K., Vigneswaran, S., In S. Kim, J. Cho, Ngo, H. H. (2004). Effect of Pre-Treatment on the Fouling of Membranes: Application in Biologically Treated Sewage Effluent. Journal of Membrane Science 234: 111-120.

Shon, H.K., Vigneswaran, S., Ngo, H. H., Ben Aim, R. (2005). Is Semi-Flocculation Effective as Pretreatment to Ultrafiltration in Wastewater Treatment? Water Research 39: 147-153.

Snyder, S., Wert, E., Yoon, Y., Westerhoff, P. (2005). Role of Membranes and Activated Carbon in the Removal of Endocrine Disruptor and Pharamceuticals During Water Treatment Process. IWA Specialty conference on Wastewater Reclamation and Reuse for Sustainability (WRRS 2005), Jeju-Do, Korea.

Soffer, Y., Ben Aim, R. and Adin, A. (2000). Membrane for Water Reuse: Effect of Pre-Coagulation on Fouling and Selectivity. Water Science and Technology 42(1-2): 367-372.

Song, L., Elimelech, M. (1995). Theory of Concentration Polarisation in Crossflow Filtration. Journal of the Chemical Society Faraday Transactions 91: 3389-3398.

Song, L. (1998). Flux Decline in Crossflow Microfiltration and Ultrafiltration: Mechanisms and Modelling of Membrane Fouling. Journal of Membrane Science 139: 183-200.

Song L., and Elimelech M. (1995). Particle Deposition onto a Permeable Surface in a Laminar Flow. Journal of colloid and interface science 173: 165-180.

Standard Methods (1998). AWWA Standard Methods for the Examination of Water and Wastewater, 20th Edition. ISBN: 0875532357. Editors: American Public Health Association, American Water Works Association and Water Environment Federation.

STOWA (2001)-14. Compendium RWZi - effluent als bron voor “ander” water (in Dutch).

STOWA (2002)-11A. MBR for municipal wasterwater treatment; Pilotplant research Beverwijk WWTP.

STOWA (2005)-35. Jong, P. de, Kramer, J.F., Slotema, W.F. and K.A. Third (2005). Exploratory Study for Wastewater Treatment Techniques and the European Water Framework Directive.

Tarabara, V. V., Hovinga, R. M., Wiesner, M. R. (2002). Constant Transmembrane Pressure Vs. Constant Permeate Flux: Effect of Particle Size on Crossflow Membrane Filtration. Environmental Engineering Science 19(6): 343-355.

Te Poele, S., van der Graaf, J.H.J.M. (2005). Enzymatic Cleaning in Ultrafiltration of Wastewater Treatment Plant Effluent. Desalination Volume 179(1-3): 73-8.

Te Poele, S. (2006). Foulants in Ultrafiltration of Wwtp Effluent. PhD Thesis. Delft University of Technology, The Netherlands.

Te Poele, Sandy and Van der Graaf, Jaap H.J. (2002). Physical and Chemical Conditioning of Effluent for Decreasing Membrane Fouling During Ultrafiltration. Membranes in Drinking and Industrial Water Production (MDIW) 5th, Mulheim an der Ruhr.

Thompson, M. and Powell, D. (2003). Case Study - Kranji High Grade Water Reclamation Plant, Singapore. IMSTEC 03. Singapore.

Thorsen, T. (1999). Membrane Filtration of Humic Substances - State of the Art. Water Science and Technology 40(9): 105-122.

Tracey, E.M., and Davis, R.H. (1999). Protein Fouling of Track-Etched Polycarbonate Micro Filtration Membranes. Journal of Colloid and Interface Science 167: 104-116.

UNIE van Waterschappen (2003). Bedrijfsvergelijking Zuiveringsbeheer 2002. Rapport (in Dutch). ISBN: 90-9017564-4.

van der Berg, G.B., Smolders, C.A. (1990). Flux Decline in Ultrafiltration

Processes. Desalination 77(1): 101-133.

Van Oss, C.J. (1993). Acid-Base Interfacial Interactions in Aqueous Media. Colloids Surfaces A: Physicochem. Eng. Aspects. 78: 1-49.

Vassilief, C., Leonard, E., Stepner, T. (1985). The Mechanisms of Cell Rejection in Membrane Plasmapheresis. Clin, Hermorheology 5.

Velasco, C., Ouammou, M., Calvo, J.I.,Hernndez, A. (2003). Protein Fouling in Microfiltration: Deposition Mechanism as a Function of Pressure for Different Ph. Journal of Colloids and Interface Science 266: 148-152.

Visvanathan, C., Ben Aim, R. (1989). Studies on Colloidal Membrane Fouling Mechanisms in Crossflow Microfiltration. Journal of Membrane Science 45: 3-15.

Vorobiev, E. (2006). Derivation of Filtration Equations Incorporating the Effect of Pressure Redistribution on the Cake-Medium Interface:Aconstant Pressure Filtration. Chemical Engineering Science 61: 3686 - 3697.

Vyas, H. K., Bennett, R.J., Marshall, A.D. (1999). Influence of Feed Properties on Membrane Fouling in Crossflow Microfiltration of Particulate Suspensions. International Diary Journal 10: 855-861.

Vyas, H. K., Bennett, R.J., Marshall, A.D. (2000). Influence of Feed Properties on the Membrane Fouling in Crossflow Microfiltration of Particulate Suspensions. International Diary Journal 10: 855-861.

Vyas, H. K., Bennett, R.J., Marshall, A.D. (2001). Cake Resistance and Force Balance Mechanism in the Crossflow Microfiltration of Lactalbumin Particles. Journal of Membrane Science 192: 165-176.

Wintgens, T., Melin, T., Schafer, A., Khan, S., Muston, M., Bixio, D. and Thoeye, C. (2005). The Role of Membrane Processes in Municipal Wastewater Reclamation and Reuse. Integrated Concepts in Water Recycling (ICWR) 2005 Wollongong, NSW, Australia.

Yiantsos, S.G., Karabelas, A.J. (1998). The Effect of Colloid Stability on Membrane Fouling. Desalination 118(1-3): 143-152.

Yuan, W., Kocic, A. and Zydney, A.L. (2002). Analysis of Humic Acid Fouling During Microfiltration Using a Pore Blockage-Cake Filtration Model. Journal of membrane science 198(1-2): 51-62.

Zhang, M., Song, L. (2000). Pressure-Dependent Permeate Flux in Ultra and Micro-Filtration. Journal of Environmental Engineering 126(7): 667-674.

Zydney, A. L. and Colton, C. K. (1986). A Concentration Polarization Model for the Filtrate Flux in Crossflow Microfiltration of Particulate Suspensions. Chemical Engineering Community 47: 1-21.

Appendix A

Experimental Equipment

Table A.1: *Main components of the ultrafiltration rig*

Item	Model
Circulation Pump	DAB Pumps KPS 30/16M N.1.01
Backflush pump	AFEC TMN Elite 600
Membrane module	X-flow F-4385
Pressure meters	Labom CB3010
Flow meter	Krohne FC 010K
Permeate Balance	Mettler PM34K
PLC	manually assembled

Table A.2: *Main equipment for physical-chemical analyses*

Item	Model
TSS precision balance	Mettler AE 240
Photometer Cuvette Tests	Spectroquant NOVA 60
Spectrophotometer (Colour, UV_{254}, EPS)	Milton Roy SPECTROMIC 401
Spectrophotometer (Humic Substances)	Perkin-Elmer Lambda 16
Turbidity meter	Hach 2100 N

COMPACT ULTRAFILTRATION MEMBRANE

F 4385

BASIC CHARACTERISTICS

- Hydrophilic tubular polyvinylidene fluoride membrane cast on a polyester carrier
- Tubular membrane available in 5.2 mm
- Structure asymmetric
- Developed for use in large-scale processes for water purification
- High performance and a very good anti-fouling behaviour
- Membranes are supplied in a standard range of elements
- Membrane elements can be backflushed for efficient membrane cleaning resulting in a higher average product flux

APPLICATIONS

- Pre-treatment RO and NF
- Surface water
- Drinking and process water production
- Recovery of sandfilter backwash water
- Effluent treatment
- Membrane bioreactor
- Waste water treatment
- Treatment of oil-in-water emulsions

MEMBRANE COMPOSITION

- Membrane material composed of polyvinylidene fluoride
- Membrane carrier is a composite polyester woven/non-woven

PERFORMANCE DATA

parameter	unit	F 4385	remarks
Clean water flux	$l/m^2.h.100$ kPa	> 1000	RO-water at 25°C
Transmembrane pressure	kPa	-100 .. + 500	
Mean pore size	nm	30	
pH		2 - 10	at 25°C
Chlorine exposure	ppm.h	250000	at 25°C
Temperature	°C	1 - 70	pH 7 and 100 kPa

Operation of membranes at any combination of maximum limits of pH, concentration, pressure or temperature, during cleaning or production, will severely influence the membrane lifetime.

220102

COMP-F4385-0204
(replaces: COMP-F4385-0143)

Figure A.1: *Membrane Data Sheet (continues . . .)*

SOLVENT RESISTANCE

Since the resistance of the membrane to solvents strongly depends on the actual process conditions, the indications given below should only be considered as guidelines.

Acids, pH > 2	+
Bases, pH < 11	+
Organic esters, ketones, ethers	−−
Aliphatic alcohols	++
Aliphatic hydrocarbons	++
Halogenated hydrocarbons	++
Aromatic hydrocarbons	+
Polar organic solvents	−−
Oils	++

CLEANING

Depending on the nature of the feed solution the following cleaning agents can be chosen:

Chemical	: NaOCl (active chlorine)	500 ppm max.
	: H_2O_2	1000 ppm max.
	: NaOH	pH ≤ 11
	: Nitric acid	pH ≥ 1
	: Phosphoric acid	pH ≥ 1
	: EDTA	pH ≤ 11
	: Citric acid	
	: Enzymatic compounds	

It is recommended to keep the pH between 1 and 11 and not to exceed a temperature of 40 °C during cleaning and/or disinfection.
If those standard cleaning techniques fail to remove the foulants, more concentrated cleaning solutions can be tried. Please contact X-Flow for recommendations.
It has to be stressed, however, that no warranty can be given on the efficiency of any cleaning nor on the membrane performance after such cleaning attempts.

STORAGE

New membrane modules can be stored as supplied.
Membrane modules should be stored in a dry, normally ventilated place, away from sources of heat, ignition and direct sunlight. Store between 0 and 40 °C.
The membrane modules should not be subjected to any freezing temperatures.
After use, UF membranes need to be stored wet at all times.
To avoid biological growth during shutdowns or storage, wet membranes should be treated with a compatible biocide. The membrane is compatible with many common disinfecting agents or biocidal preservatives. For short-term shutdowns, a daily flush with permeate quality water containing up to 2.0 ppm free available chlorine for 30 to 60 minutes may be adequate for bacteria control.
In case of long-term storage, membranes should be cleaned before the disinfection step is carried out. For disinfection, a 1% sodium metabisulfite solution can be used. In either situation, modules should be stored hydraulically filled.

For more information please write or call to:

X-Flow B.V.
P.O.Box 739
7500 AS Enschede
The Netherlands

Phone: + 31 (0)53 4287350
Fax: + 31 (0)53 4287351
E-mail: info@xflow.nl
Web site: www.xflow.nl

COMP-F4385-0204

Figure A.2: *Membrane Data Sheet (. . . continued)*

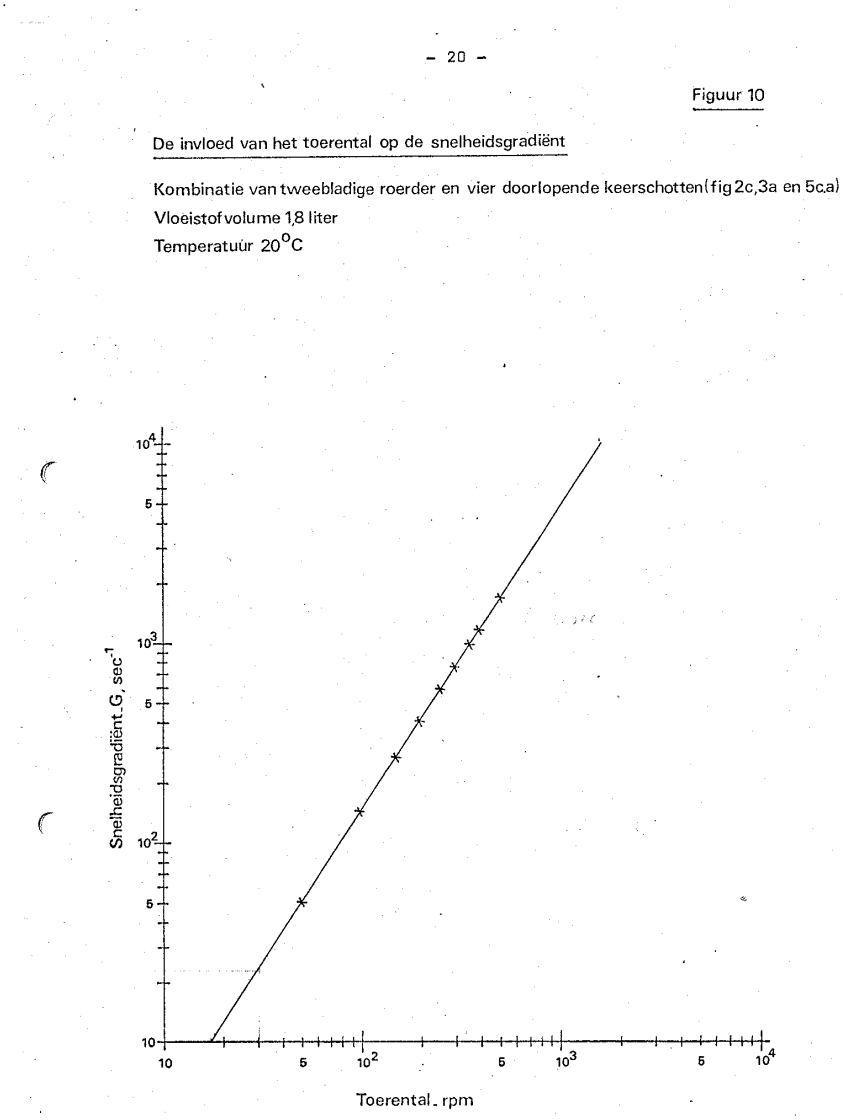

Figure A.3: *G-rpm relation for Jar Test set-up*

Appendix B

EPS Measurement

Adapted from Te Poele (2006)

Proteins

For the analysis of proteins the by Rosenberger (2003) modified method of Frølund et al. (1996), based on the method of Lowry et al. (1951) is used. For the calibration Albumin bovine, BSA, (Acros) fraction V, in a concentration range between of 0–25 mg/L is used. The concentration can be calculated with the measured extinction and calibration curve.

Reagents

- A: 143 mM NaOH and 270 mM Na_2 CO_3 in demineralised water
- B: 57 mM $CuSO_4$ in demineralised water
- C: 124 mM Na_2-tatrate, $C_4H_4Na_2O_6$, or Na-K-tatrate, $C_4H_4NaKO_6$, in demineralised water
- D: mixture of reagents A, B en C in the relation of 100:1:1
- E: Folin-Ciocalteu phenol reagent 1:2 dilution with demineralised water

Reagents A, B, C en E can be stored unlimited, reagent D has to be prepared daily.

Method

A sample of 5 mL and in addition 7 mL reagent D, is filled in a round tube and mixed in a tube mixer. After that the mixture is stored for 10 min at room temperature. Then immediately after addition of 1 mL reagent E the mixture must be mixed fast and powerful because the Folin-Ciocalteu phenol reagent is only for a short time stable in the alkaline enviro*nm*ent. The formation of the colour complex will be finished before starting the measurement. The sample-solution mixtures must be incubated for 45 min at room temperature. The adsorption is then measured in a 4 cm cuvett at a wavelength of 750 nm with a UV-VIS spectrophotometer against a reference sample of demineralised water. The formed colour complex will be stable for about 45–60 min. The samples should be measured twice and the mean value has to be calculated. The amount of proteins is expressed in mg/L.

Polysaccharides

For the analysis of polysaccharides the by Rosenberger (2003) modified method of Dubois et al. (1956) is used. For the calibration D(+)-glucose (J.T.Baker), in a concentration range between 0.5–10 mg/L is used. The concentration can be calculated with the measured extinction and calibration curve.

Reagents

- A: 5 % Phenol solution in demineralised water
- B: 95–97 % sulphuric acid

Method

A sample of 4 mL is filled in a round tube and 2 mL reagent A is added. After mixing 10 mL reagent B is added in a spout in order to get a proper mixing. Thereafter the mixture is stored for 10 min at room temperature, mixed again and incubated for 30 min at room temperature. The adsorption is then measured in a 4 cm cuvett at a wavelength of 487 nm with a UV-VIS spectrophotometer against a reference sample of demineralised water. The formed

colour complex will be stable for a long time. The samples are measured twice and the mean value is calculated. The amount of polysaccharides is expressed in mg/L.

References

Dubois, M., Gilles, K.A., Hamilton, J.K., Rebers, P.A., Smith, F. (1956). Colorimetric method for determination of sugars and related substances. Analytical Chemistry, 28: 350-356.

Frølund, B., Palmgren, R., Keiding, P.H., Nielsen, K. (1996). Extraction of extracellular polymers from activated sludge using a cation exchange resin. Water Science & Technology, 30 (8): 1749-1758.

Lowry, OH., Rosebrough, N.J., Farr, A.L., Randall. R.J. (1951). Protein measurement with the Folin phenol reagent. Journal of Biological Chemistry, 193: 265-275.

Rosenberger, S. (2003). Charakterisierung van belebtem Schlamm in Membranbelebungsreaktoren zur Abwasserreinigung (in German). PhD thesis, University of Berlin, Germany.

Te Poele, S. (2006). Foulants in Ultrafiltration of Wwtp Effluent. PhD Thesis. Delft University of Technology, The Netherlands.

Appendix C

Application of Least Square fitting

In the following pages the Matlab© code used for the cake filtration model is reported as example of the applied fitting procedure. The code for the pore blocking and pore constriction model are analogous: the only difference is that another model function "f" with corresponding derivatives is used.

Table C.1, reproduction of Table 6.4, shows the three model functions in use.

Table C.1: *Equations in use during fitting*

Model	Fitting equation
Pore blocking	$J = (J_0 - J^*) \cdot exp\left(-J_0 * k_{pb} * t\right) + J^*$
Pore Constriction	$J = J^* \left(\frac{\left[1 + \frac{\sqrt{J_0} - \sqrt{J^*}}{\sqrt{J_0} + \sqrt{J^*}} exp\left(-\frac{2\sqrt{J_0 J^*}}{r_0^2} * k_{pc}\right)\right]}{\left[1 - \frac{\sqrt{J_0} - \sqrt{J^*}}{\sqrt{J_0} + \sqrt{J^*}} exp\left(-\frac{2\sqrt{J_0 J^*}}{r_0^2} * k_{pc}\right)\right]} \right)^2$
Cake filtration	$J = \left[k_c * \frac{A_m}{J_0 R_m}\left(\frac{V}{A_m} - J^* t\right) + \frac{1}{J_0}\right]^{-1}$

DESCRIPTION OF IMPLEMENTED FUNCTION

```
% from theory
% J = ( alpha_c.*C_b.*A_m./(J_o.*R_m).*(V./A_m - J_cr.*t) + 1./J_o ).^(-1)
% here and from excel spreadsheet
% Jest = (k.*A_side./(J_mem_clean.*R_membr).*(cumVol./A_side-J_cr.*t)+1./J_mem_clean).^(-1);

% least squares

% from excel
% Jest = (k.*A_side./(J_mem_clean.*R_membr).*(cumVol./A_side-J_cr.*t)+1./J_mem_clean).^(-1);

% take the inverse eq.
% Jest.^(-1) = f(t,cumvol,k,J_cr), with J_cr = [0,150]

% establish a relation between J and Jest, err is a stochastic error with mean assumed zero
% J = Jest + err

% replace Jest in previous equation
% (J + err).^(-1) = f(t,cumvol,k,J_cr), with J_cr = [0,150]

% take initial values for k and J_cr, k0 and J_cr_0

% rewrite the equation based on the initial values k0 and J_cr_0

% Jcb_f is the jacobian of f with respect to k and J_cr, when k=k0 and J_cr=J_cr_0
% (J + err).^(-1) = f(t,cumvol,k0,J_cr_0) + [Jcb_f]*[dk;dJ_cr]

% take y to be the output of this new linearized function
% y = (J + err).^(-1) - f(t,cumvol,k0,J_cr_0)
% y = [Jcb_f]*[dk;dJ_cr]

% in least squares, the jacobian is usually represented as Phi and [dk;dJ_cr] generically as theta, so
% y = Phi*theta
% the least squares solution is (a\b is the pseudo-inverse in % matlab)
% theta = Phi\y
% k0     = k0 + dk;
% J_cr_0 = J_cr_0 + dJ_cr;

% The function is non-linear, so the process is iterated until the variation in the parameters is below a pre-defined
threshold.
% y = (J + err).^(-1) - f(t,cumvol,k0*1e9,J_cr_0)
```

FUNCTION CAKE MODEL LEAST SQUARE FITTING

```
close all


syms J k A_side J_mem_clean R_membr cumVol J_cr t real
f       = 1e9.*k.*A_side./J_mem_clean.*R_membr.*(cumVol./A_side-J_cr.*t)+1./J_mem_clean;
y       = J.^(-1) - f;
df_dk   = diff(f,k);    % =     1e9.*A_side./J_mem_clean./R_membr.*(cumVol./A_side-J_cr.*t);
df_dJ_cr = diff(f,J_cr); % =     - 1e9.*k.*A_side./J_mem_clean./R_membr.*t;

% k = alpha_c.*C_b
k0 = 6.05443E+11/1e9; % [1/m^4] % estimated by excel
% A_m
A_side = 0.07351; % [m2]
% J_cr
J_cr_0 = 0; % [L/m2*h] % estimated by excel
```

Figure C.1: *Code for Least Square fitting with cake filtration model (entire filtration period) - part 1*

```
% Rmembr
R_membr = 3.59839E+11; % [1/m]
% J_o
J_mem_clean = 298.3866766; % [L/m2*h]


% data input
data = [ ... % t [h], V [L], actual J [L/m2*h], Estim. J [L/m2*h]]
0.000  0.000  J_mem_clean J_mem_clean
0.003  0.061  295.6  248.2830642
.....
0.494  2.951  50.4    49.19788681
0.497  2.962  51.8    49.0533552
];
I = find(~(prod(data,2)>-inf));
data(I,:) = [];

% t [h], V [L], actual J [L/m2*h], Estim. J [L/m2*h]
t     = data(:,1); % [h]
cumVol = data(:,2); % [L]
J     = data(:,3); % [L/m2*h]
%Jest  = data(:,4); % [L/m2*h]

% least squares
k    = k0;
J_cr = J_cr_0;
k_history = k;
J_cr_history = J_cr;

% starting values
invf = (k.*1e9.*A_side./(J_mem_clean.*R_membr).*((cumVol./A_side)-J_cr.*t)+1./J_mem_clean).^(-1);
figure
subplot(1,2,1)
plot(t,J,'.',t,invf)
legend('J','Jest'); xlabel('time [h]'); ylabel('[L/m2*h]'); title('iteration = 1, intial values from Aldo');
subplot(1,2,2)
plot(t,(J.^(-1)-invf.^(-1)),'.')
legend('residual = J^{-1} - J_{est}^{-1}');
xlabel('time [h]');

% starting error
starterr = J - invf;
starterrsq = starterr.^2;

subplot(1,2,1)
plot(t,starterr)
title('Errors initial fitting')
ylabel('LMH')
subplot(1,2,2)
plot(t,starterrsq)
title('Squared Errors initial fitting')
ylabel('LMH^2')

% initial sum of squared errors
startSSe = sum(starterr.^2);
% initial total sum of squares
startSSt = sum((J - mean(J)).^2);
% initial coefficient of determination R2
startR2 = 1 - startSSe./startSSt;
```

Figure C.2: *Code for Least Square fitting with cake filtration model (entire filtration period) - part 2*

```
disp('Initial k [1/m] =');
disp(k0);
disp('Initial J_cr [LMH] =');
disp(J_cr_0);
disp('Initial coefficient of determination R^2')
disp(startR2)
disp('Initial sum of squared errors SSe')
disp(startSSe)


% define weight matrix
K = 0.999; % [0-1]
W = diag(K.*(t<0.002) + (1-K)); %diag(ones(length(t),1)); %

% run iterative cycle
for i=2:5,
   f       =  k.*1e9.*A_side./(J_mem_clean.*R_membr).*((cumVol./A_side)-J_cr.*t)+1./J_mem_clean;
   df_dk   =  1e9.*A_side./J_mem_clean./R_membr.*(cumVol./A_side-J_cr.*t);
   df_dJ_cr =  -1e9.*k.*A_side./J_mem_clean./R_membr.*t;

   y       = J.^(-1) - f;
   Phi     = [ df_dk, df_dJ_cr ];
   theta   = inv(Phi'*W*Phi)*Phi'*W*y; % theta = (W.^(1/2)*Phi)\(W.^(1/2)*y);
   k       = k    + theta(1);
   J_cr    = J_cr + theta(2);

   k_history(i)    = k;
   J_cr_history(i) = J_cr;

   % check results
   invf = (k.*1e9.*A_side./(J_mem_clean.*R_membr).*((cumVol./A_side)-J_cr.*t)+1./J_mem_clean).^(-1);
   figure
   subplot(1,2,1)
   plot(t,J,'.',t,invf)
   legend('J','Jest'); xlabel('time [h]'); ylabel('[L/m2*h]'); title(['iteration = ',num2str(i)]);
   subplot(1,2,2)
   plot(t,y,'.',t,[100*df_dk,10*df_dJ_cr])
   legend('residual = J^{-1} - J_{est}^{-1}','100*df/dk, f = J_{est}^{-1}', ...
      '10*df/J_{cr}, f = J_{est}^{-1}');
   xlabel('time [h]');
end

% degree of fitness in the global function
Jest = (k.*1e9.*A_side./(J_mem_clean.*R_membr).*((cumVol./A_side)-J_cr.*t)+1./J_mem_clean).^(-1);
% error
err = J - Jest;
errsq = err.^2;

subplot(1,2,1)
plot(t,err)
title('Errors final fitting')
ylabel('LMH')
subplot(1,2,2)
plot(t,errsq)
title('Squared Errors final fitting')
ylabel('LMH^2')

% sum of squared errors
SSe = sum(err.^2);
% total sum of squares
SSt = sum((J - mean(J)).^2);
```

Figure C.3: *Code for Least Square fitting with cake filtration model (entire filtration period) - part 3*

```
% coefficient of determination R2
R2 = 1 - SSe./SSt;


% uncertainty in the least squares estimates
%
% model function
% y = Phi*theta + err
% output
f = k.*1e9.*A_side./(J_mem_clean.*R_membr).*((cumVol./A_side)-J_cr.*t)+1./J_mem_clean;
y = J.^(-1) - f;
% error
err = y - Phi*theta;

% least squares estimate
% theta_est = P*Phi'*y
% information matrix
P = inv(Phi'*Phi);
% error in estimates
% theta_est - theta = P*Phi'*y - theta
%                   = P*Phi'*(Phi*theta + err) - theta
%                   = P*Phi'*err
% covariance matrix associated with error in estimates
% Q_sigma2_theta = P*Phi'*sigma2_err*Phi*P, with sigma2_err a scalar
%                = P*sigma2_err
Q_sigma2_theta = P*var(err);
% standard deviation associated with the estimates error: theta_est - theta
sigma_theta = sqrt(diag(Q_sigma2_theta));
% relative error for a 99% confidence interval for the estimates
rel_err = abs(3.*sigma_theta./[k;J_cr].*100);

figure
subplot(2,1,1)
plot([1:length(k_history)]',k_history')
title('Fitting evolution')
ylabel('k/1e9')
subplot(2,1,2)
plot([1:length(k_history)]',J_cr_history')
ylabel('J_{cr}')

% final estimated results
disp(['Estimated k/1e9 = ',sprintf('%f',k_history(end))]);
disp(['          J_cr  = ',sprintf('%f',J_cr_history(end))]);
disp('coefficient of determination R^2')
disp(R2)
disp('Sum of Squared Errors')
disp(SSe)
disp('Covariance matrix associated with error in estimates')
disp(Q_sigma2_theta)
disp('standard deviation associated with the estimates error:')
disp('sigma_theta = E{theta_est - theta}')
disp(sigma_theta)
disp('relative error for a 99% confidence interval in the estimates, [%]')
disp(rel_err)
```

Figure C.4: *Code for Least Square fitting with cake filtration model (entire filtration period) - part 4*

Appendix D

Fitting results for primary effluent

Table D.1: *Primary effluent: estimated model parameters and statistics during 30 min filtration*

	u_{cr}	TMP	J^*	k_i^*	R^2	SSe
Cake	$(m \cdot s^{-1})$	(bar)	(LMH)	$\cdot 10^{10}$ (m^{-4})	(-)	$\cdot 10^3$ $(LMH)^2$
	1	0.3	38.4	100	0.995	0.82
	1	0.5	42.1	160	0.947	27
	1	1.0	36.2	320	0.815	310
	1.5	0.3	72.8	30	0.995	0.88
	1.5	0.5	65.1	68	0.979	9.1
	1.5	1.0	66.2	20	0.857	270
	2.0	0.3	116.1	18	0.942	45
	2.0	0.5	133.5	60	0.996	1.3
	2.0	1.0	119.1	140	0.887	200
Pore Constrict.	$(m \cdot s^{-1})$	(bar)	(LMH)	(m^{-3})	(-)	$\cdot 10^3$ $(LMH)^2$
	1	0.3	60.9	0.62	0.984	3.1
	1	0.5	66.6	0.70	0.987	6.9
	1	1.0	67.8	0.76	0.975	43
	1.5	0.3	99.4	0.27	0.993	1.2
	1.5	0.5	102.7	0.50	0.986	6.3
	1.5	1.0	96.9	0.57	0.980	38
	2.0	0.3	136.1	0.18	0.944	4.2
	2.0	0.5	147.8	0.37	0.980	7.4
	2.0	1.0	139.2	0.49	0.980	37
Pore Blocking	$(m \cdot s^{-1})$	(bar)	(LMH)	(m^{-1})	(-)	$\cdot 10^3$ $(LMH)^2$
	1	0.3	63.7	0.078	0.964	6.8
	1	0.5	70.1	0.084	0.969	16
	1	1.0	72.7	0.086	0.962	64
	1.5	0.3	103.3	0.036	0.989	1.9
	1.5	0.5	105.8	0.061	0.967	14
	1.5	1.0	102.2	0.066	0.968	6.0
	2.0	0.3	139.2	0.026	0.935	5.1
	2.0	0.5	150.4	0.047	0.965	13
	2.0	1.0	143.8	0.057	0.971	52

Table D.2: *Primary effluent: estimated model parameters and statistics during min 10–30*

	u_{cr}	TMP	J^*	k_i^*	R^2	SSe
Cake	$(m \cdot s^{-1})$	(bar)	(LMH)	$\cdot 10^{11}$ (m^{-4})	(-)	$(LMH)^2$
	1	0.3	40.9	11	0.978	100
	1	0.5	44.9	17	0.987	57
	1	1.0	41.3	34	0.988	51
	1.5	0.3	75.5	3.1	0.970	32
	1.5	0.5	84.8	9.1	0.978	130
	1.5	1.0	71.2	22	0.985	99
	2.0	0.3	100.1	1.4	0.972	360
	2.0	0.5	132.5	5.9	0.962	340
	2.0	1.0	121.1	15	0.979	170
Pore Constrict.	$(m \cdot s^{-1})$	(bar)	(LMH)	(m^{-3})	(-)	$\cdot 10^2$ $(LMH)^2$
	1	0.3	55.6	0.454	0.967	1.5
	1	0.5	59.7	0.423	0.944	2.5
	1	1.0	58.4	0.344	0.925	3.2
	1.5	0.3	95.7	0.237	0.977	2.5
	1.5	0.5	96.4	0.644	0.931	4.2
	1.5	1.0	86.6	0.288	0.938	4.0
	2.0	0.3	123.0	0.130	0.969	3.9
	2.0	0.5	140.6	0.258	0.937	5.5
	2.0	1.0	132.0	0.453	0.819	41
Pore Blocking	$(m \cdot s^{-1})$	(bar)	(LMH)	(m^{-1})	(-)	$\cdot 10^2$ $(LMH)^2$
	1	0.3	57.7	0.050	0.942	2.7
	1	0.5	61.7	0.039	0.873	5.4
	1	1.0	60.6	0.024	0.803	8.5
	1.5	0.3	99.1	0.031	0.976	2.7
	1.5	0.5	98.2	0.036	0.884	7.0
	1.5	1.0	88.9	0.023	0.848	9.8
	2.0	0.3	128.0	0.019	0.968	4.1
	2.0	0.5	142.4	0.030	0.914	7200
	2.0	1.0	131.5	0.022	0.829	11

Appendix E

Flocculants Data Sheets

MSDS: 0007491
Print Date: 24-Aug-2006
Revision Date: 24-Aug-2006

SAFETY DATA SHEET

1. CHEMICAL PRODUCT AND COMPANY IDENTIFICATION

Product name: SUPERFLOC® C-492 HMW Flocculant
Synonyms: None
Product Description: Cationic polyacrylamide
Intended/Recommended Use: Water treating chemical

CYTEC AUSTRALIA HOLDINGS PTY LIMITED
ABN : 45 081 148 629
SUITE 1, LEVEL 1, 21 SOLENT CIRCUIT, BAULKHAM HILLS, NSW, 2153, AUSTRALIA

2. HAZARDS IDENTIFICATION

Hazard Classification: NON-HAZARDOUS SUBSTANCE. NON-DANGEROUS GOODS.
None required

HUMAN AND ENVIRONMENTAL HAZARDS

none

3. COMPOSITION/INFORMATION ON INGREDIENTS

HAZARDOUS INGREDIENTS

Component / CAS No.	%	(w/w)	Symbols	Risk Phrases
Adipic acid 124-04-9	~ 4		Xi	R:36

11. TOXICOLOGICAL INFORMATION

Potential health effects

none

12. ECOLOGICAL INFORMATION

This material is not classified as dangerous for the environment.
The effects on aquatic organisms are due to an external (non-systemic) mode of action, and are significantly reduced (by a factor of 7-20) within 30 minutes due to binding of the product to dissolved organic carbon and inorganic sorbents such as clays and silts.
All ecological information provided was conducted on a structurally similar product.
Acute toxicity tests conducted using environmentally representative water gave the following results:

Figure E.1: *Extract of Data Sheet Cytec Superfloc C-492*

MATERIAL SAFETY DATA SHEET

1. CHEMICAL PRODUCT AND COMPANY IDENTIFICATION

Product name: **SUPERFLOC® C-581 Flocculant**
Synonyms: None
Product Description: Polyquaternary amine in water
Intended/Recommended Use: Flocculant

CYTEC AUSTRALIA HOLDINGS PTY LIMITED
ABN : 45 081 148 629
SUITE 1, LEVEL 1, 21 SOLENT CIRCUIT, BAULKHAM HILLS, NSW, 2153, AUSTRALIA

2. HAZARDS IDENTIFICATION

Classified according to the Australian Approved Criteria for Classifying Hazardous Substances and the ADG Code

Hazard Classification: NON-HAZARDOUS SUBSTANCE. NON-DANGEROUS GOODS.
None required

HUMAN AND ENVIRONMENTAL HAZARDS

R52/53 - Harmful to aquatic organisms, may cause long-term adverse effects in the aquatic environment.

3. COMPOSITION/INFORMATION ON INGREDIENTS

HAZARDOUS INGREDIENTS

Component / CAS No.	% (w/w)	Symbols	Risk Phrases
Dimethylamine Epichlorohydrin Ethylenediamine polymer 42751-79-1	48 - 52	-	R: 52/53

Other non-hazardous ingredients to 100%

11. TOXICOLOGICAL INFORMATION

Potential health effects

PRODUCT TOXICITY INFORMATION

ACUTE TOXICITY DATA

Oral	rat	Acute LD50	6,160 mg/kg
dermal	rabbit	Acute LD50	>10,000 mg/kg
Inhalation	rat	Acute LC50 4 hr	>20 mg/l

LOCAL EFFECTS ON SKIN AND EYE

Acute Irritation	dermal	Not irritating
Acute Irritation	eye	Not irritating

ALLERGIC SENSITIZATION

Sensitization	dermal	Not sensitizing
Sensitization	Inhalation	Not sensitizing

GENOTOXICITY

Assays for Gene Mutations
Ames Salmonella Assay — No data

HAZARDOUS INGREDIENT TOXICITY DATA
No Hazardous Ingredients

12. ECOLOGICAL INFORMATION

Harmful to aquatic organisms, may cause long-term adverse effects in the aquatic environment.
All ecological information provided was conducted on a structurally similar product.
Acute toxicity tests conducted using environmentally representative water gave the following results:

Figure E.2: *Extract of Data Sheet Cytec Superfloc C-581*

MATERIAL SAFETY DATA SHEET

1. CHEMICAL PRODUCT AND COMPANY IDENTIFICATION

Product name:	**SUPERFLOC® C-592L Flocculant**
Synonyms:	None
Product Description:	Polyquaternary ammonium resin in water
Intended/Recommended Use:	Flocculant

2. HAZARDS IDENTIFICATION

Classified according to the Australian Approved Criteria for Classifying Hazardous Substances and the ADG Code

Hazard Classification: NON-HAZARDOUS SUBSTANCE. NON-DANGEROUS GOODS.
None required

HUMAN AND ENVIRONMENTAL HAZARDS

R52/53 - Harmful to aquatic organisms, may cause long-term adverse effects in the aquatic environment.

3. COMPOSITION/INFORMATION ON INGREDIENTS

HAZARDOUS INGREDIENTS

Component / CAS No.	%	(w/w)	Symbols	Risk Phrases
Polydiallyldimethyl ammonium chloride 26062-79-3	38 - 42		-	R:52/53

Other non-hazardous ingredients to 100%

11. TOXICOLOGICAL INFORMATION

Potential health effects
none

12. ECOLOGICAL INFORMATION

Harmful to aquatic organisms, may cause long-term adverse effects in the aquatic environment.
All ecological information provided was conducted on a structurally similar product.
Acute toxicity tests conducted using environmentally representative water gave the following results:

.....

SUPERFLOC C-587 and C-591 coagulants are certified with a maximum use level of 50 mg/L and C-592 & C-595 are certified with a maximum use level of 25 mg/L t
NSF/ANSI Standard 60, as produced at Cytec NSF-certified facilities.
See http:www.nsf.org/Certified/PwsChemicals/Listings.asp?CompanyName=cytec& for details

Figure E.3: *Extract of Data Sheet Cytec Superfloc C-592*

List of Figures

List of Tables

Summary

One of the emerging tools for wastewater treatment and water recycling is membranes. Membranes are used to upgrade the standard wastewater treatment plant effluent to a superior level, or even to reclaim it to potable level.

The reason behind the success of membranes in wastewater treatment lies in the fact that membranes guarantee a complete removal of particles and bacteria, by constituting a physical barrier to them. The drawback is membrane fouling, i.e. the decrease of filtration performances because of accumulation of material at the membrane surface. This is an obvious consequence of the separation process.

Because of the tendency to foul, membranes are usually applied as the final step of a complex treatment train. But can they be applied up-front, directly on untreated wastewater?

Some previous studies showed that this concept, named *direct membrane filtration*, has a high potential. In facts, micro- and ultrafiltration of untreated wastewater may produce in one single step water for reuse purposes, such as irrigation or toilet flushing. Another possibility is to use direct micro- and ultrafiltration as the starting step of a fully physical-chemical wastewater treatment scheme, based on membrane technology, with production of reusable permeate and recovery of nutrients and energy.

This dissertation studies in details the filtration characteristics of crossflow ultrafiltration of untreated wastewater, aiming at contributing operatively to the development of *direct ultrafiltration*.

The feed water of choice is municipal raw sewage, i.e. the most common form of wastewater, for which it would be worth developing a new treatment route. A crossflow ultrafiltration unit is built to perform filtration experiments in a controlled situation.

The filtration characteristics (flux decline and resistance increase over time) are studied and described at various operating conditions (crossflow velocity u_{cr}, trans-membrane pressure TMP). Additionally, the influence of pre-treatments (sedimentation and coagulation) is investigated.

Fouling is described by *filterability* (increase of resistance with time and filtrated volume) and *reversibility* (fraction of fouling removable by hydraulic cleaning, e.g. by *backflush*). Pre-existing models (*blocking laws*) are applied to the filtration curves to enable the comparison of filtration data at different operating conditions and using raw or pre-treated feed water.

Finally, based on the outcomes of the filtration tests, a preliminary estimate of the cost of the process is attempted.

At first raw sewage is tested in 30 min tests. It is confirmed that filterability depends strongly on the applied TMP and u_{cr}: excessive TMP increases fouling and is detrimental to productivity; the crossflow velocity decreases fouling. Appropriate TMP and crossflow velocity can be selected: the most advantageous operating conditions are recognised in $TMP < 0.5$ bar and u_{cr} about 1.5–2 $m \cdot s^{-1}$.

Longer filtration tests with duration 3–7 h are conducted alternating production runs and backflushes, in cyclic operating mode. At the selected operating conditions, filtration appears sustainable in time. Although a little amount of irreversible fouling is created rapidly, in the following operations become stable. In a sort of dynamic equilibrium, the fouling created during each filtration run is removed by the subsequent backflush.

At $u_{cr} = 1.5$ and 2 $m \cdot s^{-1}$, net fluxes are in the order of 70–85 LMH.

The effects of pre-treatments are limited. Effluent of primary clarifier is tested in the same way as raw sewage and compared. Results indicate a higher filterability and a very similar fouling mechanism. A possible explanation is

that with respect to raw sewage primary effluent is characterised by a smaller amount of transported solids and similar amount of dissolved organic foulants.

Coagulation produces a consistent improvement in filterability as well. However, the effect is lost rapidly during cyclic filtration. It is supposed that the recirculation through the pump induces the release of entrapped organic foulants and that the backflush procedure exposes the membrane to them.

The fitting exercise with blocking laws shows that in the case of raw sewage and primary effluent, when the stable part of the data set is considered, the cake filtration model satisfactorily reproduces observed flux values. Therefore, filterability results can be modeled and compared.

The model is based on two parameters, one related to the flux asymptotic value during unstopped filtration (J^*) and the other to the cake specific resistance ($k_c = \alpha_{cake} \cdot C_b$). Both appear strongly affected by the applied operating conditions and the water quality: J^* varies within 18–73 LMH for raw sewage and 40–132 LMH for primary effluent; whereas k_c within $5.1–37 \cdot 10^{11}$ m^{-4} for raw sewage and $2.1–6.1 \cdot 10^{11}$ m^{-4} for primary effluent.

The formation of a cake layer is ascertained on the basis of various considerations on the transported material and the analysis of flux curves. The cake layer is certainly compressible, but filtration data and modeling results show that cake compressibility is not sufficient to explain the increase of fouling with TMP. The hypothesis is that high TMP induces an increase of accumulated material or the occurrence of other fouling mechanisms (namely internal fouling).

The fraction of the total fouling that cannot be explained by simple compression increases with crossflow velocity and is bigger for primary effluent. This leads to the hypothesis that the rapid formation of a cake layer inclusive of large particles may be advantageous for the membrane, which is covered and protected from deeper, irreversible fouling. This hypothesis is further confirmed by the observation that during cyclic operations with and without coagulated water, an initial period of unstopped filtration (30 min) resulted in remarkably lower increase of resistance after 2 h.

The last topic of discussion concerns the applicability of the process.

The permeate of direct ultrafiltration differs from the conventional WWTP effluent in terms of organic load and nutrients content. This requires the identification of specific reuse applications, handling and storage practice. Preliminary cost estimates indicate an approximate range of 0.25–0.45 € $\cdot\, m^{-3}$ (this value includes only the cost of the process itself, regardless of sludge treatment, land or other). In comparison, the cost of wastewater treatment in The Netherlands (all inclusive) is in the order of 0.5–1.0 € $\cdot\, m^{-3}$, i.e. significantly higher.

Direct ultrafiltration can be implemented into the existing wastewater systems without additional expense; consequently, where the (re)use of water and nutrients is possible or necessary, the application of direct ultrafiltration may prove economically attractive.

Samenvatting

Één van de opkomende technieken voor de behandeling van afvalwater en afvalwaterhergebruik is de membraantechnologie. Membranen worden toegepast voor optimalisatie van conventionele afvalwaterzuiveringsinstallaties voor strenger effluent eisen en voor hergebruiksdoeleinden.

Het succes van de toepassing van membranen in de afvalwaterbehandeling is het feit dat membranen, zijnde een absolute fysieke barrire, zorg dragen voor een complete verwijdering van deeltjes en bacterin, maar opgeloste stoffen en vloeistoffen doorlaat. Een nadeel van het afscheidingsproces middels membranen is echter membraanvervuiling ook wel *membrane fouling* genoemd, waarmee gedoeld wordt op de afname van de filtratieprestaties door accumulatie van vervuiling in of op het membraanoppervlak.

Door de neiging om te vervuilen als gevolg van de te verwijderen stoffen, worden membranen in de afvalwaterbehandeling over het algemeen toegepast aan het eind van een aantal uitgebreide en complexe zuiveringsprocessen. De vraag is of membranen ook eerder in de zuiveringsinstallatie gebruikt kunnen worden, bijvoorbeeld direct als eerste zuiveringsonderdeel op ruw, onbehandeld afvalwater?

Eerder verkennend onderzoek heeft aangetoond dat dit concept, genaamd *directe membraanfiltratie* toepasbaar is en een aantal interessante voordelen heeft. Door behandeling van ruw afvalwater door directe micro- of ultrafiltratie kan in n zuiveringsstap een herbruikbare voedingsrijke, maar gedesinfecteerde, waterstroom geproduceerd worden, voor bijvoorbeeld irrigatie of toilet spoeling. Een alternatieve toepassing van directe micro- of ultrafiltratie is de voorbehandeling van een compleet fysisch-chemische afvalwaterzuiveringproces, volledig gebaseerd op membraantechnologie, met productie van (her)bruikbaar perme-

aat en terugwinning van nutrinten en energie.

Dit proefschrift beschrijft dan ook de filtratiekarakteristieken van crossflow ultrafiltratie van ruw afvalwater, om bij te dragen aan de ontwikkeling en toepasbaarheid van directe membraanfiltratie.

Voor de uitvoering van filtratie-experimenten is binnen het onderzoek een directe crossflow ultratfiltratie-installatie op pilot-schaal ontwikkeld die onder gecontroleerde standaard situaties kon worden bedreven. Als voedingwater van de test installatie is in dit onderzoek de meest voorkomende afvalwaterstroom gekozen: ruw communaal afvalwaterinfluent.

Met deze onderzoekopzet zijn de filtratiekarakteristieken (uitgedrukt als fluxafname en/of drukopbouw tegen de (loop)tijd) bestudeerd en beschreven voor verschillende operationele condities (waaronder het type afvalwater, voorbehandeling (bezinking) en conditionering (coagulanten en flocculanten) van het influent, de crossflowsnelheid u_{cr} en de transmembraandruk TMP).

Membraanvervuiling wordt beschreven door *filtreerbaarheid* (uitgedrukt als toename van filtratieweerstand over het membraan tegen tijd en/of gefiltreerd volume) en *reversibiliteit* (omkeerbare membraanvervuiling; het aandeel van vervuiling dat door een hydraulische reinigings(spoeling), bijvoorbeeld door een *terugspoeling*, kan worden verwijderd). Standaard filtratiemodellen (gebaseerd op verstoppingstheorien: *pore blocking laws*) zijn gebruikt voor het opstellen van filtratiecurven om inzicht te geven in de vergelijking tussen verschillende filtratiedata onder verschillende condities.

Op basis van de resultaten van de filtratietesten zijn uiteindelijk kostenanalyses uitgevoerd om de haalbaarheid en toepasbaarheid van directe membraanfiltratie definitief vast te stellen.

De eerste reeks onderzoekingen zijn uitgevoerd als korte termijn testen gedurende 30 minuten. Hiermee is de directe relatie tussen filtreerbaarheid en toegepaste TMP en u_{cr} bevestigd: een sterke toename van de TMP resulteren in een linaire toename van de membraanvervuiling en is nadelig voor de productiviteit. Daarnaast is vastgesteld dat door toename van de crossflowsnelheid membraanvervuiling afneemt. Op basis van de korte termijn testen zijn als beste

operationele condities een TMP van < 0.5 *bar* en een u_{cr} tussen 1.5-2 $m \cdot s^{-1}$ vastgesteld.

Vervolgens zijn onder verschillende condities langere termijn testen uitgevoerd gedurende 3 tot 7 uur met alternerende permeaatproductie met terugspoeling en met cyclisch bedrijf. Onder de gekozen operationele condities is het mogelijk om een langdurig stabiel en duurzaam filtratieproces te bewerkstelligen, waarbij echter relatief snel een beperkte en constante hoeveelheid onomkeer*bar*e membraanvervuiling ontstaat. In een soort als dynamisch evenwicht wordt de tijdens elke filtratielooptijd opgebouwde membraanvervuiling elke keer structureel verwijderd door de terugspoeling. Met een u_{cr} tussen 1.5 and 2 $m \cdot s^{-1}$ worden met directe membraanfiltratie structureel netto fluxes van 70–85 LMH gehaald.

Op basis van het onderzoek wordt geconcludeerd dat de effecten op de filtreerbaarheid door voorbezinking van het voedingswater beperkt zijn. De filtratiekarakteristieken van het overloopwater van verschillende voorbezinktanks zijn daarvoor herhaaldelijk vergeleken met ruw influent. Hieruit blijkt dat wel een hogere filtreerbaarheid mogelijk maar blijken zeer vergelijk*bar*e vervuilingsmechanismen op te treden. Een mogelijke verklaring hiervoor is dat, ten opzichte van ruw afvalwaterinfluent, in afloopwater van voorbezinktanks het aandeel inerte deeltjes kleiner is (met als gevolg een hogere filtreerbaarheid) maar dat de hoeveelheid opgeloste verontreinigingen die membraanvervuiling veroorzaken nagenoeg gelijk is.

Ook door coagulatie van het ruwe afvalwater kan de filtreerbaarheid structureel verbeterd worden. Echter wordt het positieve effect snel tenietgedaan door het cyclische filtratieproces. Verondersteld wordt dat door toedoen van de (recirculatie)pomp geprecipiteerde en geflocculeerde organische vervuilende stoffen weer vrijkomen en door terugspoeling in contact komen met het membraan.

De modellering van de filtratiekarakteristieken op basis van verstoppingstheorie (pore blocking laws) toont aan dat voor zowel ruw als voorbezonken afvalwater, onder een stabiele bedrijfsvoering, het koekfiltratiemodel de in de testen waargenomen fluxen reproduceert. Geconcludeerd wordt dat op basis van de koekfiltratietheorie de filtratiekarakteristieken van directe membraanfiltratie beschreven en vergeleken kunnen worden.

Het model is gebaseerd op twee parameters, de asymptotische fluxwaarde tijdens vrije, niet verstopte, filtratie (J^*) en de specifieke koekweerstand ($k_c = \alpha_{cake} \cdot C_b$). Beide parameters worden sterk benvloed door de toegepaste filtratiecondities en de afvalwatersamenstelling: de flux, J^*, varieert tussen 18–73

LMH voor ruw afvalwater en 40–132 LMH voor voorbezonken afvalwater. De specifieke filtratieweerstand, k_c, varieert tussen 5–37 $\cdot 10^{11} m^{-4}$ voor ruw afvalwater en 2–6 $\cdot 10^{11} m^{-4}$ voor afloopwater van voorbezinktanks.

De vorming van een koeklaag op het membraan wordt bevestigd door verschillende redeneringen met betrekking tot materiaaltransport in de richting van de membranen en analyses van de fluxcurves. De koeklaag blijkt samendrukbaar te zijn, maar zowel de praktijkdata als de modelresultaten tonen aan dat samendrukbaarheid (compressibility) van de filterkoek niet de maatgevend verklaring is voor de toename van membraanvervuiling door toename van TMP. De hypothese is dat een hogere TMP een toename veroorzaakt van geaccumuleerd materiaal op het membraan of bijdraagt aan andersoortige vervuilingsmechanismen (voornamelijk interen vervuiling).

Het aandeel van de totale vervuiling dat niet verklaard kan worden door eenvoudige samendrukbaarheid van de filterkoeklaag, neemt toe met de crossflowsnelheid en is duidelijk groter voor voorbezonken afvalwater ten opzichte van ruw afvalwater. Hierdoor is de veronderstelling ontwikkeld dat een snelle formatie van een koeklaag met incorporatie van grotere deeltjes en vlokken voordelig zou kunnen zijn voor membraanfiltratie, omdat het bedekte membraan beschermd wordt tegen verstopping door fijnere collodalen en ontwikkeling van niet-verwijder*bar*e vervuiling (irriversible fouling). Deze hypothese wordt onderbouwd door de waarneming dat tijdens cyclische bedrijfsvoering, met en zonder gecoaguleerd afvalwater, een initile periode van 30 minuten van vrije ongeblokkeerde filtratie optreedt met vervolgens een opmerkelijk lage drukopbouw gedurende de volgende twee uur.

Het laatste discussiepunt betreft de toepasbaarheid van het proces.

Allereerst wordt hierbij opgemerkt dat het permeaat van directe ultrafiltratie verschilt van conventionele RWZI effluent wat betreft de hoeveelheden opgeloste organische verontreinigingen en nutrinten. Dit vereist de identificatie van specifieke hergebruik toepassingen, behandeling en opslag voorzieningen.

Volgens, een voorlopige globale kostenraming geeft als kostenindicatie 0.25–0.45 $€ \cdot m^{-3}$ geproduceerd permeaat (op basis van een voorontwerp van het membraanfiltratieproces op zich zelf, los van gerelateerde processen als slibverwerking, grondkosten, etc.). Hiermee vergeleken zijn de basiskosten voor afvalwaterbehandeling in Nederland met 0.5–1.0 $€ \cdot m^{-3}$ effluent significant hoger.

Directe ultrafiltratie kan geïmplementeerd worden in bestaande zuiveringssystemen zonder bijkomende kosten en aanpassingen. Waar (her)gebruik van water en voedingsstoffen mogelijk of noodzakelijk is kan het permeaat van directe membraanfiltratie zelfs economisch rendabel geproduceerd worden.

Acknowledgments

All the work presented here and the years that I spent around it, are indissolubly tied to the people that accompanied me. Many people did actually more than just accompanying me. I would like to mention and thank gratefully the ones who contributed in a special way to the accomplishment of this dissertation, although the list that I will draw will be certainly incomplete.

Professor J.H.J.M. van der Graaf, my promotor. He offered me the opportunity to conduct this research and guided me throughout the years. He granted me a great freedom and directed my work correcting my errors discreetly and patiently. I don't recall long discussions, but his short focused comments and vivid examples. Watching him working was also a great school, and when I had difficulties he always suggested me an appropriate way to handle them.

Arjen van Nieuwenhuijzen, who advised me frequently offering his specific knowledge and experience on the topic of the research.

Prof. J. de Koning, prof. T. Melin, Thomas Wintgens and Davide Bixio for the teachings and the cooperation during the *Aquarec* project, which broadened my fields of activity and experience.

Harry Futselaar and *X-flow bv.* for providing the membranes.

Peter de Been and Joyce Arnoldus, who kindly welcomed and supported me and the students at *De Groote Lucht.*

All the colleagues of the Department of Water-Management at the TU-Delft. Herman, who welcomed and guided me at the arrival (but also on the way), and Sandy and Jelle: they have first been"tutors" and then friends and inspiring col-

leagues. Cees, Tonny, Ria and Van, who shared (or bore) the laboratory work. Eefie and Mieke, essential to the organisation and the positive atmosphere. Stefan, Arie, Maria, Adrien, Jasper, Cathalijne and Remi for the help, the nice atmosphere, the conversations and the fun. A special note is for Viviane, for we had a very similar path, and we often walked it side by side.

All the students who helped me, in rigorous order of appearance: Marta Neiva Correia, Jean Baptiste Laurens, Cherif Osman, Beatriz Varela Pinto and Benjamin Marion. They all played hard with the filthy wastewater, contributing significantly to the final outcome. Thanks also for the personal relationship and for bearing my bad moments in the lab.

Uncle Thom and Lara for reviewing the English of the text (hard task!), Joao for teaching Matlab© (harder?), and Arjen for preparing the *samenvatting*. Riki for the great work with the cover design.

To the accomplishment of the dissertation, my private life in Delft was equally important than the academic relationships. In Italy we say: "A happy cow gives better milk". There are many people I feel to thank for my happiness.

My housemates: Ciccio, Joao, Luis and Guga. You were family for years, you still have a great part in the person I am today (good and bad, of course!).

Our group of friends, with the hard-core represented by *the Buities* but not limited to them: many different people, all good people, great friends!

The glorious *Zuiderpark* from Rotterdam: for the winter trainings, the games, the time at the Club.

My family. Thank Mum and Dad for letting me go, and yet be always available and caring. I remember Mum when I left for the Master Thesis (*"You will not come back"*), and the letters she sent regularly with the invoice of the car insurance and some nice words. I remember dad, always happy and a little surprised to see me "home" in Milano.

Thank Marzia for being always close and for waking me up with Bea. Thank Massi to be always the same big brother.

To the rest of the family, including Aunts, Uncles, Grandparents, cousins and corresponding partners: thank you for being present anyway, and for your visits.

Finally I thank Lara, for the understanding and the love, and for enduring.

Publications and Congresses

2008

Bixio, D., Thoeye C., Wintgens, T., Ravazzini, A., Miska, V., Muston, M., Chikurel, H., Joksimovic, D. and Melin T. (2008). Water Reclamation and Reuse: Implementation and Management Issues. Desalination 218(1-3): 13-23.

2007

Ravazzini, A.M. , van Nieuwenhuijzen, A.F. and J.H.M.J. van der Graaf (2007). Effects of small-dosages of coagulants during crossflow ultrafiltration of raw municipal wastewater. IWA International Conference on Membranes for Water and Wastewater Treatment, Harrogate, UK, 15–17 May (Proceedings, Oral Presentation).

2006

Quevauviller, P., Thomas, O., and A. Van Der Beken (Editors) (2006). Wastewater Quality Monitoring and Treatment. Wiley Water Quality Measurement Series. ISBN: 978-0-471-49929-9. (Contribution to Chapter 5.4, *Water Reuse*, pp.329–349).

Bixio, D. and T. Wintgens, Editors (2006). Water Reuse System Management Manual Aquarec. ISBN: 9279019341. European Commission Technical Series, Bruxelles (BE). (Contribution to Chapters 12, 13 and 20).

Miska, V., Ravazzini, A.M. and J. de Koning: Aquarec Deliverable D17, Report on standard water treatment options in reuse systems. Barcelona (ES), February 2006.

2005

Ravazzini, A.M., van Nieuwenhuijzen, A.F. and J.H.J.M. van der Graaf (2005). Direct Membrane Ultrafiltration of Municipal Wastewater: comparison between filtration of raw sewage and primary clarifier effluent. Desalination 178: 51-62.

Bixio, D., B. De Heyder, Joksimovic, D., Cikurel, H., Miska, V., Muston, M., Schfer, A.I., Ravazzini, A.M., Aharoni, A., Savic, D. and C. Thoeye (2005). Municipal Wastewater Reclamation: Where Do We Stand? An Overview of Treatment Technology and Management Practice. Water Science & Technology: Water Supply 5(1): 77-85.

Ravazzini, A.M., van Nieuwenhuijzen, A.F. and J.H.J.M van der Graaf (2005). Direct Membrane Ultrafiltration of Municipal Wastewater: potential and opportunities for reuse. WRRS - Wastewater Reclamation and Reuse for Sustainability - 2005 . Jeju-Do (South Korea) 8-11 November (Proceedings, Oral Presentation).

Ravazzini, A.M., van Nieuwenhuijzen, A.F. and J.H.J.M van der Graaf (2005). Direct Membrane Ultrafiltration of Municipal Wastewater: towards sustainable operations via low fouling conditions. Particle Separation 2005, Seoul (South Korea) 1-3 June (Poster Presentation).

Ravazzini, A.M., van Nieuwenhuijzen, A.F. and J.H.J.M van der Graaf (2005). Direct Membrane Ultrafiltration of Municipal Wastewater: Sustainable conditions for constant transmembrane pressure and constant flux operations. WRRS - Wastewater Reclamation and Reuse for Sustainability - 2005, Jeju-do (South Korea) 8-11 November (Poster Presentation).

2004

Ravazzini, A.M., van Nieuwenhuijzen, A.F. and J.H.J.M van der Graaf (2004). Direct Membrane Ultrafiltration of Municipal Wastewater: comparison between filtration of raw sewage and primary clarifier effluent. MDIW - Membranes in Drinking and Industrial Water Production - 2004, L'Aquila (I), 15-17 November (Proceedings, Oral Presentation).

Van der Graaf, J.H.J.M., de Koning, J., Ravazzini, A.M. and V. Miska (2004). Treatment matrix for reuse of upgraded wastewater. IWA World Water Congress and Exhibition, Marrakech (Morocco) 19-24 September (Proceedings).

Bixio, D. De Heyder, B., Joksimovic, D., Cikurel, H., Miska, V., Muston, M., Schfer, A.I., Ravazzini, A.M., Aharoni, A., Savic, D. and C. Thoeye (2004). Municipal wastewater reclamation: Where do we stand? An overview of treatment technology and management practice. IWA World Water Congress and Exhibition, Marrakech (Morocco) 19-24 September (Proceedings).

Ravazzini, A.M., van Nieuwenhuijzen, A.F. and J.H.J.M. van der Graaf (2004). Direct Membrane Ultrafiltration of Municipal Wastewater: Operational Aspects. Euromembrane 2004, Hamburg (D), 28 September - 1 October (Poster Presentation).

Ravazzini, A.M.: Direct Ultrafiltration of Municipal Waste Water. Network Young Membrains 6, Hamburg (D), 22-24 September (Book of Abstracts, Workshop).

Miska, V., Ravazzini, A.M. and J. de Koning: Aquarec Deliverable D6 Review Report on Wastewater Treatment Unit Operations, Delft, April 2004.

2003

Ravazzini, A.M. (2003). Direct Membrane Filtration of Waste Water. Know How Special 6(3): "A look back: the Dutch membrane Congress".

Miska, V., Ravazzini, A.M. and J. de Koning: Aquarec Milestone Report M7.1, Review Report on Wastewater Treatment Unit Operations, Delft, September 2004.

Ravazzini A.M.: Direct Membrane filtration of Raw Municipal Waste Water. Network Young Membrains 5. Barcelona, 2-3 October 2003 (Book of abstracts, Workshop).

2002

Ravazzini, A.M.: MBR sludge monitoring by a laboratory crossflow membrane module. M.Sc. Thesis, Politecnico di Milano, Milano, Italy.

About the Author

Aldo Ravazzini was born in Milano, Italy, on the 8^{th} of September 1976.

After finishing the secondary school at Liceo Scientifico G. Marconi (Milano), he started the M.Sc.-course in Environmental Engineering at Politecnico di Milano. The main topics of the course were Water and Wastewater Treatment, Sanitary Engineering and Soil Decontamination, Air Pollution Control.

He successfully concluded this study in July 2002, with a thesis entitled *MBR sludge monitoring by a laboratory crossflow membrane module*. The thesis had been conducted at the Delft University of Technology, within the frame of the European exchange programs *Erasmus-Socrates* and *Leonardo*.

From November 2002 to November 2006 he was *promovendus* at the Faculty of Civil Engineering and Geosciences, Department of Water Management, section Sanitary Engineering. He was member of the research group of prof. ir. J.H.J.M. van der Graaf, working at the PhD project *Direct Ultrafiltration of Municipal Wastewater*. He also contributed to the EU-project *Aquarec, concepts for water reuse*, focusing on the technological issues of water reclamation and reuse.

From these activities he derived the interest for his actual favourite topics: membrane processes and wastewater treatment and reclamation.

In his free time he likes the most hiking, fishing, traveling, taking photographs. He used to play football until short time ago and he hopes to start again soon.

He is currently working as consultant at ILF-Engineers Italia, Department Power Plants and Desalination.